



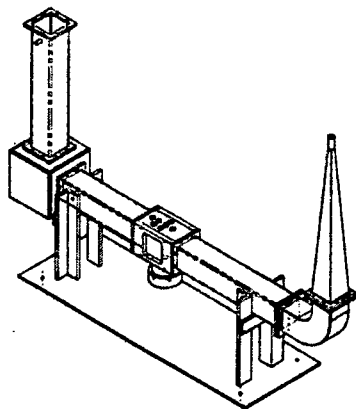
# EDGEWOOD

## CHEMICAL BIOLOGICAL CENTER

U.S. ARMY RESEARCH, DEVELOPMENT AND ENGINEERING COMMAND

**ECBC-TR-327**

### DEVELOPMENT OF THE 5-CM AGENT FATE WIND TUNNEL



**SAIC**

**Daniel J. Weber  
Mary K. Scudder  
Clayton S. Moury**

**RESEARCH AND  
TECHNOLOGY DIRECTORATE**

**Wendel J. Shuely  
John W. Molnar  
Miles C. Miller**

**SCIENCE APPLICATIONS  
INTERNATIONAL CORPORATION  
Newton Centre, MA 02459**

**December 2006**

**Approved for public release;  
Distribution is unlimited.**



# 20070406060

ABERDEEN PROVING GROUND, MD 21010-5424

### Disclaimer

The findings in this report are not to be construed as an official Department of the Army position unless so designated by other authorizing documents.

# REPORT DOCUMENTATION PAGE

Form Approved  
OMB No. 0704-0188

Public reporting burden for this collection of information is estimated to average 1 hour per response, including the time for reviewing instructions, searching existing data sources, gathering and maintaining the data needed, and completing and reviewing this collection of information. Send comments regarding this burden estimate or any other aspect of this collection of information, including suggestions for reducing this burden to Department of Defense, Washington Headquarters Services, Directorate for Information Operations and Reports (0704-0188), 1215 Jefferson Davis Highway, Suite 1204, Arlington, VA 22202-4302. Respondents should be aware that notwithstanding any other provision of law, no person shall be subject to any penalty for failing to comply with a collection of information if it does not display a currently valid OMB control number. PLEASE DO NOT RETURN YOUR FORM TO THE ABOVE ADDRESS.

<b>1. REPORT DATE (DD-MM-YYYY)</b> XX-12-06		<b>2. REPORT TYPE</b> Final		<b>3. DATES COVERED (From - To)</b> Oct 02 - Apr 06	
<b>4. TITLE AND SUBTITLE</b> Development of the 5-cm Agent Fate Wind Tunnel				<b>5a. CONTRACT NUMBER</b>	
				<b>5b. GRANT NUMBER</b>	
				<b>5c. PROGRAM ELEMENT NUMBER</b> 6R27CZ	
<b>6. AUTHOR(S)</b> Weber, Daniel J.; Scudder, Mary K.; Moury, Clayton S. (ECBC); Shuely, Wendel J.; Molnar, John W.; and Miller, Miles C. (SAIC)				<b>5d. PROJECT NUMBER</b>	
				<b>5e. TASK NUMBER</b>	
				<b>5f. WORK UNIT NUMBER</b>	
<b>7. PERFORMING ORGANIZATION NAME(S) AND ADDRESS(ES) AND ADDRESS(ES)</b> DIR, ECBC, ATTN: AMSRD-ECB-RT-DT, APG, MD 21010-5424 SAIC, 7 Wells Avenue, Newton Centre, MA 02459				<b>8. PERFORMING ORGANIZATION REPORT NUMBER</b> ECBC-TR-327	
<b>9. SPONSORING / MONITORING AGENCY NAME(S) AND ADDRESS(ES)</b>				<b>10. SPONSOR/MONITOR'S ACRONYM(S)</b>	
				<b>11. SPONSOR/MONITOR'S REPORT NUMBER(S)</b>	
<b>12. DISTRIBUTION / AVAILABILITY STATEMENT</b> Approved for public release; distribution is unlimited.					
<b>13. SUPPLEMENTARY NOTES</b>					
<b>14. ABSTRACT</b> This report describes development of a 5-cm wind tunnel designed to measure the release and retention of chemical warfare agents (CWA) from various materials under simulated environmental conditions. The wind tunnel, sized to fit within a standard chemical fume hood, provides a specified vertical velocity profile, temperature, and relative humidity (simulating the natural environment) for a sustained time period ranging from hours to weeks. The associated data acquisition instrumentation measures the time history of the vapor released during evaporation of the CWA from the material substrate whether the chemical is a sessile drop on the surface or a sorbed liquid within the substrate. The wind tunnel creates the full-scale, lower portion of the velocity profile produced by a wind-induced, atmospheric boundary layer, which passes over a full-scale drop of agent and a full-scale sample of the material substrate. This feature differentiates it from environmental type wind tunnels where scaling is required for the airflow and items being tested. The 5-cm wind tunnel has the capability to test single and multiple drops of agent. This report summarizes the design evolution, component details and operational functions. Representative data obtained in the tunnel are compared with results from other experimental sources.					
<b>15. SUBJECT TERMS</b>					
Hot wire anemometry		Chemical Warfare Agent (CWA)		Boundary Layer	
Micro tunnel		Evaporation		Adsorption	
Sorption		Atmosphere		Turbulence Absorption	
<b>16. SECURITY CLASSIFICATION OF:</b>			<b>17. LIMITATION OF ABSTRACT</b>	<b>18. NUMBER OF PAGES</b>	<b>19a. NAME OF RESPONSIBLE PERSON</b>
<b>a. REPORT</b>	<b>b. ABSTRACT</b>	<b>c. THIS PAGE</b>			Sandra J. Johnson
U	U	U	UL	179	<b>19b. TELEPHONE NUMBER (include area code)</b> (410) 436-2914

Blank

## FOREWORD

While termed a "wind tunnel", the 5-cm wind tunnel described in this report could more accurately be regarded as one element of a relatively complex experimental apparatus. (By the same token, however, it is truly a "wind tunnel" because it is used to create and study the effect of wind.) The process followed in evolving this experimental apparatus included two interacting groups within the U.S. Army Edgewood Chemical Biological Center (ECBC), Research and Technology Directorate. One group, composed of members from the Smoke and Target Defeat Team, Toxicology, Aerosol Sciences and Obscurants Senior Team, was responsible for the design, fabrication and testing of the wind tunnel component of the experimental arrangement. The evolution, installation and evaluation of the instrumentation associated with the experimental arrangement were performed by members of the Agent Chemistry Team, Physical and Chemical Sciences Senior Team. The ultimate success of the effort was due to the close working relations between these two groups, augmented by a continual interaction with other personnel and organizations involved in the Agent Fate program. While this document is primarily concerned with the development of the wind tunnel, it includes some aspects of its consequent use to demonstrate that the objectives of the effort were met. This document covers a relatively long period of time and reflects the constantly changing environment associated with an experimental development program. Accordingly, not every aspect was documented as completely or formally as desired. The intent is to present the historical sequence of how the 5-cm wind tunnel system was evolved and its subsequent validation. The bulk of the illustrations and photographs contained in the documents were extracted from the various Working Group Meetings and program reviews held by the Agent Fate Program throughout the period covered. The intent was to convey the activities involved in the evolution of a unique and complex experimental apparatus.

Blank

## PREFACE

The work described in this report was authorized under Sales Order No. 6R27CZ. This report covers work performed between October 2002 and April 2006.

The use of either trade or manufacturers' names in this report does not constitute an official endorsement of any commercial products. This report may not be cited for purposes of advertisement.

This report has been approved for public release. Registered users should request additional copies from the Defense Technical Information Center; unregistered users should direct such requests to the National Technical Information Service.

This report has been approved for public release.

### Acknowledgments

While this report deals primarily with the development and validation of the 5-cm wind tunnel, the overall effort involved other aspects related to this end. The authors wish to acknowledge the contributions of the following individuals associated with those aspects: Bob Nickol, Bruce King, John Pence, Erin Maloney, and Chris Giannaris for their efforts in developing the instrumentation and the data acquisition and reduction systems; Seok Hong and Kenneth Sumpter for the TGA data; Terance D'Onofrio for the video imaging results; and Dr. D. Durst, Dr. James Savage, Lawrence Bickford, and Dr. Frederick Berg for their managerial support throughout the developmental program.

Blank



## CONTENTS

1.	INTRODUCTION .....	17
2.	BACKGROUND .....	17
3.	5-CM WIND TUNNEL DESIGN REQUIREMENTS.....	19
4.	5-CM WIND TUNNEL DESIGN EVOLUTION .....	21
4.1	General .....	21
4.2	Plexi-Glass Test Fixture .....	22
4.3	Version 1 (Test Bed Tunnel) .....	25
4.4	Version 2 (Prototype) Tunnel .....	35
4.5	Version 2 Mod 1 (Prototype Tunnel).....	48
4.6	Version 3 (Production Tunnel) .....	52
4.7	Version 3 Mod 1 (Production Tunnel).....	67
5.	VELOCITY PROFILES .....	71
5.1	Atmospheric Boundary Layer.....	71
5.2	Specified Velocity Profiles.....	74
5.3	5-cm Wind Tunnel Velocity Profiles.....	77
6.	EFFECT OF FREE STREAM TURBULENCE .....	81
6.1	Non-Dimensional Boundary Layer.....	81
6.2	Relation to Agent Fate Test Conditions .....	84
6.3	5-cm Wind Tunnel Conditions .....	88
7.	TEST MATRIX.....	93
7.1	General .....	93
7.2	Agents.....	93
7.3	Substrates.....	93
7.4	Test Parameters.....	94
7.5	Validation Tests .....	96
7.6	Production Runs.....	97
8.	INSTRUMENTATION .....	98
9.	EXPERIMENTAL PROCEDURE.....	100
10.	5-CM WIND TUNNEL DATA.....	103
10.1	Agent Mass Balance.....	103

10.2	Evaporation Rate as a Data Metric .....	104
10.3	HD/Glass .....	105
11.	THEORETICAL ANALYSIS OF EVAPORATION RATE.....	107
12.	STATISTICAL ANALYSIS OF EVAPORATION RATE DATA .....	107
13.	AGENT FATE WIND TUNNELS.....	129
13.1	General .....	129
13.2	5-cm Wind Tunnel .....	130
13.3	10-cm Wind Tunnel .....	131
13.4	50 x 100-cm Wind Tunnel.....	132
13.5	Microbalance Facility.....	133
14.	COMPARISON OF DATA BETWEEN WIND TUNNELS .....	134
14.1	Scaling Issues.....	134
14.2	Comparison of Agent Fate Wind Tunnel Data.....	136
14.2.1	10-cm and 5-cm Wind Tunnel Data.....	136
14.2.2	TGA Data.....	138
15.	SUBSTRATE CHARACTERISTICS .....	141
15.1	General .....	141
15.2	HD/Sand .....	143
16.	CONCLUSIONS .....	146
	LITERATURE CITED .....	149
	APPENDIXES	
	A - 5-CM WIND TUNNEL DESIGN EVOLUTION .....	153
	B - ENGINEERING DRAWINGS OF 5-CM WIND TUNNEL VERSION 3 MOD 1 .....	161
	C - SUMMARY OF 10-CM WIND TUNNEL VALIDATION TEST DATA.....	179

## FIGURES

1.	Agent Fate Sequence.....	18
2.	Wind Tunnel Design Objectives.....	19
3.	Relation of Agent Fate Wind Tunnel to Environmental Tunnels and Nature.....	21
4.	Plexi-Glass Test Fixture.....	23
5.	Hot Wire Anemometer Calibration Wind Tunnel .....	24
6.	Turbulence Generator Arrangement .....	25
7.	Stainless Steel Version 1 (Test Bed) Tunnel.....	26
8.	Version 1 (Test Bed) Tunnel Blower/Exhaust Details .....	27
9.	Version 1 (Test Bed) Tunnel Turbulence Strakes and Cubes .....	27
10.	Version 1 (Test Bed) Tunnel Test Section.....	28
11.	Airflow Control Devices .....	29
12.	Lexan Version 1 (Test Bed) Tunnel .....	30
13.	Flow Straightening Elements .....	31
14.	Velocity Profile Conditioning Elements .....	31
15.	Test Section Arrangement.....	32
16.	Velocity Profiles Measured in Test Bed Tunnel With and Without Turbulence Generators.....	33
17.	Stainless Steel Version 1 (Test Bed) Tunnel.....	34
18.	Version 1 (Test Bed) Wind Tunnel Modified With Total Collection Port .....	35
19.	Original Version 2 Wind Tunnel .....	36
20.	Version 2 Tunnel with Transition Cone and Turning Vane Section .....	37
21.	Version 2 (Top View) .....	38

22.	Version 2 (Front View).....	38
23.	Miller-Nelson ECU.....	39
24.	Transition Cone .....	40
25.	Turning Vane Section .....	40
26.	Cubical Turbulence Generators.....	41
27.	Details of Cubical Turbulence Generators.....	42
28.	Test Section .....	43
29.	Mixing Tabs .....	44
30.	Sampling Section.....	44
31.	Hapsite GC-MS .....	45
32.	Blower.....	46
33.	TNO Glass Sample Cutting Set-Up.....	47
34.	Version 2 Mod 1 Tunnel .....	48
35.	Version 2 Tunnel Installed in Chemical Fume Hood .....	49
36.	Typical Agent Vapor Concentration vs. Time .....	50
37.	Typical Agent Mass Ratio vs. Time .....	50
38.	Version 3 (Production) Wind Tunnel .....	54
39.	Version 3 (Production) Tunnel Schematic (Top View).....	55
40.	Version 3 (Production) Tunnel Schematic (Front View).....	55
41.	Cut-Away View Showing Internal Elements .....	56
42.	Test Section .....	57
43.	Screw-in Piston Configuration .....	58
44.	Static Mixer .....	59

45.	Static Mixer Performance .....	59
46.	Sampling Inlet .....	60
47.	Vertical Velocity Profiles Measured Above Piston in Version 3 Wind Tunnel.....	61
48.	Version 3 (Production) Tunnel Installed in Fume Hood.....	61
49.	Version 3 (Production) Tunnel and Associated Instrumentation .....	62
50.	Graphical User Interface .....	63
51.	Variable Tube Sampler .....	64
52.	Two 5-cm Wind Tunnels Installed in Single Fume Hood .....	65
53.	Comparison Between Two Vapor Samplers and Video Information .....	65
54.	Version 3 Mod 1 (Production) Wind Tunnel .....	67
55.	Cut-Away of Version 3 Mod I (Production) Tunnel .....	68
56.	Fine Mesh for Vertical Oriented Turing Vane Section.....	69
57.	Velocity Profiles for Version 3 Mod 1 Wind Tunnel .....	69
58.	Snap-in Piston.....	70
59.	Wind Induced Atmospheric Boundary Layer .....	71
60.	Velocity Profile Nature vs. Wind Tunnel .....	72
61.	Boundary Layer Velocity Profile Nomenclature.....	73
62.	Operational Velocity Profiles Defined by Agent Fate Model Developers .....	75
63.	Operational Velocity Profiles in Physical Units.....	76
64.	Lower Portion of Operational Boundary Layer Profiles.....	76
65.	Velocity Profiles in Vicinity of Drop.....	77
66.	Measured 5-cm Wind Tunnel Velocity Profiles on Physical and Log Scales .....	78

67.	5-cm Wind Tunnel Velocity Profiles (Low Velocity Condition).....	79
68.	5-cm Wind Tunnel Velocity Profiles (Medium Velocity Condition).....	79
69.	5-cm Wind Tunnel Velocity Profiles (High Velocity Condition).....	80
70.	Velocity Profiles Measured at Center of Piston in Different Version 3, 5-cm Wind Tunnels.....	80
71.	Non-Dimensional Boundary Layer.....	81
72.	Agent Fate Operational Velocity Profiles Including Boundary Layer Regions.....	82
73.	Heights of Boundary Layer Regions for Operational Velocity Profiles.....	83
74.	Operational Velocity Values Plotted on Non-Dimensional Boundary Layer Profile.....	86
75.	Results of Experiments for HD on Glass.....	86
76.	Drop Diameter and Height for HD/Glass as a Function of Initial Drop Volume.....	87
77.	Operational Velocities at Drop Height.....	88
78.	Measured Velocity Profiles and Associated Velocity Gradients for 5-cm Tunnel.....	89
79.	Comparison Between Measured and Operational Velocity Values (Close to Surface).....	89
80.	Turbulence Intensity of 5-cm Wind Tunnel.....	90
81.	Atmospheric Turbulence Measurements at DPG Effect of Time of Day.....	91
82.	Turbulence Intensity vs. time of Day DPG.....	91
83.	Atmospheric Turbulence Measurements at DPG Effect of Altitude.....	92
84.	Turbulence Intensity vs. Height DPG.....	92
85.	Test Matrix Values.....	95

86.	Basic Test Matrix Arrangement and Coding.....	96
87.	Validation Test Matrix HD/Glass.....	97
88.	Production Test Matrix .....	98
89.	Summary of Instrumentation Used with 5-cm Wind Tunnel.....	100
90.	5-cm Wind Tunnel Reference Velocities.....	101
91.	Flow Diagram for 5-cm Wind Tunnel Data Acquisition and Analysis Process .	102
92.	Example of Video Data and Results .....	103
93.	Typical Wind 5-cm Wind Tunnel Data (9 $\mu$ l Drop of HD on Glass) .....	104
94.	3-D Plot of 5-cm Data Developed by Statistical Analysis.....	108
95.	Statistical Analysis of 5-cm Wind Tunnel Data Evaporation Rate vs. Velocity and Temperature HD on Glass for 9 $\mu$ l Drop.....	109
96.	Statistical Analysis of 5-cm Wind Tunnel Data Evaporation Rate vs. Velocity and Temperature HD on Glass for 6 $\mu$ l Drop.....	110
97.	Statistical Analysis of 5-cm Wind Tunnel Data Evaporation Rate vs. Velocity and Temperature HD on Glass for 1 $\mu$ l Drop.....	110
98.	Statistical Analysis of 5-cm Wind Tunnel Data Evaporation Rate vs. Velocity and Drop Volume HD on Glass at 15 $^{\circ}$ C.....	111
99.	Statistical Analysis of 5-cm Wind Tunnel Data Evaporation Rate vs. Velocity and Drop Volume HD on Glass at 35 $^{\circ}$ C.....	111
100.	Statistical Analysis of 5-cm Wind Tunnel Data Evaporation Rate vs. Velocity and Drop Volume HD on Glass at 50 $^{\circ}$ C.....	112
101.	Statistical Analysis of 5-cm Wind Tunnel Data Evaporation Rate vs. Temperature and Drop Volume HD on Glass at 0.22 m/s .....	112
102.	Statistical Analysis of 5-cm Wind Tunnel Data Evaporation Rate vs. Temperature and Drop Volume HD on Glass at 1.7 m/s .....	113
103.	Statistical Analysis of 5-cm Wind Tunnel Data Evaporation Rate vs. Temperature and Drop Volume HD on Glass at 3.6 m/s .....	113

104.	Statistical Analysis of 5-cm Wind Tunnel Data Evaporation Rate vs. Temperature and Velocity HD on Glass at 9 $\mu$ l Drop .....	114
105.	Statistical Analysis of 5-cm Wind Tunnel Data Evaporation Rate vs. Temperature and Velocity HD on Glass at 6 $\mu$ l Drop .....	114
106.	Statistical Analysis of 5-cm Wind Tunnel Data Evaporation Rate vs. Temperature and Velocity HD on Glass at 1 $\mu$ l Drop .....	115
107.	Statistical Analysis of 5-cm Wind Tunnel Data Evaporation Rate vs. Drop Volume and Temperature HD on Glass at 0.22 m/s .....	115
108.	Statistical Analysis of 5-cm Wind Tunnel Data Evaporation Rate vs. Drop Volume and Temperature HD on Glass at 1.7 m/s .....	116
109.	Statistical Analysis of 5-cm Wind Tunnel Data Evaporation Rate vs. Drop Volume and Temperature HD on Glass at 3.6 m/s .....	116
110.	Statistical Analysis of 5-cm Wind Tunnel Data Evaporation Rate vs. Drop Volume and Velocity HD on Glass at 50 °C.....	117
111.	Statistical Analysis of 5-cm Wind Tunnel Data Evaporation Rate vs. Drop Volume and Velocity HD on Glass at 35 °C.....	117
112.	Statistical Analysis of 5-cm Wind Tunnel Data Evaporation Rate vs. Drop Volume and Velocity HD on Glass at 15 °C.....	118
113.	Illustration of Equivalence of Reference and Test Matrix Velocities 5-cm Wind Tunnel, HD on Glass .....	119
114.	Evaporation Rate vs. Velocity at 2 m (HD on Glass - 9 $\mu$ l Drop).....	120
115.	Evaporation Rate vs. Velocity at 2 m (HD on Glass - 6 $\mu$ l Drop).....	120
116.	Evaporation Rate vs. Velocity at 2 m (HD on Glass - 1 $\mu$ l Drop).....	121
117.	Evaporation Rate vs. Velocity and Drop Volume (HD on Glass at 15 °C).....	121
118.	Evaporation Rate vs. Velocity and Drop Volume HD on Glass at 35 °C.....	122
119.	Evaporation Rate vs. Velocity and Drop Volume HD on Glass at 50 °C.....	122
120.	Evaporation Rate vs. Temperature and Drop Volume HD on Glass at 0.5 m/s .....	123



121.	Evaporation Rate vs. Temperature and Drop Volume HD on Glass at 3.0 m/s .....	123
122.	Evaporation Rate vs. Temperature and Drop Volume HD on Glass at 6.0 m/s .....	124
123.	Evaporation Rate vs. Temperature and Velocity HD on Glass for 9 $\mu$ l Drop .....	124
124.	Evaporation Rate vs. Temperature and Velocity HD on Glass for 6 $\mu$ l Drop.....	125
125.	Evaporation Rate vs. Temperature and Velocity HD on Glass for 1 $\mu$ l Drop.....	125
126.	Evaporation Rate vs. Drop Volume and Temperature HD on Glass for 0.5 m/s .....	126
127.	Evaporation Rate vs. Drop Volume and Temperature HD on Glass for 3.0 m/s .....	126
128.	Evaporation Rate vs. Drop Volume and Temperature HD on Glass for 6.0 m/s .....	127
129.	Evaporation Rate vs. Drop Volume and Velocity HD on Glass at 50 °C.....	127
130.	Evaporation Rate vs. Drop Volume and Velocity HD on Glass at 35 °C.....	128
131.	Evaporation Rate vs. Drop Volume and Velocity HD on Glass at 15 °C.....	128
132.	Statistical Trend Lines for Test Validation Data with Respect to Velocity Values at a 2 m Height.....	129
133.	Agent Fate Wind Tunnels .....	130
134.	5-cm Wind Tunnel.....	131
135.	10-cm Wind Tunnel.....	132
136.	50 x 100-cm Wind Tunnel .....	133
137.	TGA 2950 .....	134
138.	Measured Velocity Profiles for Agent Fate Wind Tunnels.....	135

139.	Reynolds Number .....	136
140.	Mean Evaporation Rate vs. Velocity for HD/Glass; 1 $\mu$ l Drop Size .....	137
141.	Mean Evaporation Rate vs. Velocity for HD/Glass; 6 $\mu$ l Drop Size .....	137
142.	Mean Evaporation Rate vs. Velocity for HD/Glass; 9 $\mu$ l Drop Size .....	138
143.	Correlation Between TGA2950 and 5-cm Tunnel .....	139
144.	TGA2950 and 5-cm Tunnel Data-6 $\mu$ l Drop .....	140
145.	TGA2950 and 5-cm Tunnel Data-1 $\mu$ l Drop .....	140
146.	Evaporation of Sessile Drop on Glass .....	141
147.	Agent Absorption in Concrete and Asphalt .....	142
148.	Comparison of Concentration vs. Time for HD on Glass and Sand.....	143
149.	Agent Mass Remaining vs. Time for HD on Glass .....	144
150.	Agent Mass Remaining vs. Time for HD on Sand .....	144
151.	Comparison of Evaporation Rate of HD on Sand and Glass .....	145

TABLES

1.	Floor Velocity Gradients for Specified Agent Fate Test Matrix Velocities .....	84
2.	Summary of 5-cm Wind Tunnel Validation Test Data.....	106

## DEVELOPMENT OF THE 5-CM AGENT FATE WIND TUNNEL

### 1. INTRODUCTION

The Agent Fate Program is sponsored by the Defense Threat Reduction Agency as a Defense Technical Objective (DTO): CB.42- Environmental Fate of Agents. The objective of the program is to measure and understand the physical-chemical processes of CWA agents on surfaces to predict their persistence and fate in operational scenarios via agent fate models. The program consists of a three parallel and interactive efforts: laboratory experiments using a variety of special wind tunnels; studies related to agent/substrate reaction and interaction chemistry and the development of predictive models using the laboratory and field test data.<sup>1</sup> Participants include research components of the Air Force, Navy and Army and their supporting contractors from the Czech Republic, United Kingdom, Netherlands and Republic of South Africa. The goal is to upgrade the threat persistence guidelines for Chemical Warfare Agents (CWA) in military field manuals and other defense activities such as the Joint Battle Management Analysis and Planning (JFOC), the Joint Effects Model (JEM) and the Joint Operational Effects Federation (JOEF).

The experimental aspects of the program involve the determination of the "secondary" evaporation of CWA (HD, VX, GD) from the surfaces of natural and man-made substrates of operational concern (glass, sand, soil, concrete, asphalt) that have absorbed the CWA agent. ("primary" evaporation takes place while the drop is airborne; prior to the drop impacting the ground.) Of prime interest is the amount of vapor volatilized and the residual agent remaining in the substrates under a set of controlled environmental conditions [wind speed, temperature, and relative humidity (RH)]. The resulting experimental data are then used to develop models to predict threat persistence for operational scenarios. The findings will then be incorporated into other models and field manuals to provide more accurate threat persistence guidance for chemical warfare defense, terrorist attacks, pesticides, and other chemical related environmental issues. This report describes the evolution and initial use of the 5-cm wind tunnel designed specifically to obtain these data.

### 2. BACKGROUND

The wind tunnel studies are intended to provide data to the model developers on the fate sequence of agent drops on different substrates under the combined influence of wind, temperature and humidity. Figure 1 describes the overall fate of agent deposited on a substrate and illustrates the sequence of events in terms of the agent vapor and agent mass being measured in the wind tunnels. The figure does not contain actual experimental data, but is intended to illustrate the types of data obtained in the wind tunnel test.

At the start of the test, a drop or drops of agent are deposited on a substrate specimen (in this illustration, the substrate is absorptive and reactive) outside of the wind tunnel. A portion of the agent forms a sessile drop on the surface while the remainder is absorbed into the substrate. For some experiments, the agent/substrate combination is then weighed. This weight is compared to the weight of the substrate alone to ascertain the weight of agent deposited.

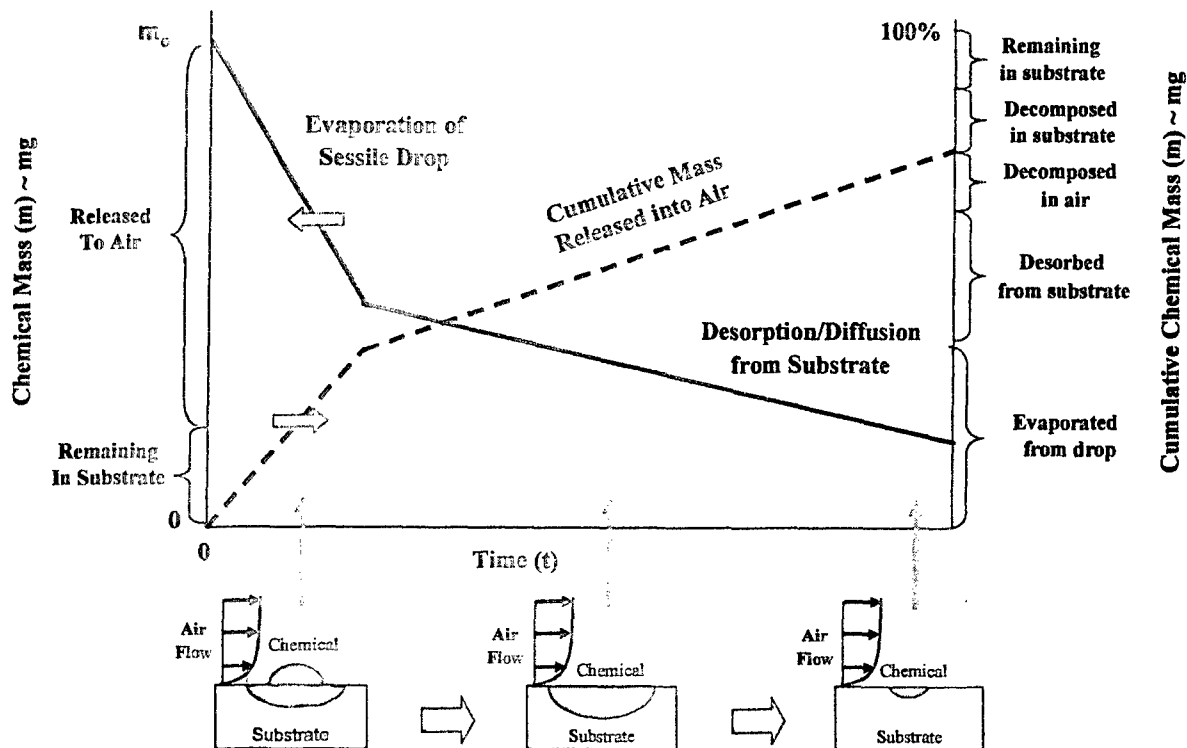


**Figure 1. Agent Fate Sequence**

The substrate sample is then inserted into the tunnel; being placed on the floor of the test section. The wind tunnel airflow is then established creating the specific velocity profile, temperature and RH conditions desired. As time passes, the chemical volatilizes into the air passing over the substrate with the resulting vapor carried away by the air stream. Eventually, the sessile drop completely volatilizes leaving only the chemical absorbed in the substrate, which then begins to desorb and volatilize. This phase exhibits a markedly lower volatilization rate than was the case for the sessile drop. Testing continues until no vapor appears to be released from the substrate. This may range from hours to weeks depending on the chemical, substrate material, drop size, velocity, temperature and RH.

Throughout this operation, the agent vapor and air mixture are collected by chemical analysis instruments such as an on-line, mass spectrometer and/or by sorbent tubes, which are used to determine the vapor mass concentration released as a function of time. The amount of agent released into the air represents the initial conditions for transport and diffusion models, which are used to predict the movement of the vapor cloud under the influence of wind over the terrain. The mass spectrometer can also be used to determine whether any of the agent decomposes in the air. After the test, the substrate can be analyzed for any residual chemical or chemical decomposition products with a variety of analytical methods including spectroscopy (e.g., in situ NMR), extraction followed by

chromatographic analysis or other methods. In this way, the fate of the chemical from each of these mechanisms can be determined for the experimental conditions evaluated. Any chemical remaining in the substrate is also a major concern because it may represent a contact hazard or be released at a future time due to rain or other effects.

### 3. 5-CM WIND TUNNEL DESIGN REQUIREMENTS

The 5-cm wind tunnel was required to satisfy a number of design objectives shown in Figure 2.

- 
- Allow testing of actual toxic agents
  - Fit entire wind tunnel in a standard chemical fume hood
  - Test full-scale drop arrays and substrates
  - Test single and multiple drops
  - Enable rapid introduction of a measured drop(s) of agent into the test section
  - Produce full-scale vertical velocity profiles based on defined, wind induced boundary layers
  - Assure velocity profiles are invariant over the substrate surface
  - Support interfacing with instrumentation for monitoring and controlling test conditions and measuring agent vapor concentration as a function of time
  - Create and maintain constant temperature and RH conditions
  - Permit visual access of drop and substrate
  - Maintain leak-proof structure
  - Minimize agent losses due to deposition on tunnel walls
  - Provide a homogeneous vapor/air mixture at sampling location
  - Represent ease of manufacture
- 

#### Figure 2. Wind Tunnel Design Objectives

A special wind tunnel had to be designed and built because no existing wind tunnels met these unique and demanding requirements.\* Since the wind tunnel was required to operate with actual toxic CWA agents, it had to be small enough to fit in a standard chemical fume hood. At the same time, the wind tunnel test section had to be large enough to accommodate multiple full-scale drops of agent on a wide range of full-scale substrate materials.

---

\* While referred to as a wind tunnel, it is not a conventional wind tunnel as employed for standard aerodynamic research and development functions and can be thought of more as a laboratory facility. By the same token, since it simulates the effect of the wind, it can truly be defined as a "wind tunnel".

At the same time, the tunnel had to be small enough (and the associated instrumentation sensitive enough) to test a single, full-scale drop of agent. No scaling of any of the testing parameters was permitted. The wind tunnel represented a unique combination of small size, low velocities and associated low pressures.

A particularly difficult requirement was to simulate defined velocity profiles matching the lower portion of an atmospheric boundary layer. The attention to duplicating the detailed vertical velocity profile over the drop/substrate was one of the main features that set this experimental arrangement apart from previous agent fate type studies. The test section also had to allow the insertion of instrumentation to establish and monitor the experimental parameters of interest. A critical consideration was to produce sustained temperature and RH conditions throughout the tunnel for periods ranging from hours to weeks. It was also desired to provide visual access to the drop/substrate via a side window.

A leak-proof wind tunnel structure was required for safety as well as for agent mass balance considerations. It is important to achieve an agent mass balance where all of the agent deposited at the beginning of the test can be accounted for at the end of the test whether as a vapor or retained in the substrate. In this regard, it was crucial to eliminate or minimize any agent losses in the tunnel due to deposition on the tunnel walls or components. The tunnel had to provide a homogeneous vapor/air mixture at the sampling port to accurately measure the agent mass released by the agent/substrate in the test section. Access locations for data acquisition and analysis instrumentation had to be available in all areas of the tunnel structure.

Throughout the design process, it was often necessary to respond to changing performance requirements as stipulated by the Agent Fate model developers or from the test results from previous tunnel designs. These included changes in the velocity profiles, temperature and RH values and different and/or additional instrumentation requirements. The resulting tunnel design had to be amenable to being fabricated in multiple units for use by different organizations in different locations. The structure was designed to be sectional so that the wind tunnel could be disassembled for decontamination. Finally, the design and validation of the wind tunnel and data acquisition/analysis system had to be completed within a period of two years.

Existing environmental wind tunnels were considered for this application, but as illustrated in Figure 3, they have limitations that preclude their use. They simulate a "scaled" velocity field over similarly "scaled" man-made and natural objects such as buildings, trees, etc. Their main function is to determine the effect of the wind on structures or the transport and diffusion of contaminants in a large scale flow field. They are large and expensive to operate and most can not test hazardous chemicals due to safety and contamination considerations.

While some large wind tunnels are being developed that might meet the requirements for environmental fate measurements with toxic materials, these are expensive to operate and their large size precludes their being used in standard chemical fume hoods or for the study of single drops of CWA. In addition, the high airflow volumes required dilute the volatilized vapor to levels that can only be analyzed after very long sampling periods, leading to loss of time resolution.

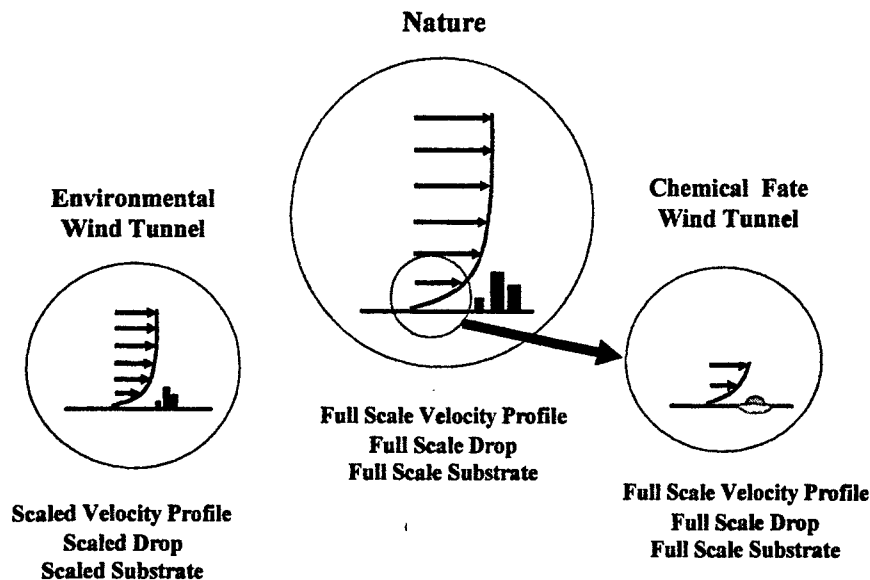


**Figure 3. Relation of Agent Fate Wind Tunnel to Environmental Tunnels and Nature**

#### 4. 5-CM WIND TUNNEL DESIGN EVOLUTION

##### 4.1 General

Development of the 5-cm wind tunnel officially began in October 2001 with a review of literature related to the design of environmental and chemical agent/simulant wind tunnels as well as references on generating representative atmospheric boundary-layers in wind tunnels. The basic design challenge was to have the overall tunnel structure fit within the dimensions of a chemical fume hood measuring 137 cm wide by 56 cm high by 40 cm deep. One of the difficulties was the unknown nature of an atmospheric boundary layer at the extreme close vicinity to the ground of interest to the Agent Fate program. Another was the fact that the full-scale drop/substrate size and the full-scale velocity conditions considered for the Agent Fate wind tunnel were unlike any conditions previously encountered in environment or conventional wind tunnels. Thus, there was little past experience or data that could be used to provide tunnel design guidance.

The use of data from previous agent fate type experimental studies is hampered by their inadequate description of the velocity profiles present. The current Agent Fate program is intended to rectify this by using defined velocity profiles that match the lower portion of a full-scale atmospheric boundary layer. One of the original concepts was to allow the vertical velocity profile to be created naturally in the wind tunnel by lining the floor of the fetch (the tunnel section located upstream of the test section) with a particular substrate material. The airflow passing through the fetch and over the substrate material would naturally form the desired velocity profile in the test section where the agent was deposited. In order for the velocity profile to fully develop, the fetch had

to be a certain number of test section diameters in length. In addition, to obtain adequate mixing of the agent vapor and the air at the sampling port located downstream of the test section, the mixing section of the tunnel had to be a certain number of test section diameters long. As will be discussed, this approach would have resulted in a tunnel length that exceeded the size constraints of the fume hood. Accordingly, turbulence generators were employed to artificially create the desired vertical velocity profile allowing a shorter fetch and a corresponding tunnel width that fits completely within the confines of the hood.

The test section size was optimized based on several competing factors. It had to be large enough to hold representative, full-scale agent drop(s) and substrate combinations yet small enough to allow the measurement of agent vapor concentrations resulting from a single small drop. As the test section cross sectional area is increased, the volume of airflow required to achieve a given velocity increases causing the concentration of a given mass of agent vapor in the air to become too diluted to be measured over the short time increments required to assess the concentration time history to the resolution desired.

High airflows also require higher volumes of heated/cooled/humidity controlled air to be supplied to the tunnel and the volume flow possible from available laboratory environmental control units to produce the 10 m/s maximum test section velocity initially required dictated an upper test section size limit of about 5-cm square. Conversely, maintaining uniform flow across the width of the test section (i.e., over the drop/substrate) becomes an issue as the test section area decreases. Boundary layers forming on the side walls and ceiling of the test section encroach into the center of the test section and adversely affect achieving the desired vertical velocity profile over the drop/substrate. This latter consideration indicated that the test section had to be greater than 4 cm square.

Based on these factors, a test section measuring 5 cm by 5 cm was adopted. A square test section cross section was chosen to provide a constant velocity profile across the width of the substrate sample. Further, this test section size was compatible with the inlet to a small DC blower, which was used to provide the airflow through the tunnel in the initial tunnel design stage. One final consideration for selecting this size was the availability of standard sized, square stainless steel tubing with a 4.85-cm inside dimension that facilitated the fabrication and reduced the cost of the tunnel. Even though the 0.45-mm thick wall tubing had an actual inside dimension of 4.85 cm, the tunnel was referred to as a 5-cm tunnel.

#### **4.2 Plexi-Glass Test Fixture**

A test fixture was designed and fabricated to specifically investigate boundary-layer development in a small wind tunnel.<sup>2</sup> The test fixture arrangement is shown in Figure 4 and consisted of a straight, 5-cm square cross sectioned, tube constructed from solvent welded, transparent Plexi-glass sheets. Transparent Plexi-glass was employed to allow visual access into the interior of the fixture. The fixture structure was attached to a wooden floor support by means of aluminum brackets. Airflow through the fixture was produced by means of a small electric squirrel cage blower located at the exhaust end of the tube. The center portion of the fixture represented the test section. Tests with the fixture commenced in June 2002.



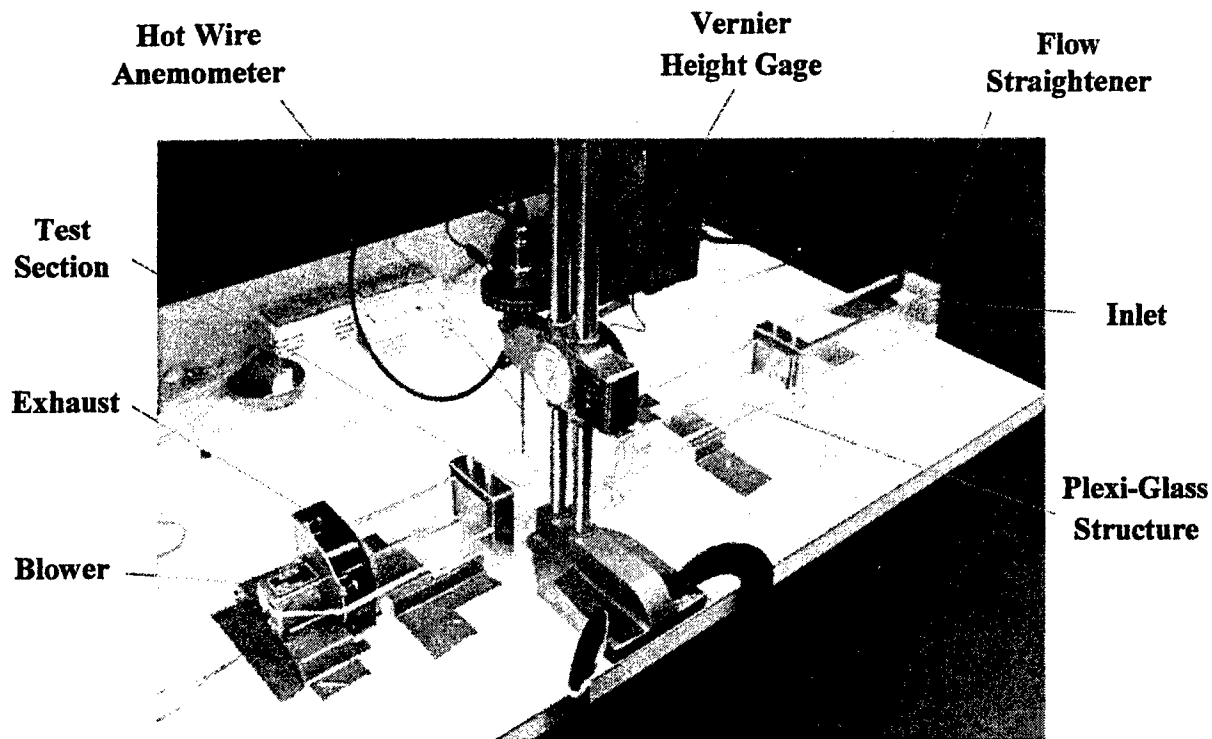


**Figure 4. Plexi-Glass Test Fixture**

Velocity measurements in the test section were achieved using a TSI Model IFA 300 hot wire anemometer; a research grade instrument that operated on the principle of constant temperature anemometry. The anemometer probe was attached to a vernier height gage, which allowed the tip of the probe to be accurately placed at different vertical positions above the test section floor. Vertical velocity surveys could be made indicating the velocity as a function of height representing the velocity profile that was critical to meeting the Agent Fate test requirements. To obtain the most accurate data possible a special hot wire calibration wind tunnel was used as shown in Figure 5. This tunnel is designed by TSI specifically for calibration of hotwire anemometers. It has a 2-cm square test section and an operating velocity range from 0.05 to 45 m/s. This tunnel allowed the hot wire anemometer calibration to be continually monitored throughout the development of the 5-cm tunnel.

Fetch lengths of 15.2, 30.5 and 45.7 cm were examined in the test fixture. A series of experiments were conducted with the various fetch lengths to evaluate the ability to create controlled and defined velocity profiles in the 5-cm sized test section. The transparent Plexi-glass permitted the position of the probe to be ascertained as well as allowing smoke visualization studies to be performed.

It was not feasible to use substrate material along the fetch to create a natural boundary layer profile due to a combination of insufficient length available to establish a fully developed boundary layer and the undefined relation of this approach to operational conditions of interest to the Agent Fate program. Accordingly, roughening devices and turbulence generators were evaluated to tailor the profile to a specific velocity profile shape. Although no specific velocity profiles had yet been defined by the Agent Fate program, the final vertical velocity profiles were expected to have a "power law" shape where the velocity was a function of the distance from the floor (height) raised to a constant exponent value (i.e., power). This was to be accomplished by the use of turbulence generators located upstream of the test section.

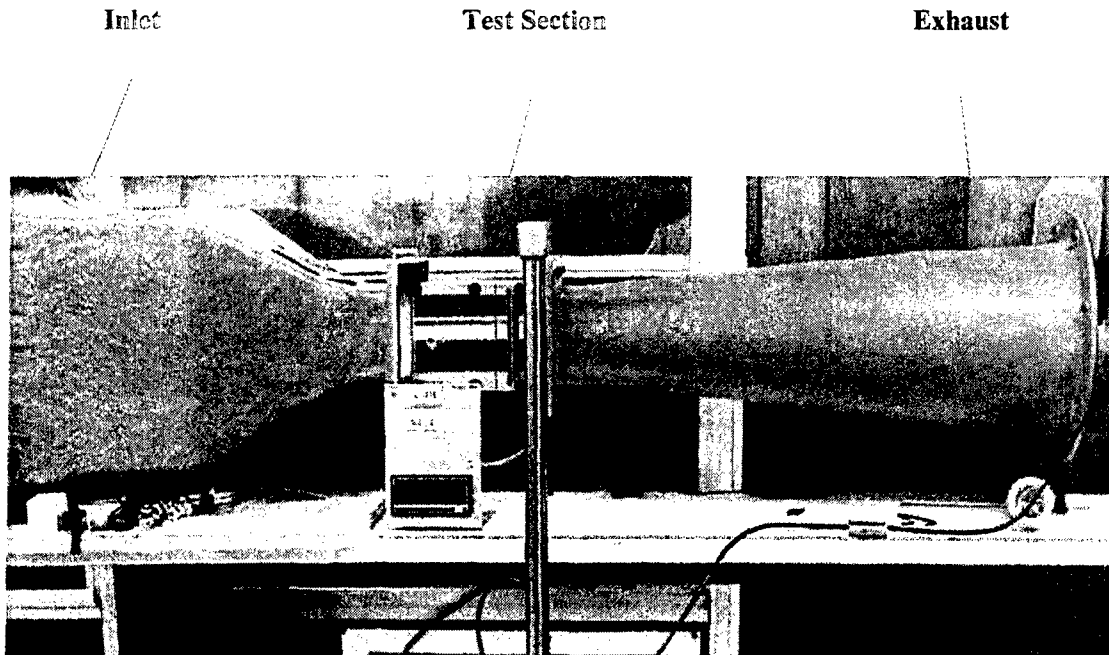


**Figure 5. Hot Wire Anemometer Calibration Wind Tunnel**

Initial velocity measurements were made with no turbulence generating devices present to provide a "clean" tunnel interior baseline. Velocity profile and turbulence intensity measurements demonstrated the need for flow straighteners upstream of the test section area to provide a stable flow condition across the width and height of the test section. This was achieved by placing an array of short tubes across the fixture entrance. A number of turbulence generating devices were then evaluated including vertical triangular strakes, chains and blocks. These devices were based on similar items employed to generate boundary layer profiles described in the literature. A combination of vertically oriented, strakes followed by an array of cubical blocks located on the floor of the fetch, as shown in Figure 6, were found to produce repeatable velocity profiles matching the nominal power law representation of an atmospheric boundary layer. The strakes were composed of five, 0.045 cm thick, flat triangular strakes measuring 0.45 cm at the base and with a height of 2.5 cm. The cubical blocks were composed of Teflon cubes glued to a flat stainless steel strip, which

was glued to the floor of the fetch. The 23 cubical blocks, each measuring 5 mm on a side, were arranged in a staggered array across the width of 9 rows along an 8.5 cm in length of the fetch. While the best results were obtained with the longer fetch lengths, to keep the overall length of the wind tunnel as short as possible, a 30.5-cm long fetch section was selected for the 5-cm wind tunnel. This gave the tunnel an overall width of 91.6 cm, which would allow it to fit within the fume hood width constraints.

The test fixture was an important step in the design of the 5-cm wind tunnel in that it demonstrated that boundary layer type velocity profiles could be created in a small wind tunnel. This fixture also established the hot wire anemometry instrumentation and methodology for subsequent measurement of the velocity profiles in later versions of the 5-cm wind tunnel.

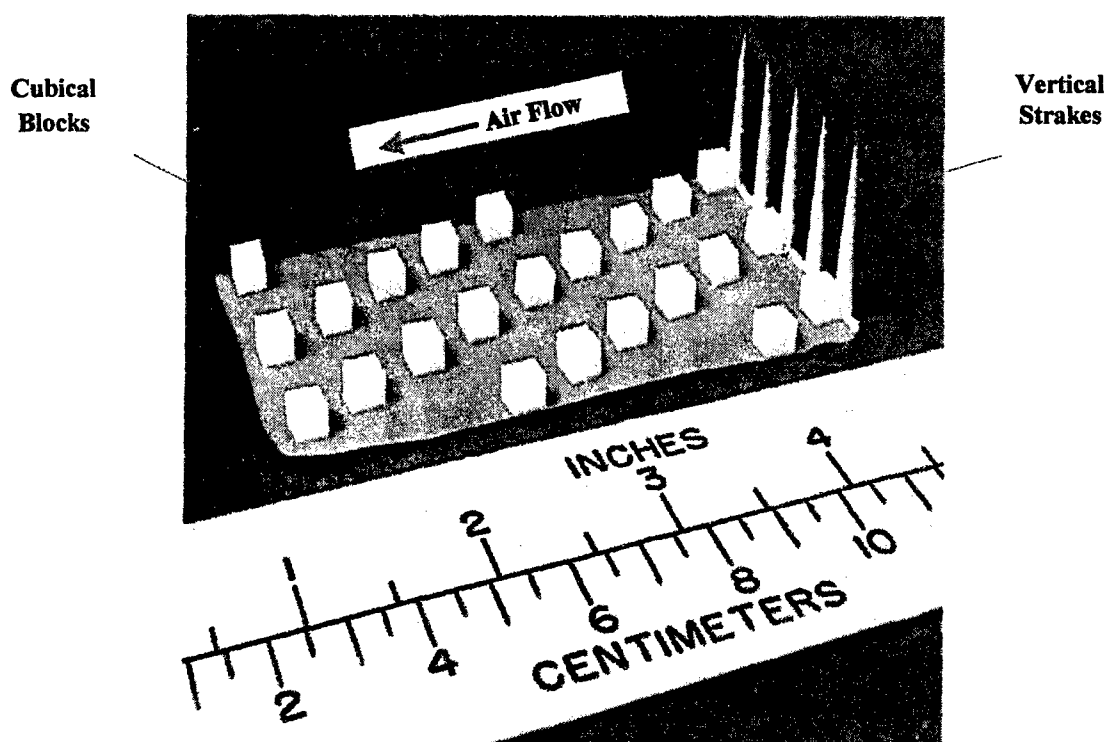


**Figure 6. Turbulence Generator Arrangement**

#### **4.3 Version 1 (Test Bed Tunnel)**

With the capability of establishing and maintaining the general velocity profile shape demonstrated, the next step was to design a test bed tunnel that could be used to evolve all of the basic components required in the Agent Fate wind tunnel including: the airflow source and controller; fetch section and final turbulence/roughening elements; test section with agent/substrate holder and instrumentation access ports; and mixing/sampling section. The resulting configuration was designated as the Version 1 (Test Bed Tunnel). Two different units were built. One was fabricated from stainless steel and was used to design the tunnel components and agent vapor

measuring instrumentation. The other was made from clear Lexan® polycarbonate plastic for flow visualization studies. Both tunnels consisted of an open circuit, straight layout with a 5-cm square interior cross section.

The stainless steel version is shown in Figure 7. The tunnel structure was fabricated from standard 4.85-cm inside dimension square tubing with the inside corners of the tubing having a 0.12-cm radius. The tunnel sections were slip fitted together with no positive attachment. Airflow in the tunnel was produced by a squirrel cage blower powered by a small brushless, variable speed DC motor located downstream of the test section as shown in Figure 8. Locating the blower downstream of the test section was done to assure that a negative pressure existed in the test section to prevent agent leakage. Air entered the fetch section through an airflow controller at the entrance to the wind tunnel. Flow straightening was accomplished by an array of straws located in the beginning of the fetch section. The air next past over the turbulence generators developed previously as shown in Figure 9. These caused the velocity profile to assume the desired “power law” shape when entering the test section.

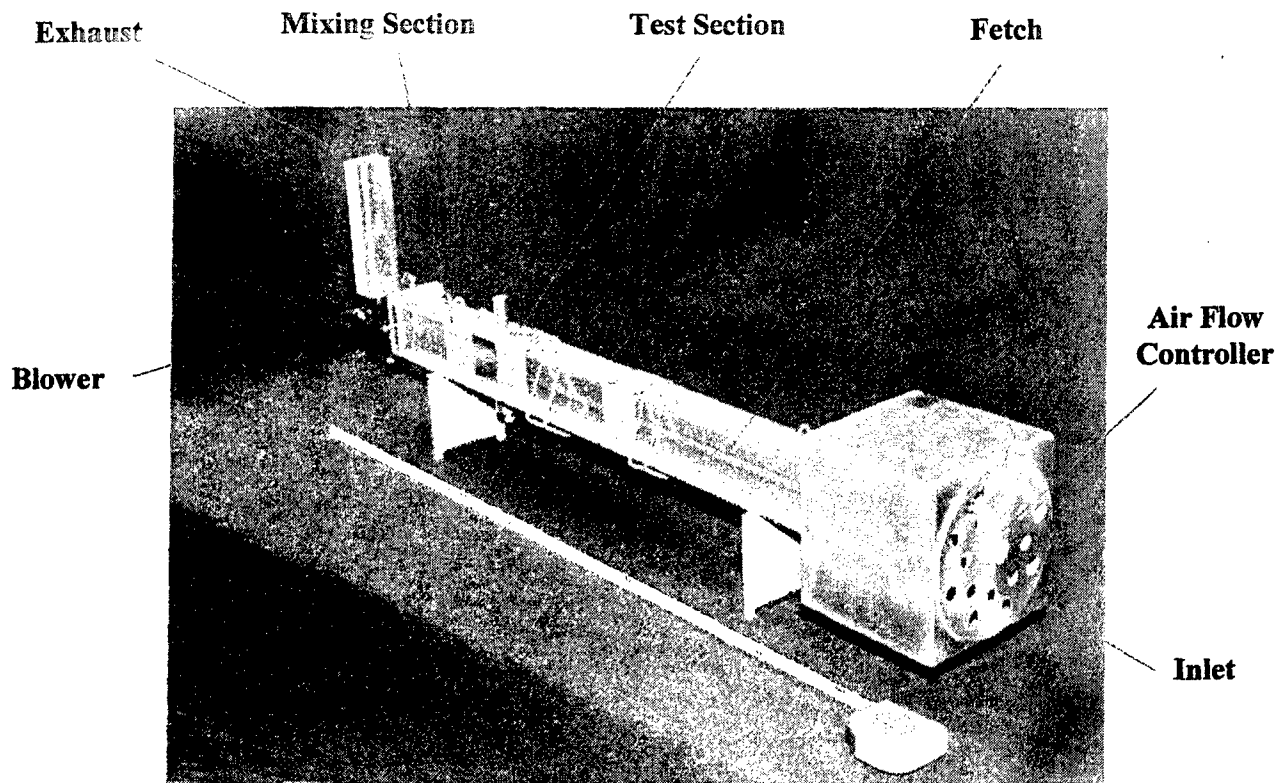


**Figure 7. Stainless Steel Version 1 (Test Bed) Tunnel**

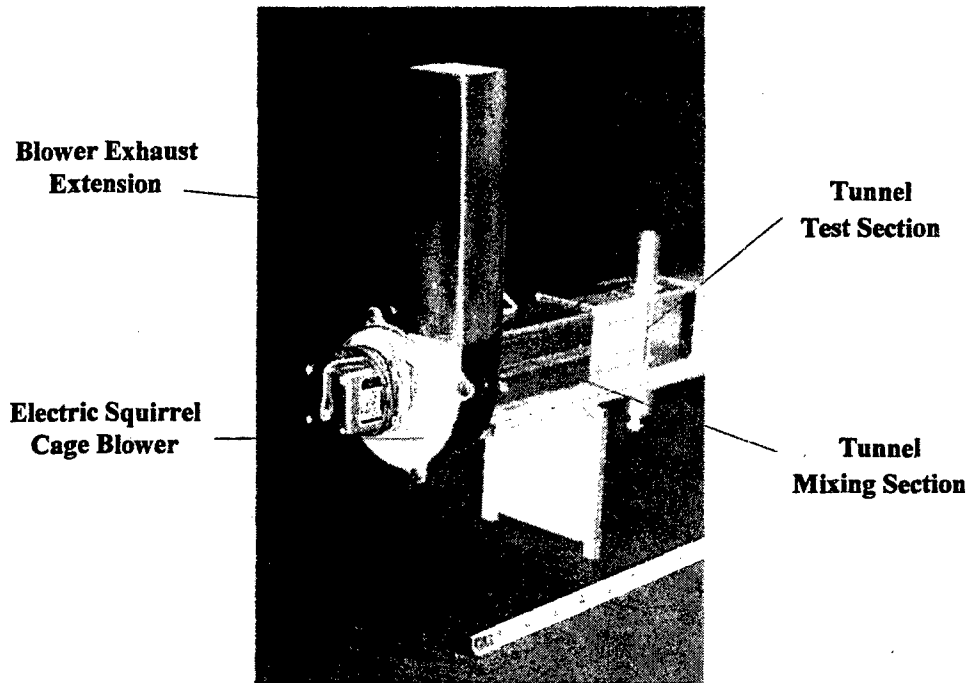


**Figure 8. Version 1 (Test Bed) Tunnel Blower/Exhaust Details**

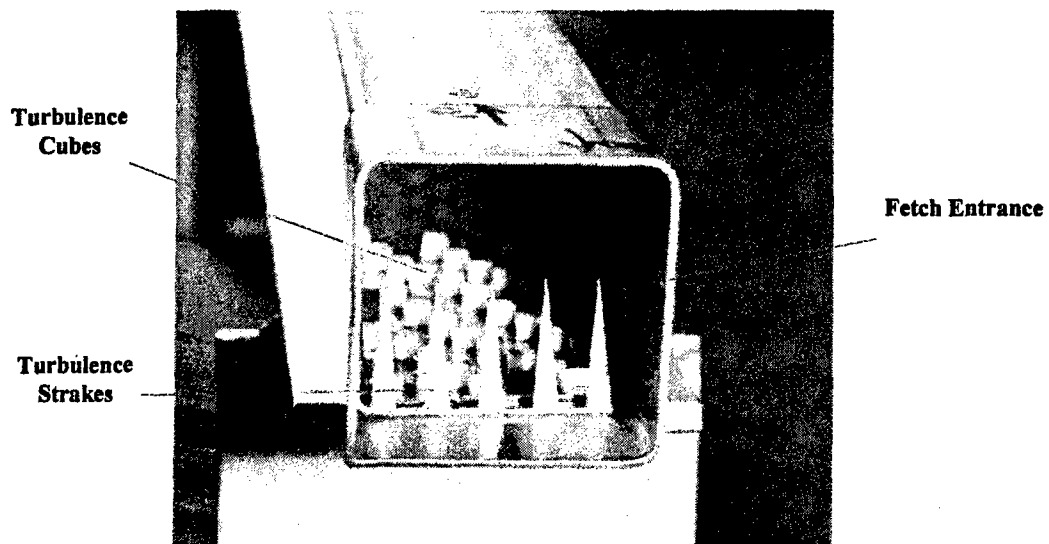


**Figure 9. Version 1 (Test Bed) Tunnel Turbulence Strakes and Cubes**

The tunnel test section is shown in Figure 10. The substrate to be tested could be placed on the top surface of a cylindrical Teflon® piston, also shown. The piston was then inserted into a hole in the bottom of the test section and positioned so that the top surface of the substrate was flush with the floor of the test section. The 2-cm diameter piston contained a flared bottom that created a tight fit to prevent vapor/air leakage between the piston and test section floor. A nylon screw projecting from the bottom of the piston allowed it to be manually inserted and withdrawn from the test section. The agent could be deposited onto the surface of the substrate by means of a syringe inserted through a stainless steel tube welded to the ceiling of the test section. The 1.6-cm diameter tube included a 1.1-cm diameter hole for agent drop insertion and was also used to introduce the hot wire anemometer probe into the test section. A 4.5-cm square window located on the side of the test section allowed observation of the agent/substrate. The flat window covered only the flat portion of the test section wall and did not extend into the curve edge of the wall. This prevented a complete side view of the drop surface/interface. The mixing section was located downstream of the test section. Two tandem, stainless steel tabs were located on the interior surfaces of each of the four walls. These acted as vortex generators to mix the vapor/air prior to its reaching the sampling section located further downstream.

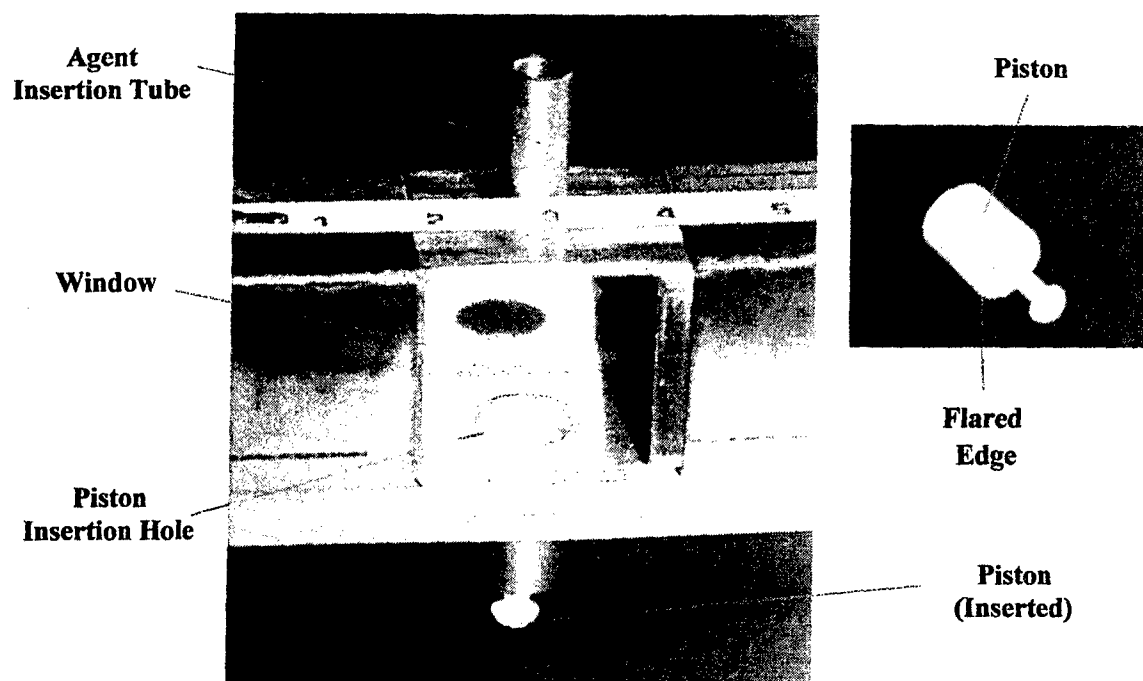


**Figure 10. Version 1 (Test Bed) Tunnel Test Section**

The two Version I tunnels were completed in June 2003. Both tunnels were used initially by the aerodynamics group for component development and velocity profile studies.<sup>3</sup> The

stainless steel version was subsequently provided to the Agent Chemistry Team in July 2003 for instrumentation installation and evaluation with actual CWA agent (HD on glass).<sup>4</sup> The tunnel was referred to as the "Wolverine". Additional modifications were made to the tunnel based on the results of testing by both groups.

Primary control of the tunnel airflow was provided by the variable speed motor located downstream of the mixing section. Finer control of the airflow was achieved by means of an airflow controller up stream of the fetch. The controller included adjustable openings into a plenum section that exhausted into the fetch. The stainless steel tunnel was initially used to evaluate various types of these airflow control devices. Three different inlet configurations were initially constructed: Multi-Slot, Multi-Hole, and Iris and are illustrated in Figure 11.

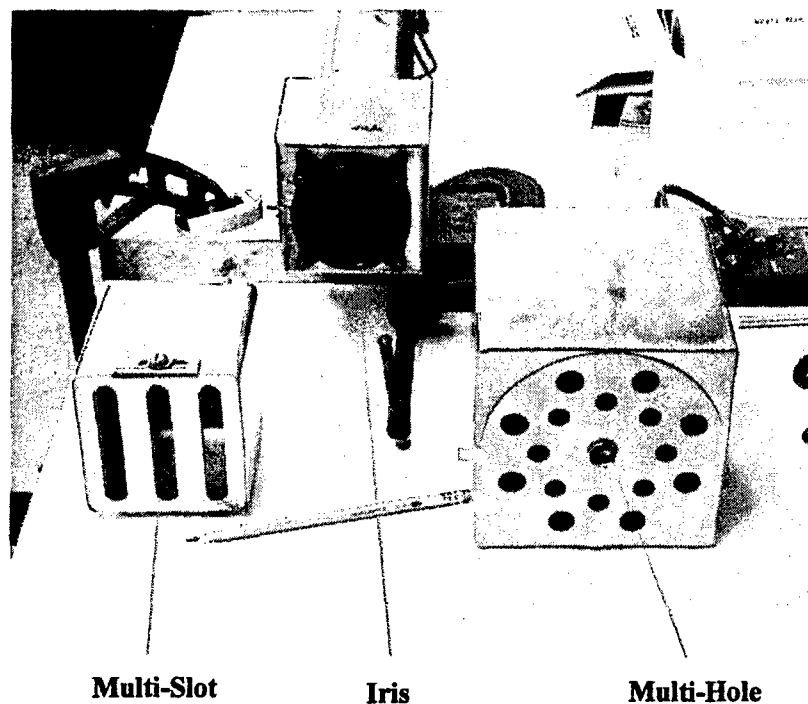


**Figure 11. Airflow Control Devices**

The latter two were evaluated in the stainless steel tunnel. Velocity profiles and turbulence intensity measurements were made for various opening settings for centerline velocities ranging from 1 to 10 m/s. These represented a nominal velocity range since the final test velocities had not been defined yet. Tests were conducted with and without the turbulence generators to investigate the effects of the devices on the tunnels internal flow. These data revealed unsatisfactory velocity profiles, especially in the critical region near the floor of the test section.

The resulting data also revealed that the repeatability of center line velocity with blower voltage (flowrate) and inlet opening was not accurate or repeatable enough to be solely relied on to monitor and adjust the tunnel velocity. The ability to correlate the test section centerline velocity with test section static pressure was also investigated. Because of the adjustable inlet area, the static pressure in the test section changed with inlet area opening. This approach was also found to be inadequate as a flow control means because of the extremely low static pressures resulting from the low velocities involved. Based on the results of these tests, the use of a dedicated, fixed position, hot wire anemometer that directly measured a reference velocity in the test section was determined to be the best approach.

The second Version I tunnel possessed the same layout, basic components and internal dimensions as the stainless steel tunnel, but was fabricated from flat, 5 mm thick sheets of Lexan® solvent welded together. As with the stainless steel tunnel, the different sections were slip fitted together without regard to sealing. Figure 12 shows the Lexan® tunnel with the associated airflow velocity measuring instrumentation. It contained the same components as the stainless steel version including the blower motor, flow straightening elements (Figure 13), turbulence generators (Figure 14), piston (Figure 15) and flow controller. Since the Lexan® tunnel was only used to investigate the velocity profiles in the test section it did not contain the vortex tabs in the mixing section.

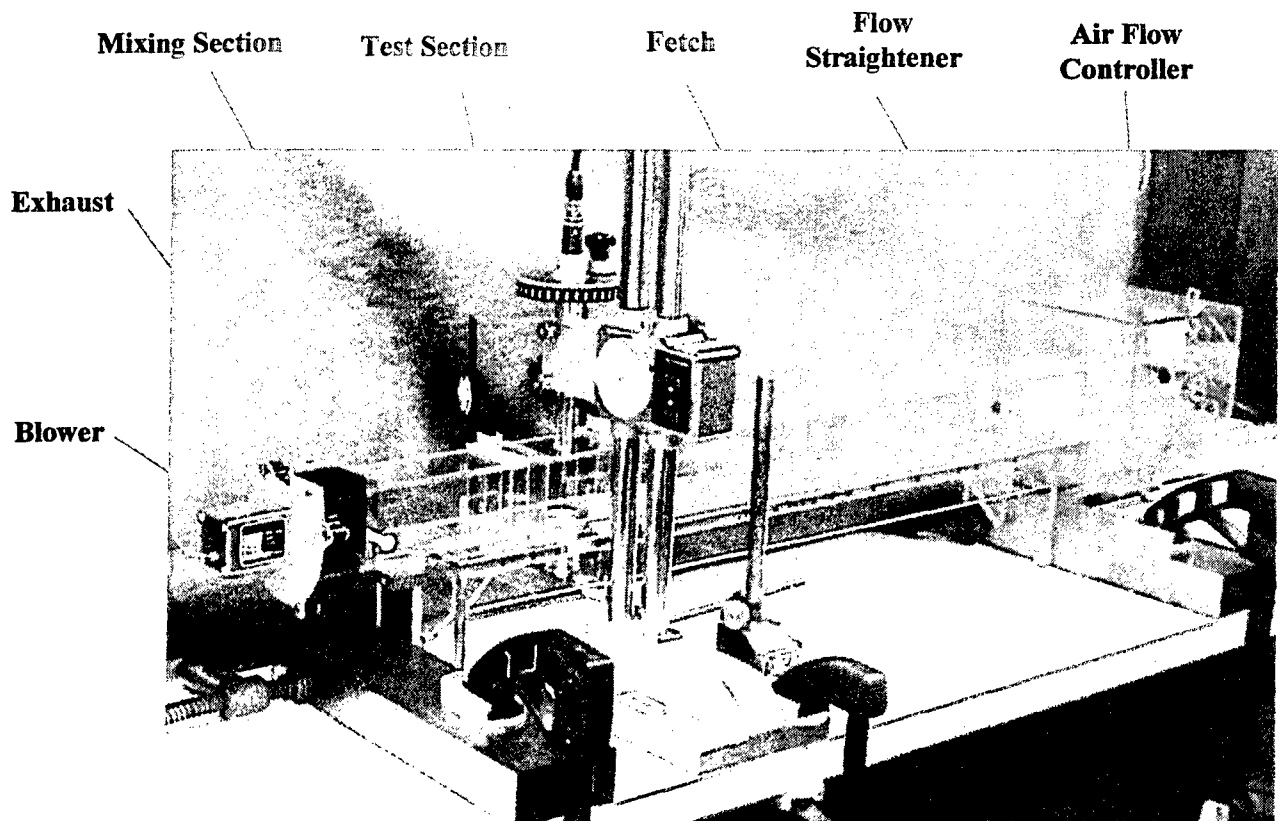
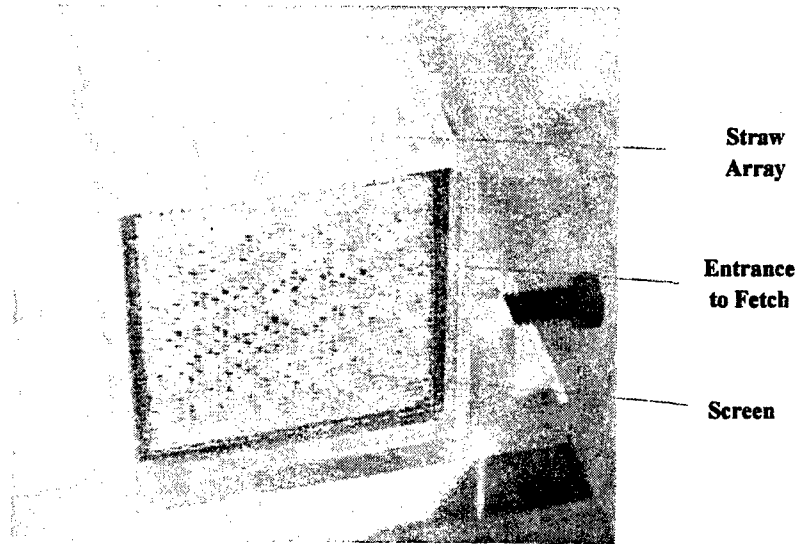
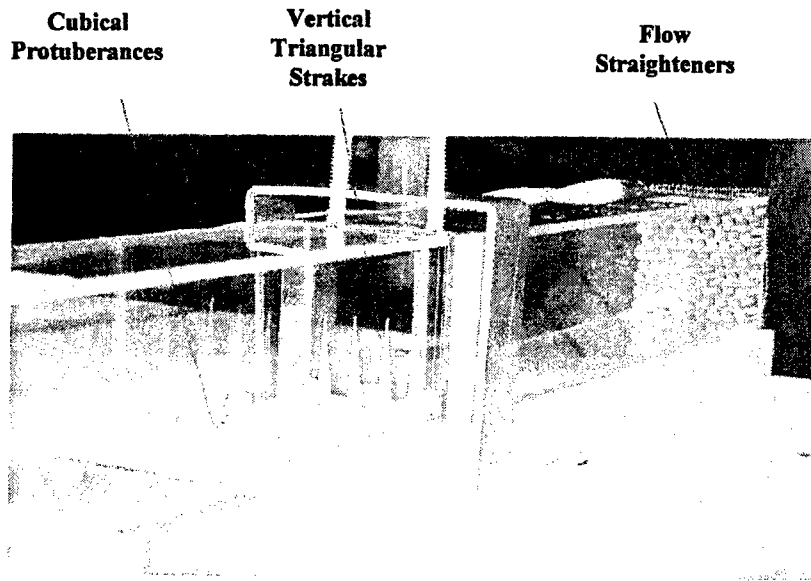


Figure 12. Lexan Version 1 (Test Bed) Tunnel





**Figure 13. Flow Straightening Elements**



**Figure 14. Velocity Profile Conditioning Elements**

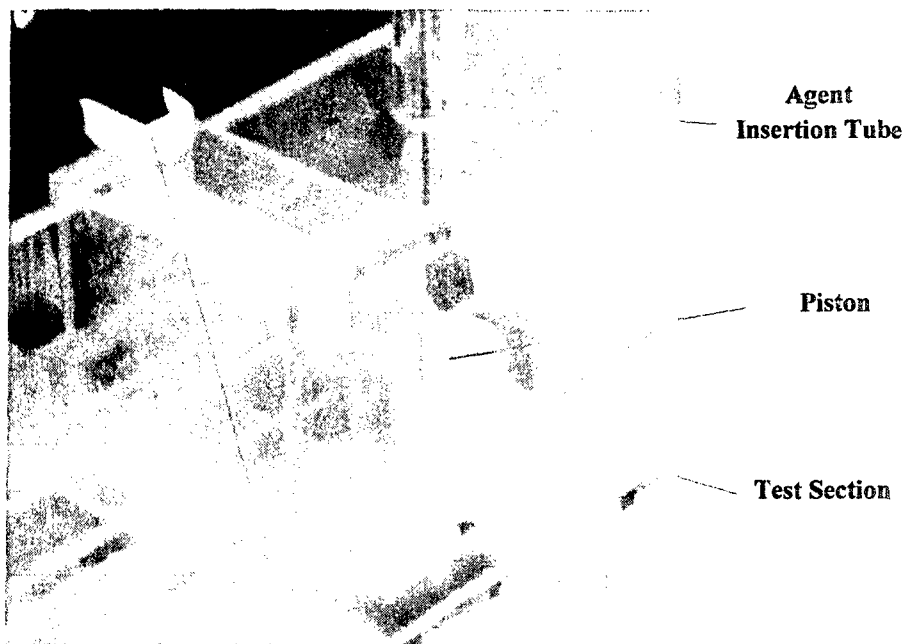


**Figure 15. Test Section Arrangement**

Smoke flow studies were also conducted with the Lexan® Version 1 tunnel to investigate the effect of motor speed in imparting any undesirable swirl associated flow asymmetries in the test section. This was found to not be the case. Experiments were then performed to correlate the center-line test section velocity with velocities near the droplet. While the specific velocity profiles for the Agent Fate studies had not yet been defined, these results showed that the velocity near the drop (approximately 1mm above the surface) could be adjusted in relation to the tunnel centerline velocity or another reference velocity in the test section. These tests also revealed that adding an extension duct to the blower exhaust resulted in a more stable flow field in the test section. This extension was found to be unnecessary in later versions of the tunnel when the sole airflow was solely provided by the Miller-Nelson ECU but was later resurrected as a sampling section.

At this point, neither specific airflow velocity values nor associated velocity profile shapes for the wind tunnel had been defined. A range of 1 m/s to 10 m/s was used for wind tunnel design guidelines. Using this range of velocities, a set of general velocity profiles was developed based on the “Law of the Wall” boundary layer theory. Profiles were evolved for a variety of friction velocities for smooth and rough surfaces and studies were performed in the Lexan Version 1 wind tunnel to establish a means of creating these profiles. Figure 16 shows the effect of the turbulence generators in creating the desired velocity profiles. Since the shear stress was a key element of these velocity profiles, measurement of the shear stress on the floor of the test section was considered as a means of comparing the flow fields between the different Agent Fate wind tunnels. This was not

possible using conventional methods due to the extremely low velocities involved, the associated low values of the resulting shear stress and space limitations.

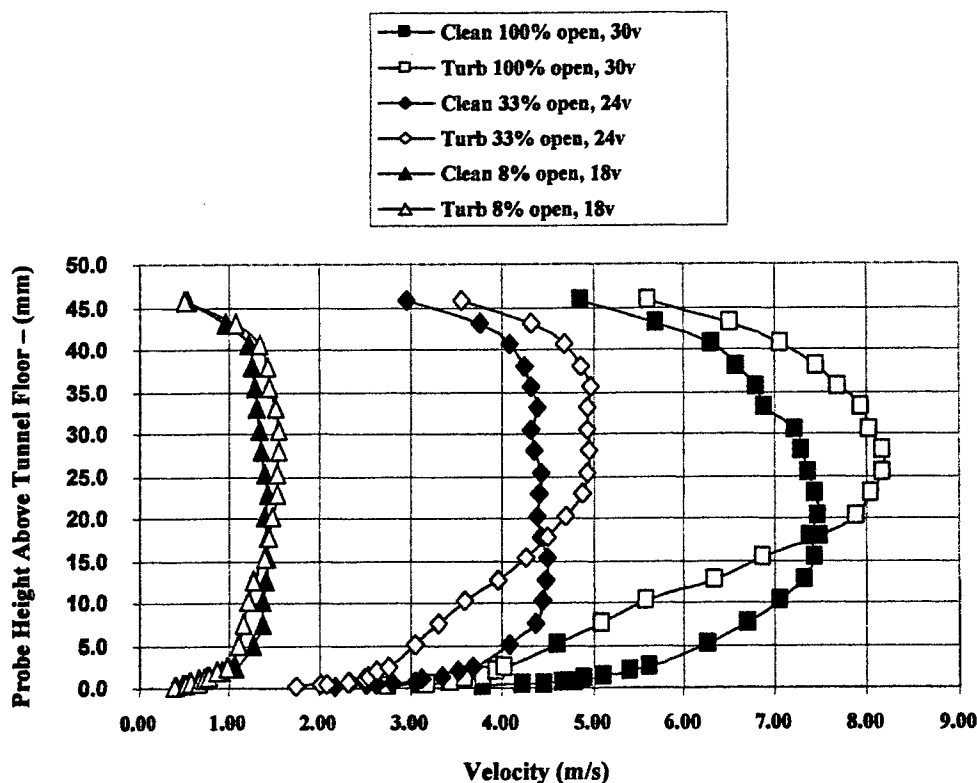


**Figure 16. Velocity Profiles Measured in Test Bed Tunnel With and Without Turbulence Generators**

Several approaches were evaluated to assure homogenous mixing of the agent vapor and air at the sampling port. One was a non-intrusive air mixer consisting of three 1.6 mm diameter tubes oriented normal to the wall around the perimeter of the mixing section. A relatively small amount of high velocity air introduced through these tubes acted to create a homogenous mixing of the agent vapor and air throughout the sampling section of tunnel. Smoke flow experiments in the Lexan Version 1 tunnel revealed that that the small diameter tubing resulted in excessive pressure drop preventing adequate flow. Also, the addition of external air mass into the tunnel would complicate measuring the agent mass balance, which was a critical requirement. Subsequently, the approach was deemed impractical and was not pursued further. Flow visualization experiments with the tunnel equipped with Chemineer, Inc., Kenics® HEV static mixers indicated that they did not produce complete homogeneous mixing by themselves. However, they had the potential to improve mixing when used in conjunction with other approaches.

The stainless steel, Version 1 tunnel was provided to the Agent Chemistry Team for use in evaluating agent vapor measuring instrumentation. The stainless steel configuration is shown in Figure 17. Tests with agent revealed that the leakage between components might influence

achieving the desired agent mass balance and indicated the need for better sealing throughout the tunnel structure. It was also shown that agent was deposited on the interior surface of the tunnel walls. This may have been sufficient to affect the ability to achieve a mass balance and it was recommended that all of the stainless steel components be treated with a protective coating process to prevent absorption of the agent.

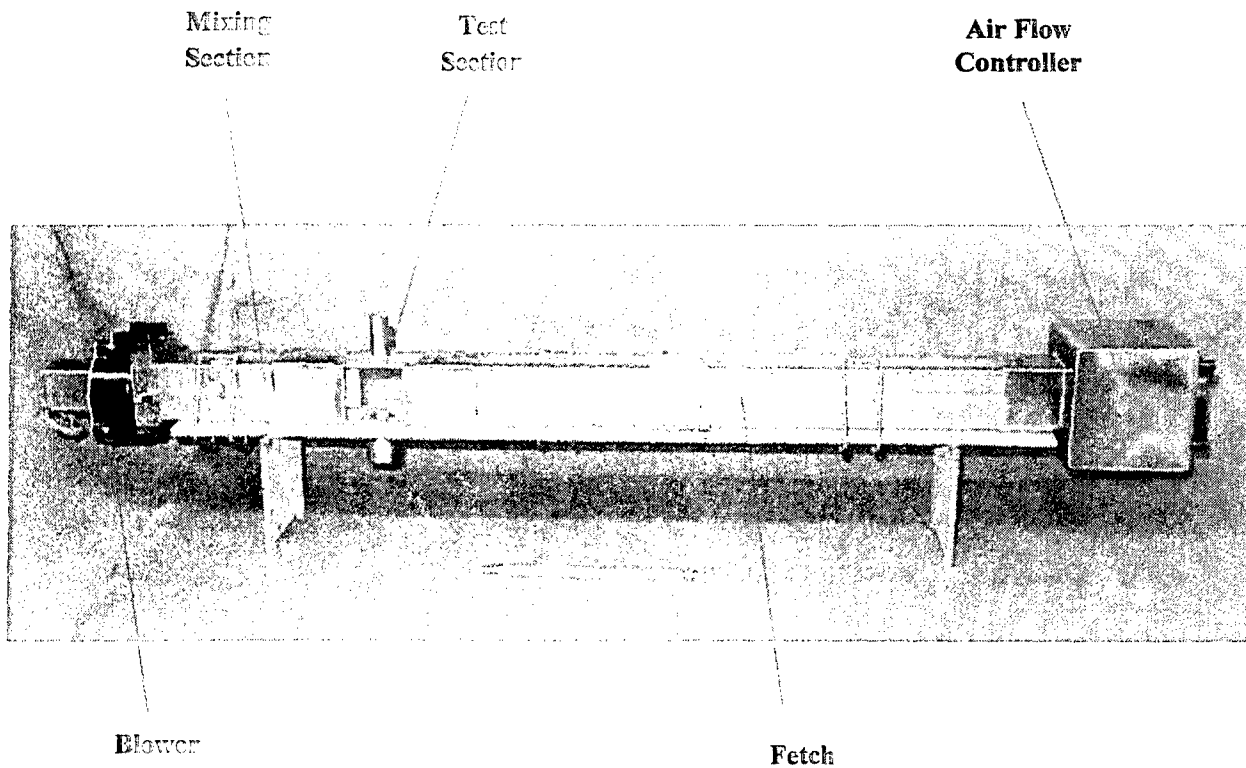


**Figure 17. Stainless Steel Version 1 (Test Bed) Tunnel**

As a side study, the 5-cm tunnel was modified to collect all of the agent/air mixture in a single port at the exit of the tunnel. In this case, the airflow had to be limited to the same 75 milliliters/min rate of the vapor analysis instrument. Concurrent Computer Fluid Dynamics (CFD) analysis indicated that this approach would only generate airflows for very low wind velocities. Although the wind tunnel test velocities had not yet been defined, it was felt that they would be too high for this approach to work and it was not pursued further. The Version 1 (Test Bed) wind tunnel modified to this configuration is shown in Figure 18.

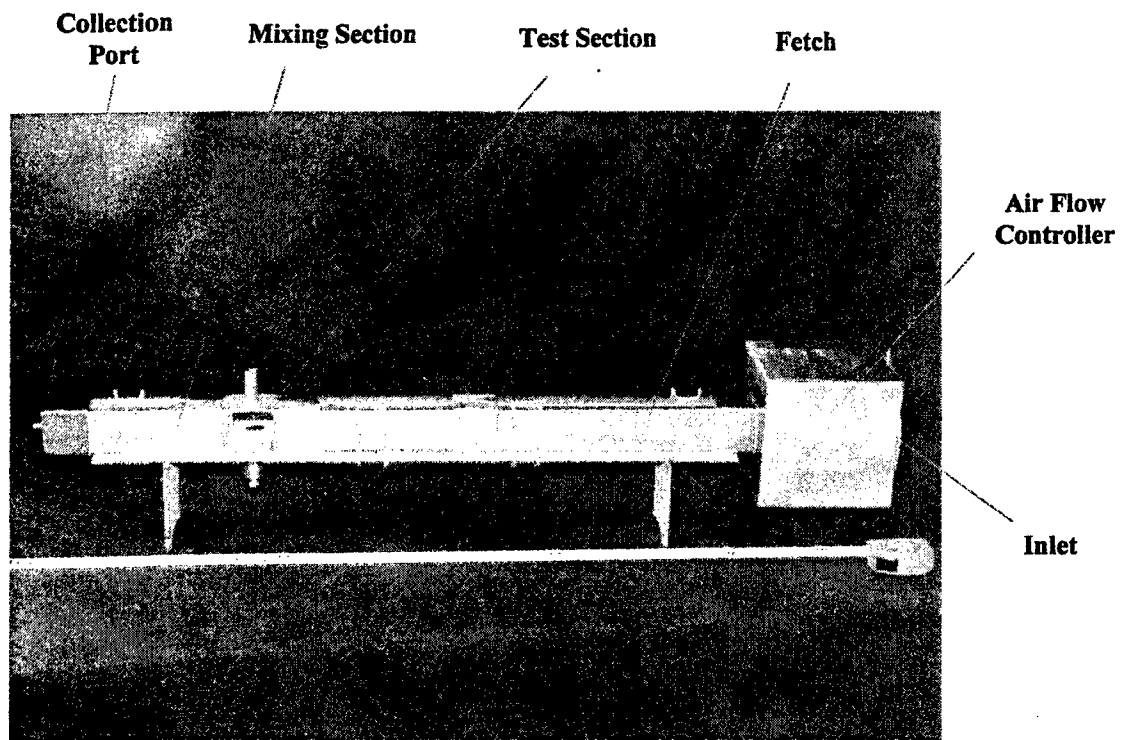


**Figure 18. Version 1 (Test Bed) Wind Tunnel Modified With Total Collection Port**

In summary, the Version 1 tunnel achieved several important accomplishments: blower location and flow asymmetry analysis; relative performance of various airflow controller designs; agent/substrate piston arrangement; ability to correlate velocity profile with a test section reference velocity, reference velocity limitations and requirements; evaluation of alternate mixing and vapor measuring approaches; and the requirement for better sealing and agent resistant coating.

#### **4.4 Version 2 (Prototype) Tunnel**

The findings from the aerodynamic and instrumentation studies with the Version 1, Test Bed Tunnel were incorporated into a Prototype tunnel configuration designated Version 2. This included more robust structural components; improved sealing; a modified test section design; an air environmental control unit; enhanced mixing elements; and the application of an agent resistant coating to the surfaces of selected components. A prime goal was to evolve a tunnel design that could be inexpensively produced in multiple units that would provide consistent experimental results. As before, two identical tunnels were fabricated: one for velocity characterization and one for agent instrumentation studies.

In March, 2004, the USAF and STI Corporation distributed a report<sup>5</sup> detailing the various parameters related to agent fate phenomena. The results of this study were used by the Agent

Fate model developers to further define the experimental test matrix for the agent fate laboratory wind tunnel experiments. This allowed specific design features for the Version 2, Prototype Tunnel to be selected.<sup>6,7</sup>

The original Version 2 Wind Tunnel configuration used the same blower unit used in the Version 1 tunnel configuration downstream of the mixing section to pull ambient air into the fetch through a square inlet cone upstream of the fetch as shown in Figure 19.

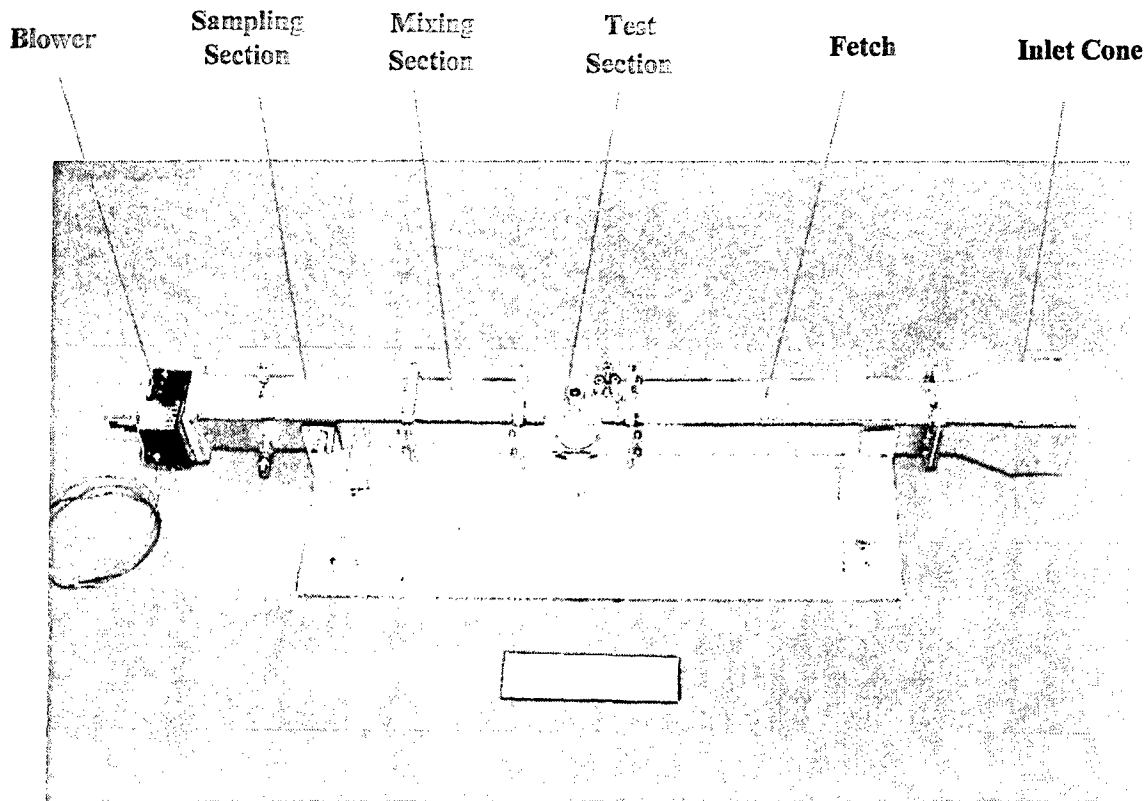


**Figure 19. Original Version 2 Wind Tunnel**

Early on, the inlet cone was replaced by a transition cone and turning vane section. This allowed the employment of the Miller-Nelson Environment Conditioning Unit (EVA) to provide the temperature and humidity controlled air to the wind tunnel. The transition cone provided a means of transitioning then airflow between the 1.2-cm diameter circular outlet of the Miller-Nelson EVA to the 5-cm square cross section of the wind tunnel fetch. Since the Miller-Nelson EVA had to be located outside of the fume hood and in front of the fume hood window, the flow from the Miller-Nelson EVA had to be turned 90° to enter the wind tunnel fetch; necessitating a turning vane section. This resulted in the “L” shaped layout shown in Figure 20.

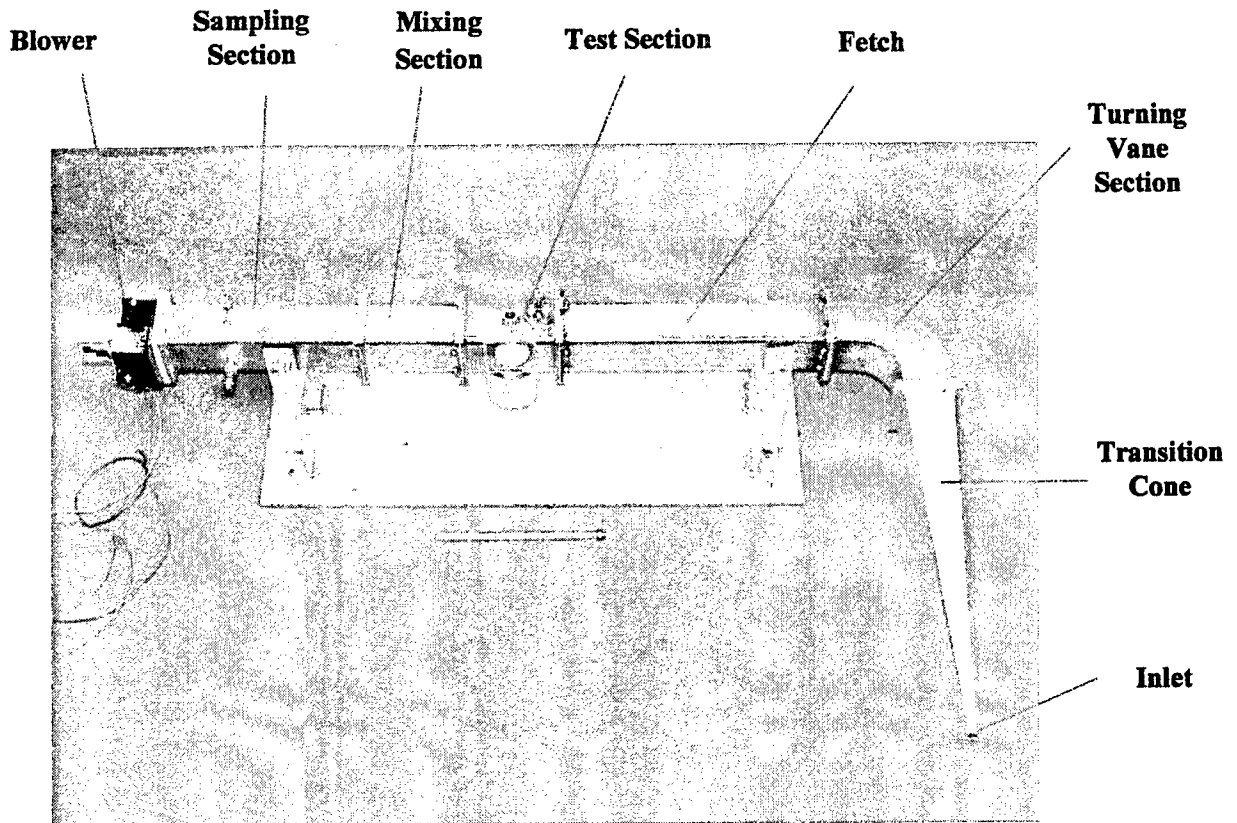


**Figure 20. Version 2 Tunnel with Transition Cone and Turning Vane Section**

The resulting Version 2 wind tunnel configuration was an open circuit arrangement with an "L" shaped layout. The overall arrangement and individual components are shown in Figure 21 and Figure 22 in a top and side view, respectively. The components consisted of a transition cone, turning vane section, fetch, test section, mixing section, sampling section and blower. The basic tunnel structure included a redesigned aluminum support structure resting on a flat aluminum base with the tunnel resting on two vertical rectangular yokes. As before, the tunnel had an overall width of 93.3 cm. Except for the transition cone, all tunnel components were fabricated from 4.85 cm internal dimension, square cross-section, stainless steel tubing.

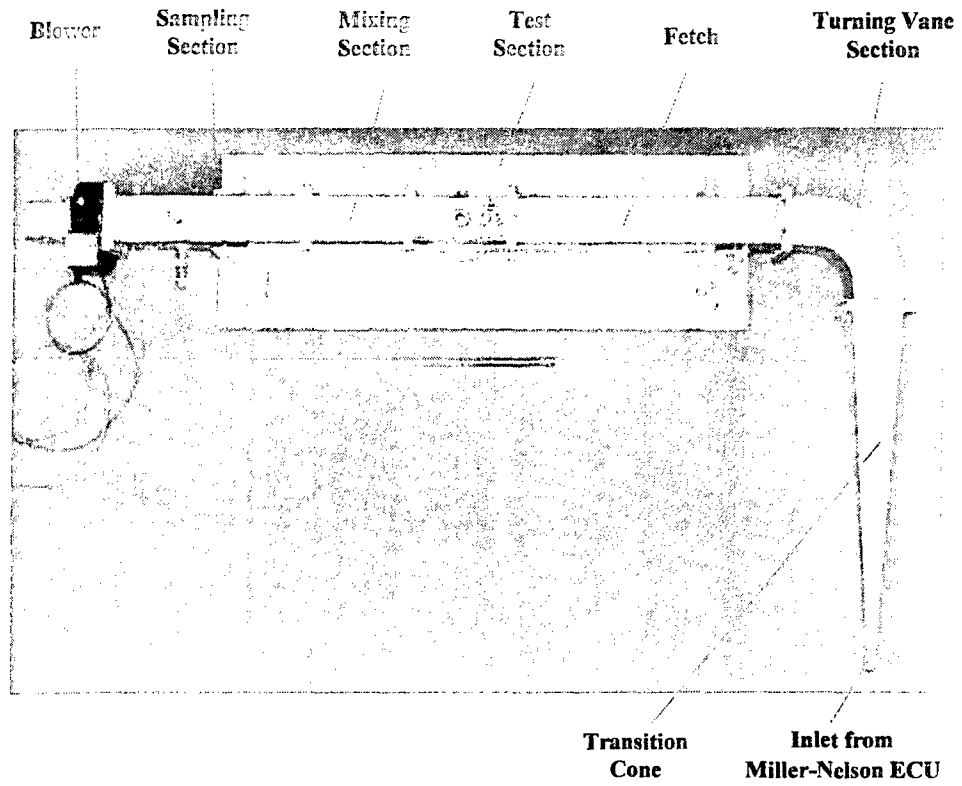


**Figure 21. Version 2 (Top View)**

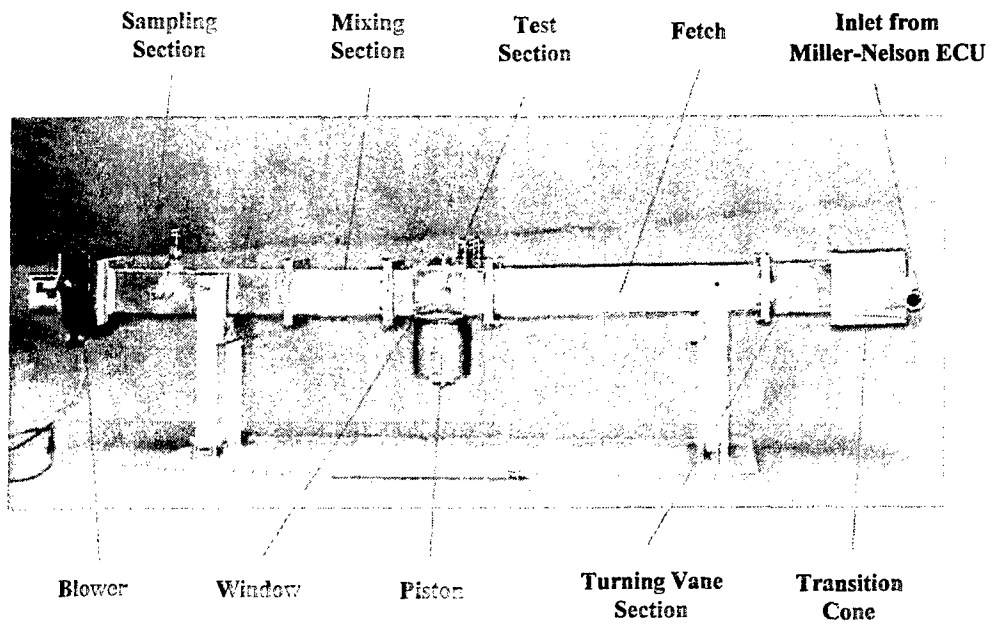


**Figure 22. Version 2 (Front View)**



After fabrication, each tunnel component was sent to the Restek Corporation where they were treated with a Silico-Steel® agent resistant coating. This was an electro-chemical process that acted to prevent the absorption of agent into the stainless steel surfaces. All of the stainless steel components included welded flanges that allowed them to be connected by screws with linear ethylene propylene rubber gaskets (fabricated from cut-up O-rings) in between.

A Miller-Nelson Environment Control Unit (ECU) was employed to provide controlled mass flow of temperature and RH conditioned air to the wind tunnel and was also used as the tunnel airflow source. The unit was located in front of the hood and directed its airflow at right angles to the wind tunnel as shown Figure 23.

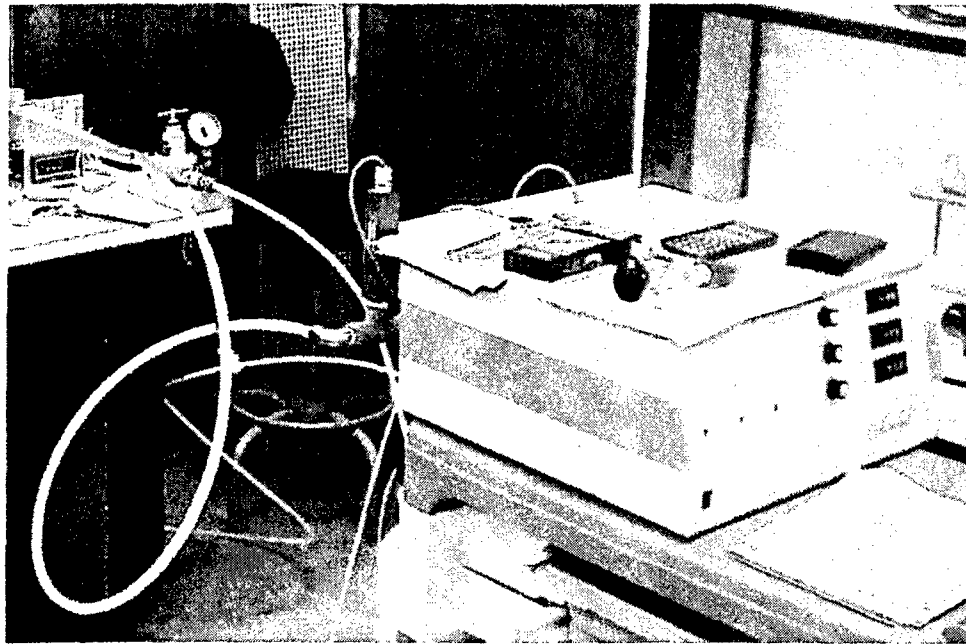


**Figure 23. Miller-Nelson ECU**

A transition cone connected the 1.2-cm diameter circular outlet of the unit to the 5-cm square inlet of the turning vane section. As shown in Figure 24, this component was made as a single piece by means of a "Rapid Prototyping" process. The item was composed of a hard plastic material with a nickel plating to provide a stronger structure as well as providing a smooth and heat resistant surface. The stainless steel turning vane section, Figure 25, contained three thin, stainless steel arc shaped "turning vanes" that directed the airflow from the Miller-Nelson through a 90° angle into the fetch. The addition of the transition cone and turning vane section gave the Version 2 tunnel its characteristic "L" shaped layout.

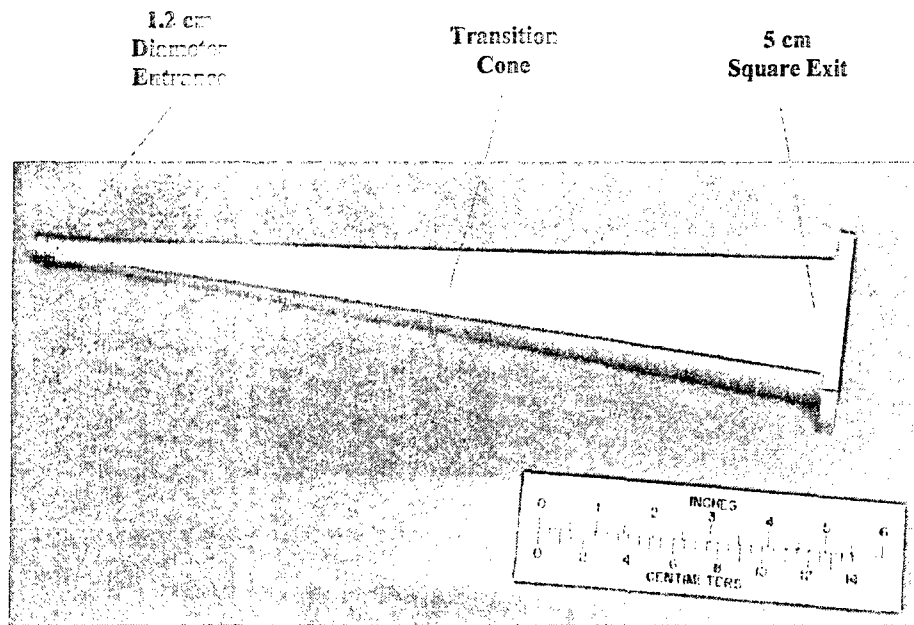


**Figure 24. Transition Cone**

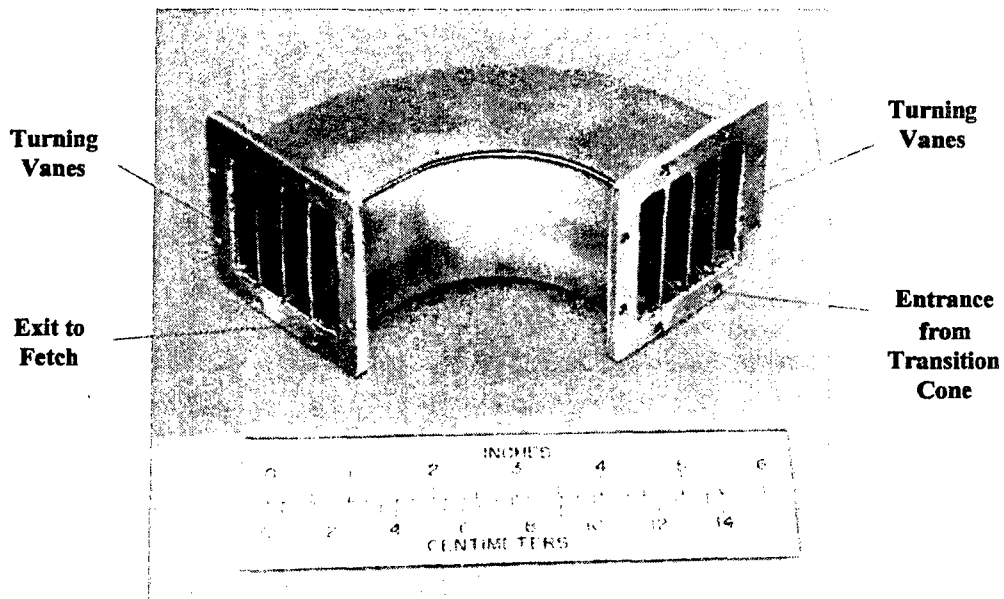


**Figure 25. Turning Vane Section**

The floor of the fetch contained the same array of 23 cubical blocks developed previously. These served as turbulence generators to form the desired velocity profile at the test section. As before, these were composed of Teflon cubes glued to a flat stainless steel strip, which was glued to the floor of the fetch. Figure 26 contains a photograph of the turbulence generator array with the dimensional details shown in Figure 27. The vertical triangular strakes were found to adversely affect the vertical velocity profiles near the center of the tunnel and did not contribute to the velocity profiles near the surface. Consequently, these were deleted as were the flow straighteners; the turning vanes providing the flow straightening function.

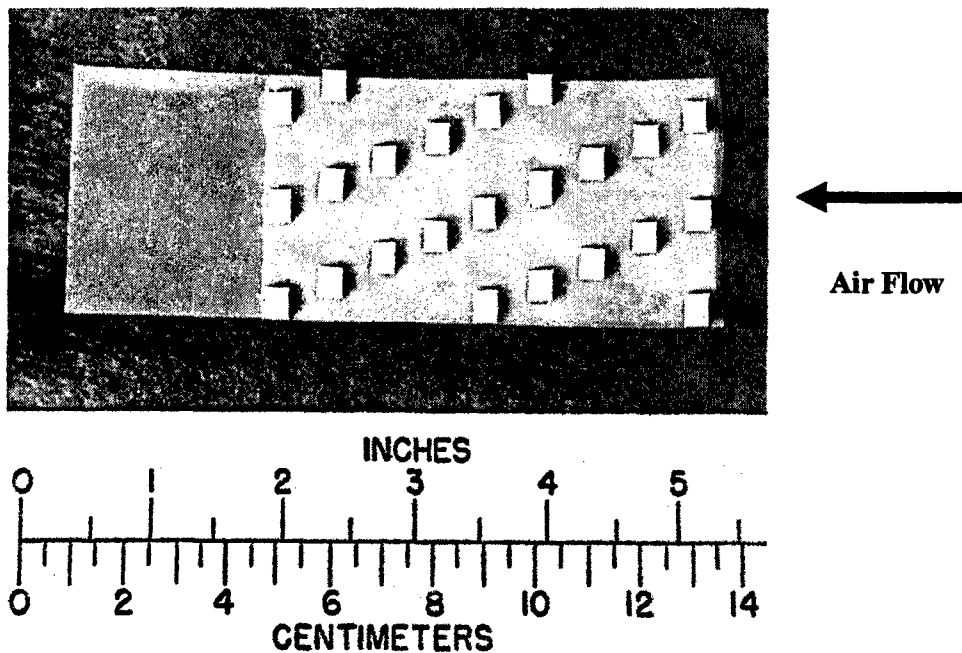


**Figure 26. Cubical Turbulence Generators**

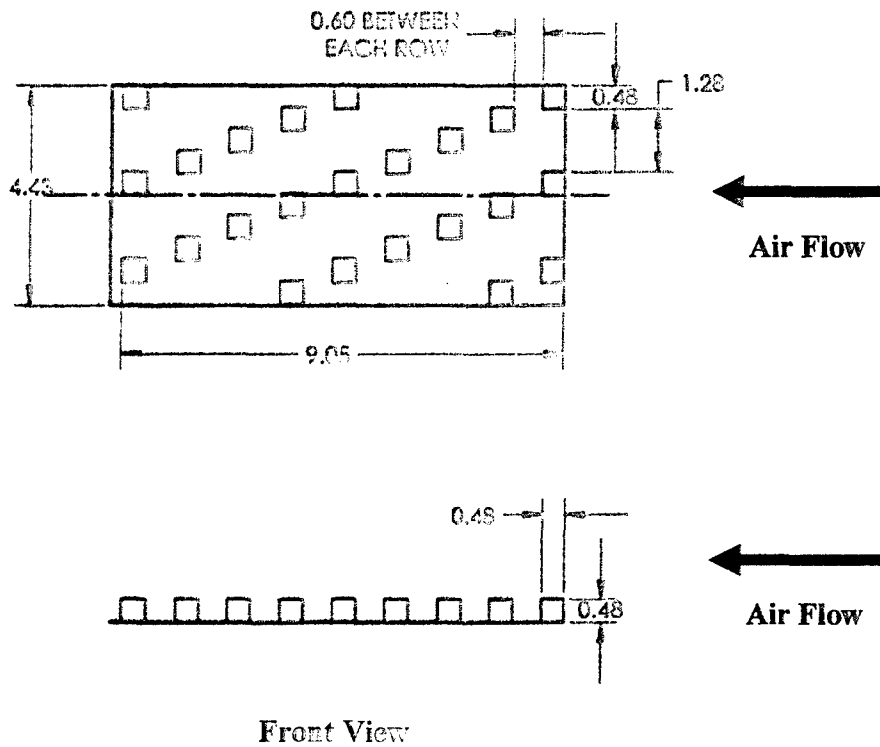


**Figure 27. Details of Cubical Turbulence Generators (Dimensions in Centimeters)**

The test section was fabricated from the same stainless steel tubing as the other tunnel components. In addition to an access tube immediately above the center of the piston, three instrumentation ports were added to the test section roof as depicted in Figure 28. The ports were welded to the test section and contained internal threads to facilitate insertion of different instrumentation devices. The test section contained a 4.5-cm square flat side window similar to that used in the Version 1 tunnel. A hollow, cylindrical, stainless steel piston receptacle projected downward from the test section floor. The outside surface of the piston receptacle was threaded to allow insertion of the piston assembly.

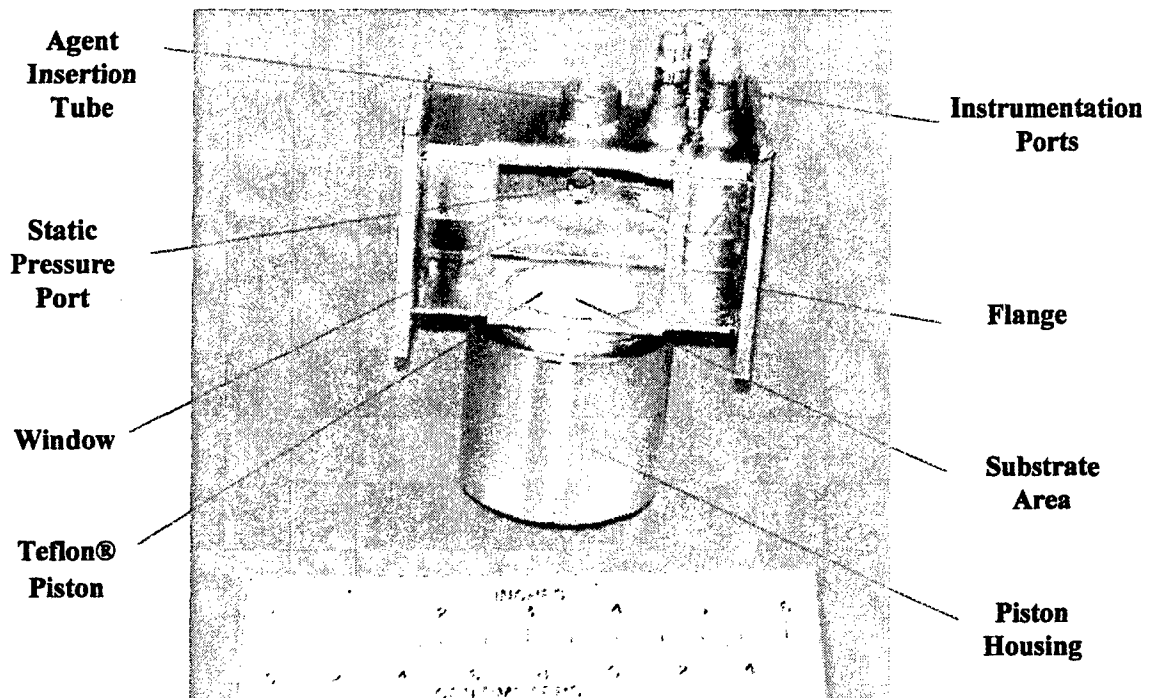


**Figure 28. Test Section**

The substrate being tested was placed in the test section by means of the piston assembly. The piston assembly was composed of a stainless steel piston housing containing a Teflon® piston. The top surface of the piston center section measured 3.8 cm in diameter and could contain either a circular or square cavity to hold the substrate sample. The outer surface of the piston housing was threaded so that it could be inserted into the piston receptacle. This placed the top surface of the substrate flush with and at the center of the test section floor. The previous flared piston design provided inadequate sealing between the piston and test section floor for agent work. Consequently, the Version 2 tunnel piston assembly included a rubber "O" ring to affect a seal between the piston assembly and the piston receptacle.

A 1.1 cm inside diameter, stainless steel tube was located in the test section ceiling immediately above the piston. This allowed insertion of the agent drop onto the top surface of the substrate being tested. Three other access holes were located in the ceiling for the hot wire anemometer probe. Two were located just upstream of and in line with the center of the piston and the other one was offset laterally. These, along with the center tube, allowed characterization of the vertical velocity profiles as well as providing a port for the reference velocity hotwire anemometer. The reference velocity was correlated to a specific vertical velocity profile over the piston. Subsequent testing revealed that the upstream location of the reference hotwire anemometer affected the velocity profile over the drop/substrate. Consequently, the reference hotwire anemometer was

relocated downstream of the center of the piston in following tunnel versions. A static pressure probe was also located in the side wall of the test section downstream of the piston.

A series of three stainless steel tabs, aligned in tandem and projecting outward from the interior surface of the mixing section walls acted as vortex generators to produce a constant concentration of agent and air. These were adapted from a Chemineer Corporation design and are shown in Figure 29. Two orthogonal sampling ports were originally located in the middle of the mixing section, as shown in Figure 30.

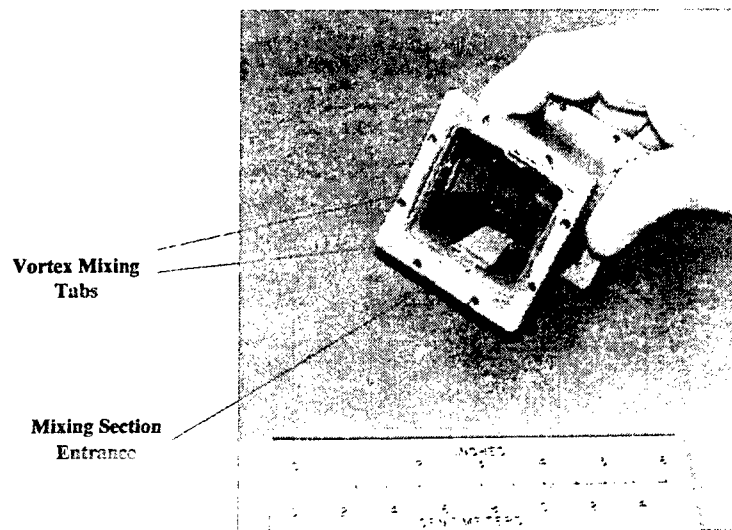


**Figure 29. Mixing Tabs**

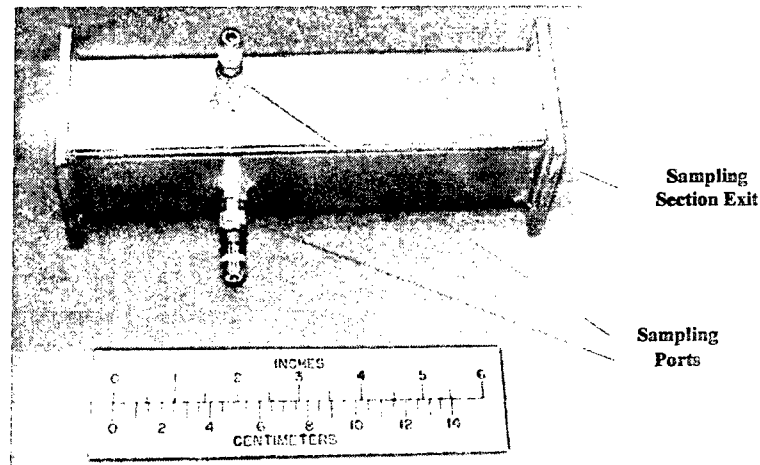


**Figure 30. Sampling Section**

An identical tunnel was provided to the Agent Chemistry Team for evaluation of various instrumentation devices and was designated the "Buckeye". Vapor concentration measurements were obtained by a Hapsite Thermal Desorption - Gas Chromatography - Mass Spectrometer (TD-GC-MS) illustrated in Figure 31. The Hapsite portable TD-GC-MS provided relatively rapid analysis of the vapor concentration as a function of time. While built for monitoring agent storage and depot areas, its ability to rapidly measure the agent concentration appeared to be ideal for the Agent Fate wind tunnel application. It was also small enough to be located by the fume hood and was available in sufficient numbers to support the anticipated Agent Fate experimental program. Subsequent tests showed that this arrangement did not result in sufficient mixing of the agent vapor/air and the sampling ports were relocated to the end of the exhaust section of the wind tunnel.



**Figure 31. Hapsite GC-MS**

As in the Version 1 tunnel, a blower, located downstream of mixing section created the tunnel's primary airflow (augmented by the Miller-Nelson ECU). The blower is shown in Figure 32. The combined effect of the upstream location of the Miller-Nelson ECU and the downstream location of the blower resulted in a slight positive static pressure in the test section.

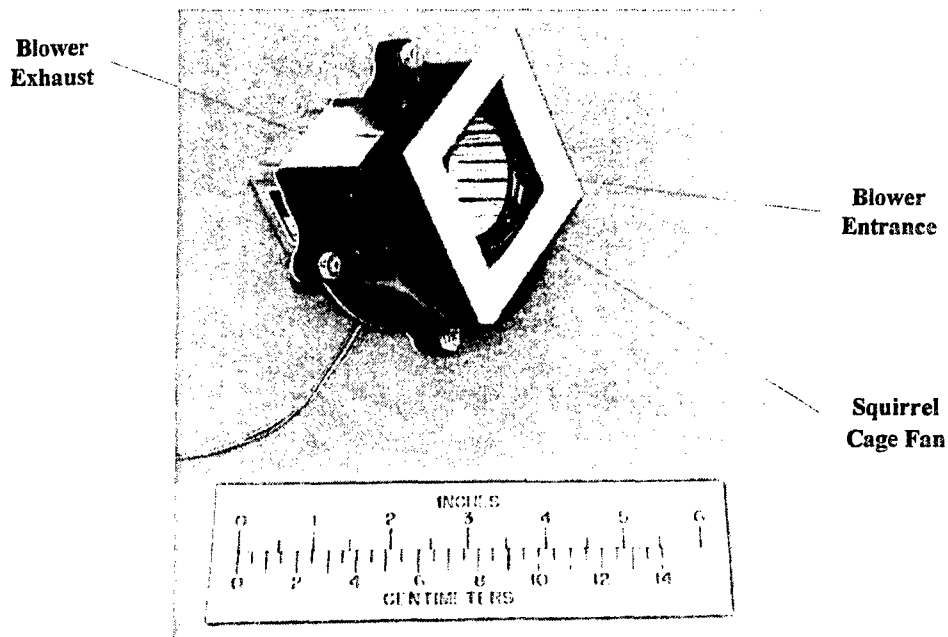


Figure 32. Blower

In May 2004, the Agent Fate model developers provided the vertical velocity profiles to be used in the wind tunnel testing program.<sup>8</sup> These profiles were based on atmospheric boundary layers for operational wind velocity conditions of 0.5, 3, and 6 m/s at a 2-m height above the ground and corresponded, respectively, to velocities of 0.22, 1.6, and 3.7 m/s at a height of 2 cm above the test section floor in the 5-cm wind tunnel. The new maximum velocity was about a third of the previous value and permitted all of the tunnel airflow to be provided by the Miller-Nelson ECU. This not only eliminated the need for the blower, but also greatly simplified the airflow control issue.

Although the blower was no longer required to provide the tunnel airflow, it was retained to improve the agent vapor/air mixing with the Miller-Nelson ECU being the sole source for the wind tunnel airflow. However, this arrangement presented a problem at the low velocity airflow condition. The low velocity required a flowrate of approximately 12 lpm, whereas the Miller-Nelson's mass flow controller would not operate below 50 lpm. To achieve the necessary low flowrate, a check valve and a secondary mass flow meter were installed between the Miller-Nelson and the wind tunnel inlet. The Miller-Nelson could be operated at a high flowrate (i.e., above 50 lpm) with the lower mass flow required for the low velocity being achieved by adjusting the check valve to direct a lower flowrate flow through the secondary mass flow meter and into the wind tunnel.

A series of tests were stipulated to validate the performance of the different Agent Fate wind tunnels. These tests involved testing various sized drops of HD agent on special TNO type glass representing a non-reactive and non-absorbent substrate. Three different glass sample diameters were required to support Agent Fate studies at the ECBC: 6mm (for the TGA Q600), 9mm



(for the TGA 2950) and 38mm (for the 5-cm tunnel). A considerable effort was put into developing a method to cut these samples from the limited amount of TNO glass provided. A water jet method was finally adapted by the ECBC Shop that could do this. The set-up is shown in Figure 33. This posed a problem because the glass had to be cut above a 0.75 m water tank into which the cut pieces would fall and it was difficult to recover the small glass samples after cutting. This was accomplished by gluing a Styrofoam backing to the original glass piece, which allowed the cut sample to float to the surface of the water bath.

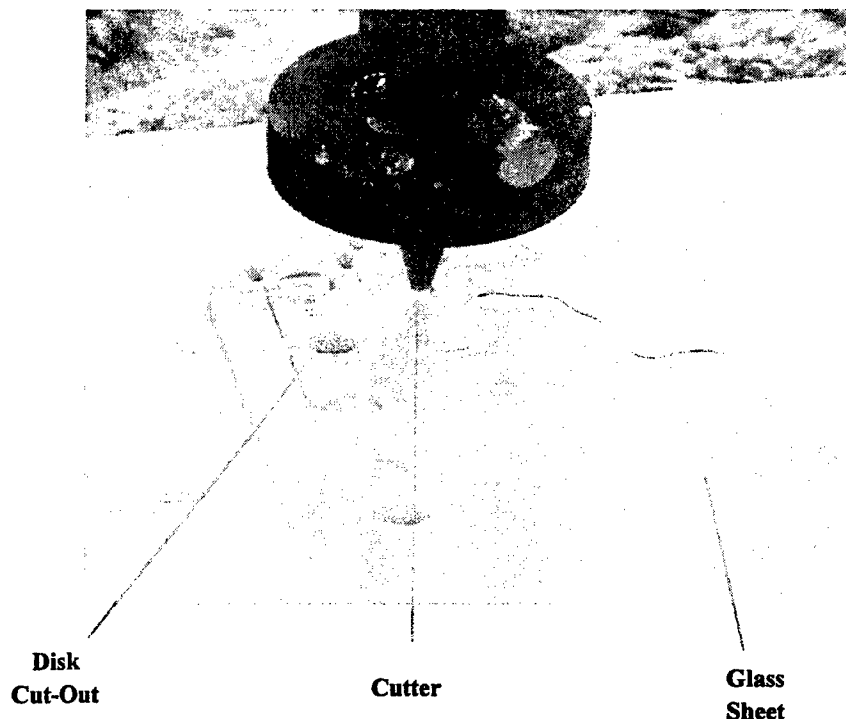


**Figure 33. TNO Glass Sample Cutting Set-Up**

Fabrication of the first Version 2 wind tunnel was completed in July 2004. It was initially used to demonstrate that the Miller-Nelson ECU could generate the airflow required for all three nominal tunnel test velocities. The flow rates required were about 400, 175, and 12 lpm for the 3.6, 1.7 and 0.22 m/s wind speeds, respectively. Vertical velocity profiles measured in tunnel test section demonstrated good agreement with the required profiles. This was followed by a series of tests demonstrating that the three nominal velocity profiles could be accurately and repeatably created by establishing a single reference velocity at a 2 cm height in the tunnel test section.

The Version 2 tunnel development provided several significant steps in the development of the 5-cm wind tunnel<sup>9, 10</sup> including: use of the Miller-Nelson ECU to provide the sole airflow source for wind tunnel; addition of transition cone and turning vane section for the Miller-Nelson ECU; ability to match specified vertical velocity profiles as provided by Agent Fate model developers; demonstration of the adequacy of a single reference velocity measurement in test

section to establish nominal velocity profiles; and the evolution of water jet method for cutting TNO glass into sample disks.

#### 4.5 Version 2 Mod 1 (Prototype Tunnel)

Feedback and additional requirements from agent testing in the Version 2 tunnel as well as changes to the test conditions desired by the model developers resulted in a series of modification to the Version 2 tunnel. Although many of these represented major changes, they all involved the basic Version 2 wind tunnel structure and components. In addition, these changes were incorporated in stages while agent testing in the Version 2 tunnel was in progress. Accordingly, the end result was a modified Version 2 tunnel and was designated Version 2 Mod 1. The final Version 2 Mod 1 configuration is shown in Figure 34 and was first installed in the chemical fume hood in August 2001.

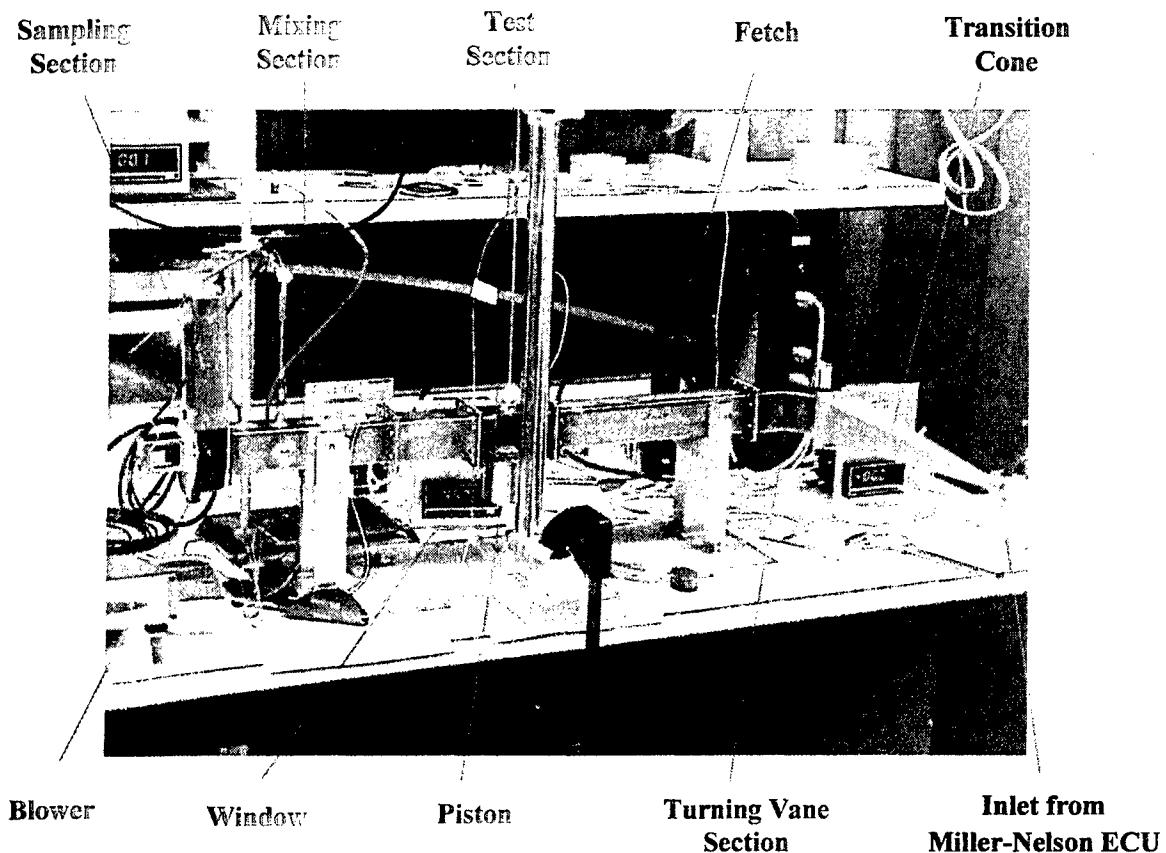
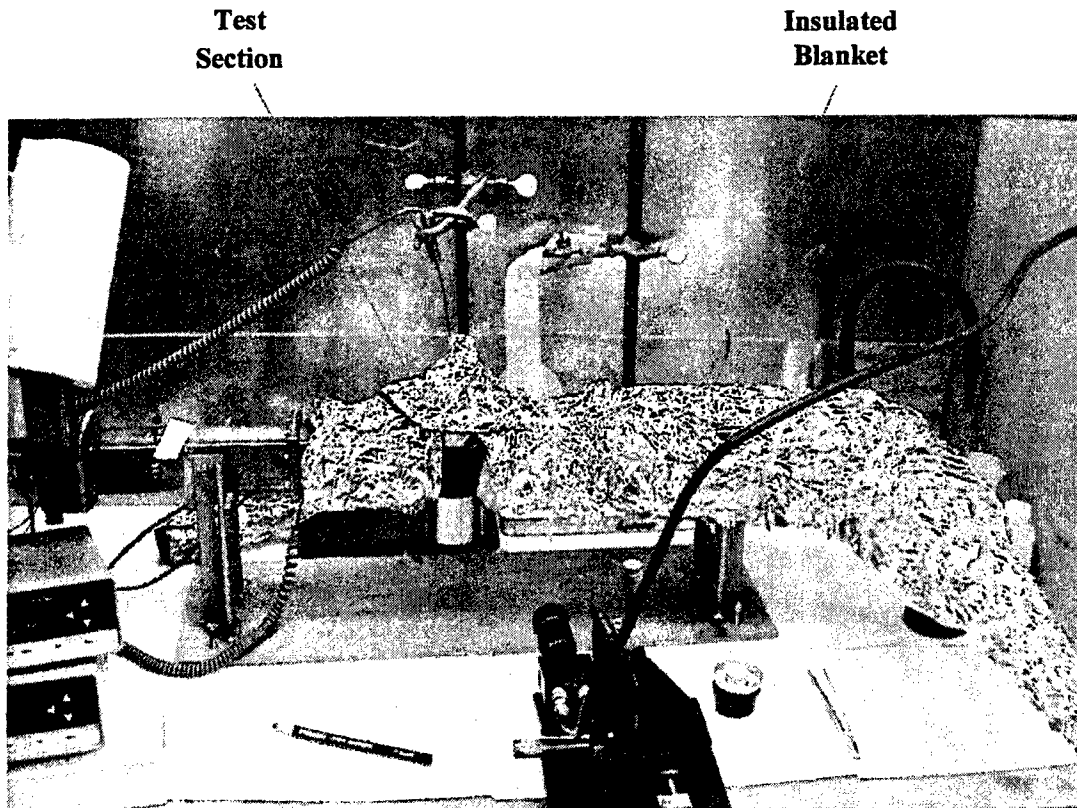


Figure 34. Version 2 Mod 1 Tunnel

A major change was the relocation of the sampling port. Smoke flow visualization experiments in the Lexan Version 1 tunnel with static tab type mixers located between the test section and the blower had indicated good mixing in a horizontal plane but poor mixing in vertical plane.

Further experiments showed that mixing in the blower exhaust section downstream of the operating blower produced good mixing across the entire area of the exhaust duct. Accordingly, the vapor sampling inlet was relocated from its original location upstream of the blower to the end of an extended length blower exhaust section (later designated as the sampling section). Agent vapor sampling was accomplished by inserting the GC-MS probe into the end of the exhaust section and locking it in place with a clamp. The vertically oriented exhaust section had a "D" shaped internal cross section to match the exit contour of the blower exit. The blower functioned purely as a mixer. Tests with the blower on and off had no effect on the vapor concentration measurement results; the air passing through the static blower squirrel cage producing a complete mixing effect. The addition of the vertical sampling section gave the tunnel it's distinctive, "Twisted S" layout.

Tests of HD on glass were conducted by members of the ECBC Agent Chemistry Team as part of the tunnel validation process.<sup>11</sup> Figure 35 depicts the Version 2 tunnel installed in the chemical fume hood. The tunnel was enclosed in a thermal insulation blanket to maintain constant temperature conditions throughout the tunnel structure.



**Figure 35. Version 2 Tunnel Installed in Chemical Fume Hood**

Samples of the agent vapor/air mixture were periodically drawn off at the sampler port and directed to the Hapsite TD-GC-MS. Typically, the Hapsite used 300 ml samples taken over a

3 min time span every 30 min. The total test depended on the agent/substrate being tested as well as the test conditions. Depending on the drop size, temperature and velocity, this could range from minutes to hours. The resulting data were stored in a computer system and reduced to a standard format. The data were initially presented as agent vapor concentration plotted versus time as illustrated in Figure 36. These data were then presented in terms of agent mass remaining from the drop/substrate as a function of time as shown in Figure 37.

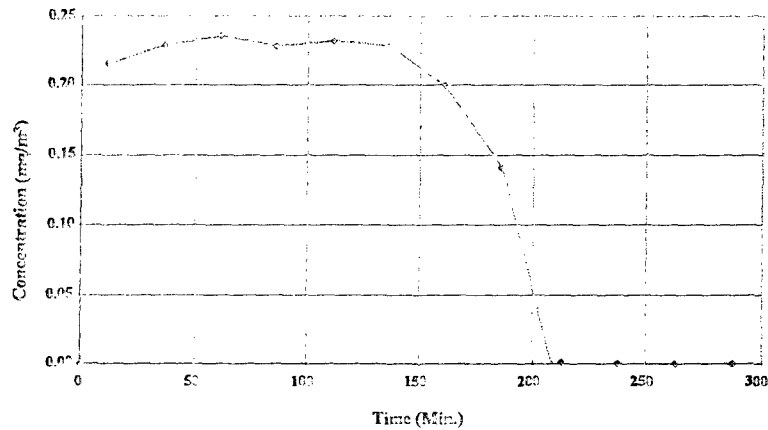


Figure 36. Typical Agent Vapor Concentration vs. Time<sup>11</sup>

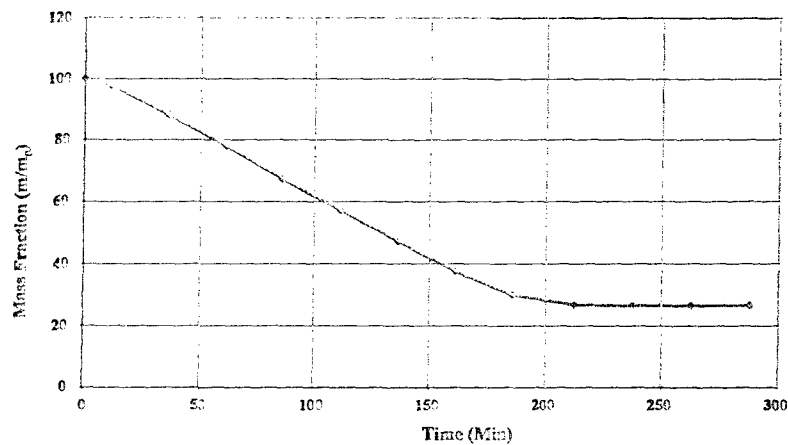


Figure 37. Typical Agent Mass Ratio vs. Time<sup>11</sup>

A measure of the successful operation of the wind tunnel and associated instrumentation system was to achieve a specified percent of agent mass recovery. For HD on glass (a non-absorbent, non-reactive substrate), the mass of HD recovered at the tunnel sampling port was to be between 95 and 105% of the original amount deposited. Achieving this agent mass recovery for HD/Glass was a self-imposed requirement for the Agent Fate wind tunnel validation tests. Once this capability had been demonstrated, agent vapor measurements could be used to determine the amount of agent absorbed and still remaining during later tests with other substrates.

Tunnel validation tests were initiated using 1  $\mu$ L drop of HD on glass at low velocity and mid-temperature in October 2004 and resulted in an 80 and 95% agent mass recovery. Video footage of the drop showed good agreement between the disappearance of the drop and the end of agent concentration readings. Agent concentration measured for a 1  $\mu$ L HD drop on glass using the Hapsite GC-MS and a separate Unity TD-GC with a Flame Photometric detector showed very similar agent concentration results. However, further testing produced erratic and inconsistent agent recovery rates ranging from 70 to 145%.

In January 2005, a Technical Assessment was performed by personnel of the ECBC 5-cm wind tunnel Working Group to identify the reason for the poor agent mass recoveries. The results of this analysis cited the following areas: tunnel leakage, inadequate instrumentation, inadequate mixing, malfunctioning instrumentation, agent deposit on interior surfaces, and hood environment flow effects. While general in nature, it was felt that these items covered the basic areas that could be causing the problem. A series of diagnostic tests were performed to verify whether these were in fact the source of the problem. It was hoped that by eliminating those items that were not the problem, the effort could focus on those areas remaining with a better chance of identifying and resolving the problem.

The tunnel was decontaminated, removed from the chemical hood and leak tested by sealing the intake and exit, pressuring the interior, totally immersing it in a water tank and observing air bubbles forming at leak points. Some leakage was noted, in particular around the blower element and the test section window. The leaks were sealed with epoxy and the tunnel was shown to be leak resistant up to an internal pressure of 13.8 kPa compared with a normal operating internal pressure of 0.5 kPa.

The length of the exhaust section was increased from 16 cm to 32 cm to enhance mixing with agent mass recovery values of 70, 75, 80, 83, and 76% being obtained. These tests were performed with a tunnel structure that had been leak checked and certified to be leak free. Two separate flow meters, one placed at the entrance to the tunnel and the other at the tunnel exit indicated identical flow rates further validating that the tunnel was leak-free. Additional tests with a 6  $\mu$ L drop of HD on Glass resulted in agent mass balances of 94, 51, 100, 102 and 75%. These findings further demonstrated that tunnel leakage was not the source of the agent recovery problem.

In addition to the temperature sensor in the test section, temperature sensors were placed in the sampling and exhaust sections of the tunnel.<sup>11</sup> These sensors revealed that a temperature controlled insulation blanket covering the entire tunnel was required to create and sustain a constant temperature throughout the tunnel. This had a profound effect on the evaporation rate measured; the resulting vapor concentration changing by two orders of magnitude bringing the 5-cm tunnel results

closer to the TGA data. It was also found that the built-in airflow controller of the Miller-Nelson ECU was incapable of providing an accurate and repeatable airflow into the tunnel. A separate Aalborg, air mass flow control unit was placed between the Miller-Nelson and the inlet to the transition cone. Once set, this automatically produced a constant airflow of temperature and humidity conditioned air into the tunnel. However, the agent mass recovery values still ranged from 93 to 145%. An Accuracy and Precision (A&P) test was performed on the Hapsite, which indicated an accuracy of about  $\pm 4\%$  and demonstrated that the Hapsite was not malfunctioning.

A Hydrogen Flame Emission Detector (HYFED) instrument was used to survey the "real-time" agent vapor concentration profiles throughout internal length and width of the tunnel exhaust section while the tunnel was operating. These data showed that the agent vapor/air concentration was homogeneous, especially for the higher velocities, indicating that inadequate mixing was not the cause of the poor mass balance. Agent mass balances consistently larger than 100% as well as post test analysis of the tunnel internal surfaces indicated that agent deposition on the interior of the tunnel was also not the cause of the problem. Finally, the addition of a shroud over the exit area of the tunnel that eliminated any airflow effects created by the hood exhaust system did not affect the mass balance thereby indicting that the hood environment was not the problem. This latter finding reduced the source of the mass recovery problem to inadequate instrumentation, which included sensors and vapor measuring devices.

The results of the diagnostic testing to confirm the root cause of the agent mass balance problem eliminated tunnel leakage, inadequate mixing, malfunctioning instrumentation, agent deposit on interior surfaces, and hood environment flow effects. This left inadequate instrumentation as the most likely source of the mass balance problem. While still representing a general area for the root cause, this finding effectively eliminated other areas that were not the cause and allowed the effort to be focused on the actual problem area. In the event, the mass balance problem was not fully resolved until the Hapsite was replaced by the Variable Tube Sampler<sup>11</sup> evolved in conjunction with the Version 3 tunnel discussed in the following section.

In summary, the Version 2 Mod.1 tunnel configuration achieved a number of significant accomplishments: zero leakage throughout the wind tunnel; automated flow control/meter at tunnel entrance; insulated and temperature controlled blankets over the entire tunnel structure; location of the sampling inlet to the exhaust section and use of the blower solely for mixing.

The Version 2 Mod 1 tunnel had an overall width of 93.2 cm and an overall height of 56.7 cm. The depth of the tunnel measured 55 cm including the transition cone, a portion of which projected beyond the front of the hood. Although the desired vapor recovery rate was not consistently being achieved, a sufficient number of modifications had been identified to warrant a new version of the tunnel for use in the production testing phase of the program.

#### **4.6 Version 3 (Production Tunnel)**

The lessons learned from the Version 2 Mod. 1 tunnel were incorporated into a tunnel configuration intended for multiple duplication to support large scale testing operations and was designated as the Version 3 (Production Tunnel). The previously separate mixing and sampling

sections located between the test section and blower were combined into a single section with the mixing vortex tabs removed. While it neither served a mixing nor sampling function, it was still referred to as the mixing section.

The Version 3 wind tunnel configuration, shown in Figure 38, was similar to the Version 2 Mod 1 tunnel retaining the same open circuit arrangement with a "Twisted S" shape layout. Figures 39 and 40 show schematics of the Version 3 tunnel denoting its major components, which consisted of a transition cone, turning vane section, fetch, test section, mixing section, static mixer and sampling section. The major changes included replacement of the blower with a static mixer and modifications to the test section. The previous aluminum support frame was retained. The Version 3 tunnel had an overall width of 93.2 cm, an overall height of 56.7 cm. and an overall depth of 55 cm. Figure 41 shows a cut-away view revealing the internal elements in the turning vane section, fetch, test section and exhaust section.

As before, except for the nickel coated, plastic transition cone, all tunnel components were fabricated from stainless steel. The fetch, mixing section and exhaust section were made from 4.85-cm internal dimension, square cross-section, stainless steel tubing. The static mixer and test section were made from stainless steel sheet and plate, respectively. The stainless steel components included welded flanges allowing them to be connected by screws with chemical resistant gasket material in between. The gaskets were fabricated from Kalrez, a rubber-like material that had superior agent resistant properties compared to the silicone rubber gaskets used in the Version 2 tunnel. The stiffer Kalrez® also provided better sealing than the more compliant, silicon rubber.

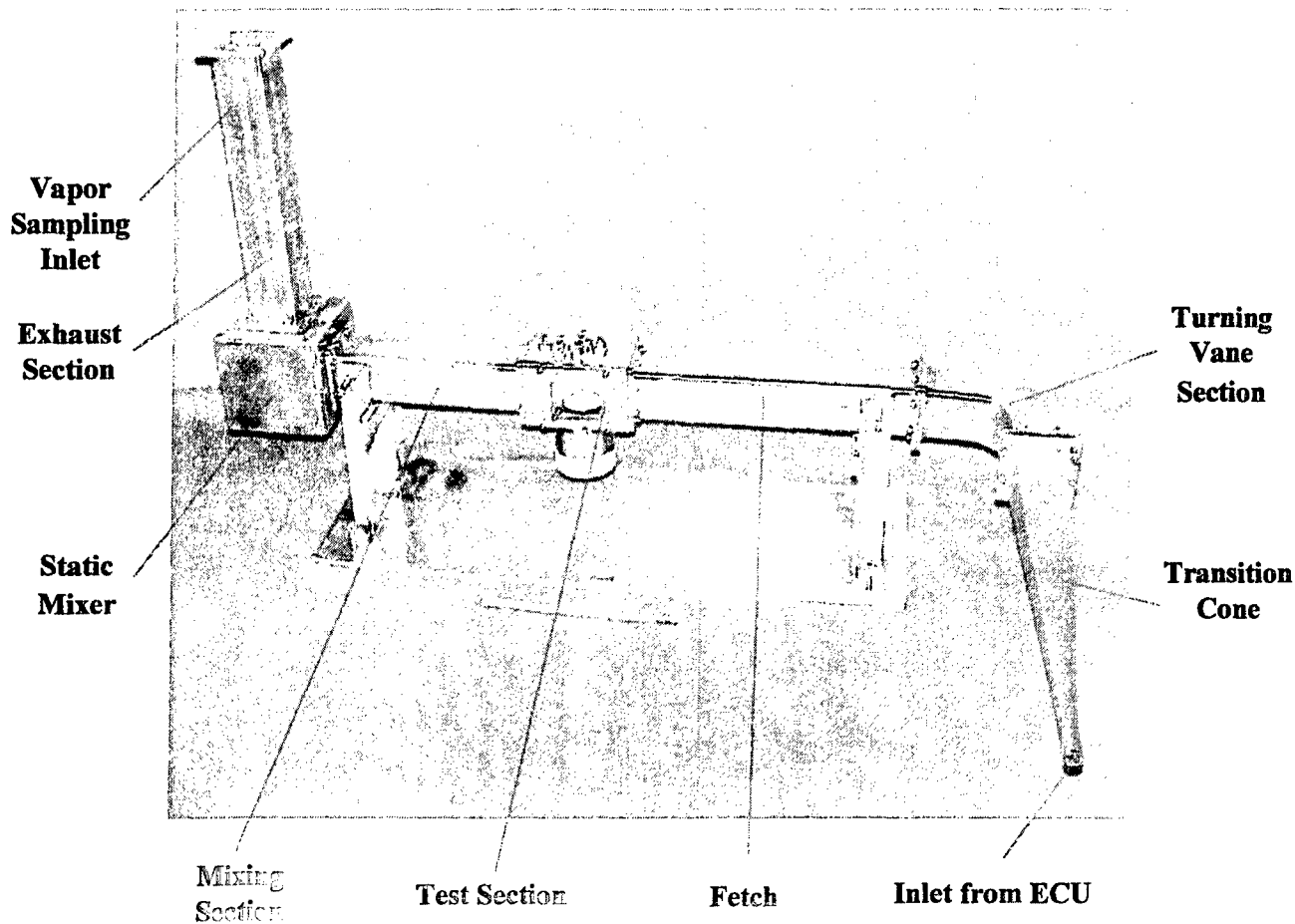


**Figure 38. Version 3 (Production) Wind Tunnel**



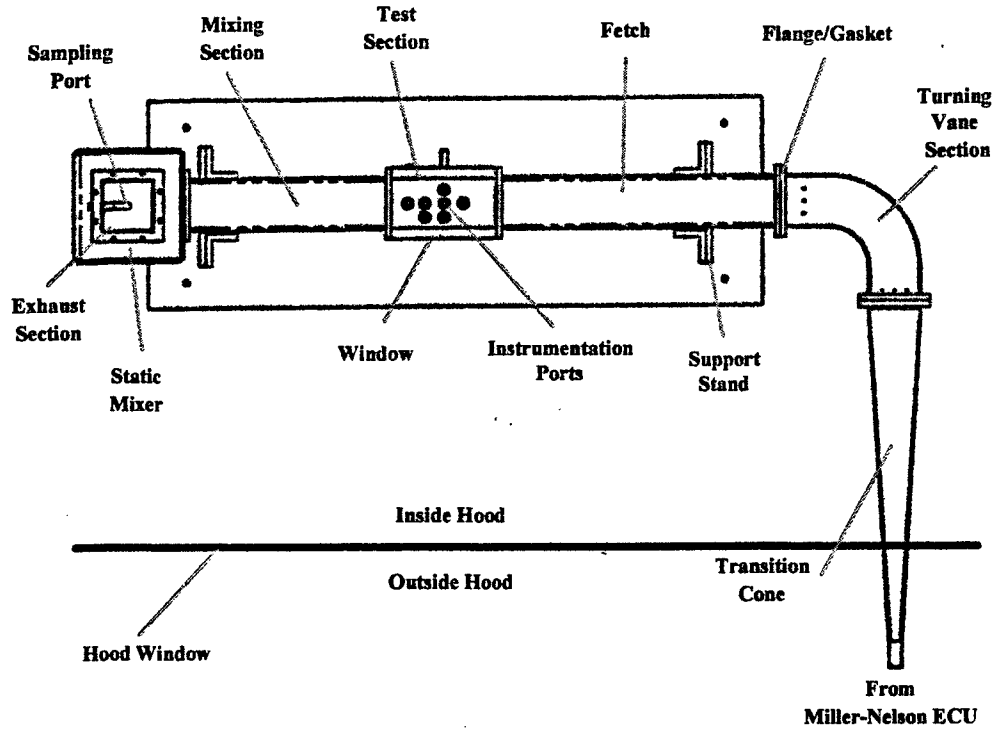


Figure 39. Version 3 (Production) Tunnel Schematic (Top View)

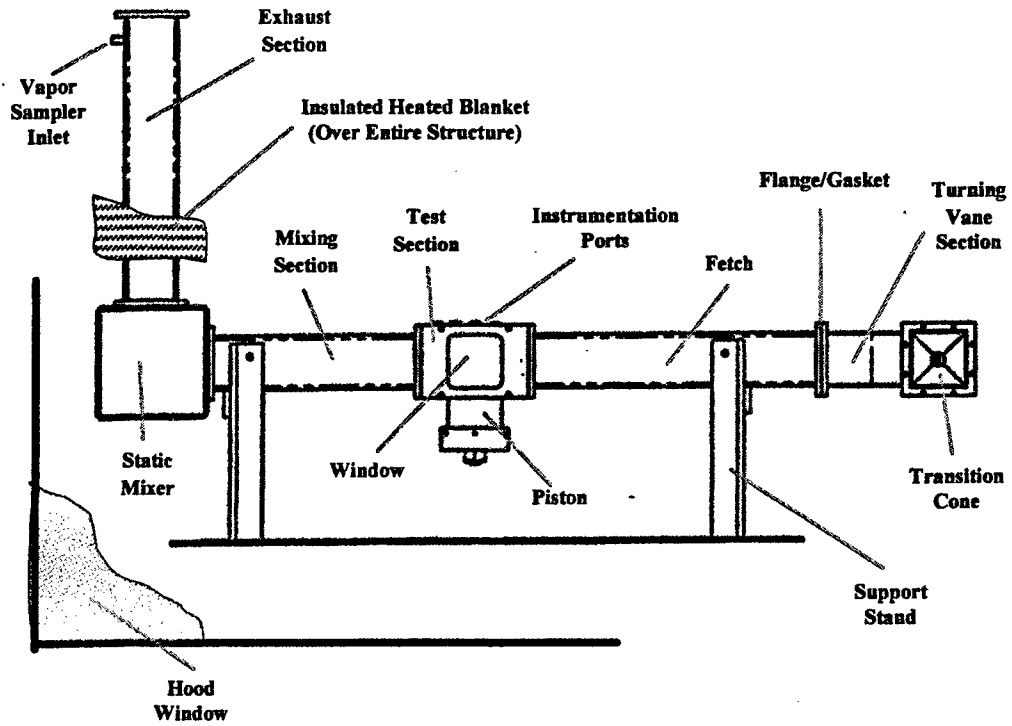
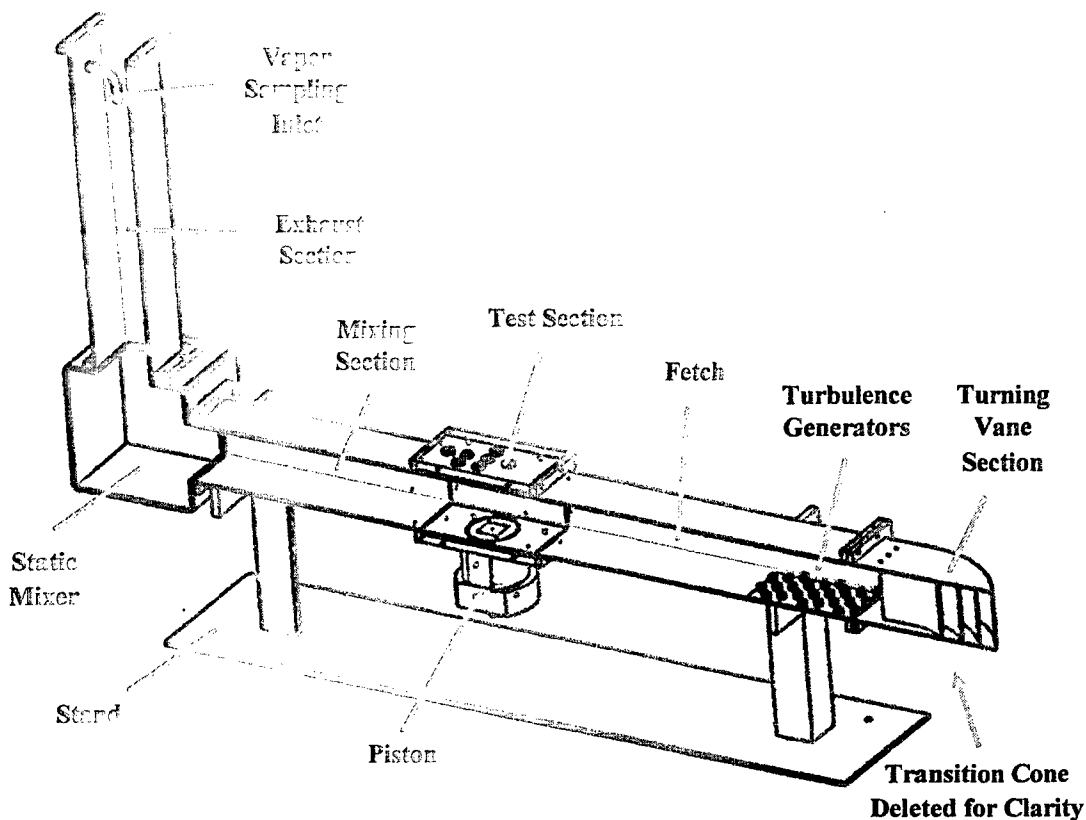


Figure 40. Version 3 (Production) Tunnel Schematic (Front View)



**Figure 41. Cut-Away View Showing Internal Elements**

The Miller-Nelson ECU provided the tunnel airflow at a prescribed temperature and RH. The Miller-Nelson was located in front of the hood and directed its airflow at into the transition cone. The previous array of 23 cubical turbulence generators was retained in the fetch to produce the desired test section velocity profiles.

The test section, shown in Figure 42, was fabricated from separate machined stainless steel plates that were screwed together with linear pieces of Ethylene Propylene (i.e., cut-up o-rings) located in machined grooves as seals. The wall thickness was increased from the previous 4.5 mm to 10.7 mm to eliminate the need for welding the instrumentation ports to the test section walls, which had a tendency to warp the walls in the Version 1 and 2 tunnels. The thicker test section walls allowed the instrumentation holes to be drilled and tapped for better attachment of the instrumentation fittings. The test section ceiling contained a total of seven instrument ports. These included an array of five attachments for the hot wire anemometer probe: a central location, an upstream and a downstream location, and a left and a right lateral location. All five positions were used for the velocity characterization surveys. The port location downstream of the center position was used for the reference velocity probe during the agent fate experiments. The test section temperature was monitored through the port located most downstream from the center port position. The static pressure port located in the center of the rear wall of the test section was retained. In

addition, a temperature/humidity sensor was located in the side wall of the test section downstream of the piston. The front wall of the test section contained a 4.5-cm square flat side window. The bottom of the window extended beyond the edge of the test section floor. This allowed an unobstructed view of the base of the sessile drop on the surface of the substrate.

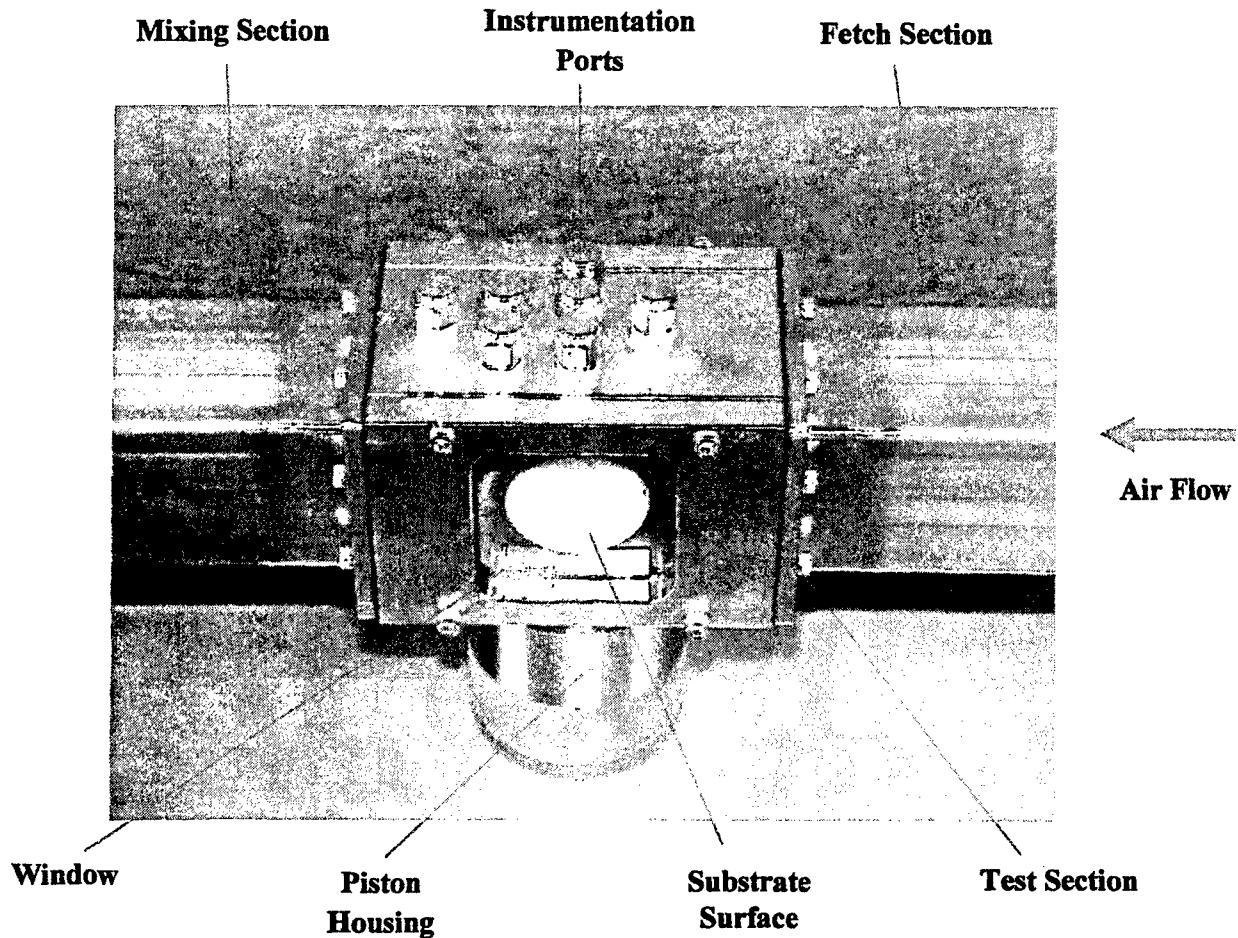


**Figure 42. Test Section**

As in the Version 2 tunnel, the same cylindrical piston, composed of a Teflon center section and a stainless steel outer body, was located in the center of the test section floor. As shown in Figure 43, the inner surface of the piston was threaded and could be screwed onto the piston receptacle projecting from the bottom of the test section floor. As before, a rubber o-ring was located in a circumferential slot on the outer surface of the piston as a seal between the piston and the piston receptacle. The top surface of the piston measured 3.8 cm in diameter and contained a shallow square cavity to hold the substrate sample. The substrate sample (whether a piece of glass, a tray of sand, or a section of concrete or asphalt) would be placed on the top surface of the piston. To accommodate different substrate thicknesses, the fine screw thread allowed the piston to be inserted to different depths so that the top surface of the substrate was flush with the floor of the test section. A knurled finish was added to the lower portion of the piston's outer surface to facilitate this adjustment.

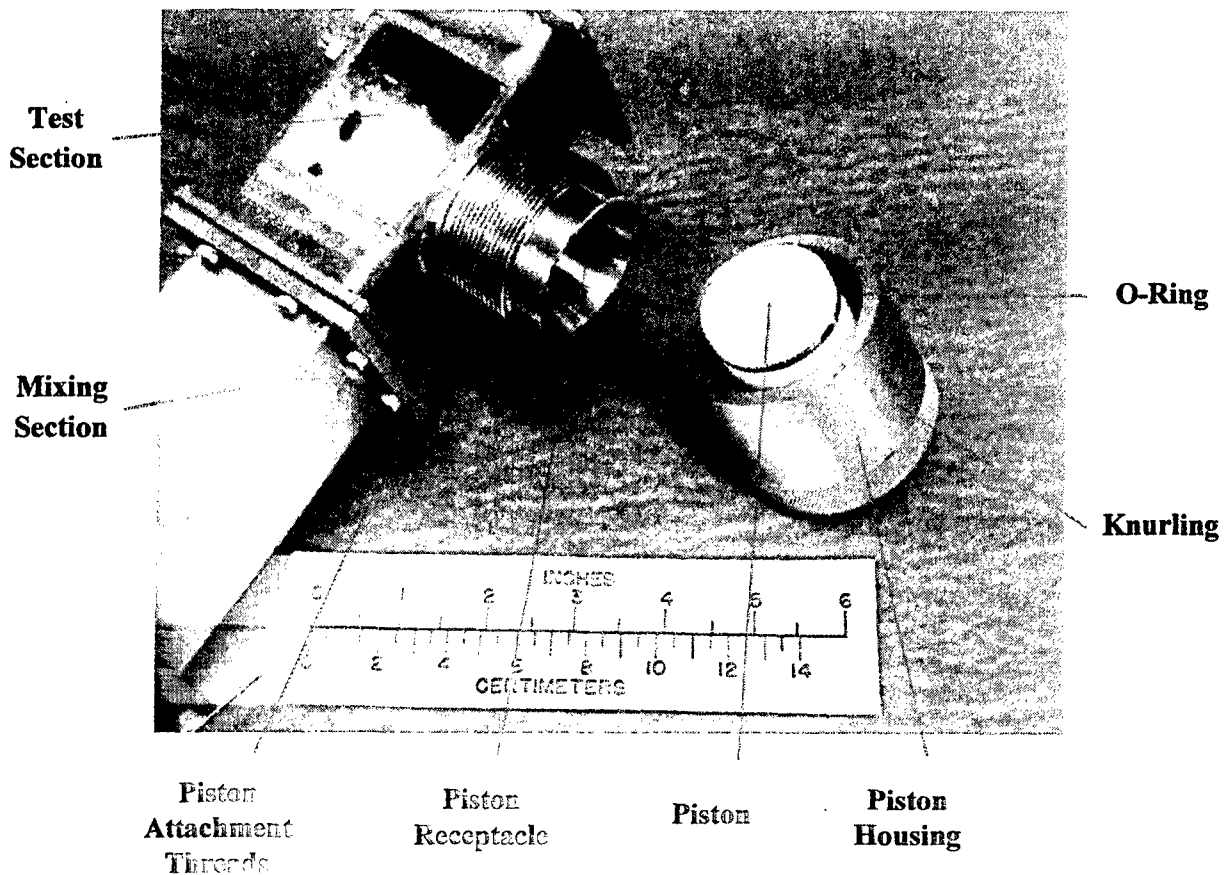


**Figure 43. Screw-in Piston Configuration**

A digital video camera viewing through the test section window measured the changing profile shape of a sessile drop as it evaporated. These results were then used to calculate the mass loss time history for HD on glass, which showed good correlation with corresponding vapor measurements. Later, a viewing port for the video camera was placed in the test section ceiling directly above the center of the piston (coincident with the velocity port). This allowed a downward viewing camera to be installed and, in conjunction with the camera viewing through the side window, allowed simultaneous, mutually orthogonal recording of the drop shape as a function of time. The downward viewing camera could also be used to record the dynamics of the absorbed agent on the surface of the substrate.

The blower previously used for mixing had been difficult to seal and was replaced by a static type mixer based on a McFarland design.<sup>12</sup> The static mixer, Figure 44, is basically a cubical box having internal dimensions of 10 cm on a side, considerably larger than either the inlet or exit ducts. The inlet duct (mixer section) and the exit duct (exhaust section) were flush with the edge of the mixing box. The airflow from the mixing section abruptly enters the mixing box where it circulates and mixes before exiting at a 90° angle into the exhaust duct. A stainless steel version of the mixer was fabricated from 3.0 mm stainless steel.

A 9 probe survey apparatus was used to measure the vapor concentration of a stimulant over the exit area of the exhaust section and indicated that the mixer provided better mixing than the blower and that a flush interface for the entrance and exit ducts provided adequate mixing.<sup>13</sup> Later concentration profiles measured across tunnel sampling region using actual agent demonstrated good mixing at the low velocity and excellent mixing at the mid and high velocities as shown in Figure 45.

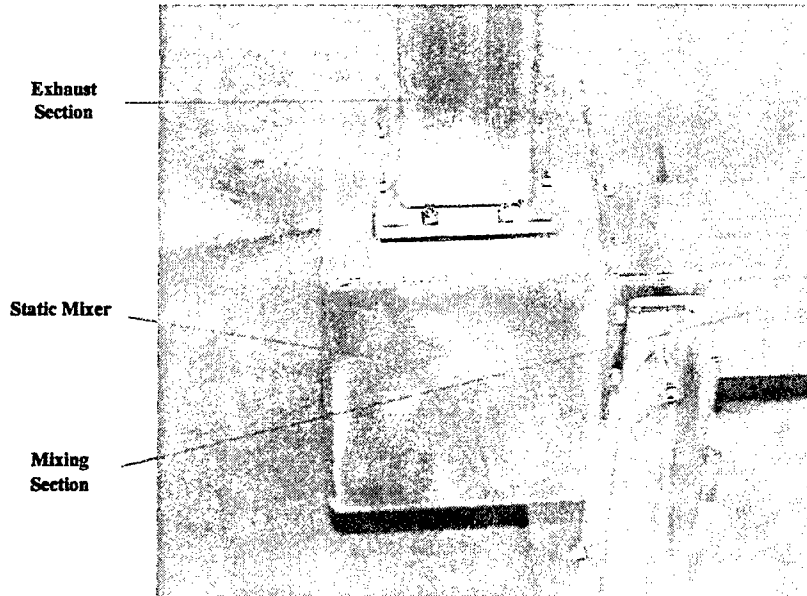


Figure 44. Static Mixer

- Vertical Profile Test
- Probe placed at 5 cm depth
- Hyfed output normalized to max

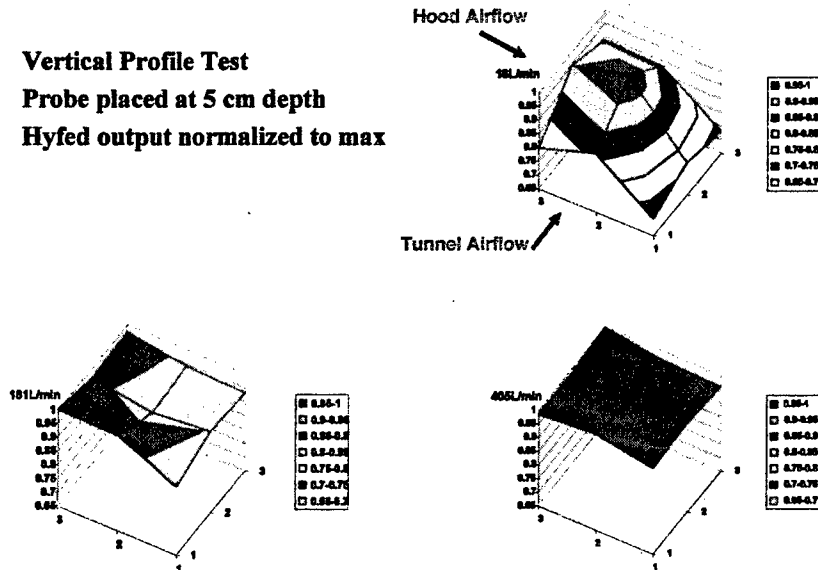
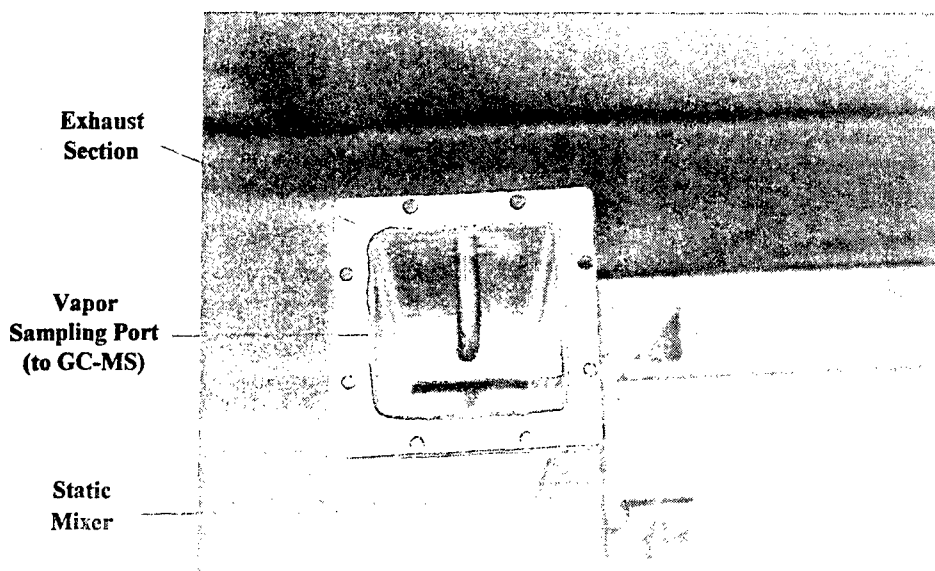


Figure 45. Static Mixer Performance<sup>13</sup>

The vapor sampling probe in the Version 2 Mod 1 tunnel had been manually inserted into the exhaust section. Minor variations in the orientation of the inlet probe to the airflow and its lateral location in the exhaust duct resulted in inconsistent vapor concentration readings. To eliminate this situation, the sampling probe was placed at a fixed position and orientation. A stainless steel tube was welded to the exhaust, entering from the side and curving through a 90° bend to face directly into the airflow as shown in Figure 46. The flexible Teflon inlet tubing for the Hapsite was inserted into the sampling tube until the leading edges of the tubes were flush. This placed the sampling inlet 5 cm from the exit of the exhaust section, on the centerline of the exhaust duct and oriented parallel to the airflow.



**Figure 46. Sampling Inlet**

Six production tunnels (3A through 3F) were initially fabricated. Each tunnel was assembled and leak checked. Tunnels 3A, 3C, 3D and 3E had a limited velocity characterization survey completed, which consisted of using a hot wire anemometer to measure the vertical velocity profiles above the center of piston for all three nominal test velocities. A total of 21 velocity and turbulence intensity measurements were made in varying height increments between 1.25 mm and 45 mm above the test section floor. An increment of 1.25 mm was used from a height of 1.25 mm to 7.5 mm and a 2.5 mm increment was used from a height of 7.5 mm to 45 mm. Two of the tunnels (3B and 3F) had a complete velocity characterization consisting of incremental vertical velocity measurements at the center position, an upwind position, a downwind position and a lateral position. Figure 47 contains representative velocity characterization data illustrating that the measured velocities match the operational values stipulated by the Agent Fate program in the vicinity of the agent/substrate. A more detailed discussion of the velocity profile issue is contained in Section 5.3.

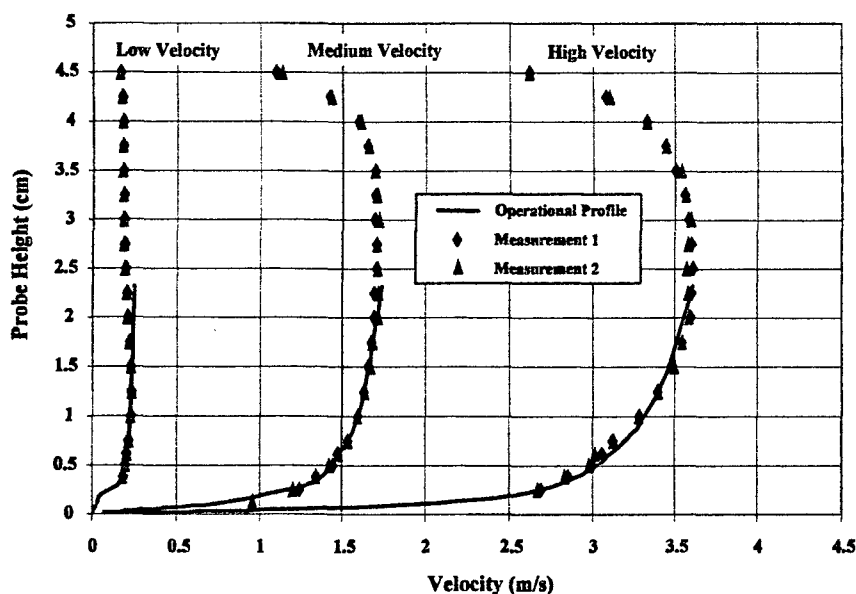


**Figure 47. Vertical Velocity Profiles Measured Above Piston in Version 3 Wind Tunnel**

In March, 2005, the first Version 3 tunnel was moved to the hood area of E3300 and initial tests were performed in April 2005.<sup>13</sup> Figure 48 illustrates the tunnel installed in the fume hood along with a person as a size reference. Details of the Version 3 tunnel and its associated instrumentation are depicted in Figure 49.

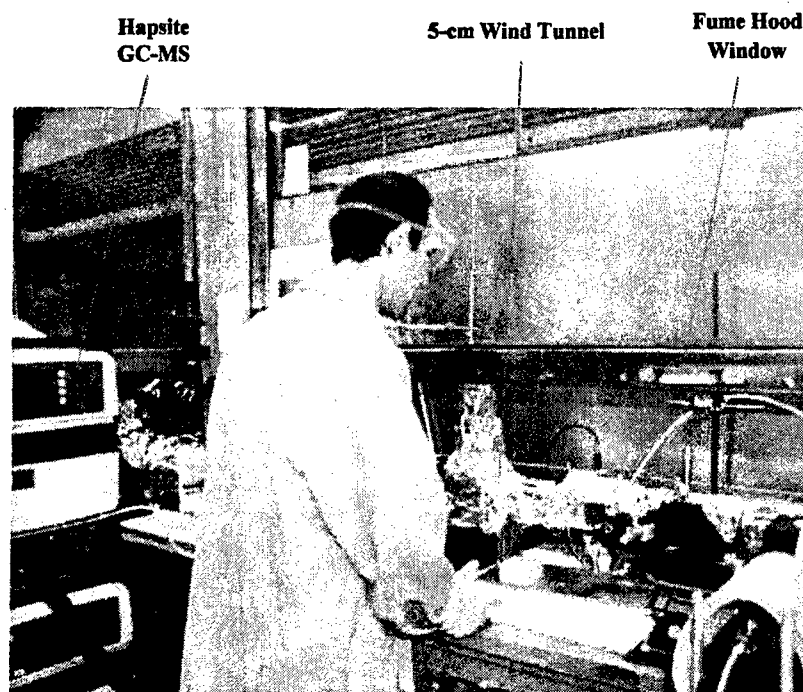


**Figure 48. Version 3 (Production) Tunnel Installed in Fume Hood**

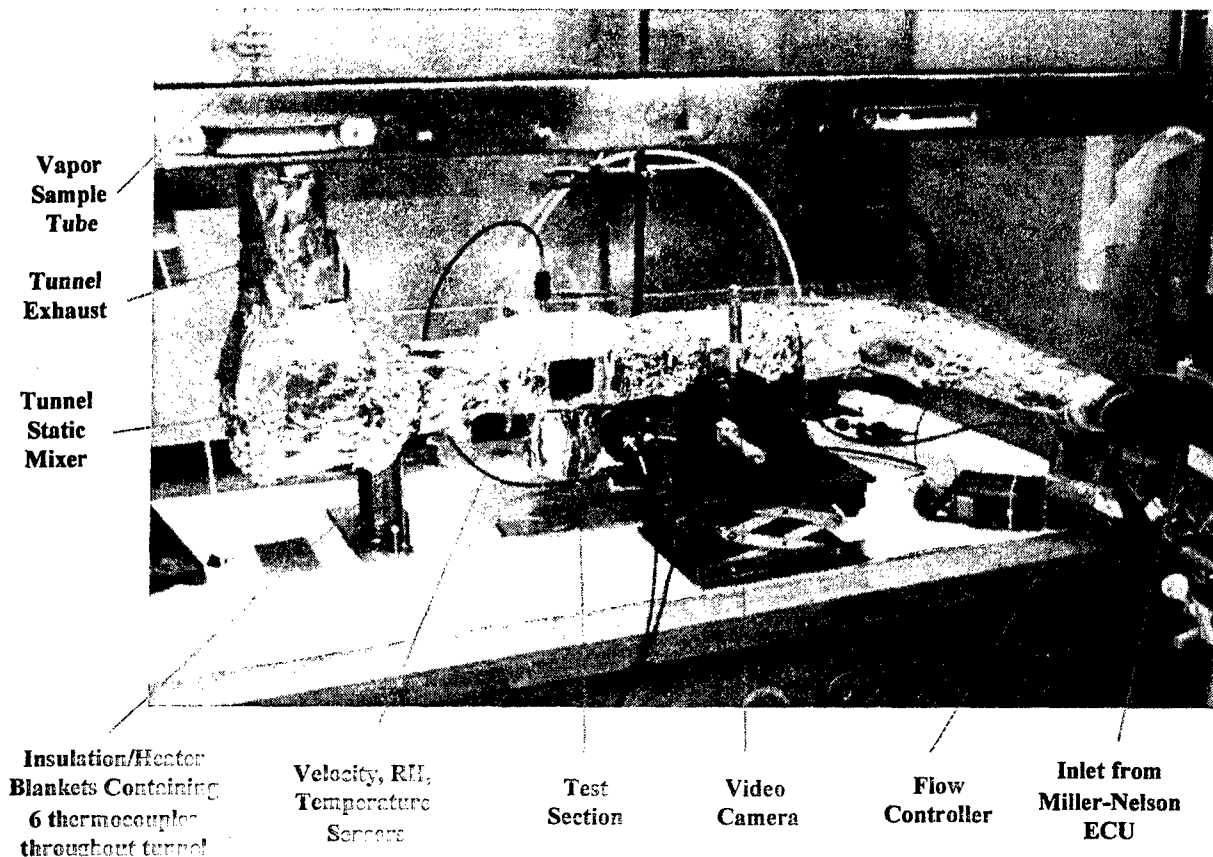


**Figure 49. Version 3 (Production) Tunnel and Associated Instrumentation<sup>11, 13</sup>**

Members of the Agent Chemistry Team developed an automated/computerized data acquisition/analysis system, which was integrated into the Version 3 wind tunnel<sup>11, 13</sup>. The settings and readings of the following instruments were incorporated into the graphical user interface computer display: the Miller-Nelson airflow, temperature, and RH settings; the Aalborg flow controller setting; the six tunnel temperature sensor readings from the transition cone, fetch, test section, piston, mixing section, mixer, and exhaust section; and the test section reference velocity and pressure readings were integrated into a graphical user interface computer display. This allowed the parameters to be set and monitored throughout the test. The real time, HYFED vapor concentration readings were also graphically displayed allowing any problems to be observed and rectified. The graphical screen is shown in Figure 50. After starting the experiment with the desired operating conditions, the system would operate automatically with the resulting data being stored in the computer for later analysis.



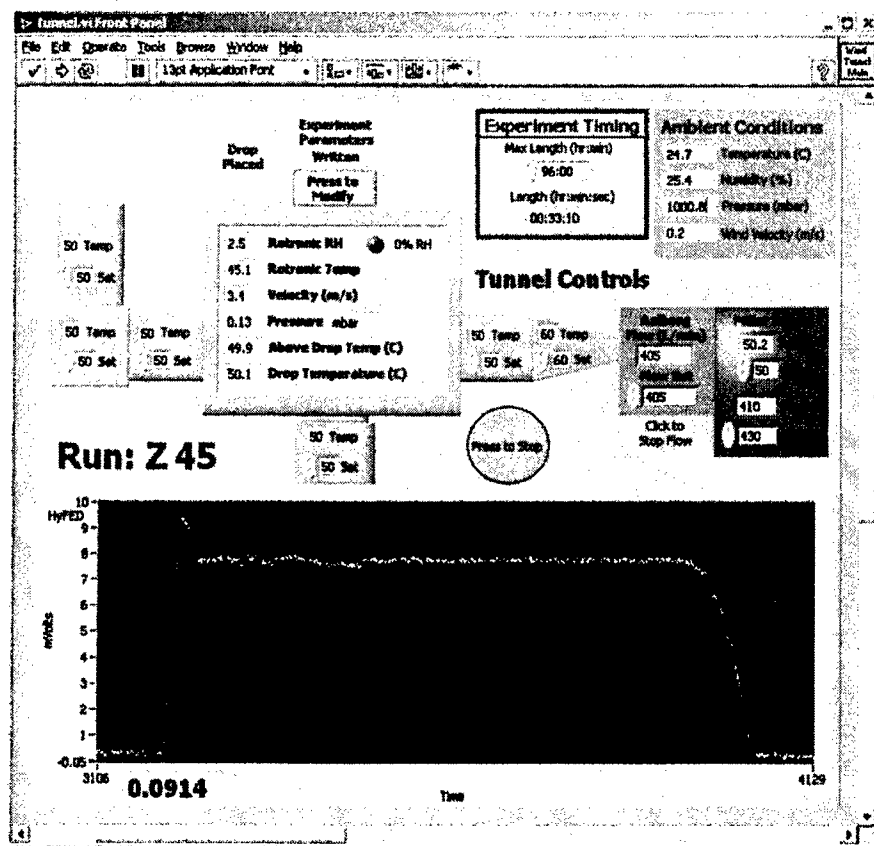


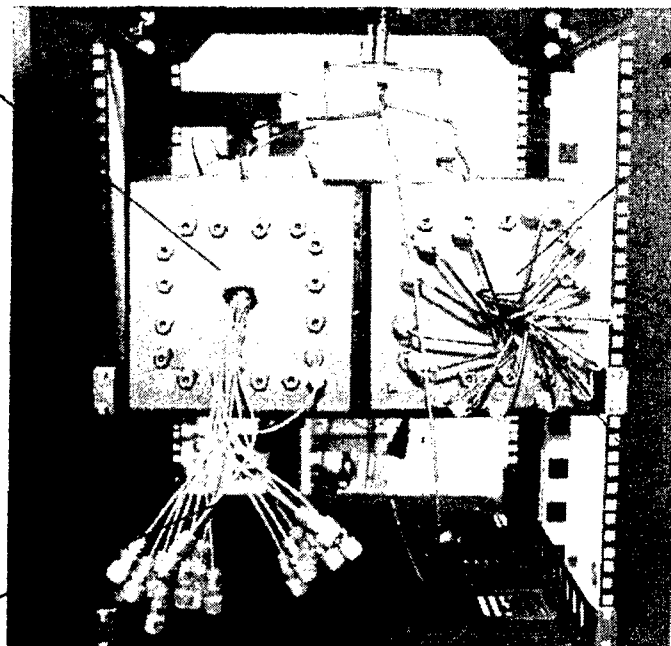
Figure 50. Graphical User Interface<sup>11, 13</sup>

During June 2005, agent mass balances in the Version 3 tunnel were shown to be consistently about  $117 \pm 1\%$ . It was conjectured that the Hapsite reference sample flowrate had a constant error of about 15%, which would explain the mass balance results. However, this rationale was not completely satisfactory due to the inability to explain the physical reason for the Hapsite error.

This situation led the Agent Chemistry Team to develop an alternate vapor collection system referred to as the Variable Tube Sampler (VTS).<sup>11, 13</sup> The VTS, shown in Figure 51, consisted of a series of 30 vapor sorbing DAAMS (Depot Area Air Monitoring System) tubes that sequentially collected the vapor/air mixture at the tunnel sample port. After the test, the content of the tubes was analyzed providing a time history of vapor concentration. Similar extraction tube arrangements were employed in other Agent Fate wind tunnel facilities (Section 13.0), but in those applications, the tubes are located internal to the wind tunnel and their outside surfaces are contaminated by the agent during a test. In the case of the 5-cm wind tunnel, the VTS is located outside of the wind tunnel and their external surfaces are not contaminated. This provided a safer, cheaper and easier testing process, especially with highly toxic agents. The VTS allows variable sampling times and flow rates to be automatically imposed, to optimize the data acquisition for a given set of test conditions. Employment of the VTS in the 5-cm wind tunnel achieved higher and more consistent agent mass recovery rates.

15-Tube Bank

15-Tube Bank



Tunnel to Tube  
Transfer Lines  
(Un-Connected)

Tunnel to Tube  
Transfer Lines  
(Connected)

Figure 51. Variable Tube Sampler<sup>11, 13</sup>

A statistical analysis of velocity profiles and evaporation rates was initiated, which established a common methodology for comparing data from the 10-cm, 5-cm and TGA facilities. The evaporation rates for HD/Glass measured in the Version 3 tunnel correlated well with data from the Agent Fate 10-cm wind tunnel and TGA instrument. This demonstrated that similar experimental data could be obtained in the different sized Agent Fate wind tunnels allowing direct comparison of data between tunnels as well as reducing the number of tests required by not requiring duplicate runs. A detailed description of these facilities and comparison of the agent evaporation data obtained during their validation tests are contained in Section 13.0 and Section 14.0, respectively.

Two different Version 3 tunnels were installed in the same chemical hood by the Agent Chemistry Team as shown in Figure 52. The tunnels were successfully operated separately and simultaneously with similar experimental results being obtained. These were both important steps in validating the plan to use multiple 5-cm wind tunnels for the Agent Fate Program.

A sideward viewing video camera was used to record the drop size as a function of time. The results were compared with vapor data from the Hapsite and a Unity Mass Spectrometer and showed excellent drop life correlation as shown in Figure 53<sup>11, 13</sup>.

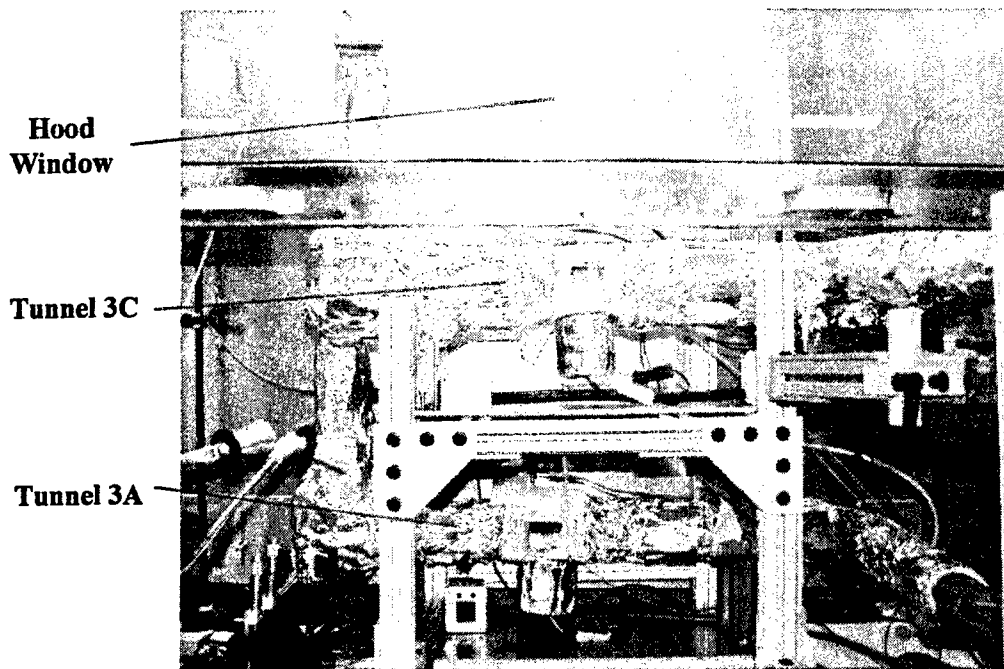


Figure 52. Two 5-cm Wind Tunnels Installed in Single Fume Hood<sup>11, 13</sup>

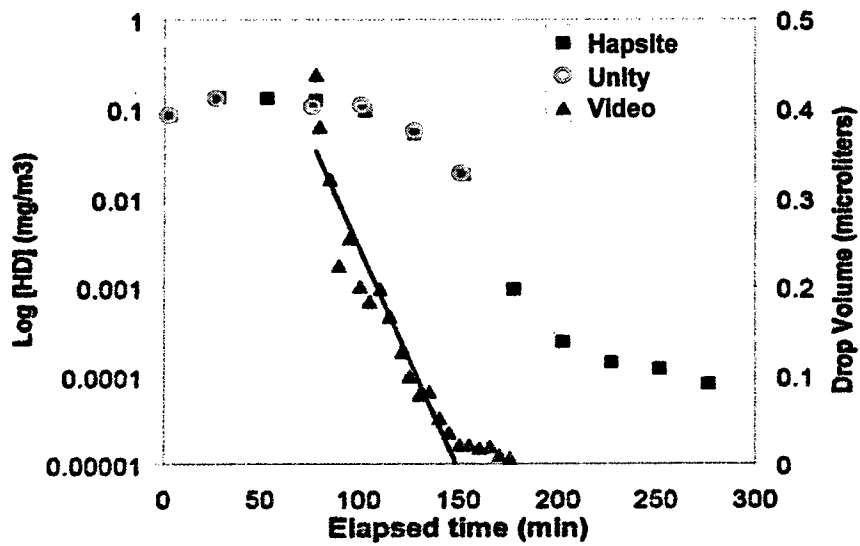


Figure 53. Comparison Between Two Vapor Samplers and Video Information<sup>11, 13</sup>

Because of the special arrangements required to achieve the low temperature test matrix conditions, it was decided to dedicate certain tunnels for medium and high temperature tests and others for cold temperature tests. Tunnels 3A (designated "Spartan") and 3C (designated "Grizzly") were used for the validation tests involving the medium and high temperature conditions. Tunnel 3D (designated "Penguin") was set up for cold temperature testing. Pre-cooled water was circulated through copper tubing installed around the tunnel components.<sup>13</sup> This tunnel was used for the cold temperature validation test conditions beginning in October 2005.

In September, 2005, a Version 3 tunnel was delivered to the Calspan University of Buffalo Research Center (CUBRC) for their use in supporting the Agent Fate program. This exemplified the ability to distribute the 5-cm tunnels to different organizations.

The Version 3 tunnel was also used to measure velocity profiles over samples of ridged concrete substrate. No differences were noted with regard to whether the ridges were oriented perpendicular or parallel to the airflow, and no differences were observed between these results and those for smooth Teflon.

The Version 3 tunnel included several significant features: Silico-Steel® coated stainless steel components; Kalrez gaskets; test section composed of rectangular, thicker test section walls bolted together; drilled and tapped instrumentation ports in test section ceiling and side wall; side test section window located flush with floor for better drop viewing; 6 instrumentation ports in test section for velocity, temperature, pressure; mutually orthogonal video camera ports in test section; temperature sensors in fetch, test section, piston and exhaust; static mixer; shortened duct between test section and mixer; extended length sampling section; square exhaust cross section; sampler located at fixed position and orientation on tunnel center-line downstream of static mixer; use of HYFED as real-time vapor analysis tool.<sup>11, 13</sup> Variable Tube Sampler (VTS) evolved; automated computer controlled airflow and temperature monitors and settings; automated computer controlled data acquisition (Hapsite and VTS); and thermal insulation and heater tape over entire tunnel structure including piston.

The Version 3 tunnel<sup>13-18</sup> achieved a number of significant milestones including: producing evaporation rate data for HD/Glass that agreed with the 10-cm wind tunnel data, equated with the results from different 5-cm wind tunnels and compared well with TGA data; generating velocity profiles that matched operational values stipulated by model developers; correlating video measurements of agent drop evaporation with vapor measurements; achieving simultaneous operation of two 5-cm wind tunnels in the same chemical fume hood; demonstrating the operation of dedicated medium/hot and cold tunnels; and providing duplicate 5-cm wind tunnels to other research organizations. This was the version of the 5-cm tunnel that was used for the 5-cm wind tunnel validation tests with HD on glass. It was also used for the initial absorbent substrate tests involving HD on sand. With minor changes, this design became the Version 3 Mod 1 tunnel described in the next section.

4.7

Version 3 Mod 1 (Production Tunnel)

The Version 3 Mod 1 tunnels were intended to be installed in larger capacity chemical hoods. A new support structure was designed allowing a group of three Version 3 tunnels to be installed in a single hood. This arrangement required the Miller-Nelson units to be located to the side of the hood permitting the hood sash to be closed during testing operations. To accomplish this, the transition cone was placed in a vertical orientation giving the tunnel a "U" shaped layout as shown in Figure 54. As can be seen in Figure 55, except for this feature, the Version 3 Mod 1 tunnel is identical to the Version 3 tunnel.

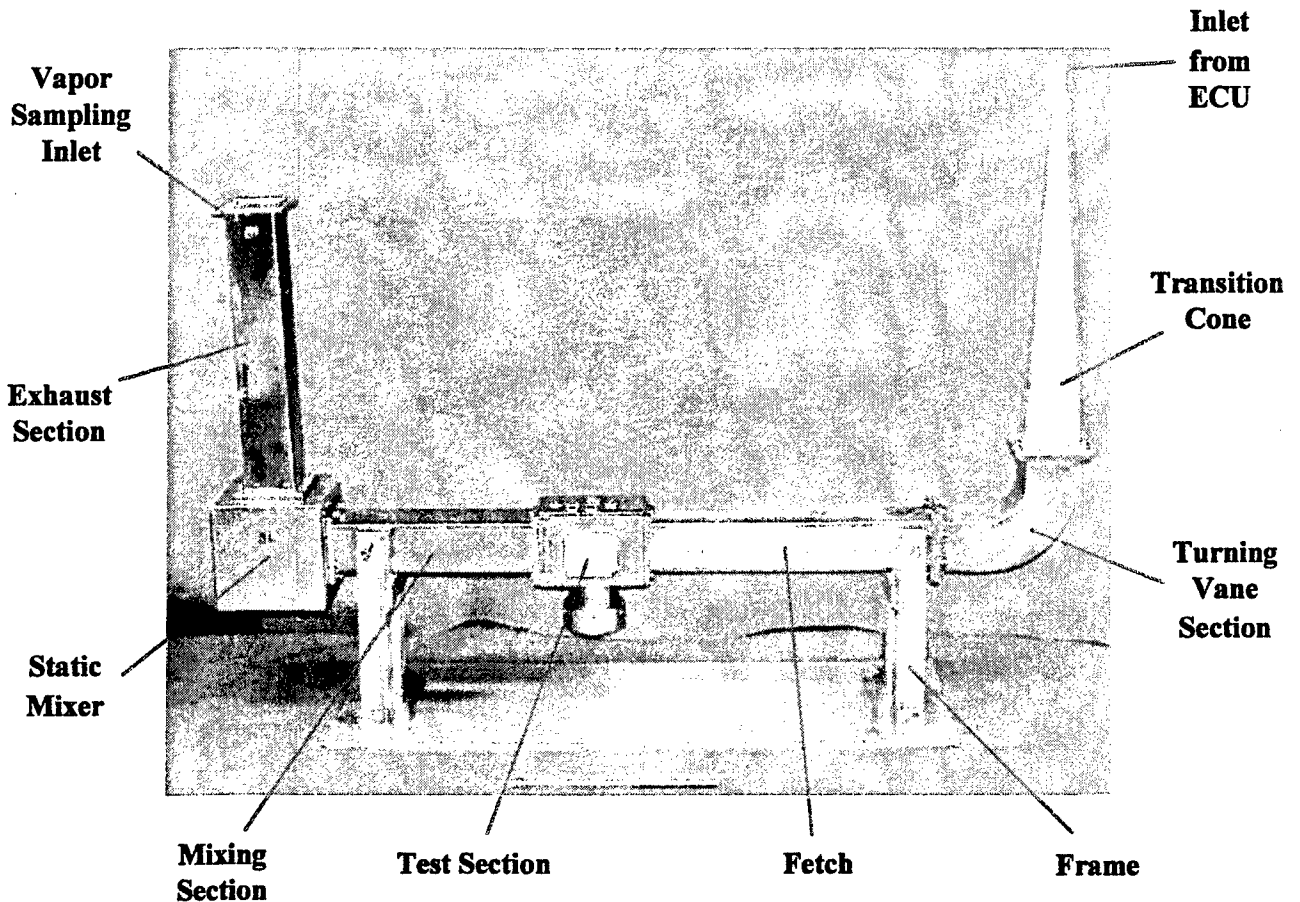
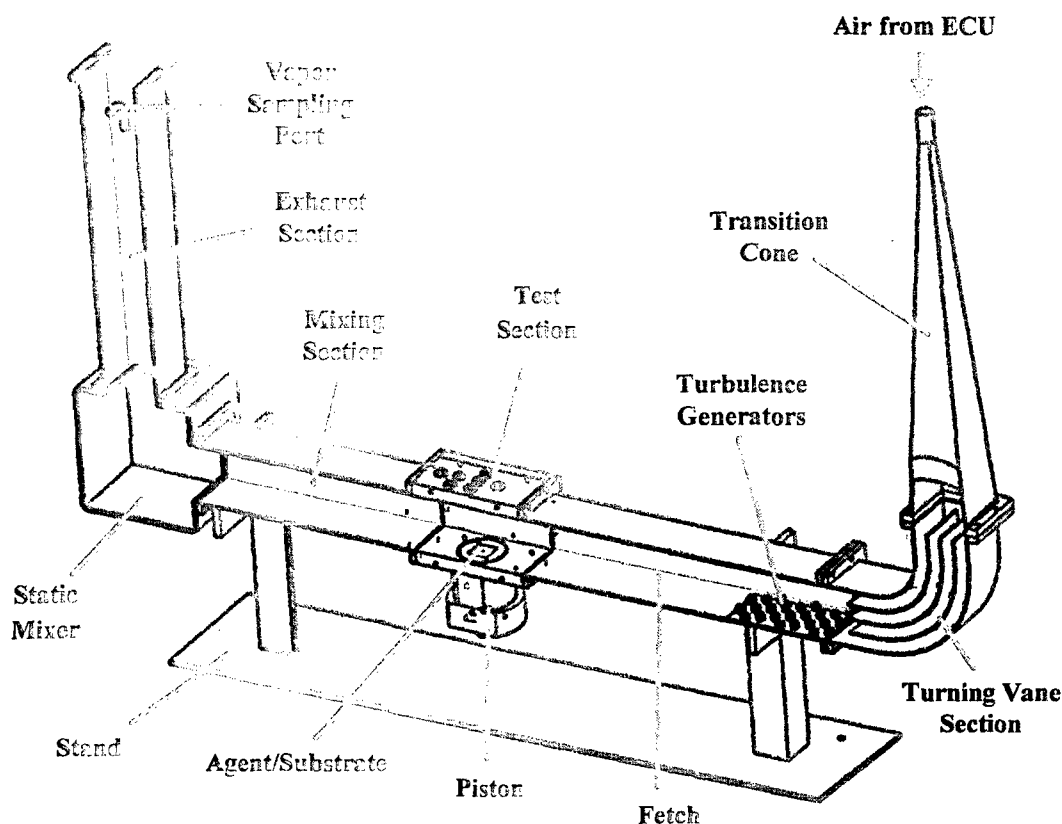


Figure 54. Version 3 Mod 1 (Production) Wind Tunnel



**Figure 55. Cut-Away of Version 3 Mod 1 (Production) Tunnel**

The horizontal orientation of the turning vane section of the Version 3 tunnel configuration resulted in any flow disturbances due to the vanes to act in a horizontal plane. While this influenced the variance of the profiles in a lateral sense, it had little effect on the more critical shape of the vertical velocity profiles. However, the vertical orientation of the turning vane section of the Version 3 Mod 1 tunnel configuration resulted in vane induced flow disturbances to act in a vertical plane and, consequently, had a greater influence on the shape of the vertical velocity profiles. As a consequence, the Version 3, Mod 1 tunnel required an inlet screen to eliminate airflow perturbations produced by the turning vanes. A 24 x 24 mesh per inch, 0.36 mm diameter wire screen was located at the exit of the turning vane section (the entrance of the fetch) as shown in Figure 56. Figure 57 illustrates that the good match to the operational velocity profiles was retained. Another improvement was to shorten and provide insulation/temperature control for the transfer line between the tunnel and the VTS eliminating the need for any post-test corrections to the agent mass balance.

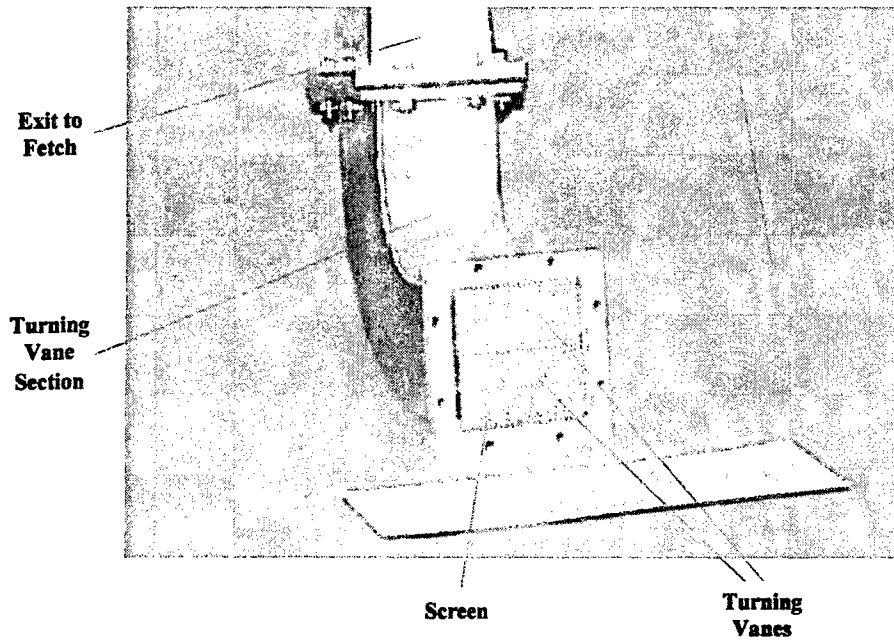


Figure 56. Fine Mesh for Vertical Oriented Turing Vane Section

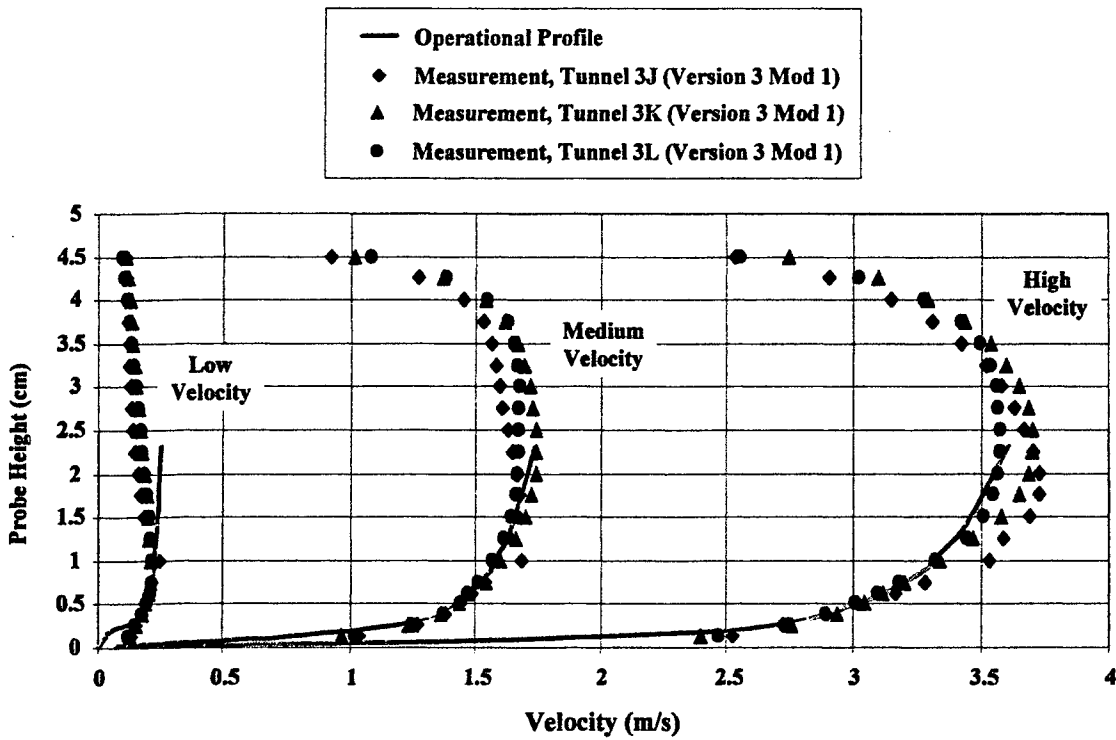


Figure 57. Velocity Profiles for Version 3 Mod 1 Wind Tunnel

Another modification involved replacing the screw-in piston with a snap-in piston. This improved design allowed a more rapid insertion and removal from tunnel than the previous screw-in piston greatly reducing the time delay for the temperature to stabilize and to start the measurement of evaporation data during the crucial early portion of the test. Adjusting the piston insertion depth to place the top of the substrate flush with test section floor was accomplished by a threaded attachment between the piston and the piston holder. The snap-in piston is illustrated in Figure 58.

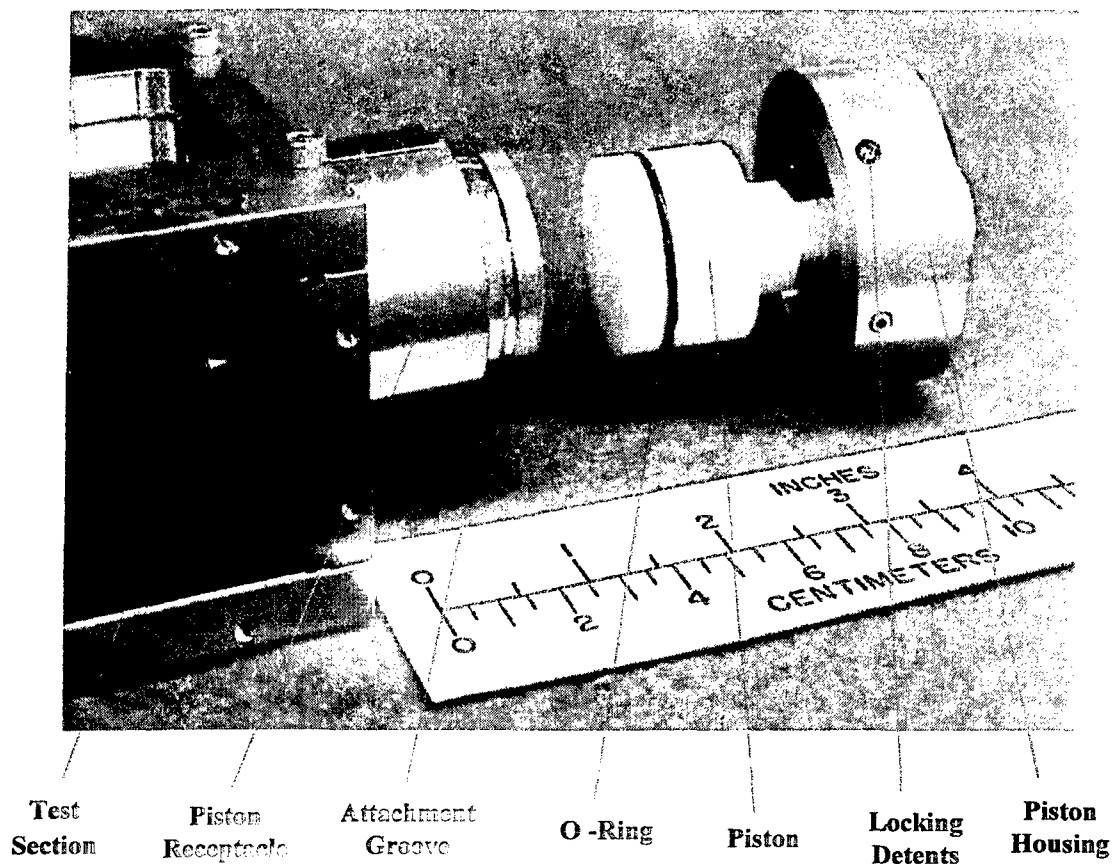


Figure 58. Snap-in Piston

For testing with VX, all Version 3 Mod 1 tunnels were electro-polished and Sulfinert® coated. The Sulfinert® treatment provided an order of magnitude increase in resisting absorption of VX compared with the Silico-Steel® process.

A concise summary of the 5-cm wind tunnel design evolution is contained in Appendix A. The Version 3 Mod 1 tunnel represents the 2006 development stage of the 5-cm wind tunnel and is being used for the major portion of the Agent Fate production testing. Accordingly, this particular version is presented in detail in Appendix B.



## 5. VELOCITY PROFILES

### 5.1 Atmospheric Boundary Layer

One of most critical elements of the wind tunnel is to simulate the effect of the wind on the drop/substrate. Previous experimental studies of agent evaporation from surfaces under air flow conditions<sup>19</sup> are of limited value for the current Agent Fate program because of the inadequate description of the velocity profiles present in their experimental arrangements. Most of these studies employed average flowrates or volumes passing over the drop area rather than utilizing vertical velocity profiles that more closely simulated a boundary layer produced by the wind. Accordingly, one of the goals of the Agent Fate program was to use realistic and defined vertical velocity profiles in all of its experimental operations.

In general, a steady wind is characterized by a horizontal velocity that decreases with altitude; ranging from a nominal velocity at some altitude to zero at the earth's surface as illustrated in Figure 59. This atmospheric "boundary layer" type velocity profile can extend to several hundred feet above the ground. The shape of the associated velocity profile is influenced by several factors such as the weather (atmospheric pressure, temperature, RH, etc.); terrain, foliage (trees, bushes, etc.), buildings and other man-made structures and the ground composition (roughness, ground temperature, etc.).

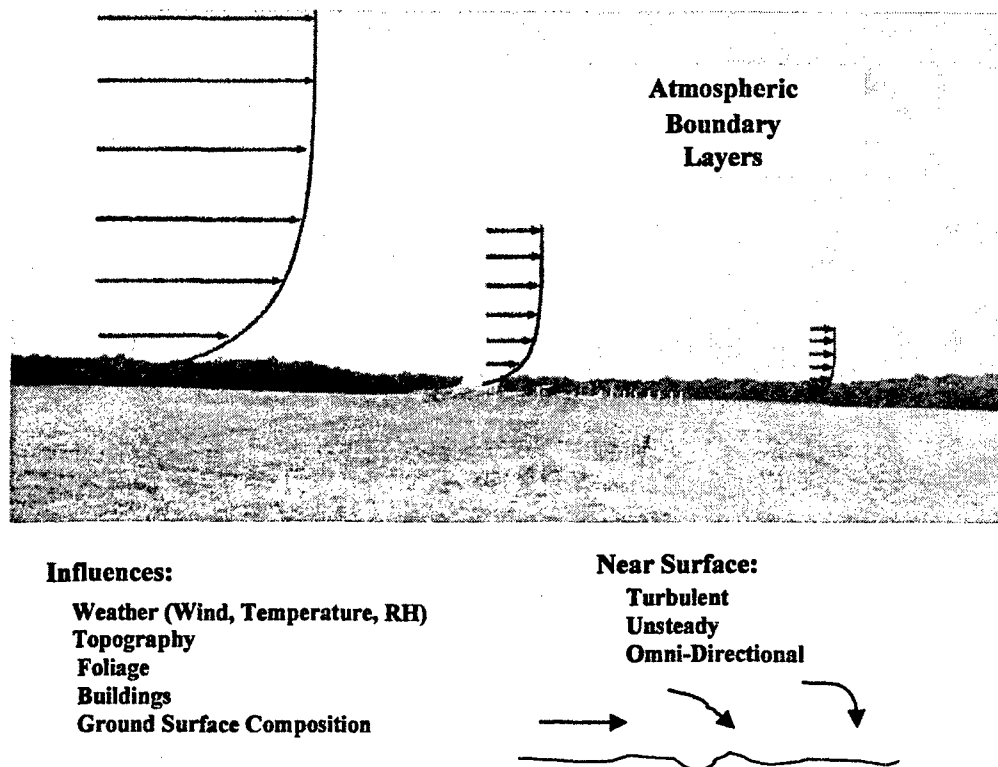
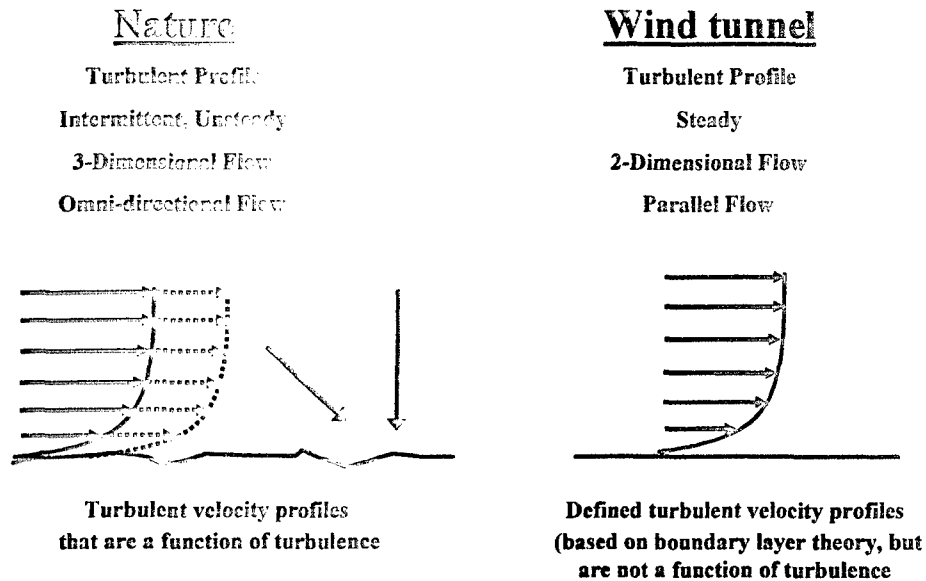


Figure 59. Wind Induced Atmospheric Boundary Layer

On a macro-scale, an atmospheric boundary layer can be ideally envisioned in terms of a steady, horizontal velocity profile. However, close to the surface, the wind effects are characterized by intermittent, unsteady, omni-directional and swirling motion, frequently approaching the ground in a near perpendicular attitude, as illustrated in Figure 60. This near-ground region is the main area of interest to the Agent Fate studies because this is where the agent and substrate are located.\* Defining a set of controlled airflow conditions for the wind tunnel experiments that are representative of the lower portion of the atmospheric boundary layer was an important facet of the Agent Fate program. It should again be emphasized that the droplets, surface materials, and velocity profiles are not scaled for these tests. The droplet and substrates are full size, which leads to the challenging problem of matching the atmospheric wind profile near the droplet.



**Figure 60. Velocity Profile Nature vs. Wind Tunnel**

\*With all of the uncertainties involved in the actual environment: varying wind, temperature, substrate, etc. only a general idea of the agent vapor can be predicted, regardless of the accuracy of the data that the model is based on. While the type, amount and drop size of the agent may be known fairly well, the specific substrate it is applied to is known to only a very limited degree with regard to the type and extent of the various ground conditions, which can be a combination of grass, bushes, pavement, buildings, bare ground, vehicles, etc. For example, in the case of grass, is the grass short or high; is there clover and weeds in it; are there dirt patches, etc.? All of these factors result in an agent hazard prediction that can only be estimated to order of magnitude terms. These factors should be kept in mind when assessing the accuracy, precision and repeatability of any experimental data used in these models. Fine details in the experimental data are lost in the overall uncertainties of the operational conditions being modeled.

In its simplest terms, an atmospheric boundary layer velocity profile can be expressed as the so-called, "power" law (sometimes referred to as "Frost Curves").

$$u/U_0 = (y/Y_0)^p$$

Where  $u$  = velocity at height  $y$

$U_0$  = Reference velocity (usually the maximum velocity at the maximum altitude)

$y$  = Height

$Y_0$  = Reference height (height at reference velocity)

$p$  = Exponent (power) value

While this expression suffices for most atmospheric boundary layer applications, it is not adequate for use in the Agent Fate program where a more detailed description is required. A turbulent boundary layer, which is characteristic of the velocity profiles used in the Agent Fate program, is actually composed of three distinct regions as depicted in Figure 61. These include a "laminar sub-layer" region that extends from the surface outward; a "turbulent" region that extends inward from the outer edge of the boundary layer; and a "buffer" region between the two where the transitions from one to the other occurs. In the laminar sub-layer region, the velocity is proportional to the height above the surface whereas in the turbulent region, the velocity is proportional to the height raised to a power (i.e., logarithmic).

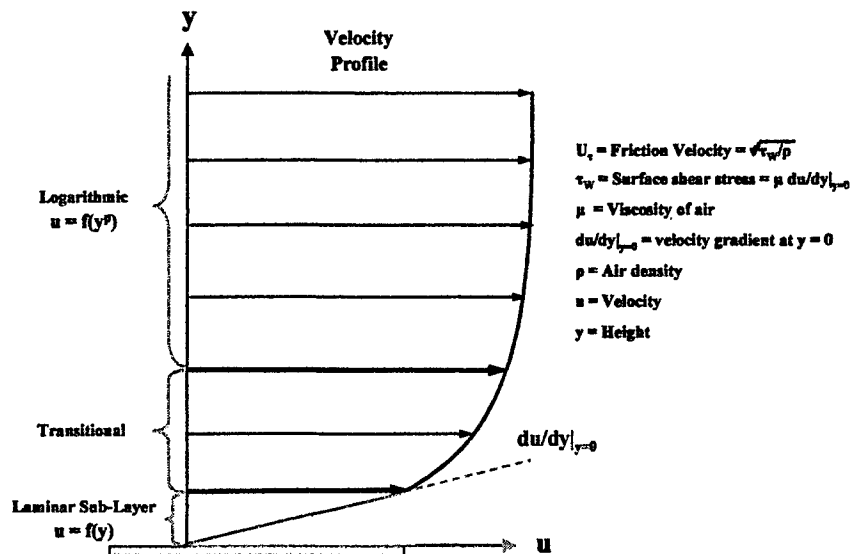


**Figure 61. Boundary Layer Velocity Profile Nomenclature**

In the laminar region, the vertical velocity profile is linear with the height above the surface and is expressed by the following equation:

$$u/U_\tau = U_\tau y/\nu$$

Where  $u$  = velocity at height  $y$

$U_\tau$  = Friction Velocity, which is proportional to the surface shear stress

$y$  = height above surface

$\nu$  = kinematic viscosity of the air

Note that the velocity is directly proportional to the height.

The vertical velocity profile in the turbulent region is a logarithm function of the height above the surface and is expressed, for a smooth surface, in the following equation known as the "Law of the Wall".

$$u/U_\tau = (1/\kappa) \ln(U_\tau y/\nu) + C$$

Where  $\kappa$  is the Von-Karman constant (usually = 0.4)

$C$  is a constant (usually = 5.5).

Note that the velocity is a logarithmic function of the height.

Thus, no surface roughness height is required, which helped to simplify the wind profiles developed for the Agent Fate program. The smooth surface assumption was thought to be a good approximation for glass, concrete, asphalt, sand and soil. However, for grass and vegetation, the smooth surface assumption may not be correct and a surface roughness factor may be required. For this stage of the program, this additional complexity was not pursued.

## 5.2 Specified Velocity Profiles

The approach adopted by the Agent Fate program was to define a set of nominal vertical velocity profiles, based on boundary layer theory and the "operational" wind conditions of interest to the model developers. While somewhat arbitrary and for simplified conditions, they represent a practical bridge between the variable turbulent, unsteady and omni-directional airflow in nature and the turbulent, steady and parallel flow of the wind tunnel.

A set of three "operational" boundary layer velocity profiles were defined by the model developers as standard conditions for the wind tunnel studies.<sup>8</sup> Figure 62 contains the original graph provided by the model developers and defines the near surface velocity profiles of an atmospheric boundary layer on a flat surface with some degree of roughness for wind speeds of at a 2 m height above the ground of 0.5, 3.0 and 6.0 m/s. These wind velocity conditions were selected based on operational conditions intended to be included in the final Agent Fate models. The velocity profiles were developed using boundary layer theory and are based on three values of friction

velocities representing relatively smooth surfaces (glass, metal, concrete and asphalt). The choice of these friction velocities defined their respective velocity profiles.

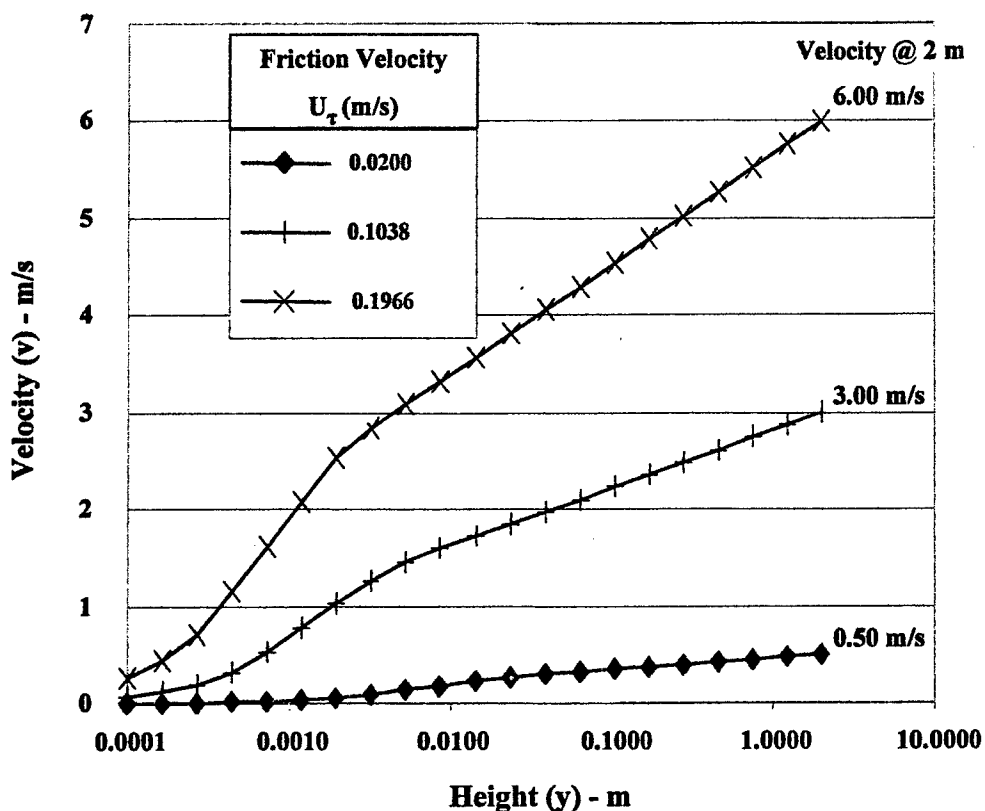


**Figure 62. Operational Velocity Profiles Defined by Agent Fate Model Developers**

Figure 63 shows the three operational velocity profiles in non-logarithm units and provides a better physical “feel” for the shape of the velocity profile. While the operational velocity profile is defined for a wind velocity at a height of 2 m, the 5-cm wind tunnel only needs to duplicate the velocity profile up to a maximum height of 2 cm as shown in Figure 64. Above this height, the velocity profile is affected by the ceiling boundary layer and, more important, does not influence the airflow in the vicinity of the drop/substrate. At a height of 2 cm in the 5-cm wind tunnel, these result in velocities of 0.22, 1.7 and 3.6 m/s for the 0.5, 3.0 and 6.0 m/s test matrix velocities, respectively. Previous hot wire anemometer measurements in the 5-cm wind tunnel test section had demonstrated that the stipulated operational vertical velocity profiles were created for these reference velocities. Thus, setting the 2-cm reference velocity at a specific test matrix value was sufficient to establish the associated operational vertical velocity profile.

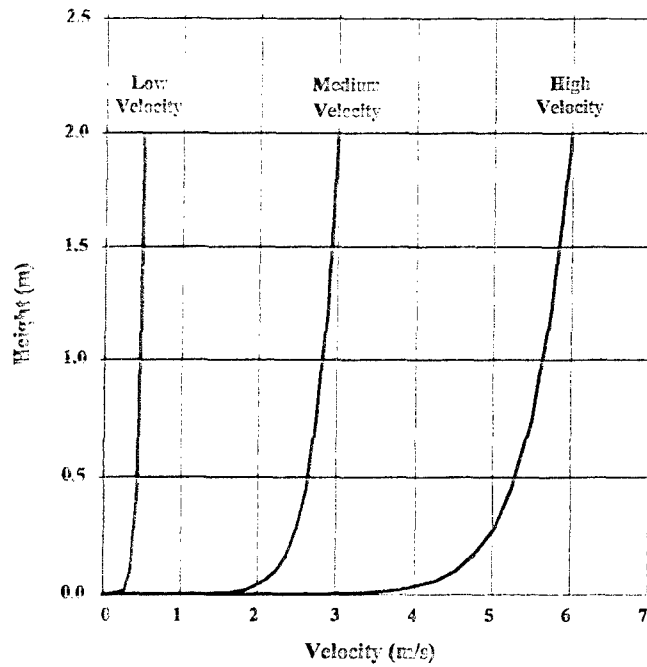


Figure 63. Operational Velocity Profiles in Physical Units

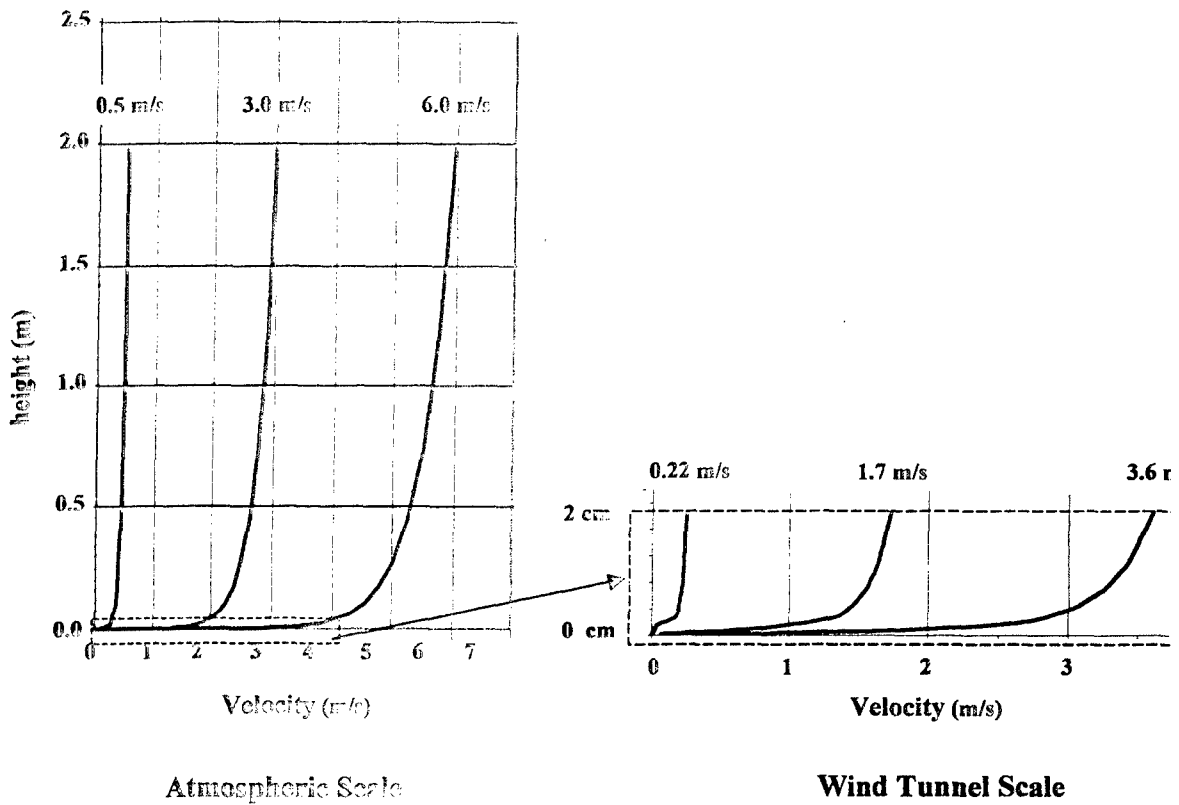
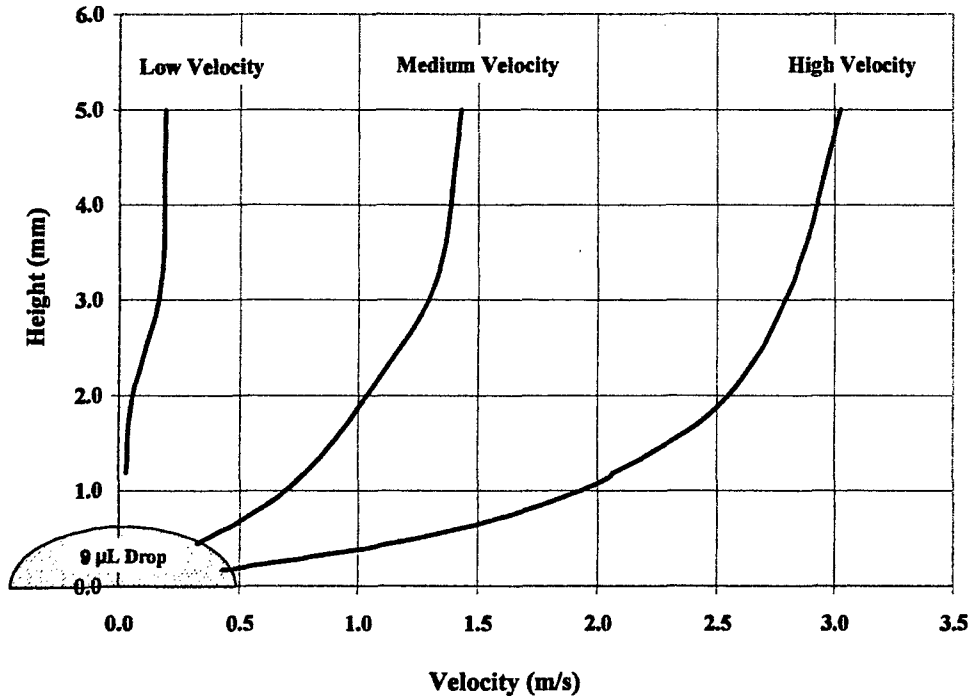


Figure 64. Lower Portion of Operational Boundary Layer Profiles

Figure 65 depicts the three operational velocity profiles up to a height of 2 cm above the floor of the wind tunnel relative to a typical agent drop size. The 9  $\mu\text{L}$  drop shown (the largest unthickened drop size to be tested) is about 0.5 mm in height (about the same size as the head of a pin) illustrating its extremely small size. Even though the drop is extremely small, it still experiences an appreciable velocity. The velocity at the top surface of the drop ( $y = 0.5 \text{ mm}$ ) is about 20-33% of the nominal "free stream" velocity in the tunnel and 10-20% of the velocity at the 2 m reference height.



**Figure 65. Velocity Profiles in Vicinity of Drop**

### 5.3 5-cm Wind Tunnel Velocity Profiles

Vertical velocity profiles were measured above the center of the piston in the 5-cm, Version 3 wind tunnel for each of the three nominal test velocities and are shown in logarithmic and physical units in Figure 66 and compared with the respective operational values stipulated by the Agent Fate program and illustrate the close agreement achieved.

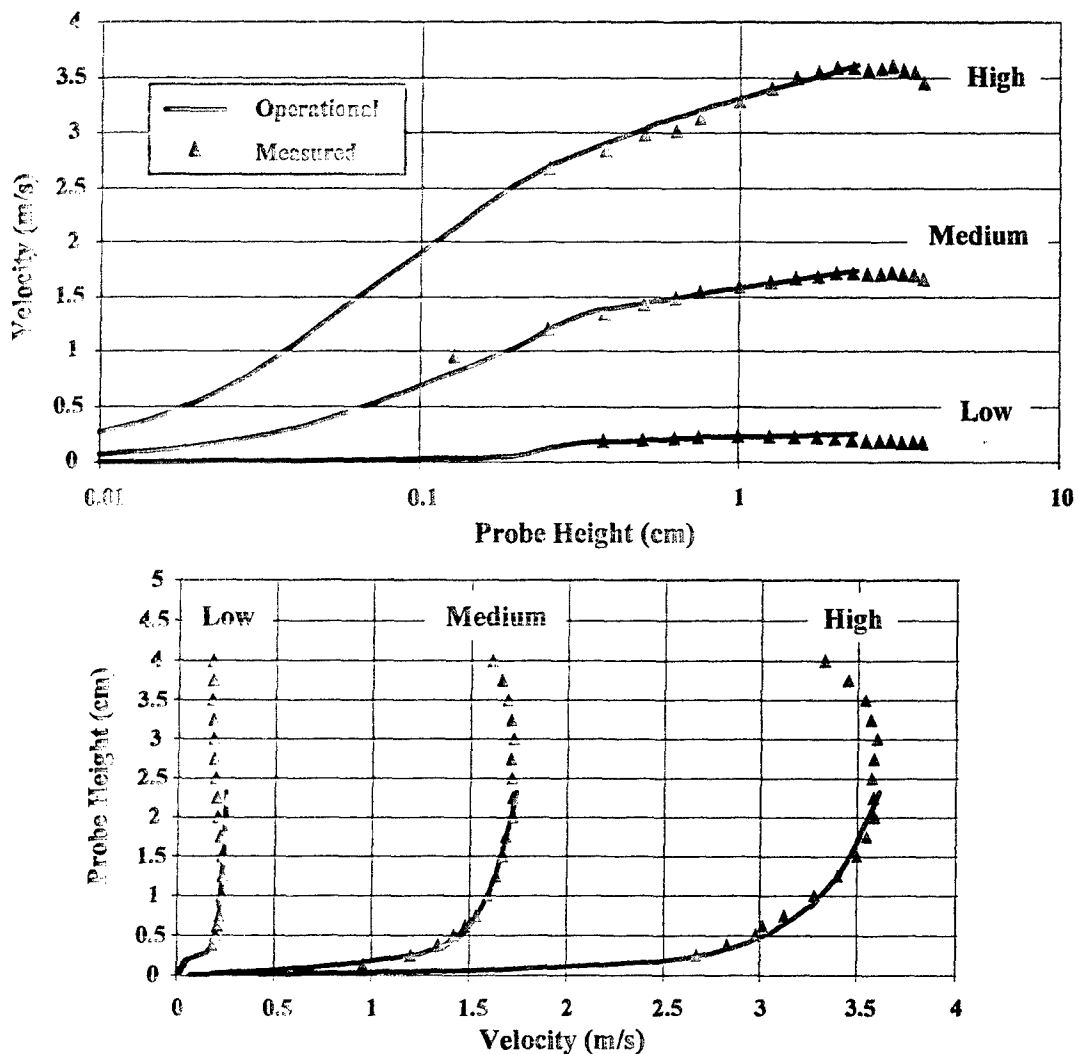


**Figure 66. Measured 5-cm Wind Tunnel Velocity Profiles on Physical and Log Scales**

The vertical velocity profiles in the test section were fully characterized by measuring the velocity profiles at five lateral locations relative to the center of the piston (i.e., center, upstream, downstream and left and right lateral). These are shown compared to the operational profiles in Figure 67 through Figure 69 for the low, medium and high operational velocity profiles, respectively. These data illustrate that similar vertical velocity profiles are produced over the entire top surface of the piston (near the test section floor where the drop/substrate is located).

As noted previously, a design goal for the 5-cm wind tunnel was to allow it to be built in large numbers and used in multiple locations. Figure 70 shows the velocity profiles measured in five different 5-cm wind tunnels. All profiles are quite similar; with any small differences at the mid-height gradually disappearing with the profiles overlaying each other at the critical region near the droplet. This demonstrates that the velocity profiles can be duplicated in different tunnels; an essential requirement for using multiple 5-cm wind tunnels to support the Agent Fate Program.



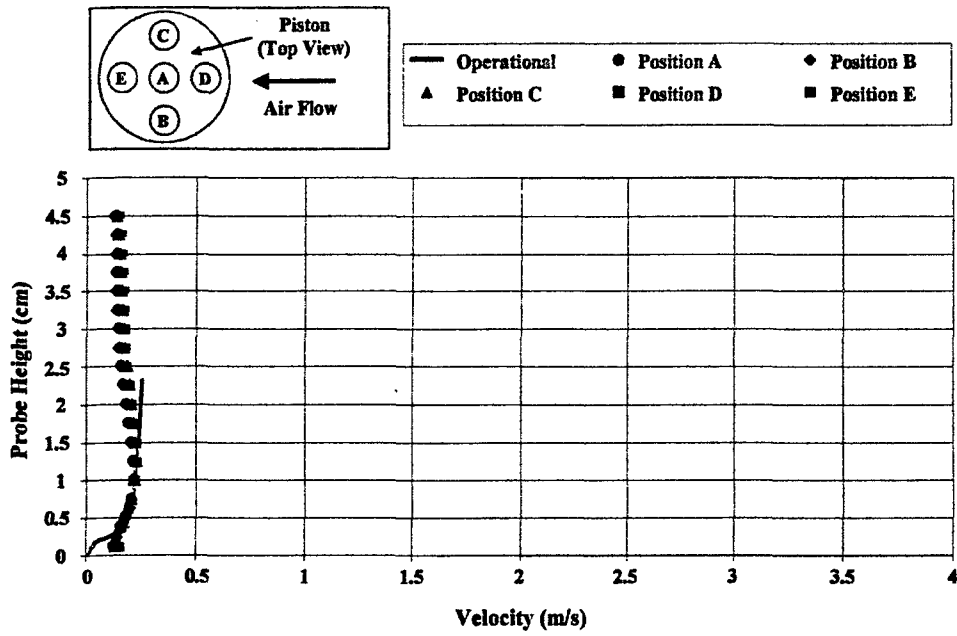


Figure 67. 5-cm Wind Tunnel Velocity Profiles (Low Velocity Condition)

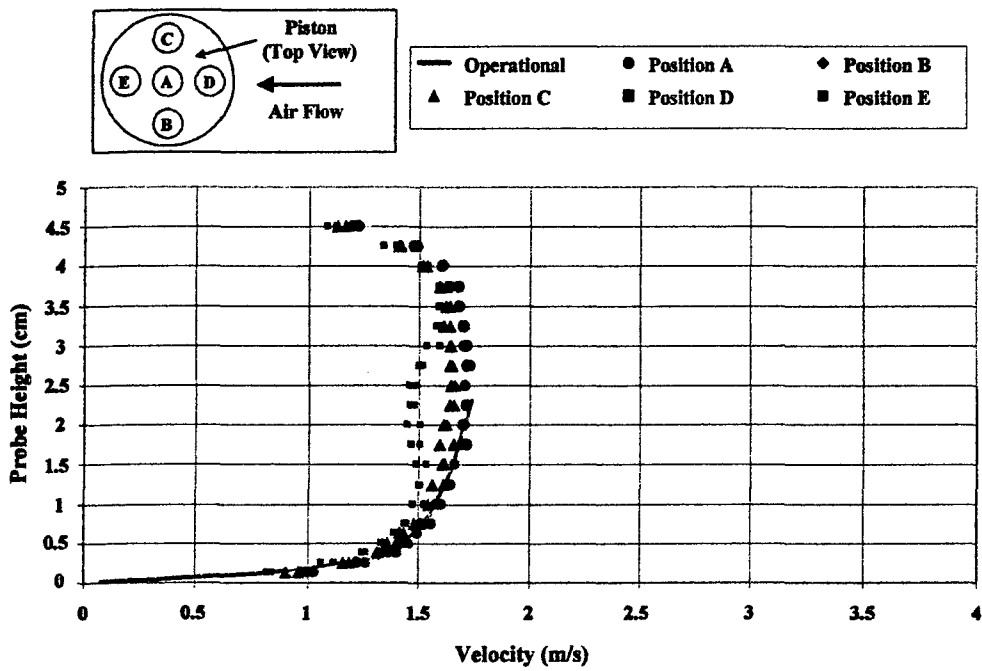
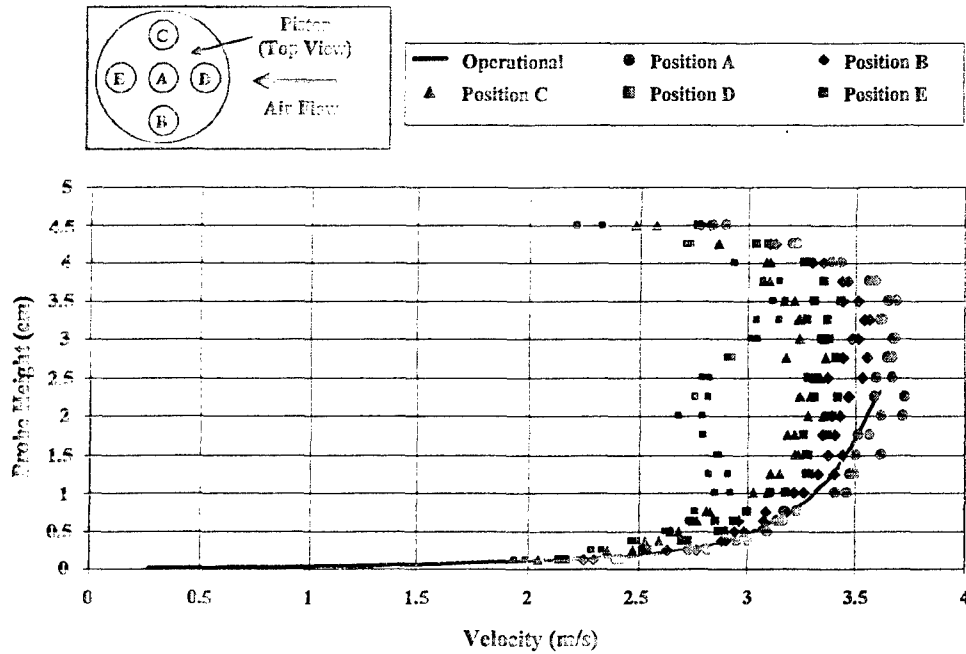
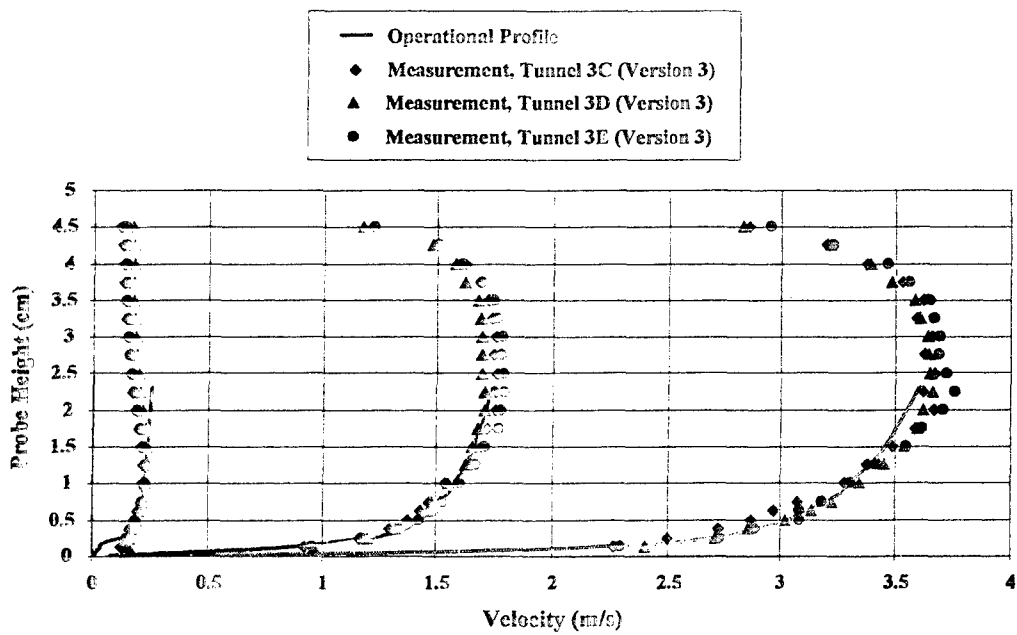


Figure 68. 5-cm Wind Tunnel Velocity Profiles (Medium Velocity Condition)



**Figure 69. 5-cm Wind Tunnel Velocity Profiles (High Velocity Condition)**



**Figure 70. Velocity Profiles Measured at Center of Piston in Different Version 3, 5-cm Wind Tunnels**

## 6. EFFECT OF FREE STREAM TURBULENCE

### 6.1 Non-Dimensional Boundary Layer

Figure 71 contains a generalized, semi-log plot of the boundary layer velocity profile depicting its fully laminar and fully turbulent shapes.<sup>20</sup> The velocity profiles are presented in terms of the non-dimensional velocity and height.

Where

$$u^+ = \text{Non-dimensional velocity} = u/U_\tau$$

$$y^+ = \text{Non-dimensional height} = U_\tau y/\nu$$

$$U_\tau = \text{Friction velocity} = \sqrt{\tau_w/\rho}$$

$$\tau_w = \text{Surface shear stress} = \mu \left. \frac{du}{dy} \right|_{y=0}$$

$$\mu = \text{Absolute viscosity of air}$$

$$\rho = \text{Density of air}$$

$$\nu = \text{Kinematic viscosity of air} = \mu/\rho$$

$$u = \text{Horizontal velocity}$$

$$y = \text{Height above test section floor}$$

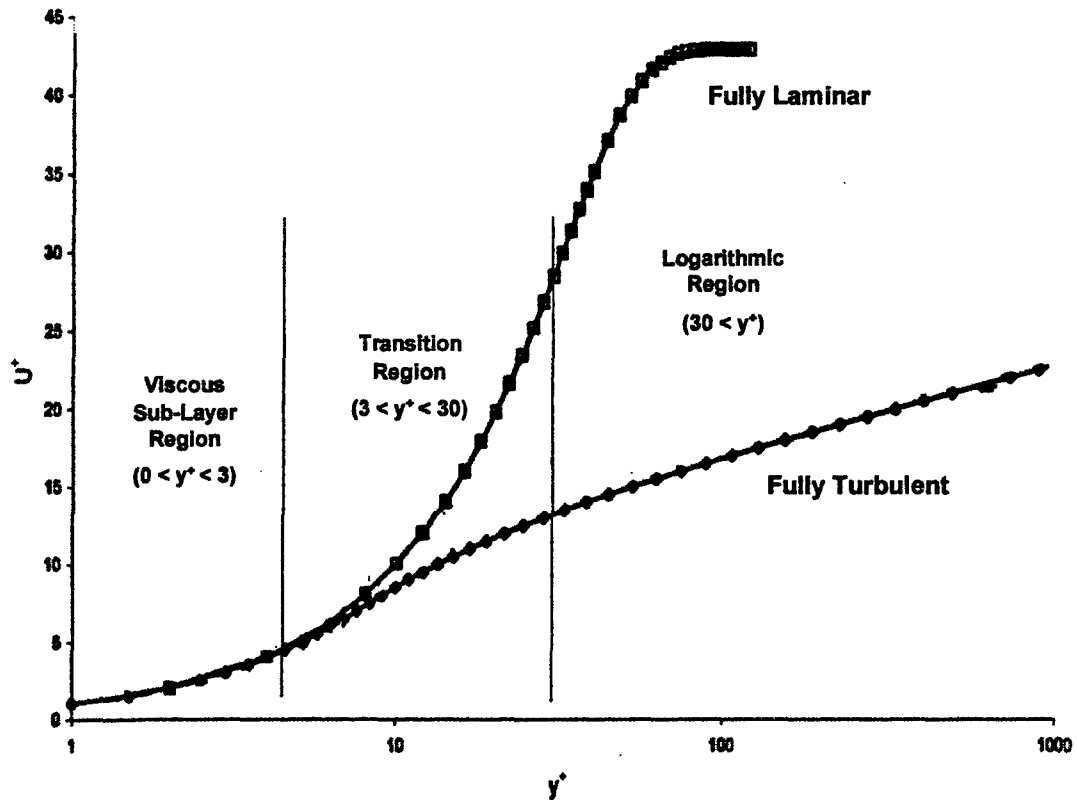
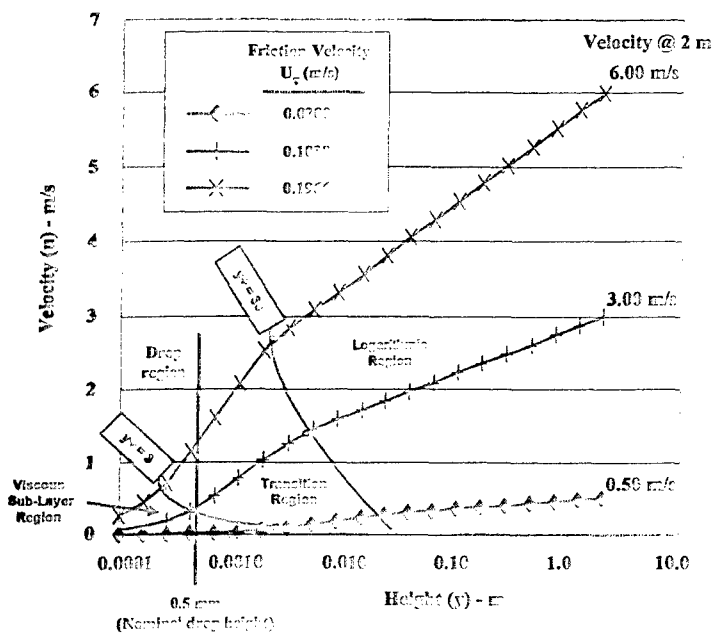


Figure 71. Non-Dimensional Boundary Layer

The viscous sub-layer ( $0 < y^+ < 3$ ) is characterized by the velocity being proportional to the height (in non-dimensional terms  $u^+ = y^+$ ). Viscous effects dominate in this region and evaporation of a drop in this region is not affected by the turbulence in the upper regions (for a given surface shear stress (i.e., friction velocity) condition). The logarithmic region ( $y^+ > 30$ ) is characterized by the velocity increasing logarithmically with height. In this region, inertial effects dominate and various degrees of free stream turbulence can be present. The buffer layer ( $3 < y^+ < 30$ ) is a transition region between the viscous sub-layer and the logarithmic region. In this region, the viscous effects diminish as the inertial effects increase with increasing height.

Figure 72 shows the velocity values at different heights above the floor of the wind tunnel test section as defined for the Agent Fate wind tunnels. In the viscous sub-layer region ( $0 < y^+ < 3$ ), the velocity is linear with height and is characterized by a non-linear curve in this logarithmic plot. The outer boundary of this region is indicated by the  $y^+ = 3$  line. Note that the thickness of the linear, viscous sub-layer is inversely proportional to the value of the magnitude of the test velocity condition ranging from 2.5 mm for the low velocity profile to 0.25 mm for the high velocity profile. The outer portion of the profile ( $y^+ > 30$ ) where the velocity is a logarithmic function of the height is characterized by a linear relation for the logarithmic scale used. The inner boundary for this region is indicated by the  $y^+ = 30$  line. This region has an inner boundary ranging from 25 mm for the low velocity to 2.5 mm for the high velocity. The “transition” region representing the transition area between the viscous sub-layer and logarithmic regions lies in between.



Upper Limits of Boundary Layer Regions

U m/s	y+ = 3 mm	y+ = 30 mm
0.5	2.5	25
3.0	0.5	5
6.0	0.25	2.5

Where:

U = Reference velocity @ 2 m

y+ = 3 = Outer edge of viscous sub-layer region

y+ = 30 = Outer edge of transition region

Figure 72. Agent Fate Operational Velocity Profiles Including Boundary Layer Regions

The heights for the different boundary layer regions (laminar sub-layer, transitional and logarithmic) for the operational velocity profiles are shown in physical units in Figure 73. Note that all regions extend to greater heights (i.e., are “thicker”) at the lower velocities. This figure also points out the very small thicknesses for the laminar sub-layer and transitional regimes. These can be expressed as a percentage of the 2 m height at which the velocities are defined. For the low and high velocities, respectively, these range from 0.25 to 0.02% for the upper extreme of the laminar sub-layer to 1.0 to 0.1% for the lower extreme of the logarithmic regime. Note also, that the 5-cm wind tunnel includes all three regions for all three velocity profiles.

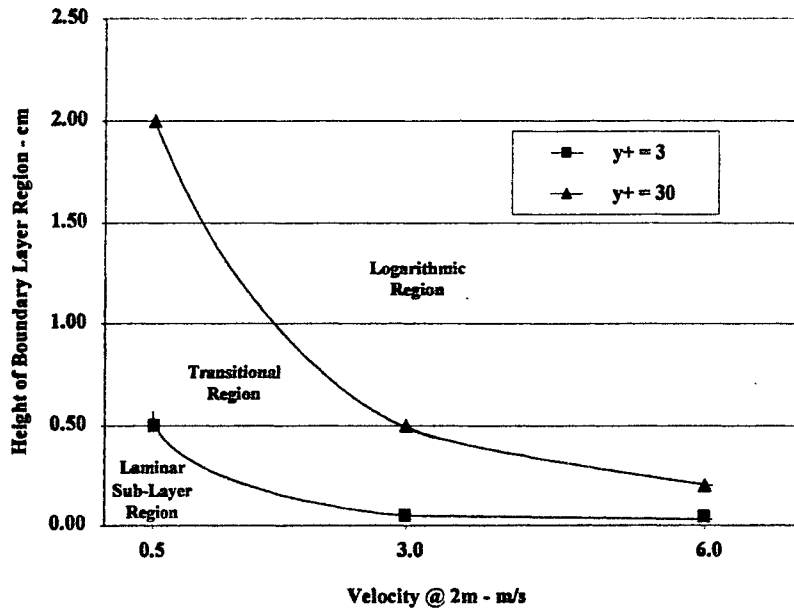


**Figure 73. Heights of Boundary Layer Regions for Operational Velocity Profiles**

Free stream turbulence results from random velocity fluctuations occurring in any air stream whether in an atmospheric boundary layer or in a wind tunnel. The 5-cm wind tunnel forces the creation of a turbulent boundary layer by introducing turbulence to the flow via the turbulence generators located upstream of the test section. The formation of a turbulent boundary layer and its characteristic velocity profile depend on having a certain level of free stream turbulence present in the airflow (the more turbulence, the fuller the profile). However, its velocity profile (representing a specific friction velocity and a corresponding shear stress at the surface) is relatively insensitive to the free stream turbulence level as long as it remains within a certain range of values. While the evaporation rate of a chemical/substrate is influenced by the shear stress at the surface, the question arises as to how evaporation rate is further affected by the specific level of the free stream turbulence.

6.2

Relation to Agent Fate Test Conditions

The following analysis relates the velocity profiles used in the Agent Fate wind tunnels to the general, non-dimensional boundary layer shape to determine in what regime the agent evaporation occurs and to assess the effect of free stream turbulence on the resulting evaporation. It should be noted that the Agent Fate program is concerned only with predicting the initial evaporation of the agent. The subsequent movement of the agent vapor cloud throughout the atmosphere is predicted by separate Transport and Diffusion models. These latter models are heavily influenced by the wind and free stream turbulence in the air.

The velocity gradient at the floor of the test section can be computed from the friction velocities specified for the Agent Fate test matrix velocities, see Table 1.

**Table 1. Floor Velocity Gradients for Specified Agent Fate Test Matrix Velocities**

V@ 3m m/s	$U_\tau$ m/s	$\frac{du}{dy} _{y=0}$ sec <sup>-1</sup>
0.5	0.200	24.2
3.0	0.1038	652.2
6.0	0.1966	2,339.7

Where

$$U_\tau = \sqrt{\tau_w/\rho}$$

$$\tau_w = \mu \frac{du}{dy}|_{y=0}$$

$$\nu = \mu/\rho$$

$$\frac{du}{dy}|_{y=0} = U_\tau^2/\nu$$

These can be used to compute the associated non-dimensional boundary layer terms. The following are examples for computing the non-dimensional velocity and height at for the three test matrix velocity profiles at a height of 1 mm:

V = 0.5 m/s @ 2 m

$$u = 0.024 \text{ m/s}; y = 1 \text{ mm}$$

$$U_\tau = \sqrt{\nu \times \frac{du}{dy}|_{y=0}} = \sqrt{0.00001652 \times 24.2} = 0.020 \text{ m/s}$$

$$y^+ = yU_\tau/\nu = (0.001 \times 0.020)/0.00001652 = 1.21$$

$$u^+ = u/U_\tau = 0.024/0.020 = 1.20$$

V = 3.0 m/s @ 2 m

$$u = 0.65 \text{ m/s}; y = 1 \text{ mm}$$

$$U_{\tau} = \sqrt{\nu \times du/dy|_{y=0}} = \sqrt{0.00001652 \times 652.2} = 0.1038 \text{ m/s}$$

$$y^{+} = yU_{\tau}/\nu = (0.001 \times 0.1038)/0.00001652 = 6.28$$

$$u^{+} = u/U_{\tau} = 0.65/0.1038 = 6.28$$

$V = 6.0 \text{ m/s @ } 2 \text{ m}$

$$u = 2.30 \text{ m/s; } y = 1 \text{ mm}$$

$$U_{\tau} = \sqrt{\nu \times du/dy|_{y=0}} = \sqrt{0.00001652 \times 2339.7} = 0.1966 \text{ m/s}$$

$$y^{+} = yU_{\tau}/\nu = (0.001 \times 0.1966)/0.00001652 = 11.90$$

$$u^{+} = u/U_{\tau} = 2.30/0.1966 = 11.70$$

Note that in all three cases, the equal values of  $u^{+}$  and  $y^{+}$  indicate that these points all lie in the laminar region of the boundary layer.

Figure 74 shows the plot of the operational velocity values defined as test conditions for the Agent Fate wind tunnels for heights of 1, 10 and 20 mm above the floor of the wind tunnel test section including the maximum free stream velocity for the 5-cm Tunnel. Note that the 1 mm points for all three operational velocities lie on the laminar shape whereas the points at 10 and 20 mm lie on the turbulent shape. The low velocity at 1 mm is well within the viscous sub-layer region and the two higher velocities are in the transition region. However, even the latter two points, are in laminar flow as evidenced by their equal values of  $u^{+}$  and  $y^{+}$  indicating that the velocity is linear with height.

A series of experiments were conducted to determine the maximum height of a sessile drop of agent. These experiments used agent drop sizes corresponding to those used in the Agent Fate test matrix and involved HD agent on glass (a non-absorbent, non-reactive agent/substrate surface) to produce a drop having the maximum height possible. The results are pictorially displayed in Figure 75. The drops are shown relative to the head of pin demonstrating their extremely small size. Note that sessile drops are formed in all cases and, due to spreading, the nominal height achieved for all three drop sizes used in the Agent Fate program (1, 6 and 9 microliters) was about 0.5 mm as shown in Figure 76.

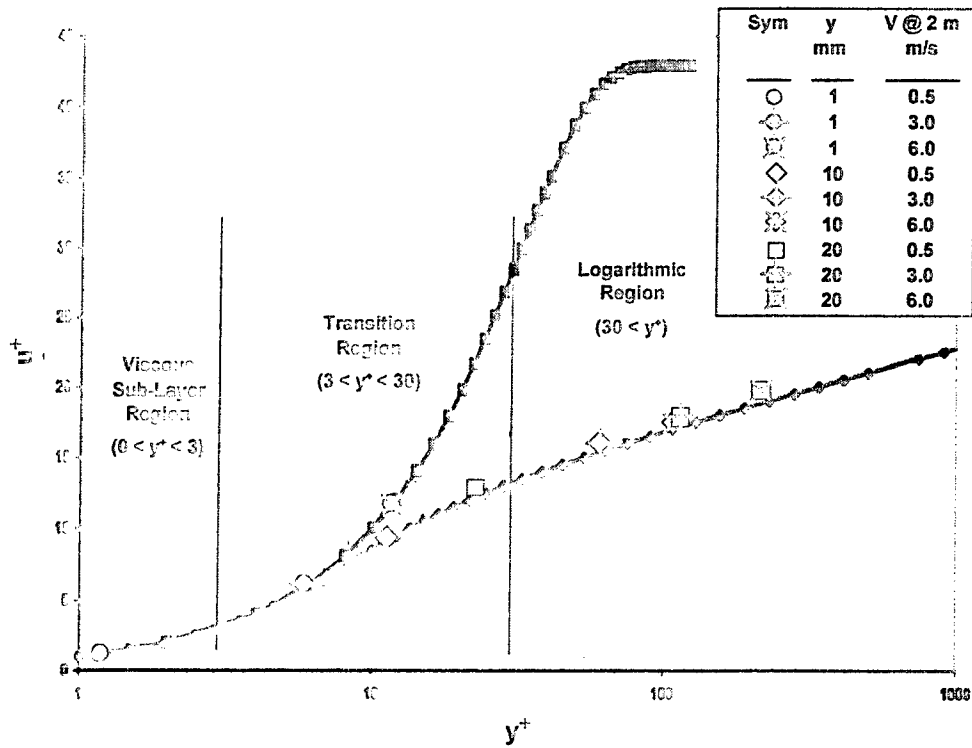


Figure 74. Operational Velocity Values Plotted on Non-Dimensional Boundary Layer Profile

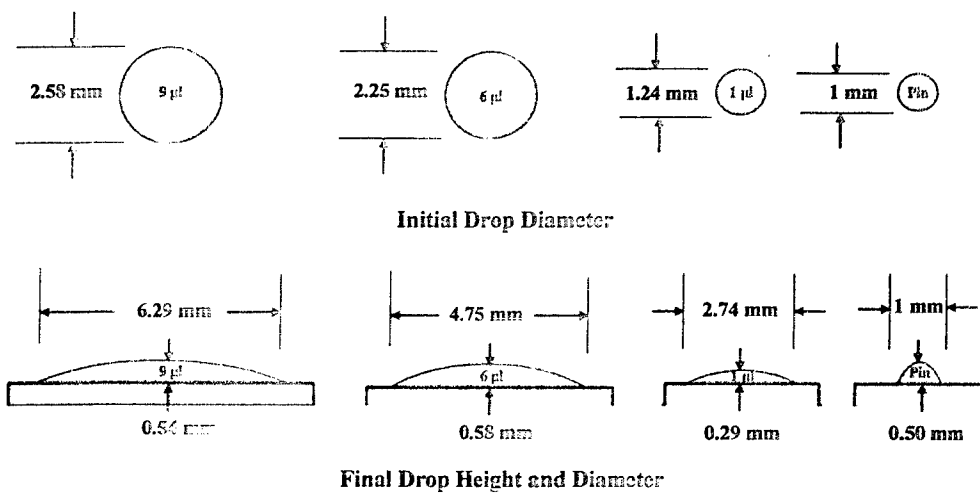
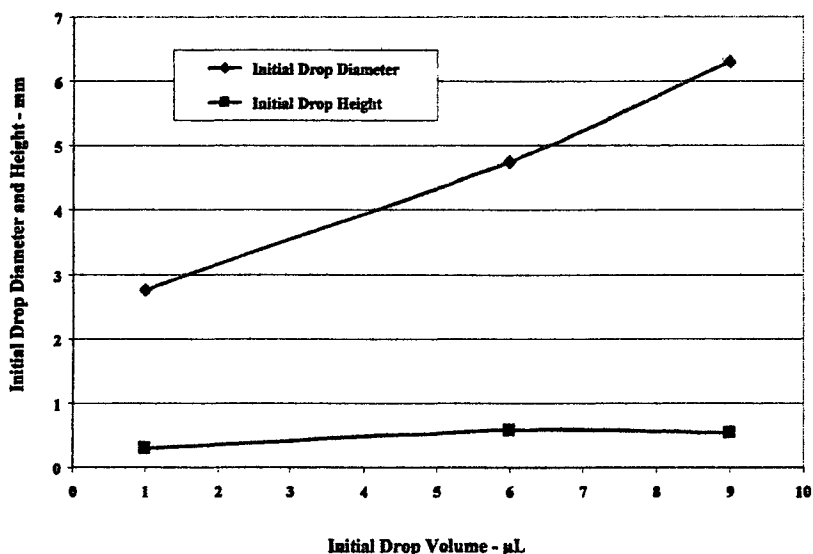


Figure 75. Results of Experiments for HD on Glass





**Figure 76. Drop Diameter and Height for HD/Glass as a Function of Initial Drop Volume**

Figure 77 shows where the top of the 5mm high drop would lie in the generalized boundary layer profile for each of the three test matrix velocities. Even at this low height, the upper two velocities are close to, but not within, the viscous sub-layer. However, the fact that their  $u^+$  and  $y^+$  terms are equal indicates that they are both still in the laminar region of the turbulent boundary layer.

The 5mm drop height on glass represents the highest projection of agent into the wind tunnel for the range of drop sizes being considered in the test program in that any sorbent substrate situation would result in essentially no drop height. Since the largest agent drop would always be in the laminar flow area of the velocity profile, its evaporation will not be influenced by the free stream turbulence level in the main wind tunnel airflow. Therefore, while the different Agent Fate wind tunnels may have different levels of free stream turbulence, it will not influence the evaporation rate data obtained.

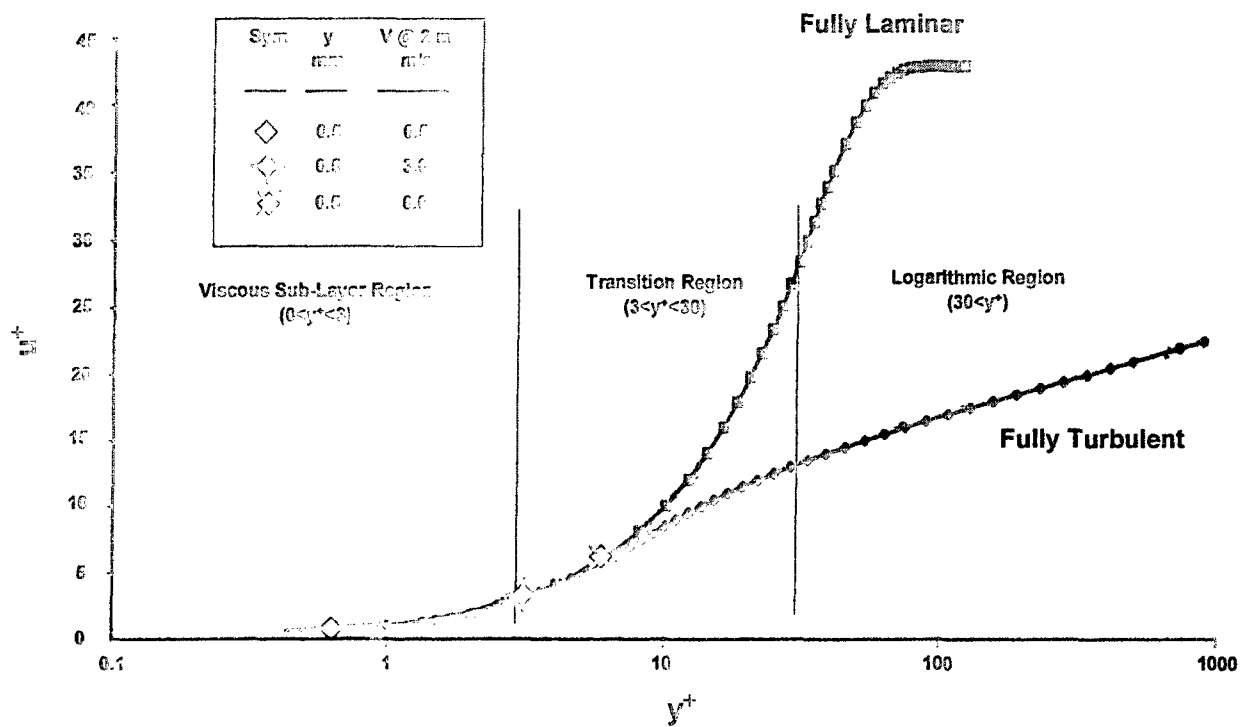


**Figure 77. Operational Velocities at Drop Height**

**6.3 5-cm Wind Tunnel Conditions**

Figure 78 shows the actual velocity values measured in the 5 cm tunnel at a height of 0.5 mm compared with their corresponding operational values. Note that all of the measured velocities are slightly higher than their corresponding operational values. This results in higher shear stresses at the surface and results in the measured velocities lying more out of the viscous sub-layer region of the boundary layer profile than for the operational cases. However, as shown in Figure 79, the measured velocity profile points are all close to the operational velocity profile points with respect to their locations in the same regions of the boundary layer, and thus should have a similar evaporation effect on the agent drop.

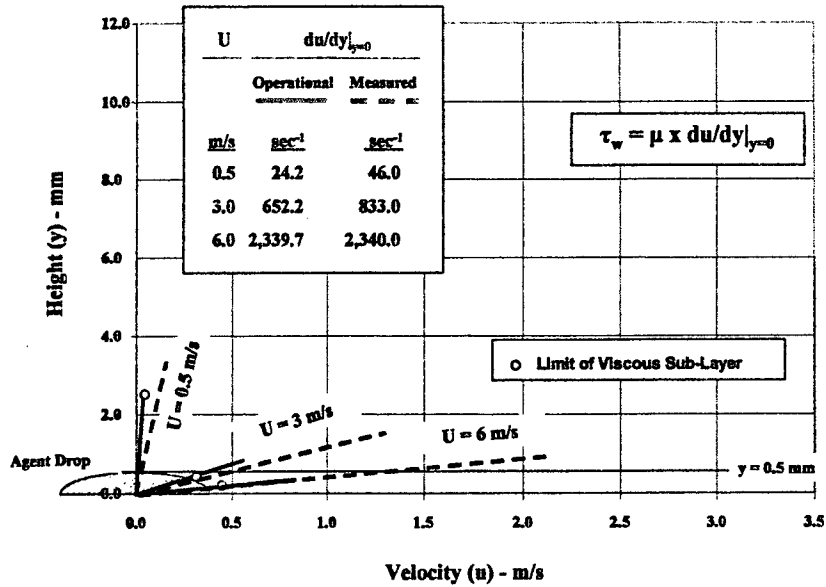


Figure 78. Measured Velocity Profiles and Associated Velocity Gradients for 5-cm Tunnel

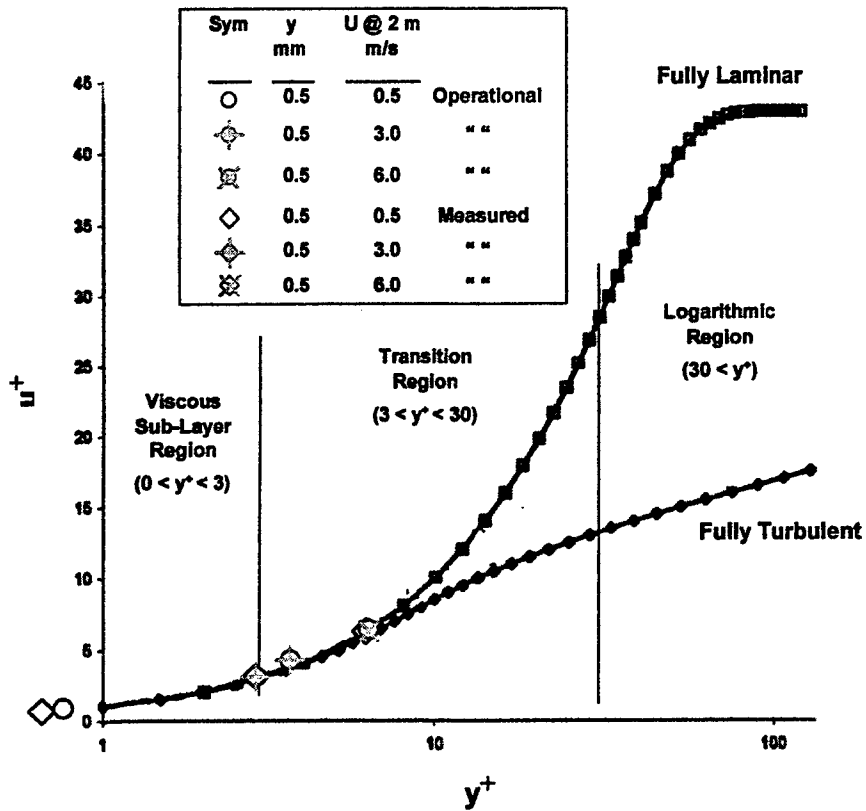


Figure 79. Comparison Between Measured and Operational Velocity Values (Close to Surface)

Free stream turbulence intensities were measured in the 5-cm wind tunnel for each of the three velocity conditions and are shown in Figure 80. Here the root mean square of the three orthogonal velocity fluctuations (due to turbulence) is referenced to the local total velocity. Thus, while the absolute free stream turbulence level is fairly constant throughout the tunnel, the intensity increases near the floor because the total velocity (the denominator in the turbulence intensity) decreases near the floor. As can be seen, the turbulence intensity ranges from about 0.5 to 2% for the low velocity and about 4 to 14% for the medium and high velocities. The low velocity data exhibits a markedly lower turbulence level and profile compared to the higher velocities further illustrating the laminar nature of the low velocity profile.

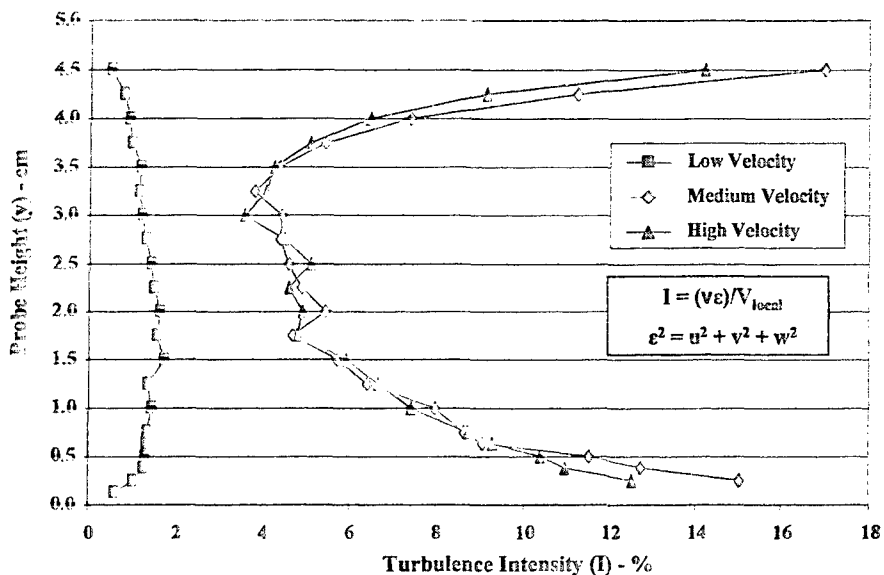


Figure 80. Turbulence Intensity of 5-cm Wind Tunnel

An appreciation of how this compares with the turbulence level in an atmospheric boundary layer can be gained by Figure 81, which contains atmospheric data obtained over a 24-hr period at Dugway Proving Ground.<sup>21</sup> The wind velocity and the square of the free stream turbulence intensity are shown as a function of time of day for an altitude of 120 m AGL. Note that the wind velocity ranges from 2 to 11 m/s with an average value of about 5 m/s during the day (0600 to 1800) and ranges from 0.5 to 4 m/s with an average value of about 3 m/s during the night (1800 to 0600). As shown in Figure 82, for the 120 m height, the turbulence intensity ranges from about 1 to 4% during the day and about 2 to 6% at night. This relates to an average turbulence intensity of about 3% during the day and about 3.5% during the night. The turbulence level is greater at night because while the absolute turbulence levels are about the same for day and night, the wind velocity (to which the turbulence is referenced) is lower during the night, resulting in a larger intensity value.

Figure 83 shows the wind velocity and turbulence level as a function of altitude measured just before sunrise. Note that the wind velocity increases with altitude up to a height of

about 360 m ranging from about 0.5 m/s near the ground to 10 m/s at 360 m/s. At the same time, the turbulence level remains fairly constant over the same altitude range. Thus, the turbulence intensity decreases with increasing altitude. Figure 84 shows the turbulence intensity as a function of altitude. Note that the turbulence intensity decreases with increasing altitude ranging from about 14% at ground level to about 0.2% at 300 m. At 120 m, the wind velocity is about 2.5 m/s and the turbulence intensity is 1.3%.

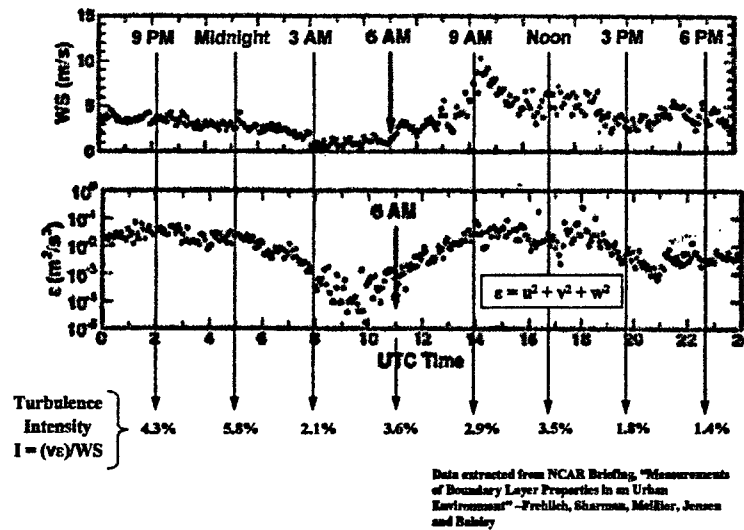


Figure 81. Atmospheric Turbulence Measurements at DPG Effect of Time of Day (z =120 m)

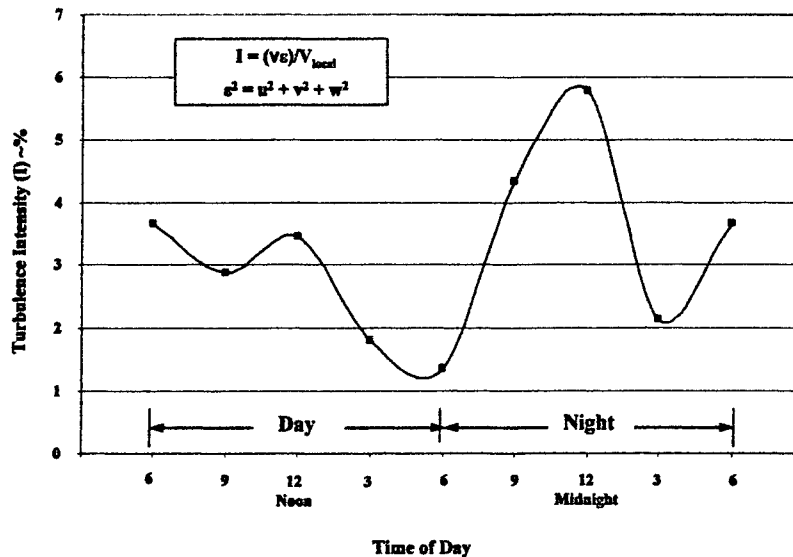


Figure 82. Turbulence Intensity vs. time of Day DPG, Height = 120 m

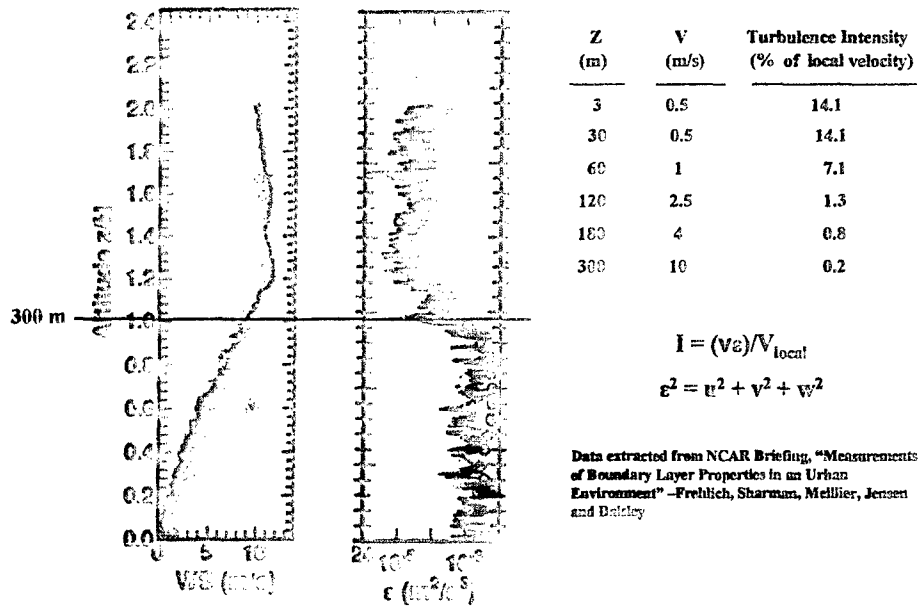


Figure 83. Atmospheric Turbulence Measurements at DPG Effect of Altitude, 6 AM

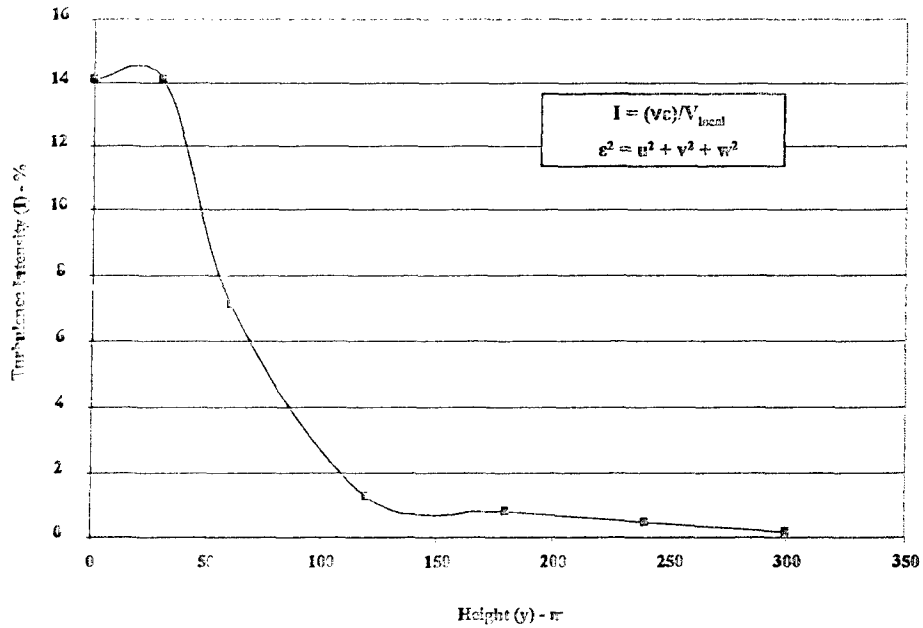


Figure 84. Turbulence Intensity vs. Height DPG, 6 PM

While this is a single example of the free stream turbulence levels in an atmospheric boundary layer, it is representative and illustrates that the 5-cm wind tunnel has a similar free stream turbulence levels. However, as noted previously, the free stream turbulence level in the wind tunnel does not affect the evaporate rates of the agents since the friction velocities and associated specific surface shear stresses are controlled.

## **7. TEST MATRIX**

### **7.1 General**

A test matrix consisting of a common set of test conditions was stipulated by the model developers for all Agent Fate wind tunnels and included the agents and substrates as well as the test parameters consisting of temperature, drop size, velocity and RH.

### **7.2 Agents**

The agents to be investigated are shown listed in order of their priority:

HD

VX

GD

Thickened VX

Thickened GD

### **7.3 Substrates**

A key feature of the substrate was its interaction with the agent. The substrates were resolved into four basic categories<sup>5</sup>:

1. non-absorptive, non-reactive
2. absorptive, non-reactive
3. non-absorptive, reactive
4. absorptive, reactive

The specific substrates to be tested were prioritized as follows along with their general substrate interaction characteristics noted above:

<u>Substrate</u>	<u>Category</u>
1. Glass	non-absorptive, non-reactive
2. Sand/Clay	absorptive, non-reactive
3. Concrete	absorptive, reactive
4. Asphalt	absorptive, reactive
5. Grass	absorptive, reactive

It should be noted that the Substrate/Category relation depends on the agent in that different agents interact differently with the various substrates. For example, some agents react with glass and sand. Also, variations in the same general type of substrate can affect its interaction with a chemical. For example, concrete can vary in surface texture, granularity and chemical composition. Except for grass, full-scale samples of all of the substrates listed can be tested in the 5-cm wind tunnel. Because its physical dimensions are too large for the 5-cm and 10-cm tunnels, grass can only be tested in large wind tunnel facilities with test section heights of approximately 0.5 m or greater.

#### 7.4 Test Parameters

The wind tunnel test matrix consists of three temperatures, three agent drop sizes (which could involve single and multiple drops), three velocities (as previously described) and two relative humidities. The original test matrix is shown in Figure 85.<sup>5</sup> These values were intended to cover a 5 to 95 percentile operational probability for three operational areas: Europe, Mid-East and Asia. The values have been modified as shown in light of practical limitations associated with the wind tunnel testing process. For example, the original small drop size of 0.0005  $\mu\text{l}$  required multiple drops to produce a sufficient amount of vapor for measurement by the instrumentation. It was determined that these drops could not be deposited onto the substrate and inserted into the tunnel before major evaporation occurred. Accordingly, the minimum drop size was increased to 1.0  $\mu\text{l}$  (with some tests to be performed with a 0.1  $\mu\text{l}$  drop in the 5-cm tunnel. Similarly, 90% RH values could not be created in the wind tunnel without condensation occurring.<sup>11</sup> Consequently, the maximum RH values were decreased to 50%. Temperatures of 0 °C were also found to be very difficult to create and sustain and was increased to 15 °C. Another problem was experienced in testing at 25 °C (near room temperature) and this was changed to 35 °C.



Agent	Temperature (° C)		
	Low	Mid	High
HD	15	35	<del>35</del> 50
VX	<del>0</del> 15	<del>25</del> 35	<del>35</del> 50
GD	<del>0</del> 15	<del>25</del> 35	<del>35</del> 50

Level	Neat Agent	
	Drop (µm)	Drop (µL)
Low	100	<del>0.0005</del> 0.1 to 1.0
Mid	750	<del>0.2</del> 6.0
High	2,600	<del>9.2</del> 9.0

Level	2m Wind Speed (m/s)
Low	0.5
Mid	3.0
High	6.0

Level	Thickened Agent	
	Drop (µm)	Drop (µL)
Low	200	<del>0.0042</del> 1.0
Mid	1,200	<del>0.91</del> 6.0
High	4,000	33.5

Level	Relative Humidity (%)		
	Low(°C)	Mid(°C)	High(°C)
Low	<del>35</del> 0	<del>20</del> 0	<del>5</del> 0
Mid	<del>05</del> 50	<del>35</del> 50	<del>45</del> 50
High	<del>95</del> 50	<del>90</del> 50	<del>90</del> 50

Note: Crossed out values indicate change from initial Test Requirements Document

Figure 85. Test Matrix Values<sup>5,11</sup>

To facilitate testing, a nomenclature code was established to define the first three test conditions. A set of three symbols: -, 0, and + were used to designate whether the test conditions were low, medium or high values of the temperature, drop size and velocity, respectively. Some variation in these values occurred depending on the agents and substrates being tested. Also, as the testing and modeling progressed, the test matrix was changed in that certain data were no longer needed. For example, it was found that the evaporation of HD was not affected by RH; thus, only a single RH value was tested. As shown in Figure 86, the testing arrangement is based on a "design of experiments" approach where the center point condition for the medium temperature (0 0 0) is repeated 6 times with the remaining points repeated twice.<sup>5</sup>

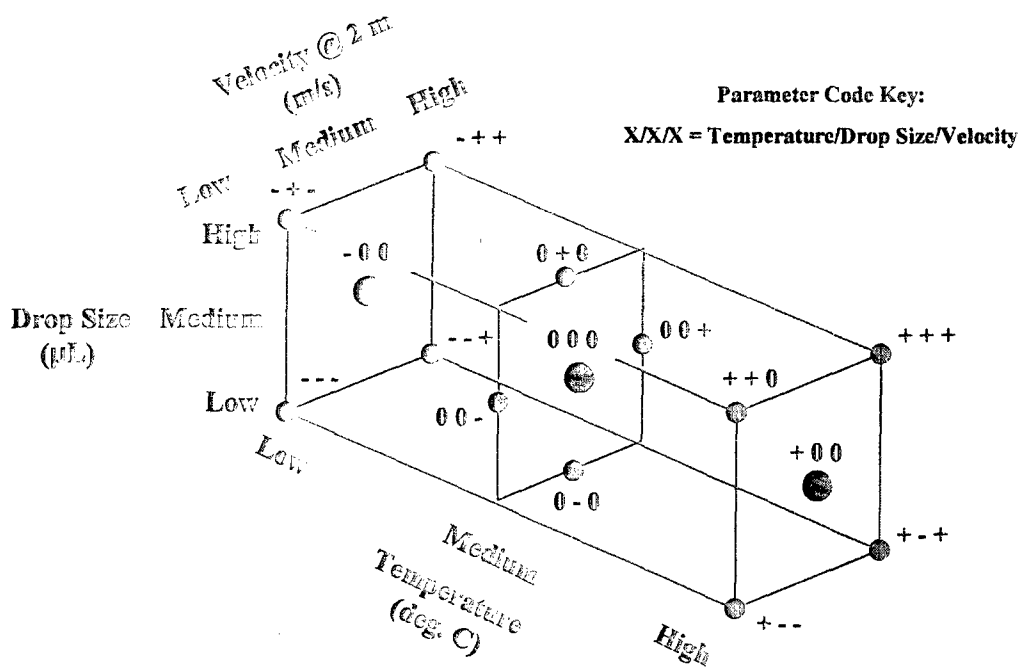


Figure 86. Basic Test Matrix Arrangement and Coding<sup>5</sup>

7.5

Validation Tests

A special test matrix was used to validate the various Agent Fate wind tunnels. These tests involved HD on glass, which is non-absorbent and non-reactive. This represented the simplest experimental situation and the absence of any absorption and reaction meant that all of the agent vapor could be accounted for by the vapor measuring instrumentation. This allowed the possibility of achieving a 100% agent mass balance that was an important factor for validating the wind tunnel operations. For other agent/substrate combinations such as agents that absorb or react with the substrate, a 100% agent mass balance based solely on vapor sampling is not possible. Thus, the HD on glass combination represented an ideal test for validating the operation of the wind tunnel and the vapor sampling techniques employed. The resulting data also provided a baseline set of data to allow comparison and interpretation of the data resulting from the more complex absorbent and reactive substrates.

Their nominal values are indicated below:

Temperature: 0, 35, 50 °C

Drop Size: 1, 6, 9 µL

Velocity @2 m: 0.5, 3.0, 6.0 m/s (defined operational wind conditions)

RH: 0%

These tests were originally to be performed at RH values of 0 and 50%. However, the fact that HD evaporation is not affected by humidity, allowed these tests to be performed in the 5-cm wind tunnel at 0 % RH. This resulted in 34 test runs required for the validation phase. Termed the "Validation" test matrix, it involved HD on glass (the glass representing a non-absorbent, non-reactive substrate) and is shown in three-dimensional diagram form in Figure 87.

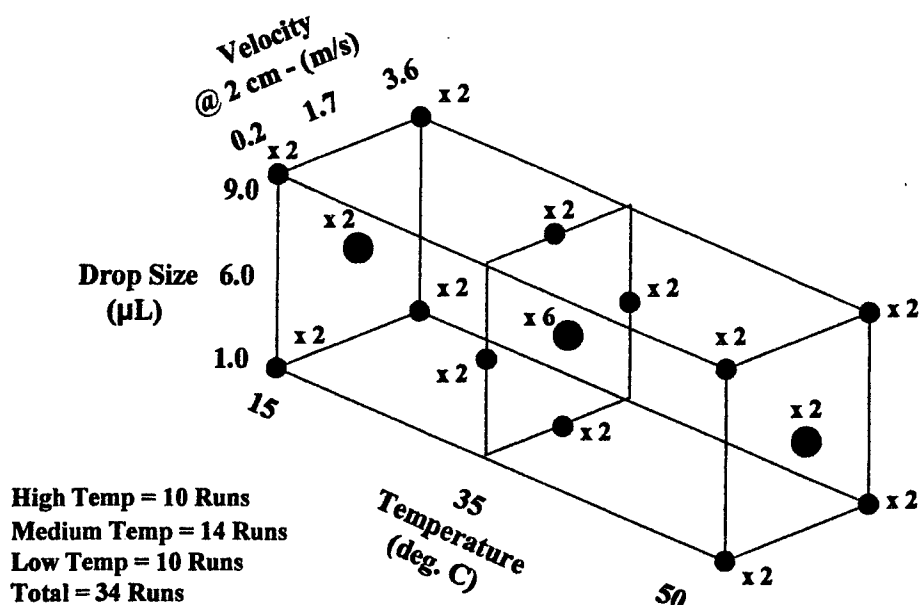


Figure 87. Validation Test Matrix HD/Glass<sup>5</sup>

## 7.6 Production Runs

With the "Validation" tests completed, the program then entered the "production" testing phase. This involved testing agents with the more complex substrates. These tests involved a slightly different test matrix shown in Figure 88. The only difference between the production and validation test matrix is that the former includes different low and mid temperatures and, in the case of VX and GD, requires testing at multiple values of RH. The resulting test program involves a total of 54 runs. Note also, that the RH values used are a function of the temperature.

\* Temperature: VX/ED

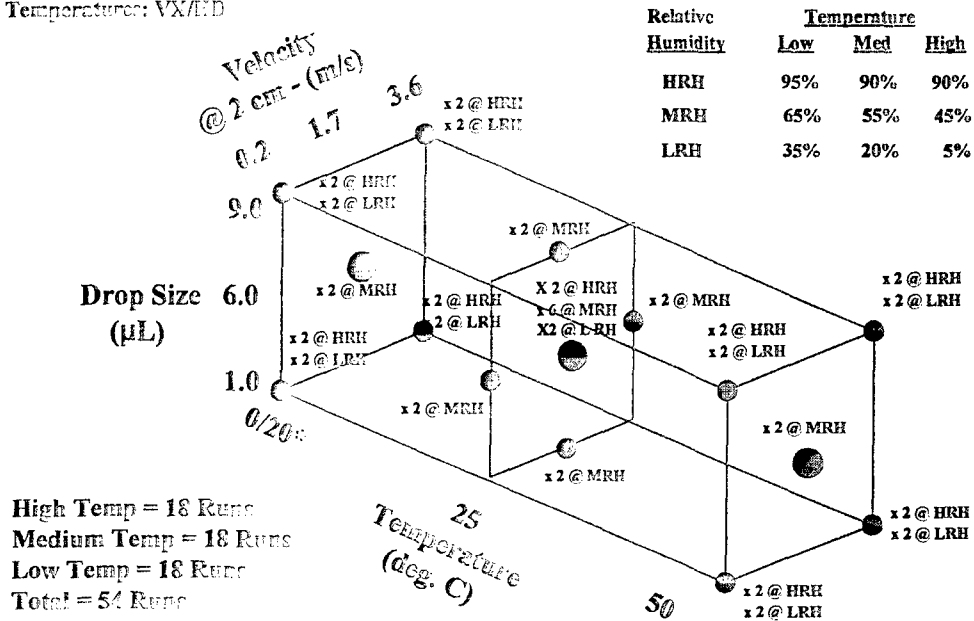


Figure 88. Production Test Matrix<sup>5</sup>

## 8. INSTRUMENTATION

Data acquisition and associated instrumentation for the 5-cm wind tunnel was the primary responsibility of the Agent Chemistry Team. Data acquisition represents an extremely challenging aspect due to the strict need to maintain the liquid and volatilized agent and substrate at a constant temperature throughout the wind tunnel and to accurately measure the large range of vapor concentration levels produced over the duration of the experiment. An array of sensors and control elements were required to establish and maintain the constant velocity, temperature and RH conditions<sup>11, 13</sup>:

- Aalborg mass flow sensor and controller at entrance to transition cone
- Wall temperature sensors in transition cone, fetch, test section, piston, mixing section and static mixer
- Air Temperature sensor in test section
- RH sensor in test section
- Reference velocity hot wire anemometer in test section

In addition, the entire tunnel structure was covered with a thermal insulation and temperature controlled blanket.

Three different instruments were employed to measure the agent vapor concentration at the sampling location in the exhaust section of the wind tunnel:

- Variable Tube Sampler (VTS) sampling port in exhaust section
- Hapsite GS/MS sampling port in exhaust section
- HYFED vapor analyzer probe in exhaust section

The Variable Tube Sampler (VTS) was selected as the primary means of vapor sampling after extensive testing of several different types of instruments. Samples of the chemical vapor/air mixture are periodically drawn off at the sampler port and directed to the VTS, which is composed of two banks of 15 standard, DAAMS vapor collection tubes. The flowrate of agent/air into a tube can be adjusted and, when the tube is full, switched to a fresh one.

The Hapsite is a portable, Thermal Desorption - Gas Chromatography - Mass Spectrometer (TD-GC-MS) and provides a relatively rapid analysis of the vapor concentration as a function of time. The Hapsite samples 225 ml of agent vapor/air over a 3-min time increment. A period of 30 min is then required to analyze the sample and provide the concentration value measured. The system is automatically purged and a new sample taken.

The HYFED samples a 250 ml/min flowrate of agent vapor/air mixture every 5 s and indicates the agent vapor concentration on a real-time basis. However, it only provides qualitative values of concentration. While not accurate enough to be used as a main vapor measuring instrument, it is employed for pre-test screening to provide an estimate of maximum concentration values for the test. These results were used to determine whether to employ the VTS, Hapsite or a combination of the two as well as to determine their optimum sampling time increment settings.

Additional insight was gained through the use of digital video cameras that viewed the drop/substrate through the side window as well as from a port in the test section ceiling. These provided orthogonal views of the sessile drop and the resulting recordings were analyzed to provide the drop volume time history. This was particularly important in validating the vapor measurement data, particularly the total drop life time. An internal light was later added to the test section to illuminate the substrate area for enhanced observation and recording purposes. Figure 89 graphically depicts the instrumentation used to monitor, control and acquire the data during each 5-cm wind tunnel run.

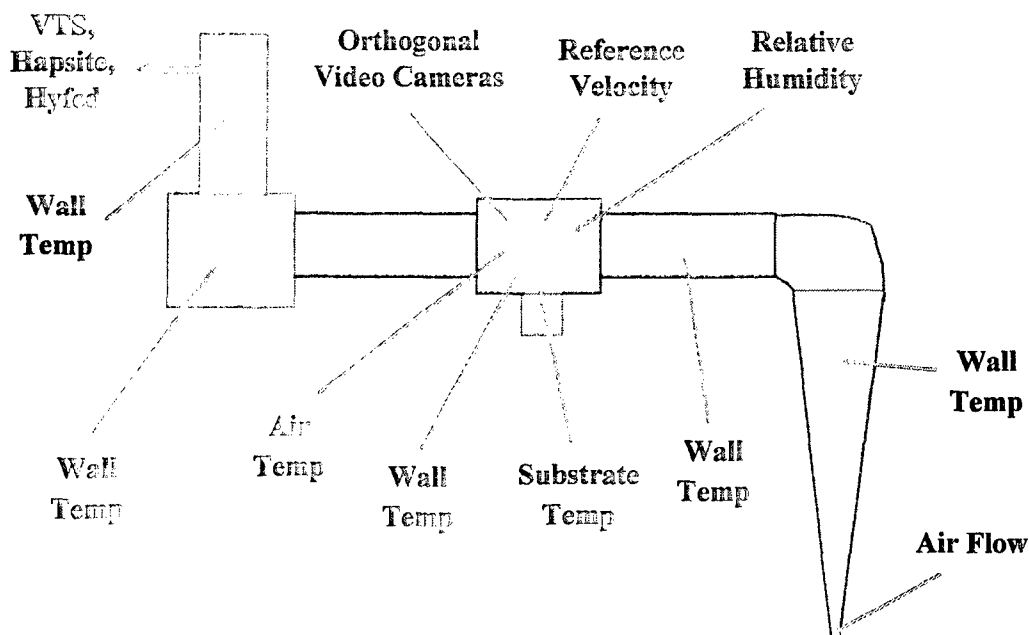


**Figure 89. Summary of Instrumentation Used with 5-cm Wind Tunnel<sup>11,13</sup>**

## 9. EXPERIMENTAL PROCEDURE

This section describes the experimental procedure evolved by the Agent Chemistry Team.<sup>4, 6, 11, 13, 14, 16, 18</sup> As noted previously, while the main test apparatus is termed a wind tunnel, it represents a highly complex laboratory experimental arrangement. Its use involves the measurement of phenomena which, because of the small scales and accuracies involved, had no historical precedence in the scientific community. In addition to requiring new and unique measuring instrumentation, special testing procedures had to be evolved to achieve the desired results.

A typical testing procedure began with the substrate being tested placed on the piston, which was then inserted into the tunnel. The tunnel was then operated at the desired test conditions sufficiently long to achieve constant airflow and temperature conditions throughout. The tunnel airflow was then turned off to allow the piston to be extracted from the tunnel. The substrate was removed and the agent deposited on to the surface of the substrate by means of a manually operated pipette. In some instances, the substrate was weighed before being inserted into the wind tunnel (for other tests, weighing was not performed). Next, the substrate with the agent was placed back onto the piston and the piston was reinserted in the tunnel. The wind tunnel airflow was re-established and a few minutes were required for the tunnel to again achieve the constant temperature and velocity conditions desired.

The tunnel air flowrate was established by measuring the velocity in the test section at a reference height above the test section floor using a hot wire anemometer and adjusting the Aalborg flow controller to achieve the test matrix reference velocity desired (in the initial phase of testing, this reference height was 2 cm, but was later changed to 1 cm to obtain a velocity setting closer to the drop/substrate). Based on the previous velocity characterization\*, this provided the stipulated velocity profile in the test section as shown in Figure 90. The velocity values at a 2 cm height are the source of the 0.22, 1.7, and 3.6 m/s for the low, medium and high operational velocities, respectively.

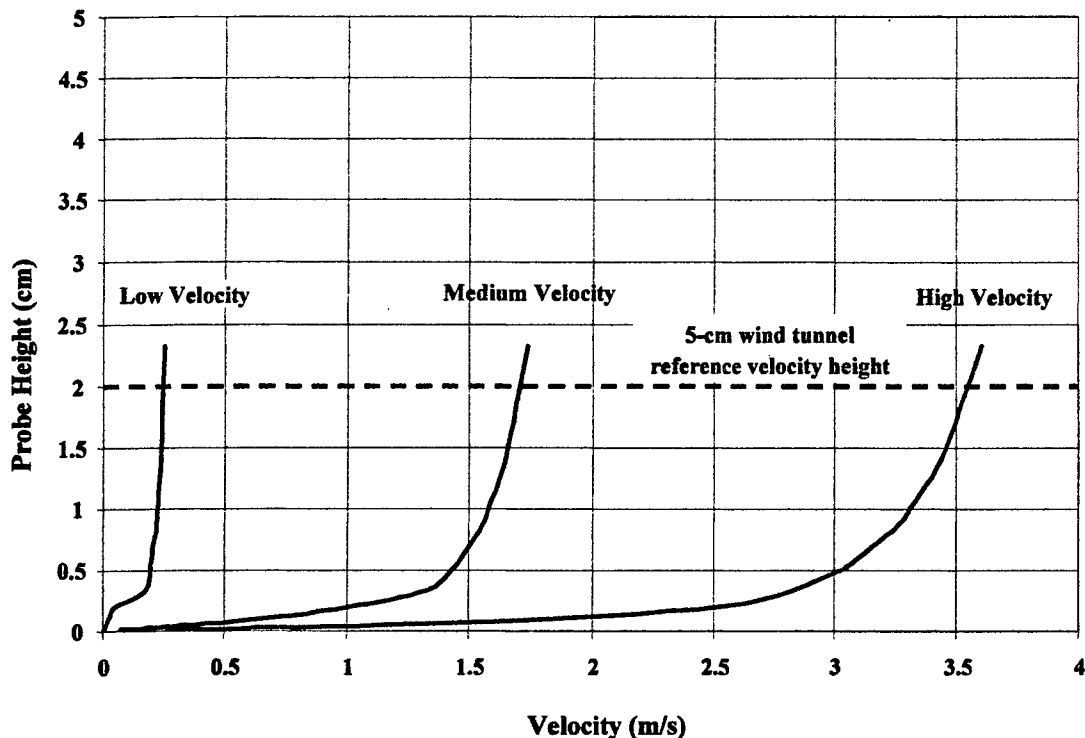


**Figure 90. 5-cm Wind Tunnel Reference Velocities**

An initial "scouting" run was usually made at the desired test conditions using a real time HYFED vapor detector. This determined the length of experiment, the approximate concentration range, the sampling period, requirement for any split ratios, and the optimum time increment between sampling. From these data, a decision was made as to which type of vapor collection instrument to use: the Hapsite (for relatively long run times) or the Variable Tube Sampler (for relatively short run times) or a combination of the two. The VTS was usually employed for mid-temperature and high temperature experiments and the Hapsite for cold temperature experiments.

\*Weber, D.; Scudder, M.; Moury, C.; Shuely, W.; Molnar, J.; Miller, M. Velocity Profile Characterization for 5-cm Agent Fate Wind Tunnel; U.S. Army Edgewood Chemical Biological Center: Aberdeen Proving Ground, MD; 2006, UNCLASSIFIED REPORT, unpublished data.

Samples of the agent vapor/air mixture were periodically drawn off at the sampler port and directed to the Hapsite and/or the VTS. In the case of the VTS, the tubes were transferred to an automated tube desorber system for analysis by an Agilent GC/MS. The total test time depended on the agent/substrate being tested as well as the test conditions and could range from 30 min to 48 hrs. The resulting data were automatically stored in the associated computer system are reduced to standard form as prescribed by the Agent Fate Program. All aspects of the data acquisition system are computer controlled. The data acquisition and analysis process is diagrammed in Figure 91.

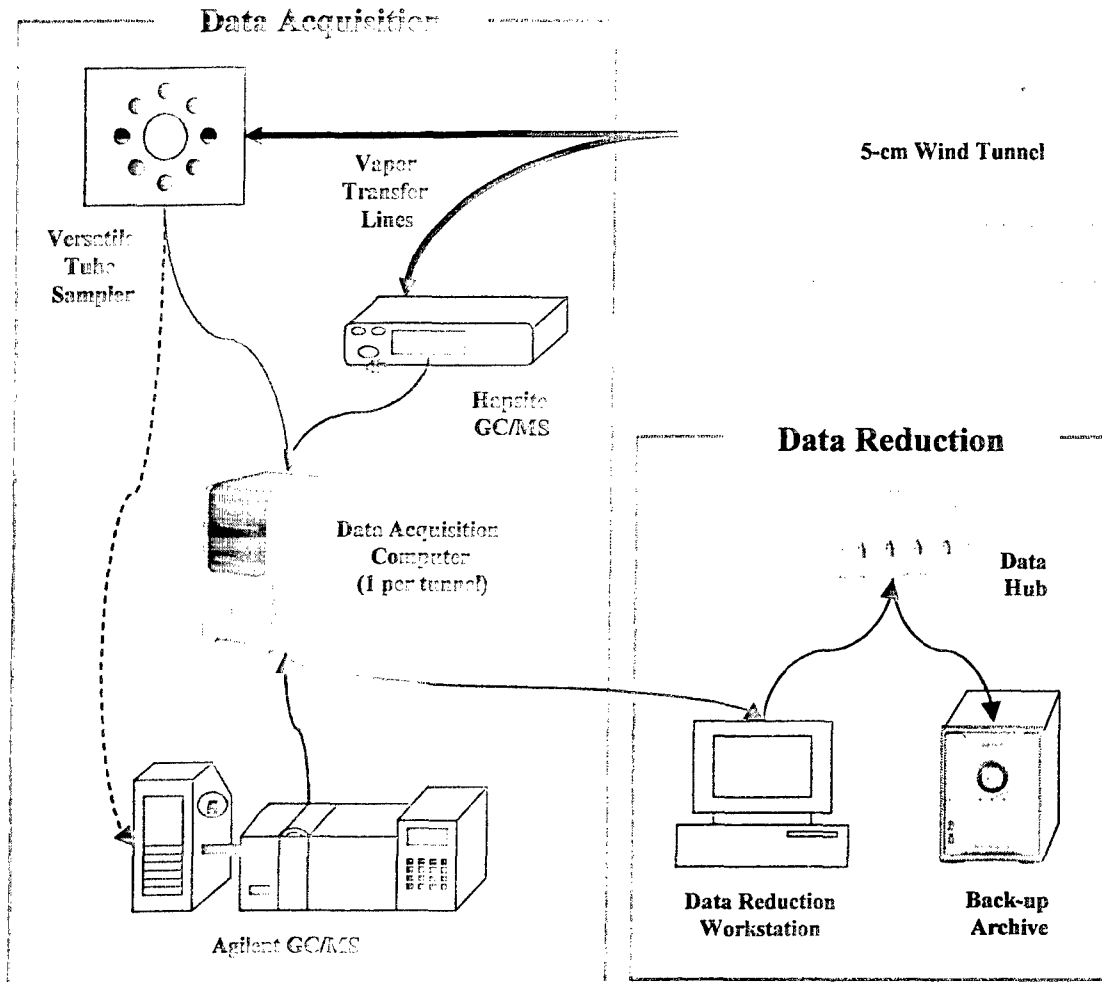


**Figure 91. Flow Diagram for 5-cm Wind Tunnel Data Acquisition and Analysis Process<sup>11, 13</sup>**

Figure 92 shows video measurements of the agent drop volume as a function of time and compares the evaporation rate computed from these results with data obtained through agent vapor measurements.



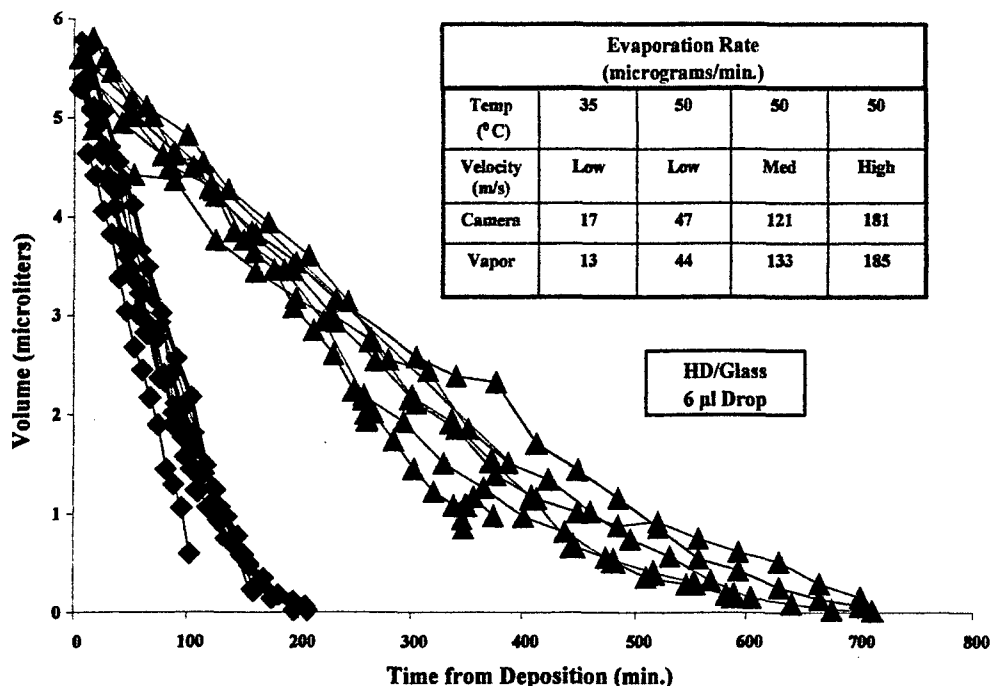


Figure 92. Example of Video Data and Results<sup>11, 13</sup>

## 10. 5-CM WIND TUNNEL DATA

### 10.1 Agent Mass Balance

A near 100% agent mass balance (i.e., accounting via vapor analysis, extraction or other losses) for all the agent initially deposited on the substrate) was initially considered as a key factor in demonstration of the operational validity of the wind tunnel and instrumentation arrangement. As anticipated, there were numerous independent processes that caused the agent mass balance to differ from a perfect 100%. Many of these were resolved during the development process. However, achieving a perfect mass balance was probably never a realistic goal and goals of 95 to 105% or wider ranges were proposed as practical alternatives. Reasons for deviations from a perfect mass balance can be attributed to three areas: wind tunnel design issues; vapor analysis issues; and complex interactions between the two. Only the discussion of wind tunnel design issues will be considered here.

Considerable difficulties in achieving the desired agent mass balance of 95 to 105% were experienced during the development of the 5-cm wind tunnel. This was mainly resolved by assuring that the airflow, wind tunnel walls and agent/substrate remained at a constant temperature throughout the test and the use of the Variable Tube Sampler for agent vapor sampling. Although the desired agent mass balance was not achieved for many of the 5-cm tunnel validation tests, the non-absorbent, non-reactive nature of the HD/glass tested allowed the actual mass balance obtained to be used as a correction factor for the measured evaporation rates.

10.2

Evaporation Rate as a Data Metric

All of the data from the wind tunnel tests were provided to the model developers in a designated format for use in generating Agent Fate models. While not representing the only data of interest to the Agent Fate model developers, the initial evaporation rate was an easy to calculate and physically meaningful metric to use to assess the quantitative values and parametric trends of the wind tunnel data.<sup>13, 14, 16, 18</sup> The agent mass remaining vs. time was a standard plot obtained during the wind tunnel tests. The slope of this curve over a particular time increment represents the evaporation rate during that time period. These evaporation rates can be used to formulate trends with the various test parameters as well as establishing correlation with theoretical analyses and other experimental results.

A standardized, statistical process was established for reducing the wind tunnel data to a common format so that the data from each of the Agent Fate wind tunnel facilities could be directly compared. The experimental agent mass vs. time data obtained from each facility was assessed using various curve fitting techniques including cubic spline, 3<sup>rd</sup> degree polynomial and linear spline with the latter being found to provide the best fit. In the case of HD on glass, this approach divides the agent mass remaining vs. time data trace into three linear segments. As shown in Figure 93, the result is a very accurate fit over the entire range of validation test matrix conditions including the tail-off at the end. This good fit was present for data from the 5-cm and 10-cm wind tunnels.

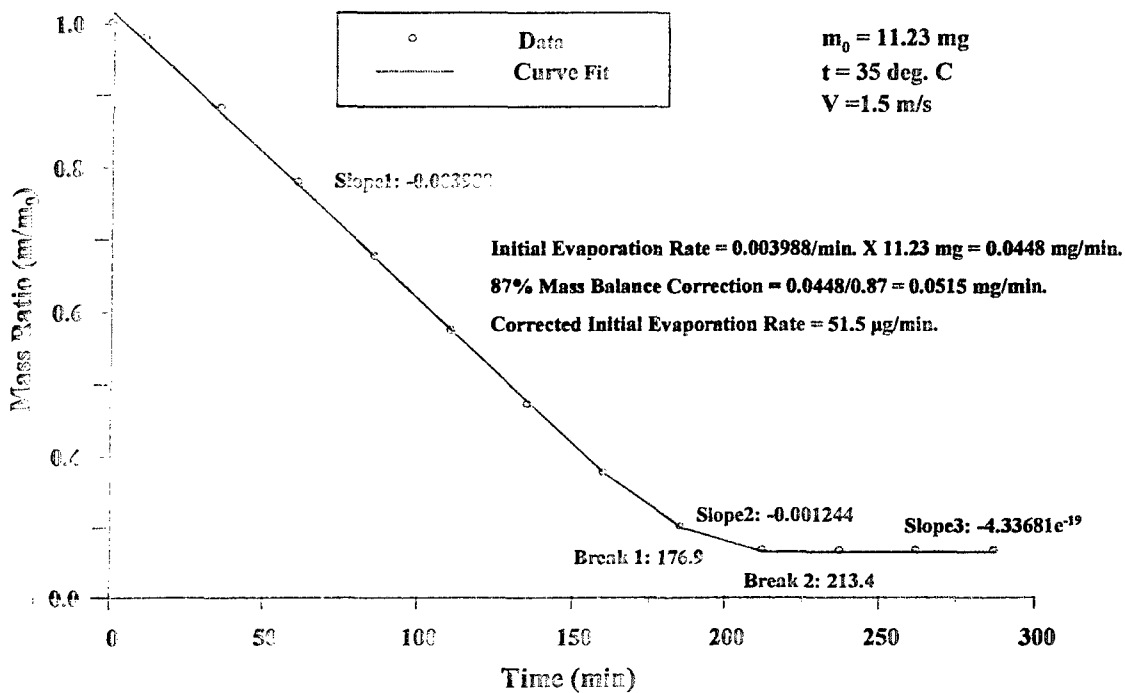


Figure 93. Typical Wind 5-cm Wind Tunnel Data (9 µl Drop of HD on Glass)

Based on the results of the previous statistical evaluation, the initial evaporation rate was selected as a standard term for comparing the data from the various Agent Fate wind tunnels. For HD on glass, the evaporation rate vs. time curve can be resolved into three distinct and constant slopes. The slope of this curve at any point in time represents the evaporation rate at that time. The initial slope is the steepest and relates to the highest evaporation rate. It typically lasts for about 50 to 90% of the drop life and represents a near constant evaporation rate over that time period. The second distinct slope lasts for about 5 to 25% of the total drop life and is less steep than the first indicating a slightly lower evaporation rate. The third slope lasts for the final 0 to 25% of the drop life and represents a very low evaporation rate or a zero slope plateau, indicating the absence of HD volatilization. The initial slope and its associated evaporation rate can be easily and accurately measured and provides an excellent metric to assess the repeatability of a particular tunnel as well for comparison of data between different tunnels.

The evaporation is proportional to the surface area of the droplet exposed to the air and the surface area depends on the drop shape during evaporation. Three linear slopes describe the two basic shapes the sessile drop assumes during the evaporation process. During the initial phase, the drop height (and volume) decrease while its base area on the surface of the substrate remains constant. The contact angle between the outer edge of the drop and the substrate constantly changes. Since the surface area is decreasing only very slightly as the drop volume decreases with a constant base, the slope will be near linear. The third linear evaporation phase occurs as the drop diameter (and base area) diminishes and ends when the drop is completely evaporated; this is a non-linear process, but can be approximated by a linear slope for small intervals. In some cases, the third slope represents a return to the zero-concentration baseline, which is the case in Figure 93. The contact angle remains constant during this latter phase. The second or middle linear region represents the transition between the two phases and this small, non-linear region can also be approximated with a linear slope.

Figure 93 also illustrates the correction process to account for the mass balance. This involves dividing the measured evaporation rate by the fractional mass balance. Note, that in Figure 93, after a correction for the 87% mass balance to a nominal 100%, the Break 1 to Break 2 points define a middle region of about 8% of the drop life with the third region representing less than 1%.

It should be noted that the three slope mass change with time characteristic of HD on glass would not necessarily be the case for other agents and substrates, especially if no sessile drop is present. However, it provides a simple and straight forward means of evaluating and comparing data from the Agent Fate Validation runs. The data sets discussed in the flowing sections compare the validation test results obtained from the various Agent Fate wind tunnels.

### **10.3      HD/Glass**

As noted previously, the agent mass loss due to evaporation for HD on glass is linear with time over a considerable proportion (on the order of 50%) of the total drop life. This slope represents a constant evaporation rate for the agent and provides an operationally meaningful term to assess the results of the wind tunnel tests. Table 2 summarizes the mean evaporation rates measured in the 5-cm tunnel during its validation tests<sup>6, 11, 13</sup>. While several repeat runs had been performed at

each test matrix condition, for clarity, only the mean or average values are presented. The data spread for all of the combinations of conditions tested was relatively small resulting in distinct groupings of the data.

The initial validation tests were performed in Tunnel 3A (Spartan) at medium and high temperature conditions. When the second tunnel (Tunnel 3C, Grizzly) was brought online, tests were conducted at condition (+ 0 0). The resulting evaporation rate closely matched that previously achieved in the 3A tunnel demonstrating the feasibility of using multiple 5-cm wind tunnels in the Agent Fate program. Subsequently, for the 5-cm validation tests, the data for the mid and high temperatures were obtained in tunnels 3A and 3C and the low temperature data were obtained in Tunnel 3D (Penguin).

**Table 2. Summary of 5-cm Wind Tunnel Validation Test Data<sup>6, 11, 13</sup>**

Code	Temperature deg. C	Drop Size μl	Velocity @ 2cm m/s	Velocity @ 2 m m/s	Mean Evaporation Rate μg/min.
- - -	15	1	0.22	0.5	1.5
- 0 -	15	6	0.22	0.5	3.1
- + -	15	9	0.22	0.5	4.1
-- 0	15	1	1.7	3	
- 0 0	15	6	1.7	3	11.7
- + 0	15	9	1.7	3	
-- +	15	1	3.6	6	5.6
- 0 +	15	6	3.6	6	
- + +	15	9	3.6	6	19
0 - -	35	1	0.22	0.5	
0 0 -	35	6	0.22	0.5	20
0 + -	35	9	0.22	0.5	
0 - 0	35	1	1.7	3	14.5
0 0 0	35	6	1.7	3	37.6
0 + 0	35	9	1.7	3	53.7
0 - +	35	1	3.60	6	
0 0 +	35	6	3.60	6	63.2
0 + +	35	9	3.60	6	
+ - -	50	1	0.22	0.5	21.6
+ 0 -	50	6	0.22	0.5	42.8
+ + -	50	9	0.22	0.5	51.2
+ - 0	50	1	1.7	3	45.6
+ 0 0	50	6	1.7	3	100.2
+ + 0	50	9	1.7	3	196
+ - +	50	1	3.6	6	66.9
+ 0 +	50	6	3.6	6	
+ + +	50	9	3.6	6	272

As can be seen from Table 2 not all of the validation test matrix conditions were measured. This was due to technical difficulties experienced in evolving a satisfactory wind tunnel configuration and associated instrumentation, which took more time than anticipated. Accordingly, once it was felt that sufficient HD on glass tests had been conducted to validate the experimental

arrangement, program schedule considerations required progressing into testing of other substrates. While not representing the complete set of test conditions originally desired, the non-linear nature of the data as well as the ability of the resulting data to validate the operation of the 5-cm wind tunnel was subsequently demonstrated as described in Sections 11.0 and 12.0.

## 11. THEORETICAL ANALYSIS OF EVAPORATION RATE

To assess the dependence of the evaporation rates measured in the wind tunnel validation tests to the main parameters involved, a theoretical analysis was completed<sup>22</sup>. The analysis was based on the evaporation of a sessile drop of liquid on a non-absorbent, non-reactive surface under the influence of a velocity profile that is linear based on a 2-dimensional integral boundary layer technique. This airflow condition is similar to that present in the viscous sub-layer of the boundary layer flow being simulated in the Agent Fate wind tunnels and provided a significant insight into the influence of velocity, drop size and temperature on the evaporation rate. The results indicated that the evaporation rate is a non-linear function of velocity and drop diameter. Specifically, the evaporation rate is a function of the friction velocity to the 0.67 power.

$$M = 0.624 C(T) [U_\tau d/\nu]^{2/3}$$

Where

M = Drop evaporation rate

C(T) = Combination of air and vapor thermodynamic variables

$U_\tau$  = Friction Velocity =  $\sqrt{\nu} (du/dy)|_{y=0}$

d = Drop diameter

$\nu$  = Kinematic viscosity

The analysis indicated that the evaporation rate is proportional to the velocity and drop size to the 2/3<sup>rd</sup> power. This means that the evaporation rate will tend to flatten out with increasing velocity and drop size. This was not visually apparent from the plot of evaporation rate vs. velocity, but was later verified by the statistical analysis of the 5-cm wind tunnel data.

## 12. STATISTICAL ANALYSIS OF EVAPORATION RATE DATA

As noted previously, only 19 of the 27 validation test matrix data points were obtained for HD on glass in the 5-cm wind tunnel. A statistical analysis of the validation test data from the 5-cm wind tunnel was performed.<sup>23</sup> The analysis had several purposes. One was to determine whether the existing data points were sufficient to assess the non-linearity of the trends predicted by the theoretical study or if additional data points were required. The statistical analysis also provided a

means of evaluating off-design data point values where the exact velocity, drop size or temperature established in the wind tunnel was not exactly equal to the desired test matrix value. Finally, it provided a means of comparing the data between the various Agent Fate wind tunnels.

In the case of the 5-cm tunnel, 17 unique conditions were run out of the 27 possible combinations required by the validation test matrix. This resulted in a G-Efficiency\* of 63%. The approach was to perform a regression procedure based on only the interior points and use the corner points of the test matrix to check the predictive validity of the resulting model. These revealed trend curves for the evaporation rate as a function of velocity, drop size and temperature.

Most significantly, the analysis indicated that the evaporation rate was a non-linear function of velocity where the evaporation rate flattens out with increasing velocity. This finding confirms the results of the theoretical analysis noted previously. This was not apparent from visualizing the plot of evaporation rate vs. velocity data, but could be extracted by the statistical analysis process. A series of 2-D and 3-D plots were formulated depicting the evaporation rates vs. the three basic parameters. Figure 94 illustrates the 3-D plot of Evaporation Rate as a function of velocity and drop size for the 35 °C temperature test condition as determined from the statistical analysis of the 5-cm wind tunnel data. Note that the evaporation rate is a non-linear function of velocity and drop size.

While additional data would be desirable to more accurately establish the trend lines and to provide check points, the analysis demonstrated that sufficient data points were available to validate the wind tunnel, indicate non-linear relationships between the parameters, and to compare the data between the different Agent Fate wind tunnels.

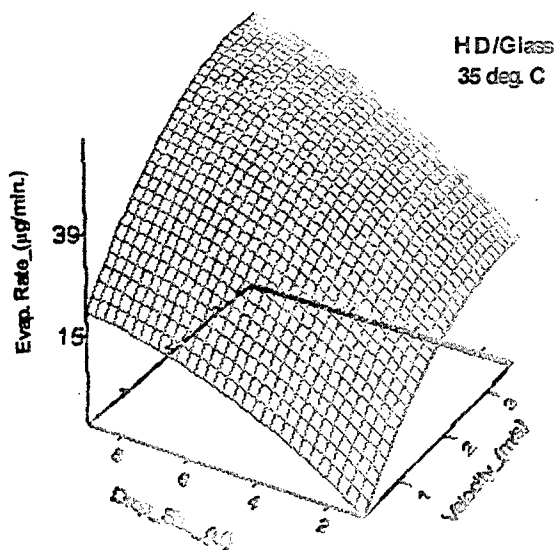


**Figure 94. 3-D Plot of 5-cm Data Developed by Statistical Analysis<sup>23</sup>**

- Note: A higher G-efficiency means that there will be higher correlations among the effects estimates making a cleaner analysis of the data possible. G-efficiencies in excess of 50% are considered to be adequate for yielding good predictive models over the design space.

Following this statistical approach, the 5-cm wind tunnel validation test data were used by the authors to develop the plots<sup>24</sup> shown in Figures 95 through 112. The figures contain both the statically determined constant parameter value trend lines as well as the individual experimental data points used to develop the lines. The figures are presented in sets of three with each set showing the Evaporation Rate plotted against a different set of the three main test matrix parameters: Velocity, Temperature, and Drop Volume. Accordingly, each plot presents a slightly different perspective as to the relative effects of each parameter. It should be noted that the trend lines shown in each plot provide a predictive capability only for the test data set within the domain of values used in the validation test matrix. Interpolation within these boundaries gives very good agreement with experimental data. However, extrapolation beyond these boundaries is not valid.

Figures 95 through 97 contain Evaporation Rate vs. Velocity and Temperature for the three drop volumes, respectively. These plots clearly reveal the non-linear nature of Evaporation Rate on Velocity. Also of note is that the low velocity is very close to a “no-wind” condition providing just enough airflow to prevent any accumulation of agent vapor around the drop.

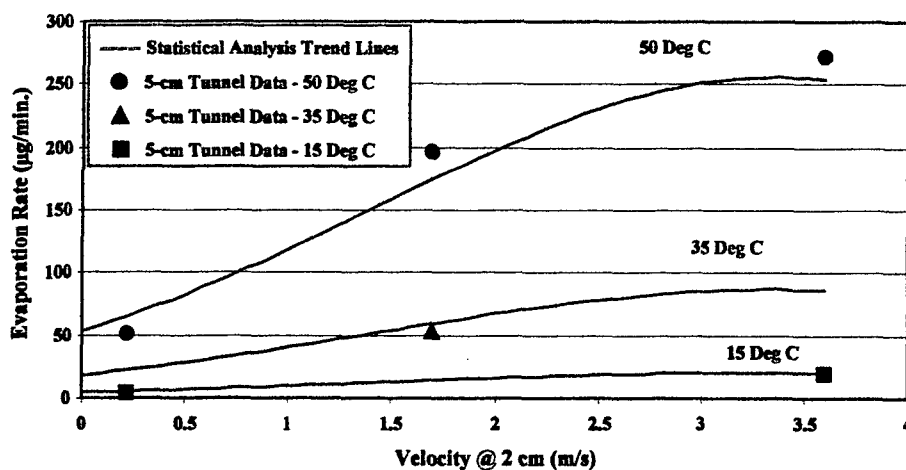


**Figure 95. Statistical Analysis of 5-cm Wind Tunnel Data Evaporation Rate vs. Velocity and Temperature HD on Glass for 9 µl Drop**

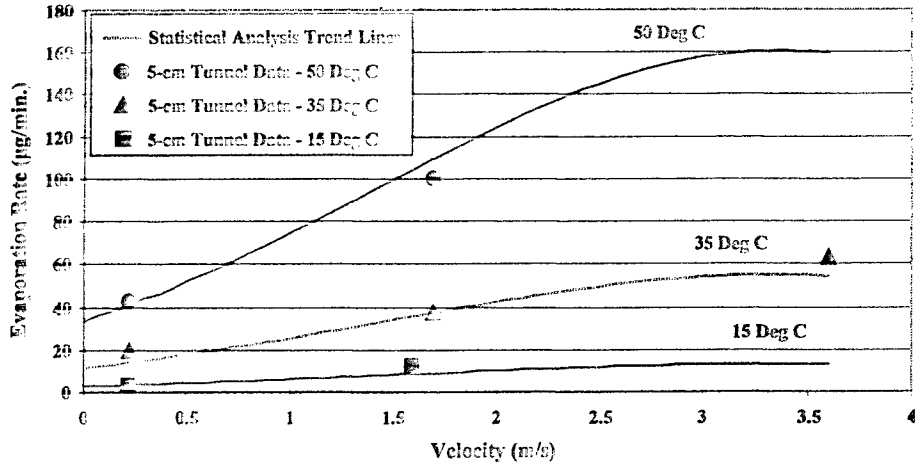


**Figure 96. Statistical Analysis of 5-cm Wind Tunnel Data Evaporation Rate vs. Velocity and Temperature HD on Glass for 6 µl Drop**

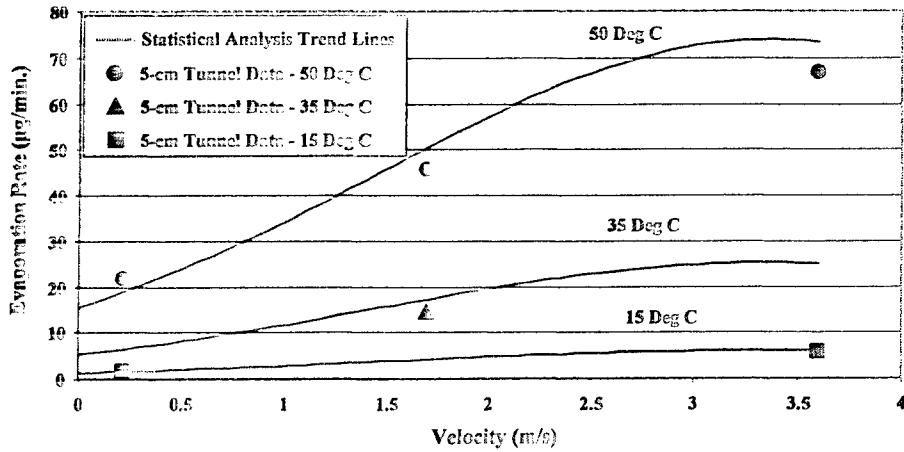


**Figure 97. Statistical Analysis of 5-cm Wind Tunnel Data Evaporation Rate vs. Velocity and Temperature HD on Glass for 1 µl Drop**



Figures 98 through 100 portray Evaporation Rate vs. Velocity and Drop Size for the three Temperatures, respectively.

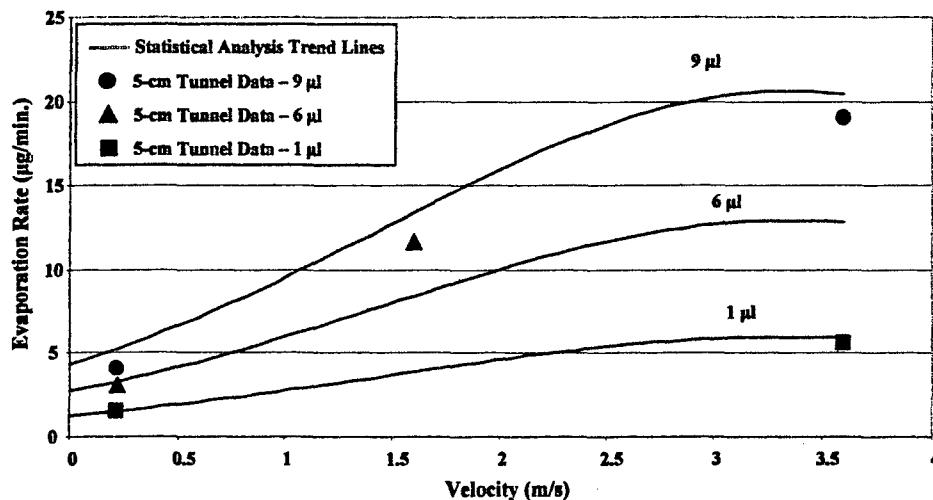


Figure 98. Statistical Analysis of 5-cm Wind Tunnel Data Evaporation Rate vs. Velocity and Drop Volume HD on Glass at 15 °C

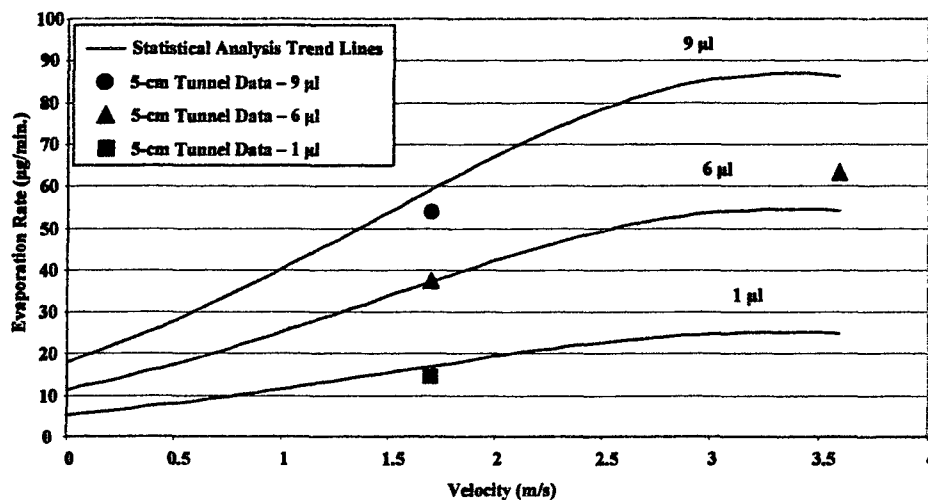
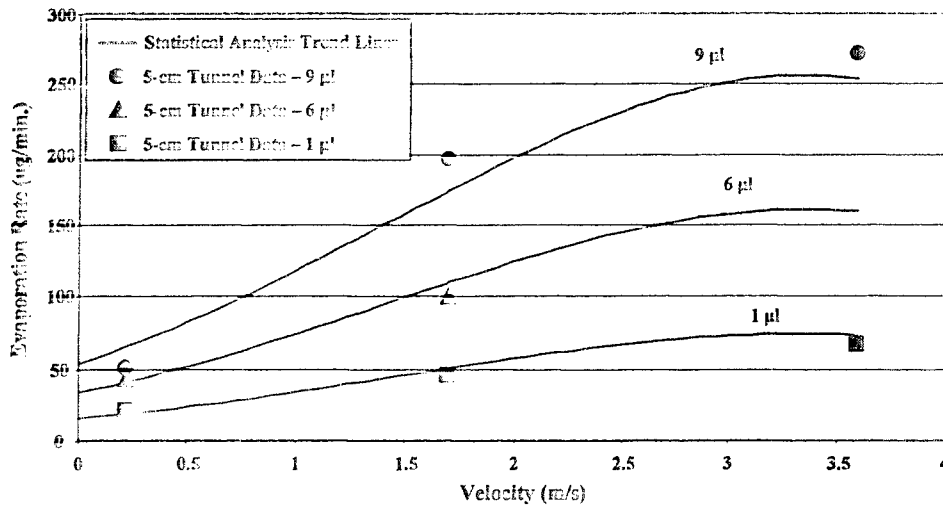
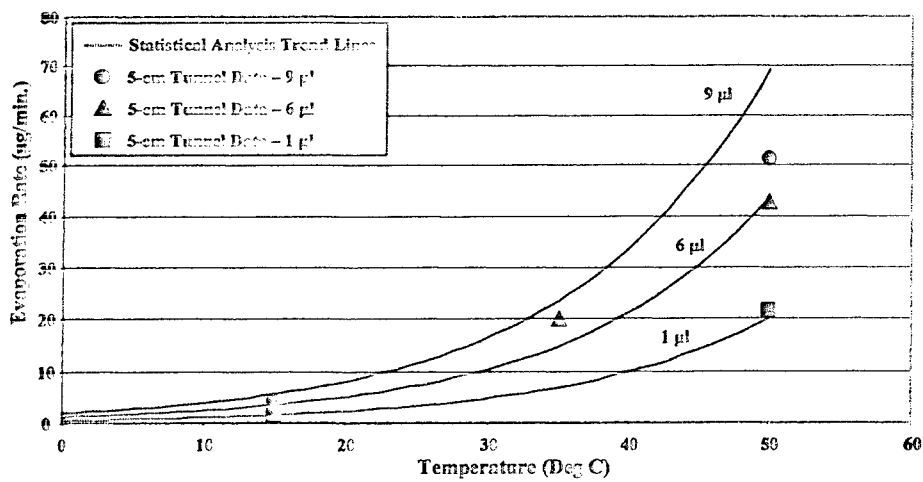


Figure 99. Statistical Analysis of 5-cm Wind Tunnel Data Evaporation Rate vs. Velocity and Drop Volume HD on Glass at 35 °C



**Figure 100. Statistical Analysis of 5-cm Wind Tunnel Data Evaporation Rate vs. Velocity and Drop Volume HD on Glass at 50 °C**

Figures 101 through 103 present Evaporation Rate vs. Temperature and Drop Size for the three Velocities, respectively, and emphasize the strong non-linear effect of temperature.



**Figure 101. Statistical Analysis of 5-cm Wind Tunnel Data Evaporation Rate vs. Temperature and Drop Volume HD on Glass at 0.22 m/s**

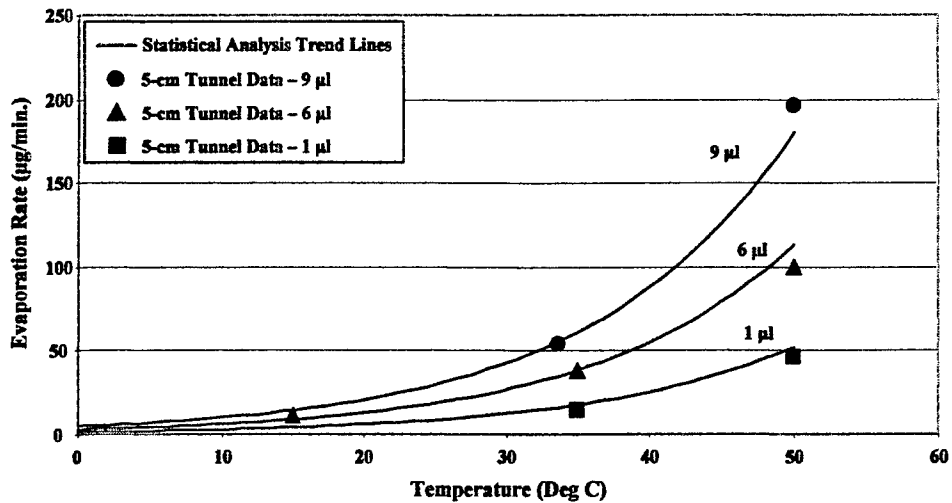


**Figure 102. Statistical Analysis of 5-cm Wind Tunnel Data Evaporation Rate vs. Temperature and Drop Volume HD on Glass at 1.7 m/s**

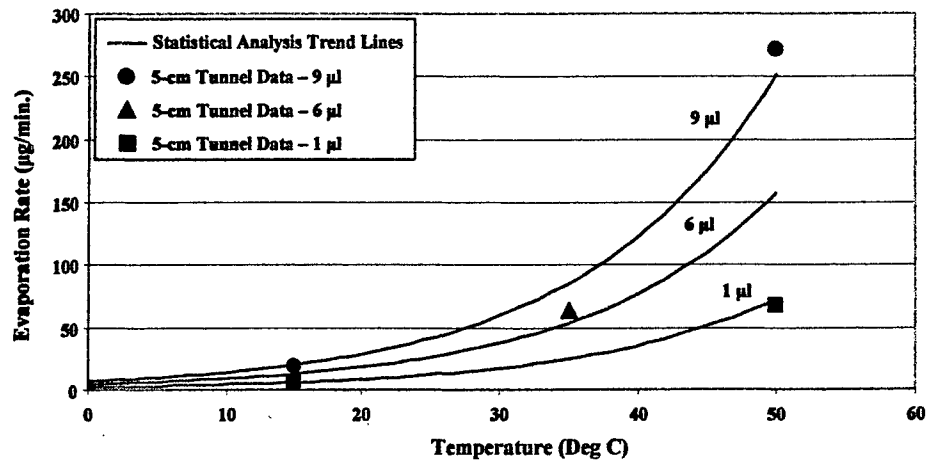


**Figure 103. Statistical Analysis of 5-cm Wind Tunnel Data Evaporation Rate vs. Temperature and Drop Volume HD on Glass at 3.6 m/s**

Figures 104 through 106 show the Evaporation Rate vs. Temperature and Velocity for Drop Volumes of 9, 6 and 1  $\mu\text{l}$ , respectively.

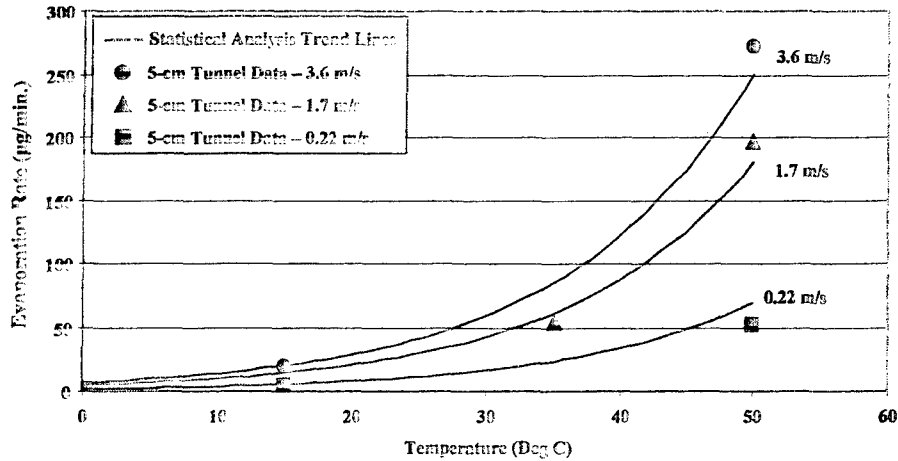


**Figure 104. Statistical Analysis of 5-cm Wind Tunnel Data Evaporation Rate vs. Temperature and Velocity HD on Glass at 9  $\mu\text{l}$  Drop**

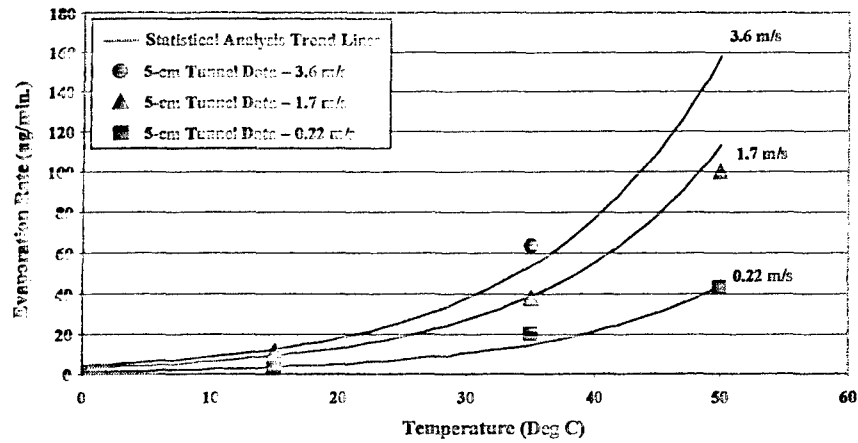


**Figure 105. Statistical Analysis of 5-cm Wind Tunnel Data Evaporation Rate vs. Temperature and Velocity HD on Glass at 6  $\mu\text{l}$  Drop**

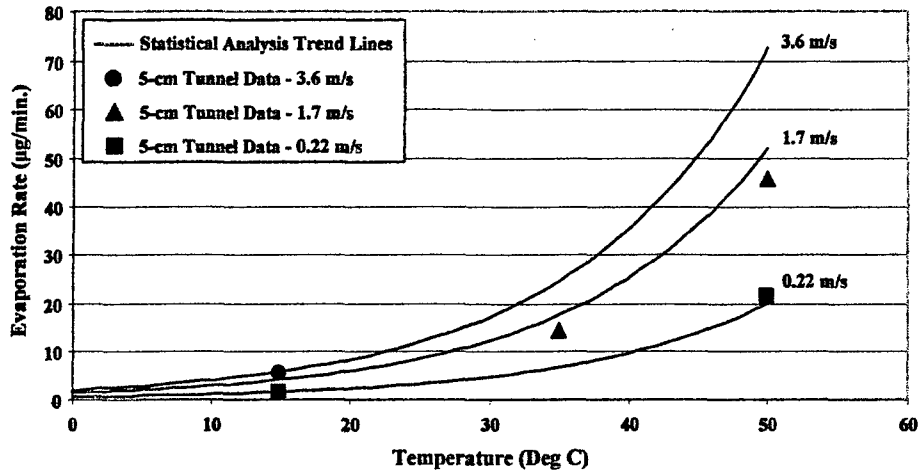


**Figure 106. Statistical Analysis of 5-cm Wind Tunnel Data Evaporation Rate vs. Temperature and Velocity HD on Glass at 1 µl Drop**

Figures 107 through 109 show Evaporation Rate vs. Drop Volume and Temperature for Velocities of 0.5, 3.0 and 6.0 m/s, respectively.

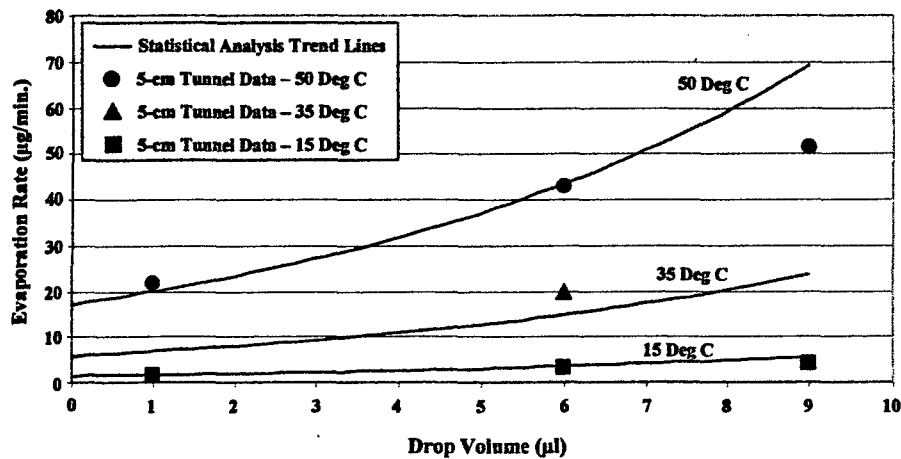


**Figure 107. Statistical Analysis of 5-cm Wind Tunnel Data Evaporation Rate vs. Drop Volume and Temperature HD on Glass at 0.22 m/s**

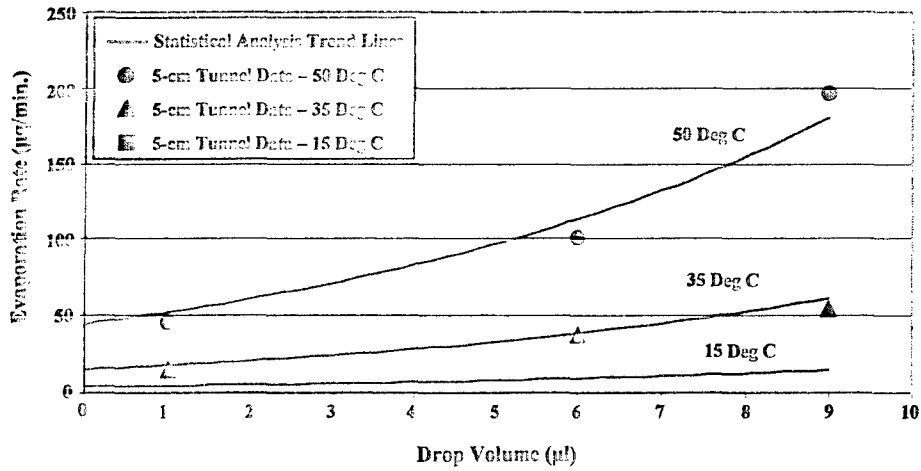


**Figure 108. Statistical Analysis of 5-cm Wind Tunnel Data Evaporation Rate vs. Drop Volume and Temperature HD on Glass at 1.7 m/s**

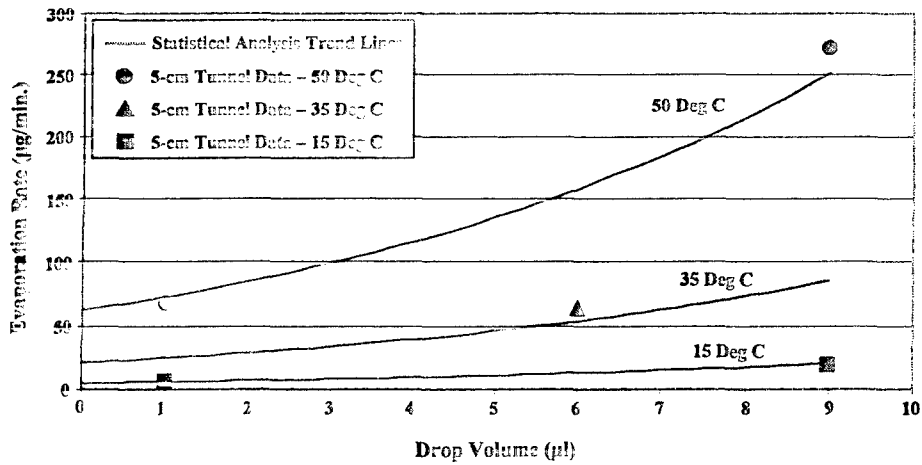


**Figure 109. Statistical Analysis of 5-cm Wind Tunnel Data Evaporation Rate vs. Drop Volume and Temperature HD on Glass at 3.6 m/s**

Figures 110 through 112 show Evaporation Rate vs. Drop Volume and Velocity for Temperatures of 50, 35 and 15 °C, respectively.

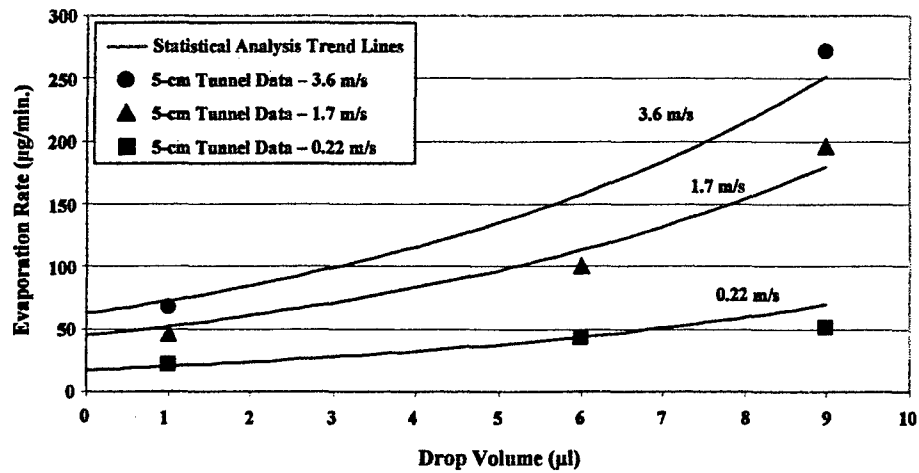


Figure 110. Statistical Analysis of 5-cm Wind Tunnel Data Evaporation Rate vs. Drop Volume and Velocity HD on Glass at 50 °C

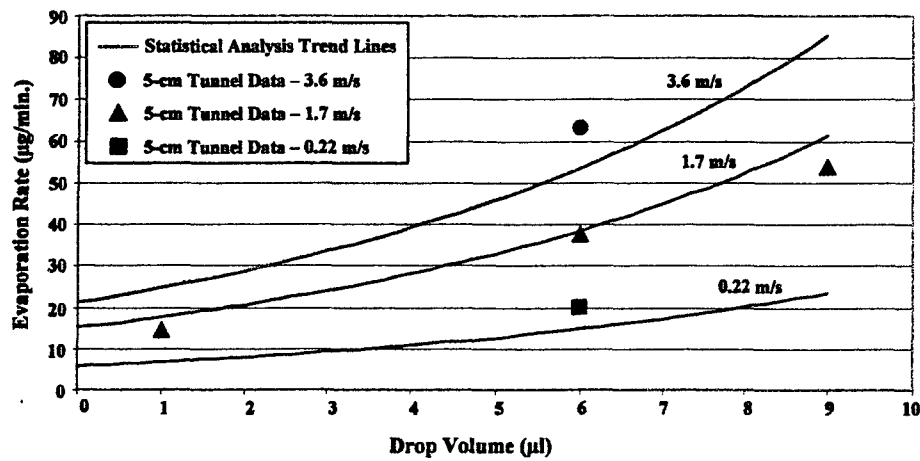
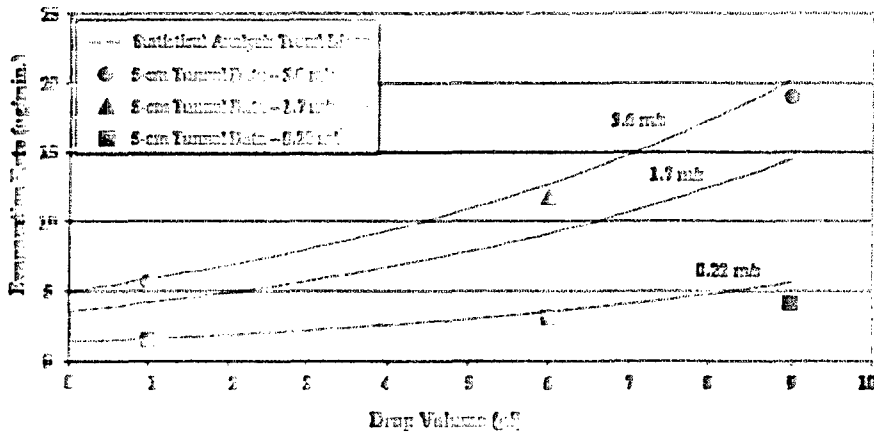


Figure 111. Statistical Analysis of 5-cm Wind Tunnel Data Evaporation Rate vs. Drop Volume and Velocity HD on Glass at 35 °C



**Figure 112. Statistical Analysis of 5-cm Wind Tunnel Data Evaporation Rate vs. Drop Volume and Velocity HD on Glass at 15 °C**

The velocity values shown in the wind tunnel data plots to this point are the reference values measured at a height of 2 cm above the tunnel test section floor. These were the velocity values contained in the wind tunnel data reporting format and were used in the plots for the sake of clarity and to allow direct reference to the wind tunnel data. However, as noted previously, these velocity values equate to the operational vertical velocity profiles stipulated by the model developers and which are present in all of the Agent Fate wind tunnels. Accordingly, it would be more appropriate and consistent to present the Agent Fate wind tunnel data in terms of the operational velocity values at a 2 m height. These operations velocities have been shown to correspond to their respective reference velocities through velocity characterization of the 5-cm wind tunnel.<sup>28</sup> For example, Figure 113 shows a representative set of 5-cm wind tunnel data for the evaporation rate of HD on Glass data plotted against the reference velocity (value at a 2 cm height) and the operational velocity (value at a 2 m height) both of which represent the same vertical velocity profile.



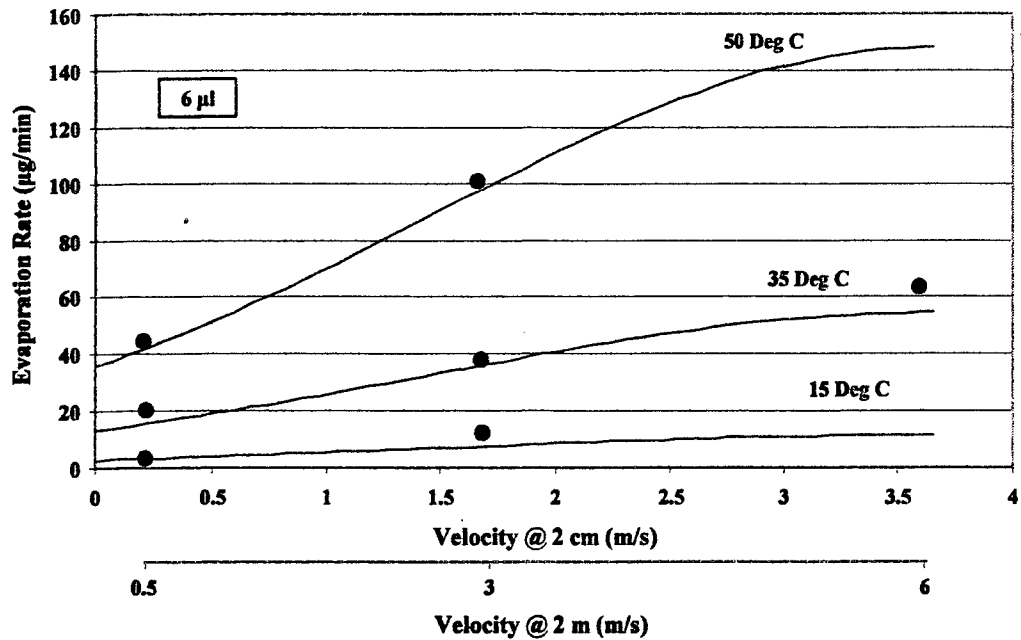


**Figure 113. Illustration of Equivalence of Reference and Test Matrix Velocities 5-cm Wind Tunnel, HD on Glass**

The previous HD on Glass data plots are repeated in Figures 114 through 131 in terms of the more relevant operational velocity values. Figures 114 through 116 show the Evaporation Rate vs. Velocity and Temperature for the three Drop Volumes, respectively.

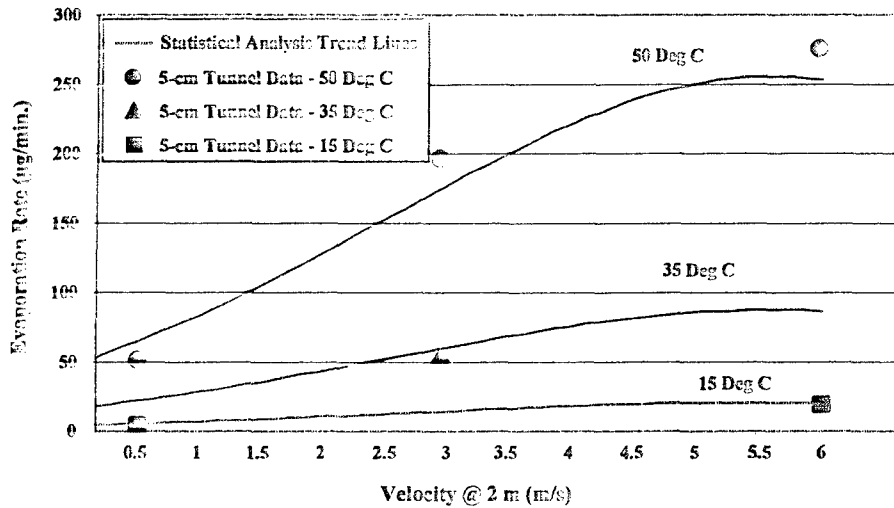


Figure 114. Evaporation Rate vs. Velocity at 2 m (HD on Glass - 9 µl Drop)

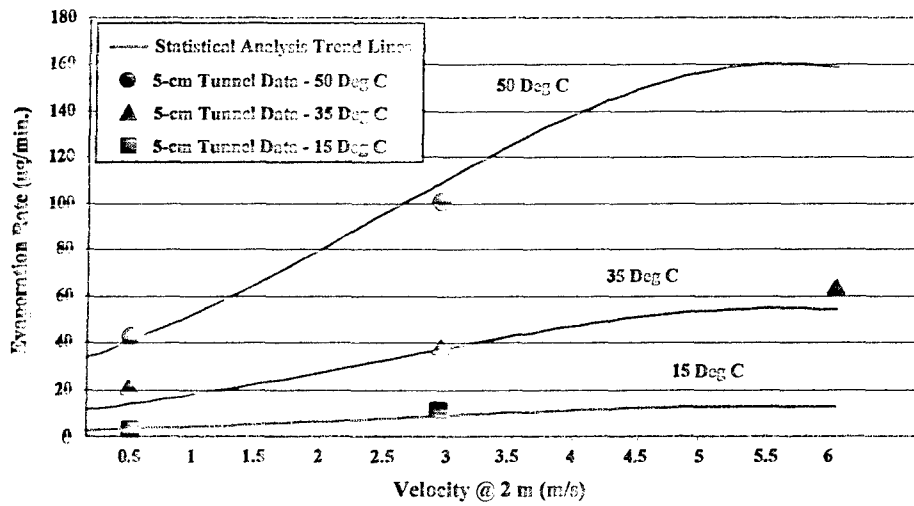


Figure 115. Evaporation Rate vs. Velocity at 2 m (HD on Glass - 6 µl Drop)

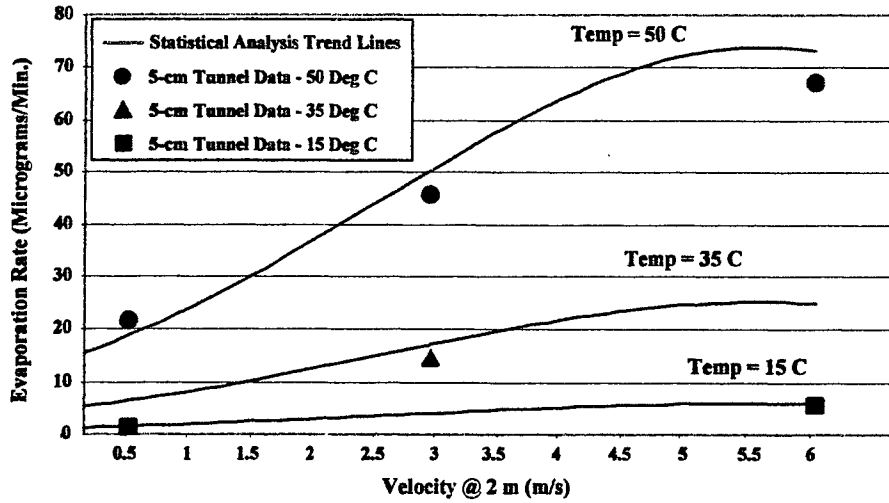


Figure 116. Evaporation Rate vs. Velocity at 2 m (HD on Glass - 1 µl Drop)

Figures 117 through 119 show the Evaporation Rate vs. Velocity and Drop Volume for constant temperatures of 15, 35, and 50 °C, respectively.

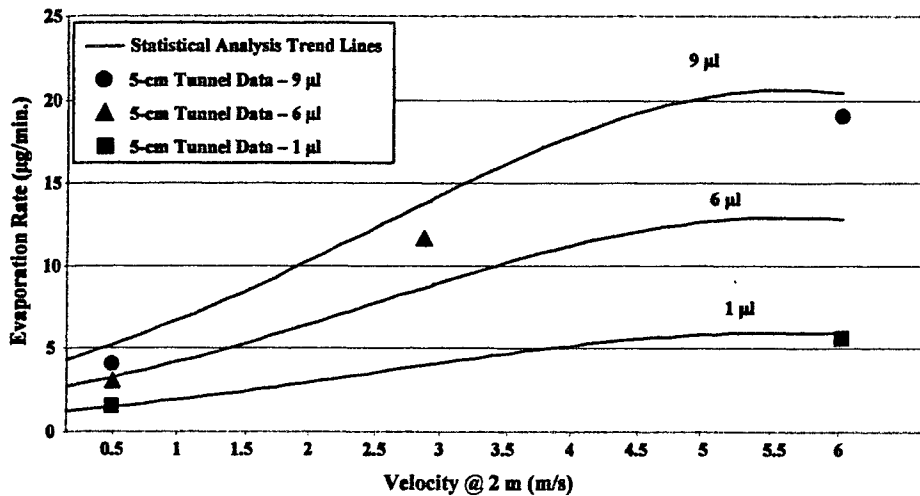


Figure 117. Evaporation Rate vs. Velocity and Drop Volume (HD on Glass at 15 °C)

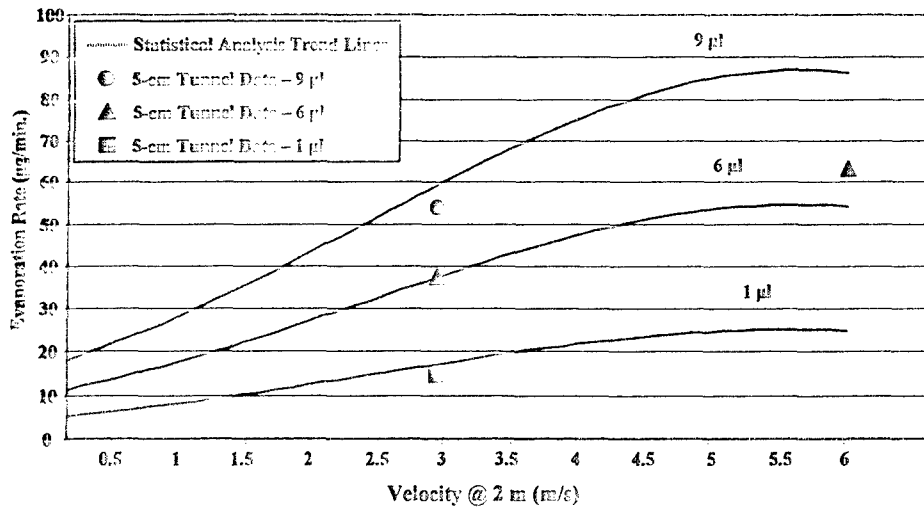


Figure 118. Evaporation Rate vs. Velocity and Drop Volume HD on Glass at 35 °C

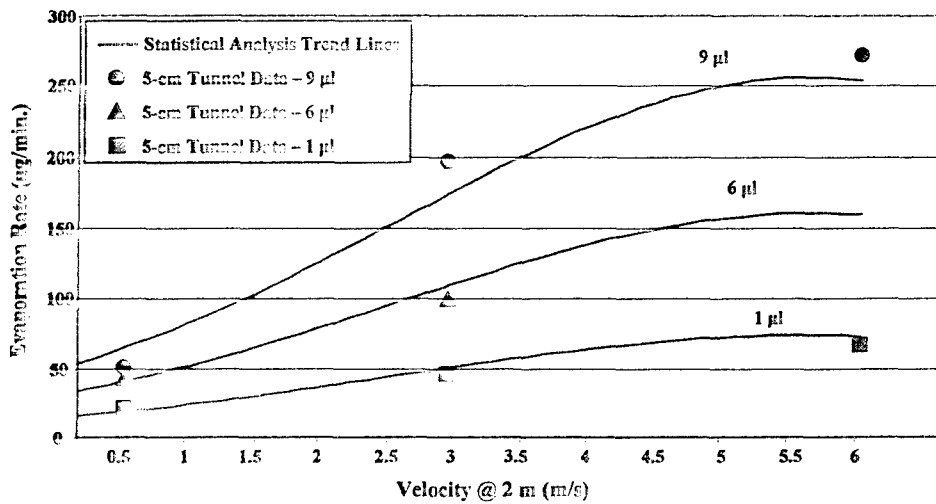


Figure 119. Evaporation Rate vs. Velocity and Drop Volume HD on Glass at 50 °C

Figures 120 through 122 present Evaporation Rate vs. Temperature and Drop Size for Operational Velocities of 0.22, 1.6 and 3.7 m/s, respectively.

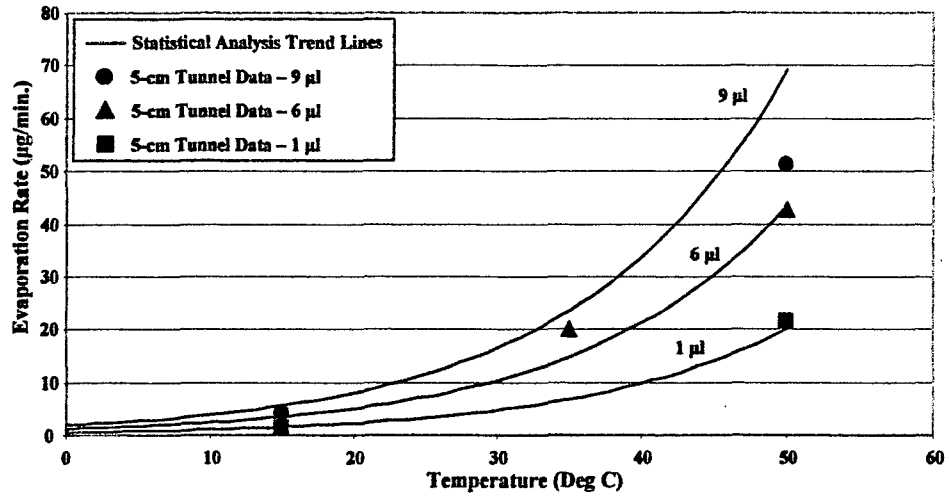


Figure 120. Evaporation Rate vs. Temperature and Drop Volume HD on Glass at 0.5 m/s

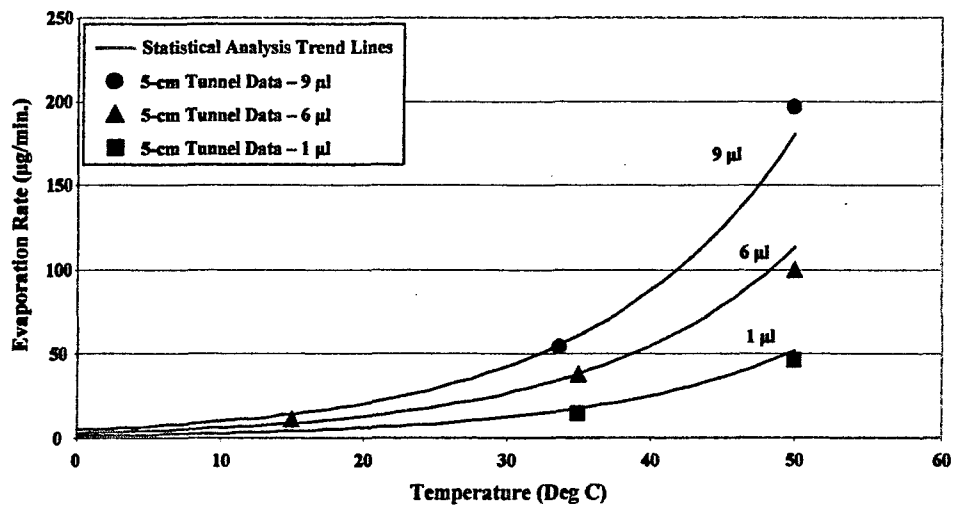
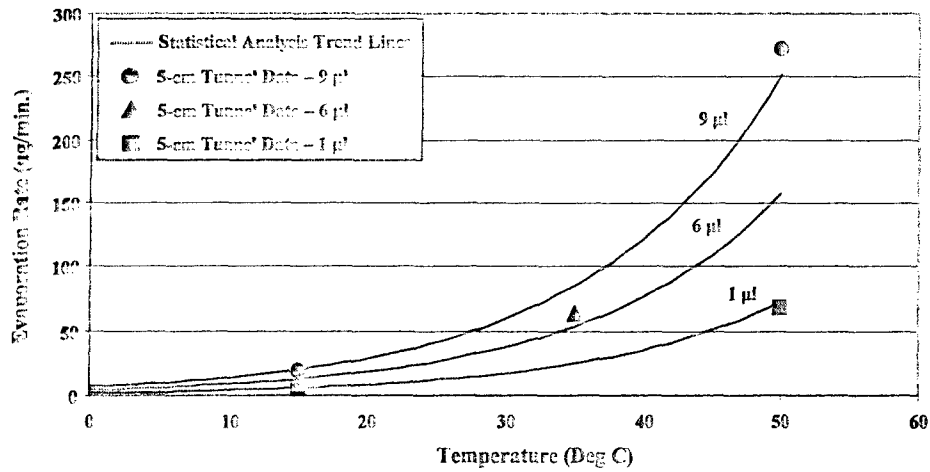
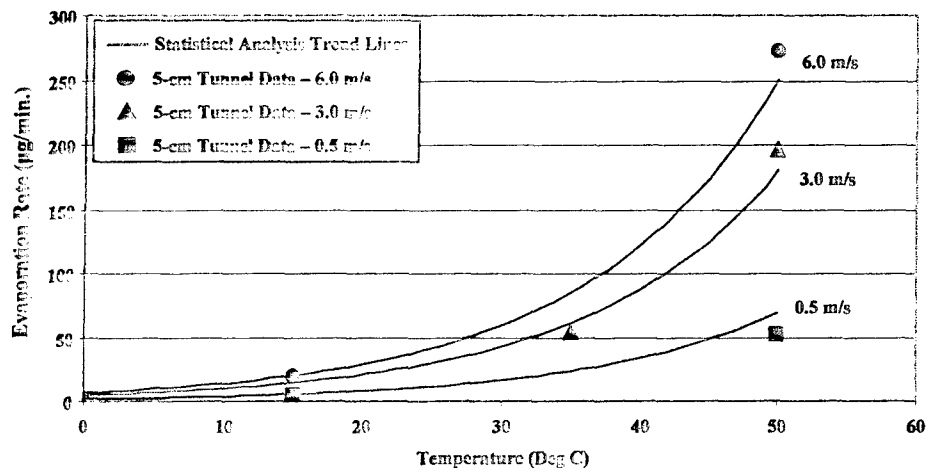


Figure 121. Evaporation Rate vs. Temperature and Drop Volume HD on Glass at 3.0 m/s



**Figure 122. Evaporation Rate vs. Temperature and Drop Volume HD on Glass at 6.0 m/s**

Figures 123 through 125 show the Evaporation Rate vs. Temperature and Velocity for Drop Volumes of 9, 6 and 1 µl, respectively.



**Figure 123. Evaporation Rate vs. Temperature and Velocity HD on Glass for 9 µl Drop**

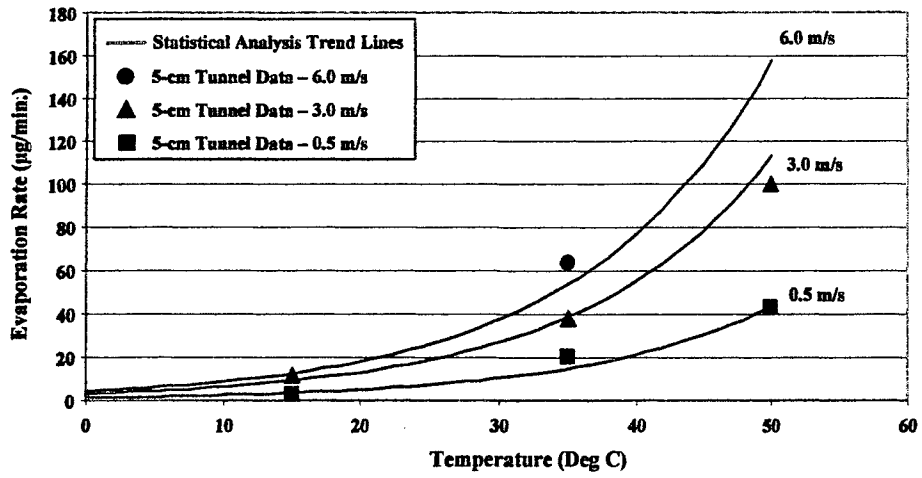


Figure 124. Evaporation Rate vs. Temperature and Velocity HD on Glass for 6 µl Drop

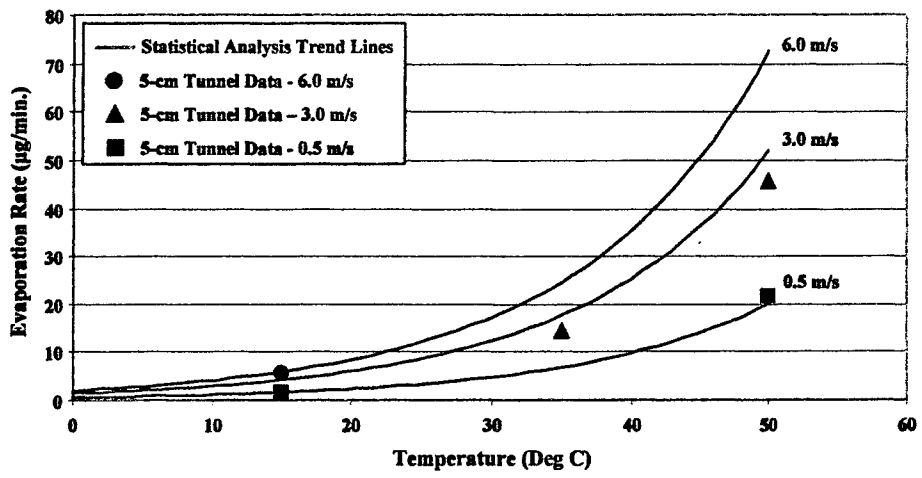
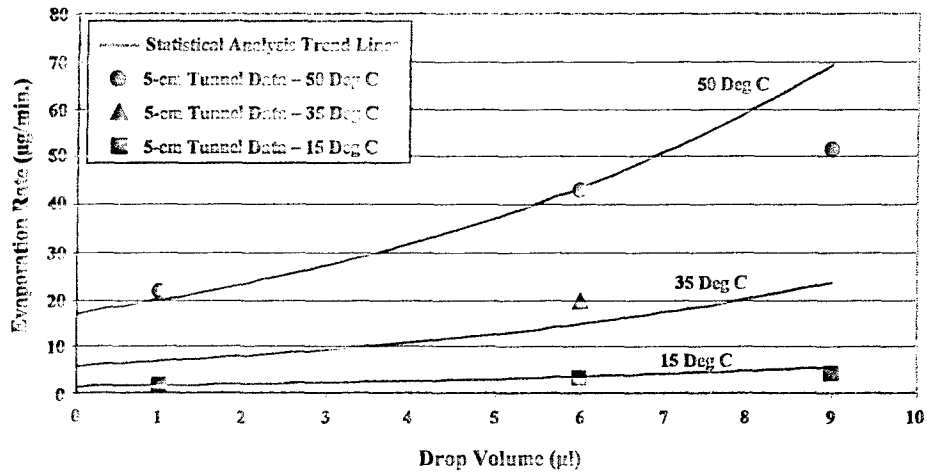
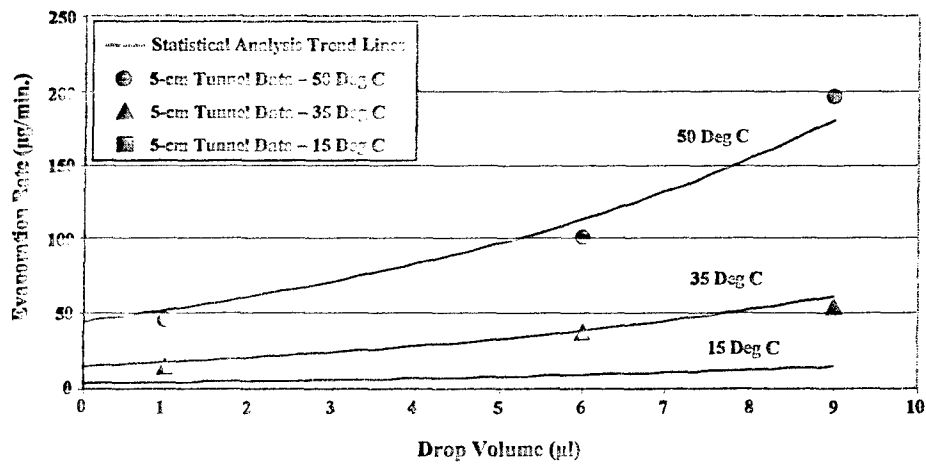


Figure 125. Evaporation Rate vs. Temperature and Velocity HD on Glass for 1 µl Drop

Figures 126 through 128 show Evaporation Rate vs. Drop Volume and Temperature for Velocities of 0.5, 3.0 and 6.0 m/s, respectively.



**Figure 126. Evaporation Rate vs. Drop Volume and Temperature HD on Glass for 0.5 m/s**



**Figure 127. Evaporation Rate vs. Drop Volume and Temperature HD on Glass for 3.0 m/s**



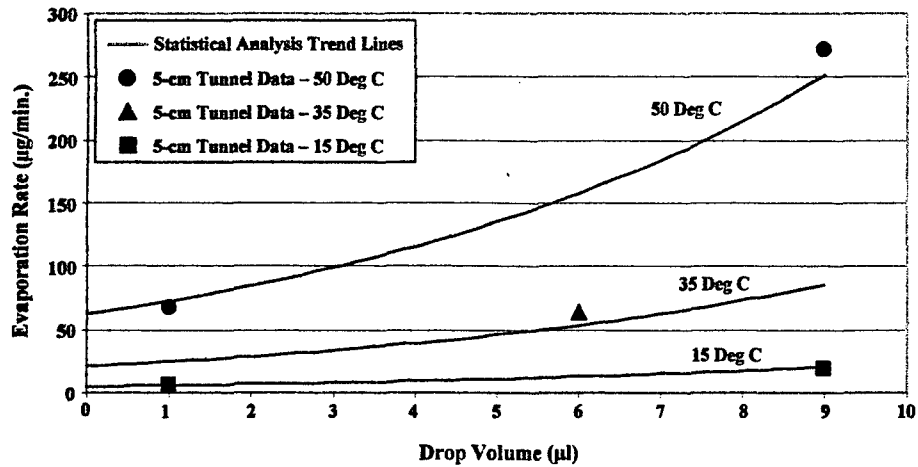


Figure 128. Evaporation Rate vs. Drop Volume and Temperature HD on Glass for 6.0 m/s

Figures 129 through 131 show Evaporation Rate vs. Drop Volume and Velocity for Temperatures of 15, 35, and 50 °C, respectively.

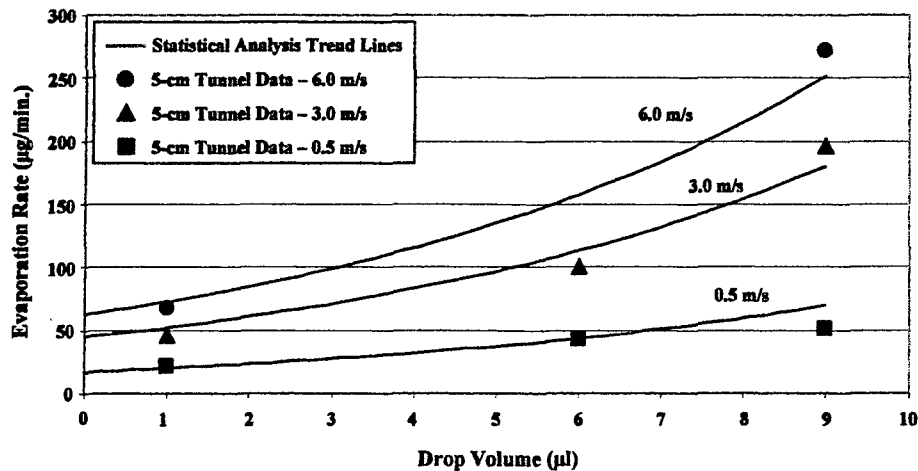


Figure 129. Evaporation Rate vs. Drop Volume and Velocity HD on Glass at 50 °C

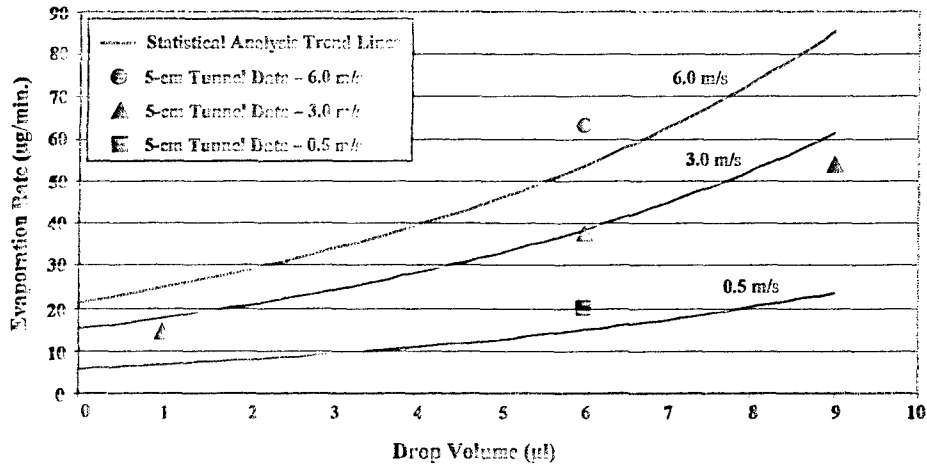


Figure 130. Evaporation Rate vs. Drop Volume and Velocity HD on Glass at 35 °C

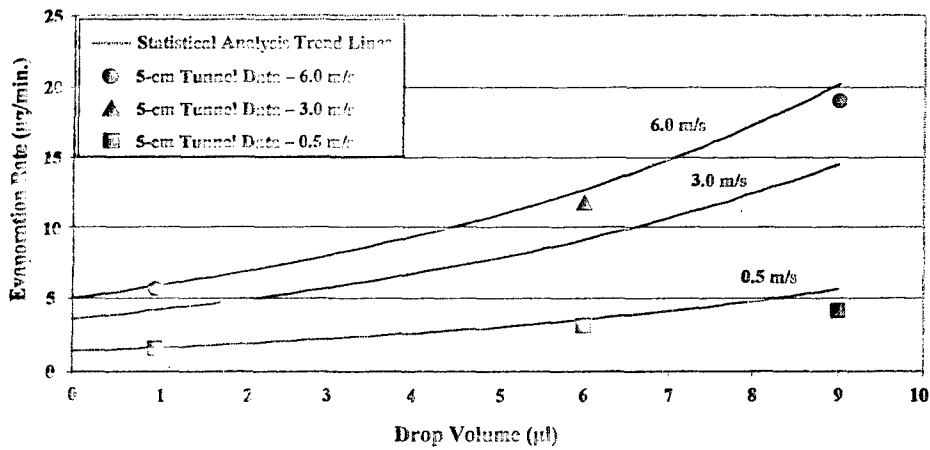


Figure 131. Evaporation Rate vs. Drop Volume and Velocity HD on Glass at 15 °C

Figure 132 summarizes all of the statistical trend lines for HD on Glass as determined from tests in the 5-cm wind tunnel in terms of the nominal validation test matrix term values. The results of the wind tunnel validation tests are presented in a single plot. Note that for the test matrix conditions, the Evaporation Rate value ranges from 0 to 300 micrograms/min. This figure illustrates that the Agent Fate wind tunnels should provide adequate data accuracy for the uses intended, especially in the context of the large uncertainties and variability present in operational situations.

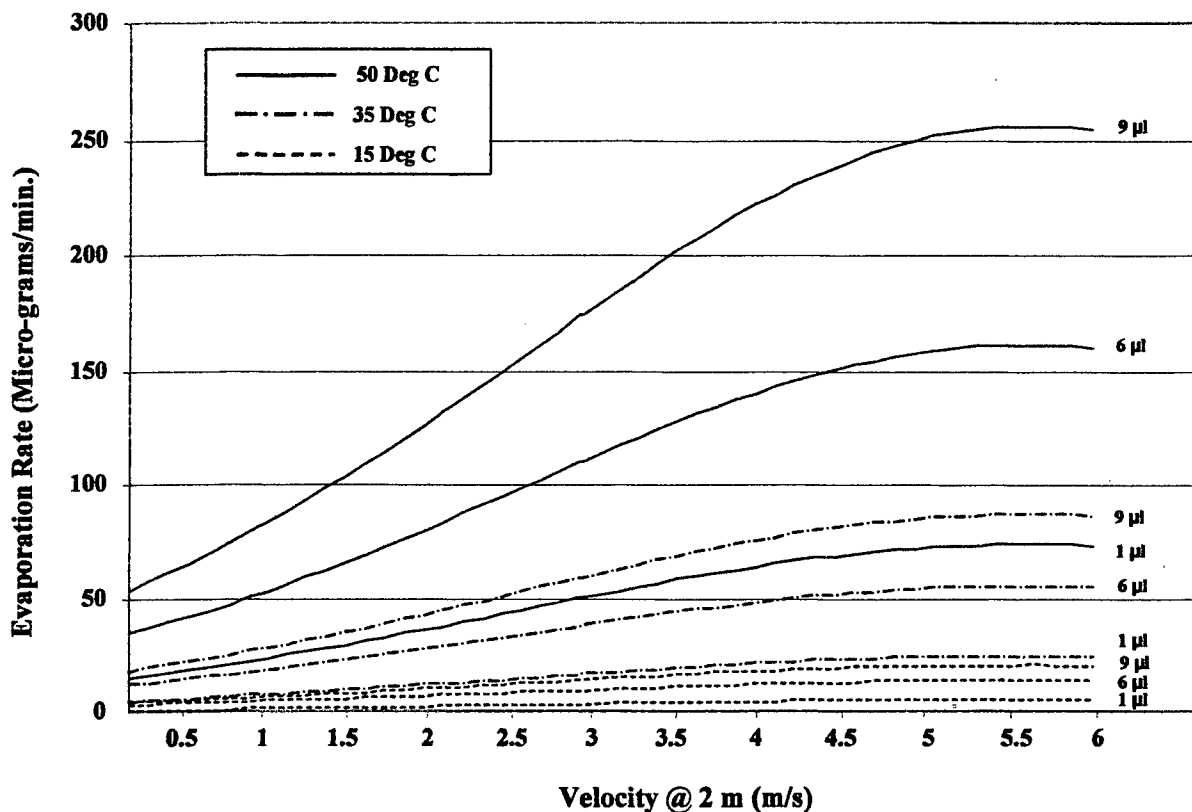


Figure 132. Statistical Trend Lines for Test Validation Data with Respect to Velocity Values at a 2 m Height

### 13. AGENT FATE WIND TUNNELS

#### 13.1 General

Three different wind tunnel facilities are being used to support the Agent Fate program. Figure 133 depicts the general outlines and sizes of the wind tunnels.<sup>25, 26</sup> As noted, these tunnels range considerably in size and each has specific features that allow it to be particularly applicable to certain of the agent/substrate combinations or test conditions. The next three figures

summarize each of the tunnels with regard to its physical characteristics, any special features and operational status.

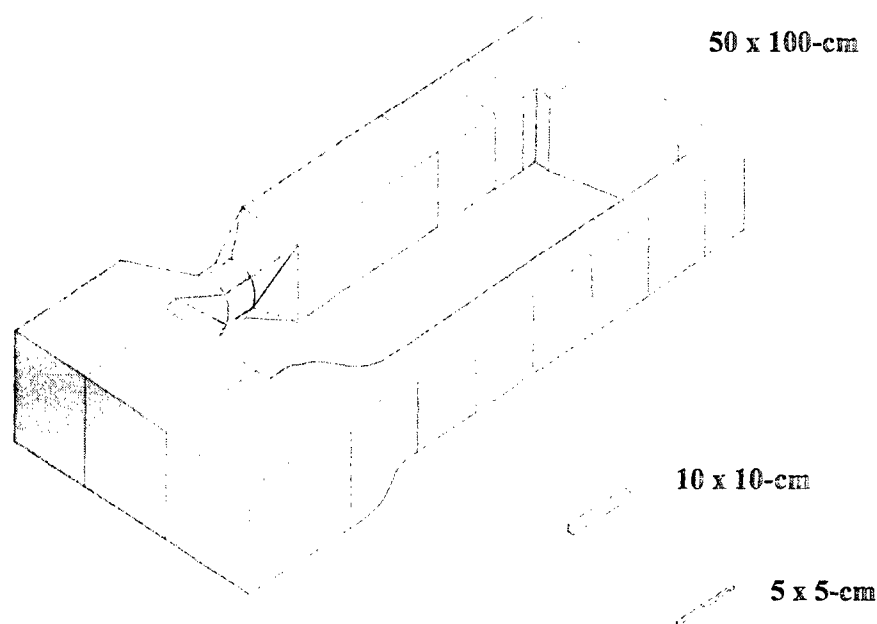
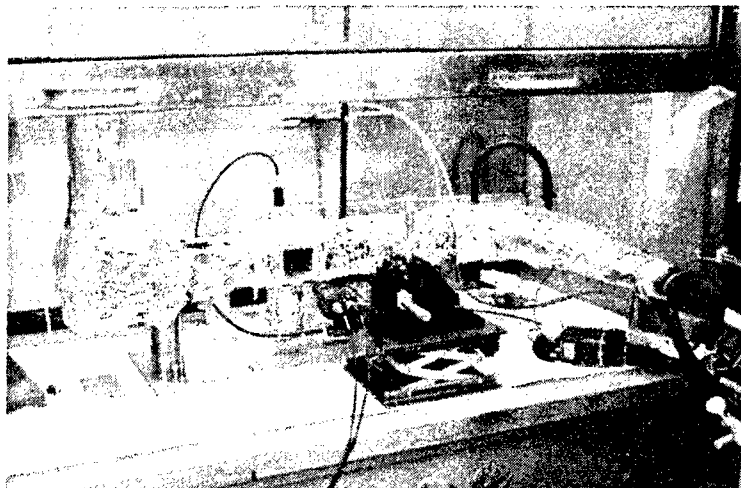


**Figure 133. Agent Fate Wind Tunnels (to same scale)<sup>25, 26</sup>**

### 13.2 5-cm Wind Tunnel

The ECBC 5-cm wind tunnel is summarized in Figure 134. It was designed and built specifically for the Agent Fate program by the ECBC, Aberdeen Proving Ground, MD. It can test single and multiple drops in a semi-automated fashion and can test all agent/substrate combinations except grass. Mixing of the agent vapor/air is enhanced by a static mixing box located downstream of the test section. During a test, samples of the agent/air mixture are collected by an array of vapor collection tubes located at the tunnel exit. Their contents are later analyzed by a TD-GC-MS. An on-line GC-MS can also be used to analyze the agent/air vapor during the test. The tunnel was sized so that multiple tunnels could fit into a standard chemical laboratory fume hood. A total of 12 tunnels have been fabricated. The first tunnel was completed in the spring of 2005 and validation testing was performed between July 2005 and January 2006.



**5-cm Wind Tunnel**

**Characteristics**

**Type: Open circuit**  
**Size: 5 x 5-cm test section:**  
**Width = 93 cm**  
**Height = 57 cm**  
**Depth = 55 cm**  
**Power: Conditioned air supplier**  
**Wind speed: 0 - 4 m/s**  
**Temperature: 0 - 55°C**  
**Humidity: 0 - 60%**

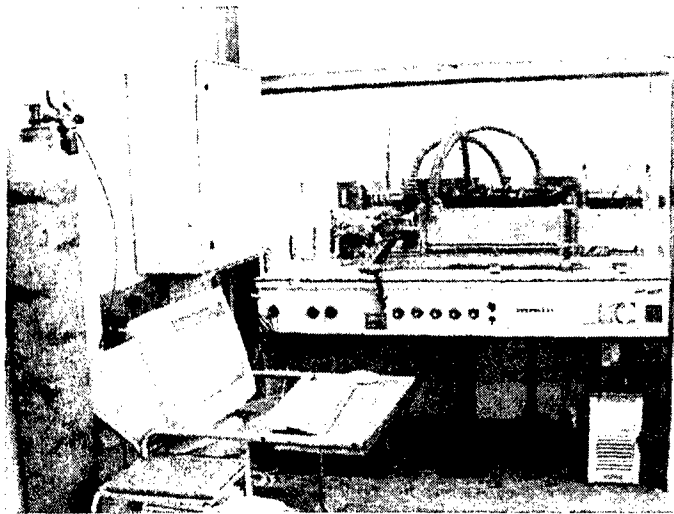
**Features**

**3.8 cm diameter substrate area**  
**Manual drop insertion (0.1 - 9 $\mu$ L)**  
**Single and multiple drops (1 - 6+)**  
**Agent vapor sampling of mixed effluent**  
**Vapor collection tubes**  
**On-line GC-MS**  
**Imaging digital video system**  
**GC-MS/NMR analysis of agent decomposition in air and substrate**  
**Compatible with standard fume hood**  
**High testing rate due to automation, multiplexing and multiple tunnels**  
**Measures all substrates except grass**

**Figure 134. 5-cm Wind Tunnel**

**13.3 10-cm Wind Tunnel**

Figure 135 describes the Czech 10-cm wind tunnel.<sup>27</sup> It is operated by the Military Technical Institute of Protection (MTIPS) in BRNO, Czech Republic. This tunnel was designed and built by MTIPS under an Air Force contract specifically for the Agent Fate program. The 10-cm wind tunnel consists of six stainless steel modules. The walls of the modules are temperature controlled through a water bath system. Environmental conditioning of the air is accomplished in a separate chamber and is connected with temperature controlled ductwork. It can test a multiple drop array in a highly automated fashion and can test all agent/substrate combinations except grass. Mixing of the agent vapor/air is enhanced by a static mixer located 5 cm downstream of the contaminated sample. An auto-sampler collects samples of the agent/air at the tunnel exit at a pre-determined position. Samples are analyzed with a GC-MS after the test. Two 10-cm wind tunnels are currently in operation. Designed prior to the start of the Agent Fate program DTO, the first wind tunnel was completed in the summer of 2004 with validation testing completed between October 2004 and April 2005. Major improvements were made to the wind tunnel in the fall of 2005 and a second wind tunnel, a mirror image of the improved tunnel, was completed in the winter of 2005 with validation testing for both completed in the spring of 2006.



**10-cm Wind Tunnel**

**Characteristics**

**Type: Open circuit**  
**Size: 10 x 10-cm test section**  
 Width = 100 cm  
 Depth = 10 cm  
 Height = 10 cm  
**Power: Conditioned air supplier**  
**Wind speed: 0 - 5 m/s**  
**Temperature: 5 - 50°C**  
**Humidity: 5 - 95%**

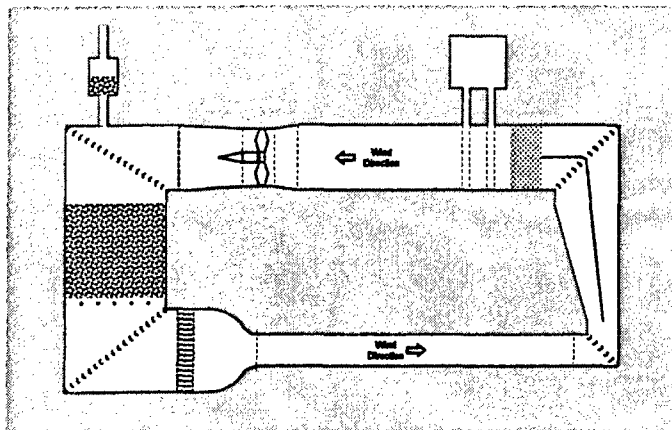
**Features**

**5 x 5-cm drop/substrate area**  
**Manual drop insertion (1-9µL)**  
**Multiple drops (9-25) in rectangular array**  
**Agent vapor sampling of mixed effluent**  
**Imaging digital video system**  
**Vapor collection tubes**  
**Off-line GC-MS**  
**Automated operation**  
**Measures all substrates but grass**

**Figure 135. 10-cm Wind Tunnel<sup>27</sup>**

**13.4 50 x 100-cm Wind Tunnel**

The 50 x 100-cm wind tunnel, summarized in Figure 136, is operated by the Defense Science and Technology Laboratory at Porton Down, U.K.<sup>25, 26</sup> It had been built prior to the Agent Fate DTO, but was modified to meet the Agent Fate program requirements. It can test a multiple drop array in a highly automated fashion and is large enough to test agent on grass. It operates by periodically collecting samples of the agent/air just downstream of the agent array and analyzing them with a GC-MS during the test. Unlike the other Agent Fate wind tunnels, the agent vapor/air mixture does not undergo secondary mixing; the sample being taken directly from the original vapor plume formed by the agent/substrate. The tunnel became operational in the fall of 2005 and validation was completed between October 2005 and January 2006.



**50 x 100 - cm Wind Tunnel**

**Characteristics**

**Type:** Closed circuit with in-line filter

**Size:** 50 x 100-cm test section

**Width =** 920 cm

**Depth =** 440 cm

**Height =** 100 cm

**Power:** Electric Fan

**Wind speed:** 0 - 10 m/s

**Temperature:** 5 - 55°C

**Humidity:** 10 - 60%

**Features**

**50 x 28-cm drop/substrate area**

**Automated drop insertion (1-9 µL)**

**Multiple drops (30) in 2 lateral rows**

**Vapour sampling of plume  
(no artificial mixing)**

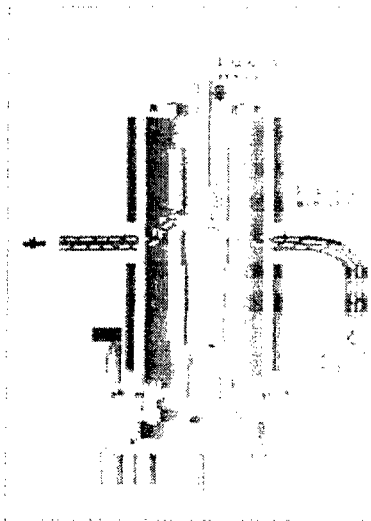
**On-line GC-MS**

**Can test grass**

**Figure 136. 50 x 100-cm Wind Tunnel<sup>25,26</sup>**

**13.5 Microbalance Facility**

A Thermal Gravimetric Analyzer (TGA) is a standard microbalance instrument that has been modified to allow a steady air stream to pass over the weighing pans containing the agent drops.<sup>28</sup> This facility provides quantitative and qualitative data that can be used to better understand and interpret data from the larger wind tunnels. The difficulty with these instruments is the small size that only allows their use for non-absorbing and a limited number of absorbent substrates. Its velocity profiles were determined by a combination of experimental and CFD techniques.<sup>3</sup> The TGA 2950 is shown in Figure 137. The TGA was extensively used to perform studies to identify the specific effects of the different test parameters on the agent evaporation. These results were used to help reduce the number of test conditions required for the Agent Fate program.



TGA 2950

#### Characteristics

Type: Open circuit

Size: 0.55 cm diameter test section:

Width = 58.4 cm;

Height = 53.3 cm;

Depth = 35.6 cm

Power: Conditioned air supplier

Wind speed: 50 - 2000 milli-liters/min.

Temperature: 35 - 55°C

Humidity: 0 - 60%

#### Features

10 x 10-mm drop/substrate area

Manual drop insertion (1-6µL)

Single drop

Agent vapor sampling of mixed effluent

Off-line GC-MS

Measures all substrates but concrete, asphalt and grass

Figure 137. TGA 2950

## 14. COMPARISON OF DATA BETWEEN WIND TUNNELS

### 14.1 Scaling Issues

As noted previously, the Agent Fate wind tunnel testing conditions involve full-scale agent/substrate samples in the presence of a full-scale velocity profile. All of the Agent Fate wind tunnels are required to have the same test matrix velocity profiles as discussed previously, Figure 138 shows how closely the velocity profiles for the three tunnels match the three test matrix velocity profiles. Accordingly, there are no scaling issues to be considered.



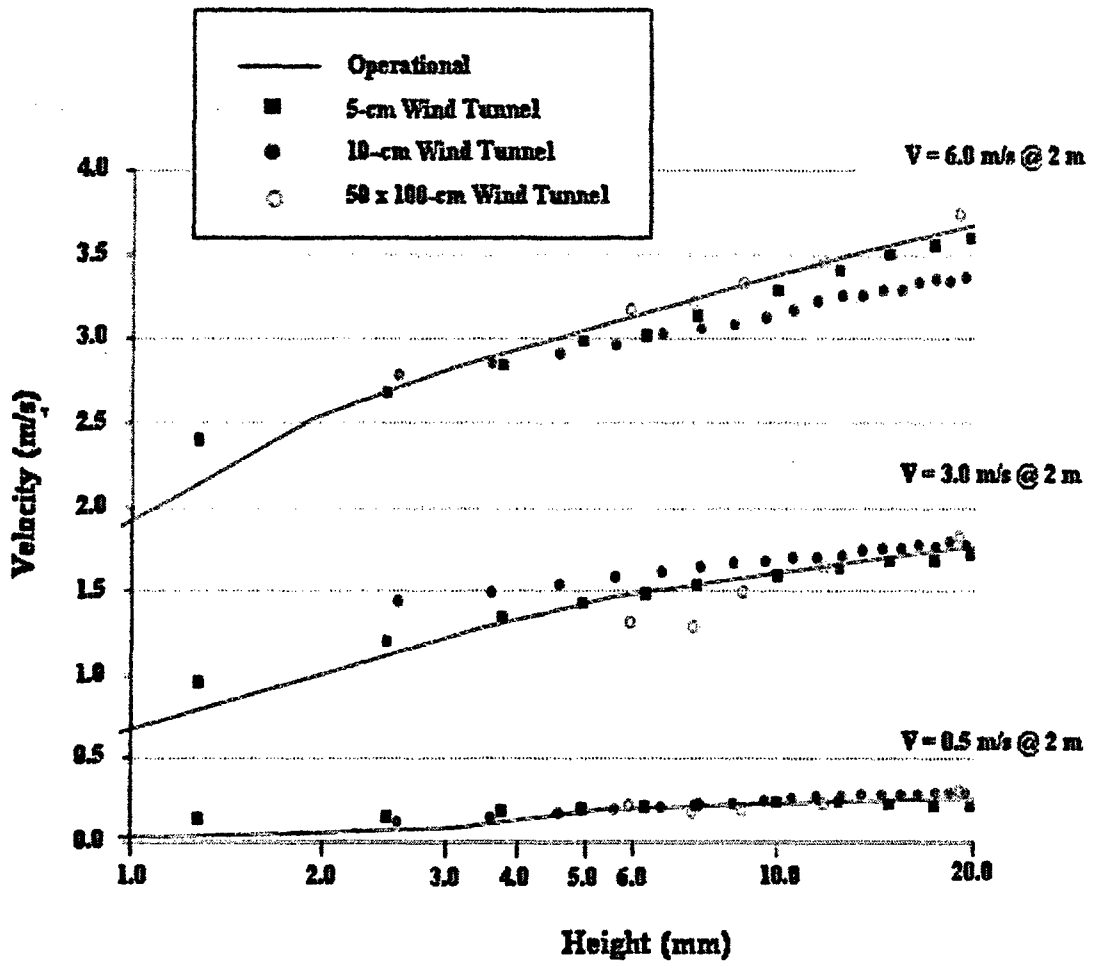


Figure 138. Measured Velocity Profiles for Agent Fate Wind Tunnels

Figure 139 depicts the factors relating to the Reynolds number, which is an important similitude ratio used in standard wind tunnels. In the Agent Fate situation, all terms in the Reynolds Number are full-scale values illustrating that no scaling of Reynolds number is required. Similar considerations of other non-dimensional fluid dynamic and thermodynamic scaling factors also demonstrate that no scaling is necessary.

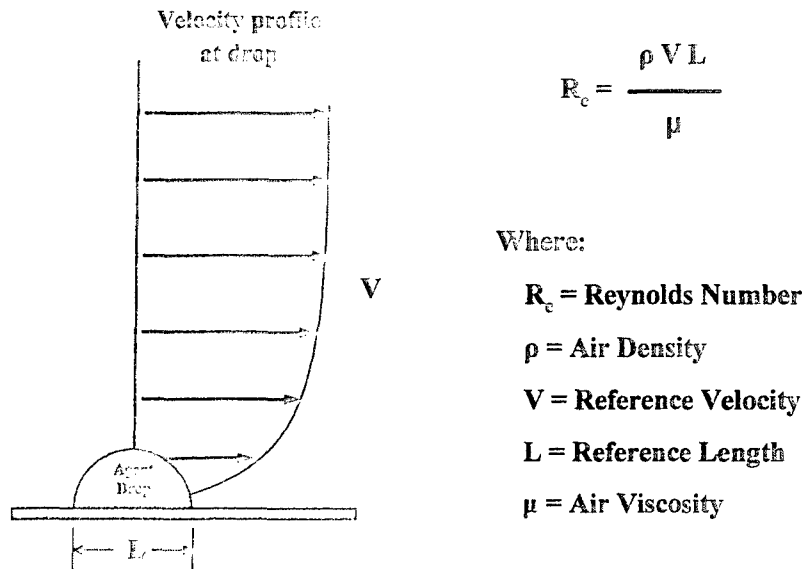


Figure 139. Reynolds Number

14.2 Comparison of Agent Fate Wind Tunnel Data

14.2.1 10-cm and 5-cm Wind Tunnel Data

Figure 140 through Figure 142 summarize the mean initial evaporation rate as a function of velocity and temperature for a 1, 6 and 9 micro-liter drop of HD/Glass, respectively, obtained from the 10-cm<sup>27</sup> and 5-cm<sup>11</sup> wind tunnels. These plots include the same constant value trend lines determined from the statistical analysis described in section 12.0. Evaporation rate data from the 10-cm wind tunnel are shown in tabulated form in Appendix C. It should be noted that the data from the 10-cm tunnel were obtained for an array of 9 to 25 drops whereas the data from the 5-cm tunnel were obtained from a single drop of agent. In the case of the 10-cm wind tunnel, the total evaporation rate is divided by the number drops to give an average evaporation rate per drop. Except for the questionable data point for the 10-cm tunnel at 3 m/s\*, these figures illustrate the good agreement between the two different sized facilities.

\*The maximum velocity for the 10-cm tunnel was limited to a reference velocity of 3 m/s at a 2 cm height (for the mid and large drops sizes) rather than the required 3.6 m/s to prevent drop movement due to airflow. This problem has not been noted in the 5-cm tunnel. This may be due to differences in the physical properties of the weapons grade HD used in the 10-cm wind tunnel tests and the more pure, CASARM grade HD agent used in the 5-cm wind tunnel tests.

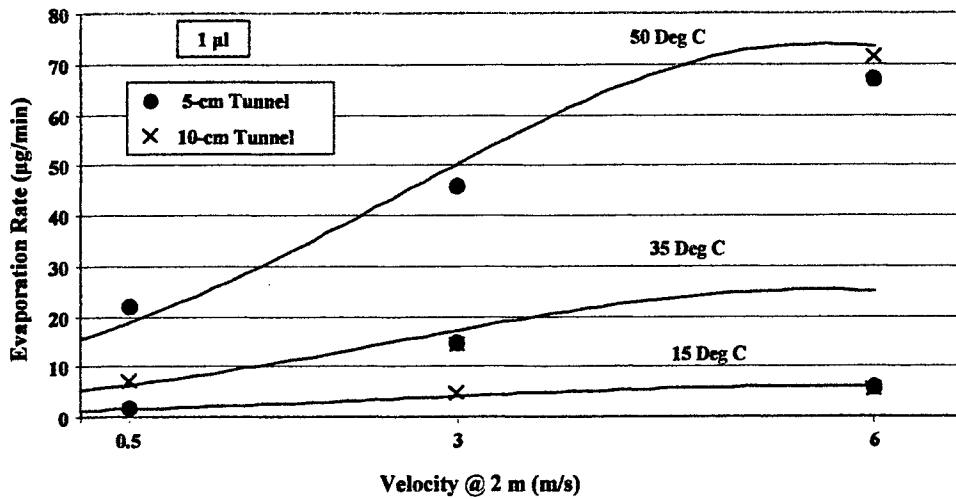


Figure 140. Mean Evaporation Rate vs. Velocity for HD/Glass; 1 µl Drop Size

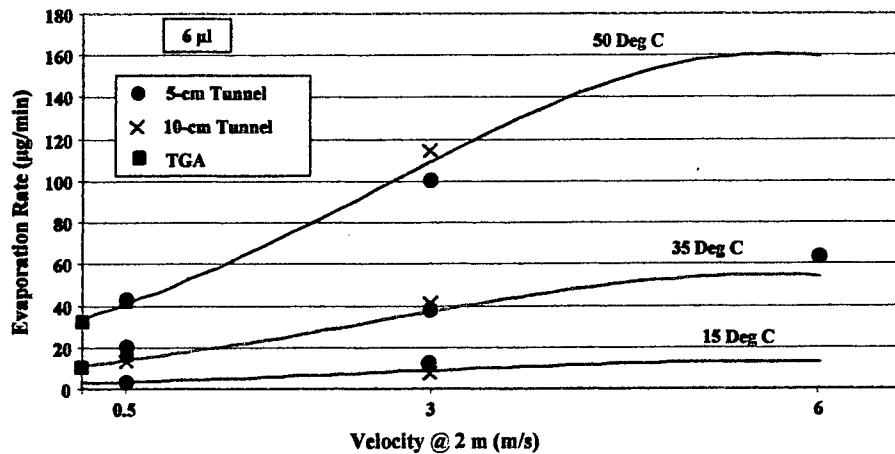
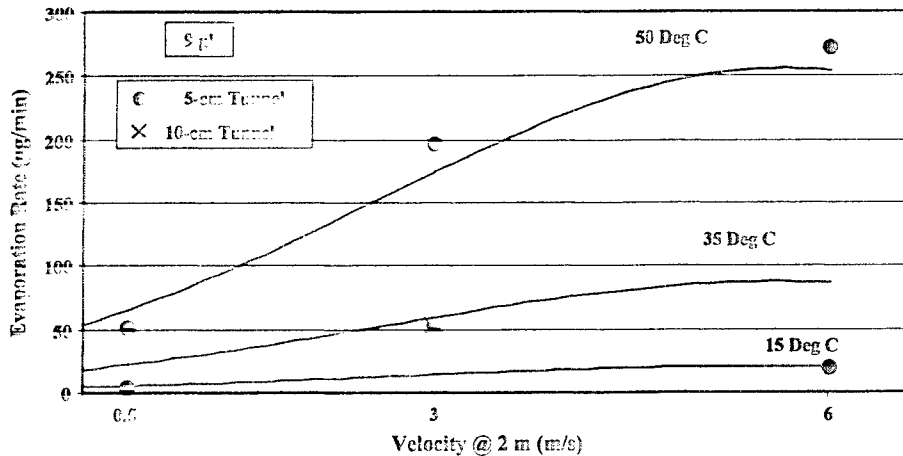


Figure 141. Mean Evaporation Rate vs. Velocity for HD/Glass; 6 µl Drop Size



**Figure 142. Mean Evaporation Rate vs. Velocity for HD/Glass; 9 µl Drop Size**

The experimental evaporation rates of HD on glass from 5-cm and 10-cm Agent Fate wind tunnels obtained during the validation tests were statistically analyzed for the three critical variables, temperature, velocity and drop size.<sup>23</sup> These included 19 and 13 unique combinations for the 5-cm tunnel and 10-cm tunnel, respectively, representing subsets of originally planned - but not completed - 27-trial (3 X 3 X 3) full-factorial experimental designs to be run in each tunnel. By employing data transformations of the response and control variables, the required number of trials needed to well-fit evaporation rate data to a linear model is greatly reduced over what is required to obtain a comparably well-fitting empirical quadratic model. This allows subsets of the data to be used to fit the model and the balance of the trials to be used as checkpoints. In the case of the 19-unique trials for the 5-cm tunnel, the physics-based model fit to the 11 inner-most trials is shown to accurately predict the observations at the 8 outer-most (extrapolated) variable combinations. This bodes well for the potential need to make predictions at wind velocities beyond which the tunnels can be used to generate data. While the combined data from both tunnels show that there are statistically significant effects between the tunnels, it is not practically significant compared to the effects associated with temperature, velocity, and drop size, which are about an order of magnitude greater.

#### 14.2.2 TGA Data

A series of TGA-EGA tests were conducted for comparison with the 10-cm and 5-cm tunnel data.<sup>29</sup> TGA tests were conducted with a single drop of HD on glass at a constant temperature, but for a range of air flowrates. The same statistical data reduction method was used to process the data obtained in the TGA2950 facility. It was not possible to characterize the detailed velocity profile for the different flowrates in the TGA due to its small size. A TGA flowrate corresponding to a test matrix velocity condition in the 5-cm wind tunnel was determined by matching the evaporation rates for HD on glass for the TGA to that obtained in the 5-cm tunnel at the same test matrix

temperature condition. This analysis used TGA and 5-cm tunnel data for a 6  $\mu$ l drop of HD on glass at temperatures of 35 and 50 °C. As shown in Figure 143, the analysis indicated that the TGA produced the same evaporation rate as the 5-cm tunnel for both temperatures only at a flowrate of 600 lpm. Since this evaporation rate corresponded to the low velocity condition of the test matrix in 5-cm tunnel, it was concluded that the TGA did provide the same “effective” velocity for that condition.

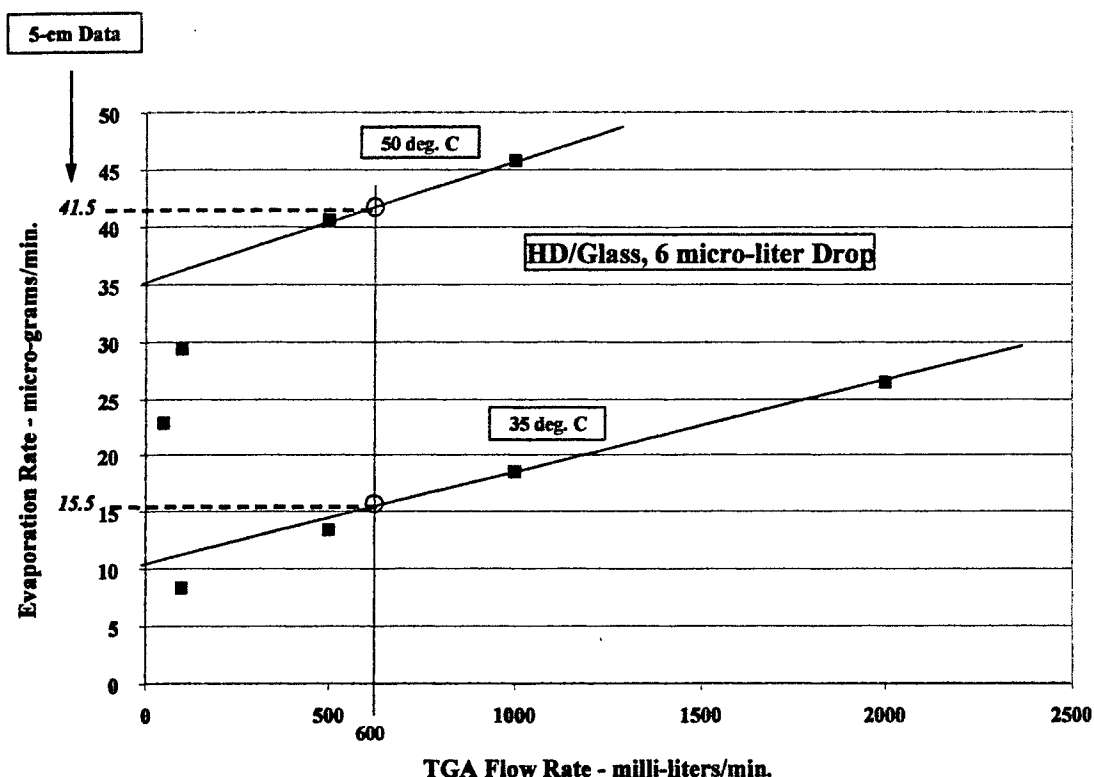


Figure 143. Correlation Between TGA2950 and 5-cm Tunnel

It was also hoped that the TGA tests would indicate the “zero airflow” evaporation rate of HD on glass. This would provide another data point to correlate with the 10-cm and 5-cm tunnel data (by extrapolating their evaporation rates to the zero velocity case). As can be seen in Figure 144, the evaporation rate drops off drastically at the lower flowrates. It is not known whether this phenomenon is due to saturation of the air surrounding the drop due to the small volume of the TGA or whether this is an actual effect at the low velocity condition. A linear extrapolation of the constant temperature curves to the zero flowrate produces a “zero velocity” evaporation rate that appears to match the 10-cm and 5-cm tunnel data in Figures 144 and 145.

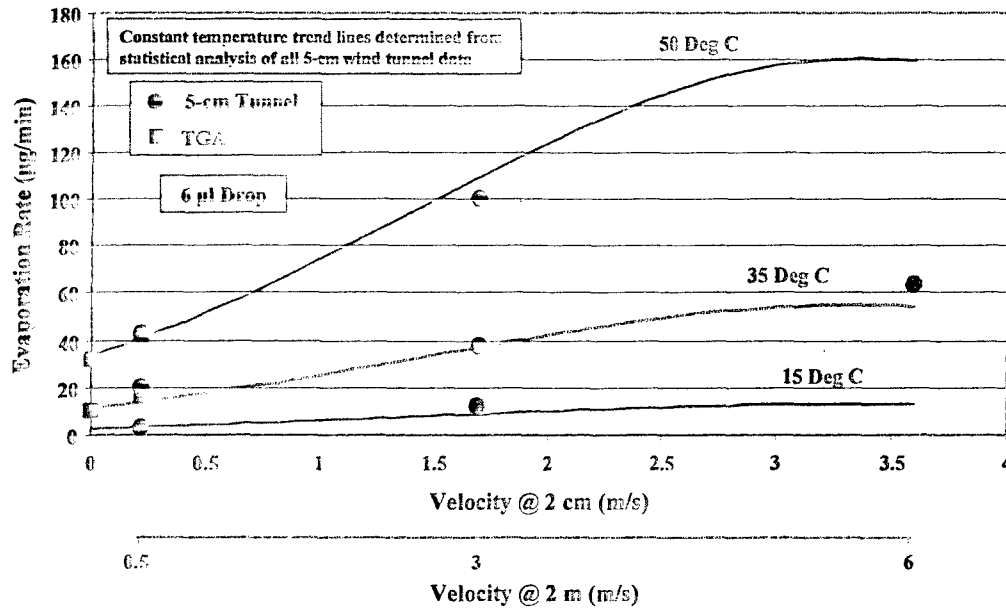


Figure 144. TGA2950 and 5-cm Tunnel Data-6 µl Drop

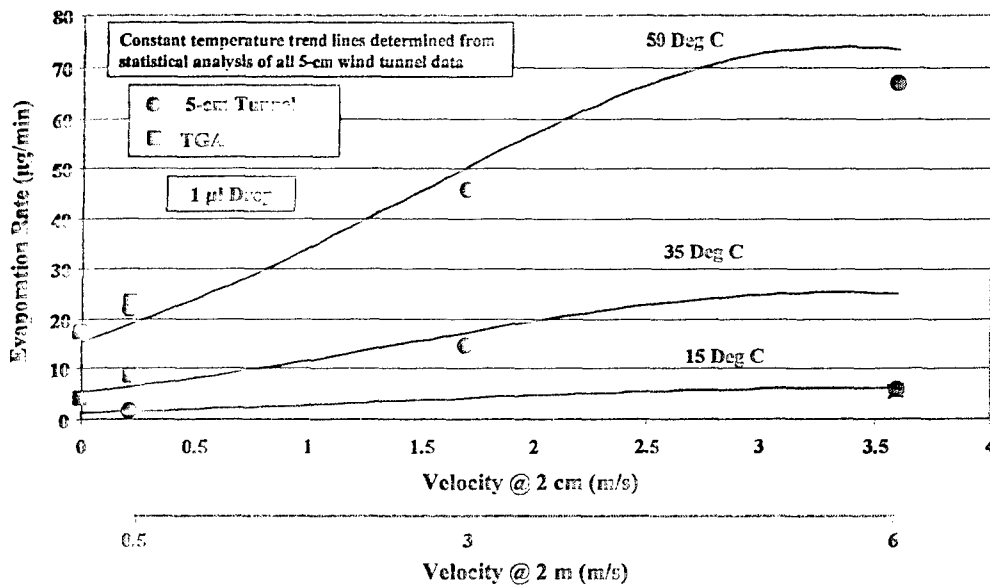


Figure 145. TGA2950 and 5-cm Tunnel Data-1 µl Drop

## 15. SUBSTRATE CHARACTERISTICS

### 15.1 General

The most important aspect of the Agent Fate program was to assess the hazard posed by any agent remaining in the substrate. This presents an immediate contact hazard for anyone touching the surface of the substrate soon after the event as the potential for the agent desorbing at a later time resulting in a vapor and a contact hazard. Another issue is the possibility that some of the agent can react with the substrate and form harmless as well as hazardous by-products.

The various substrates being considered in the Agent Fate program have significantly different interactions with the various agents. As shown in Figure 146, HD agent on glass forms a sessile drop that neither reacts with nor is absorbed by the glass.<sup>30</sup> Sand will rapidly absorb agents, but may not react with some.

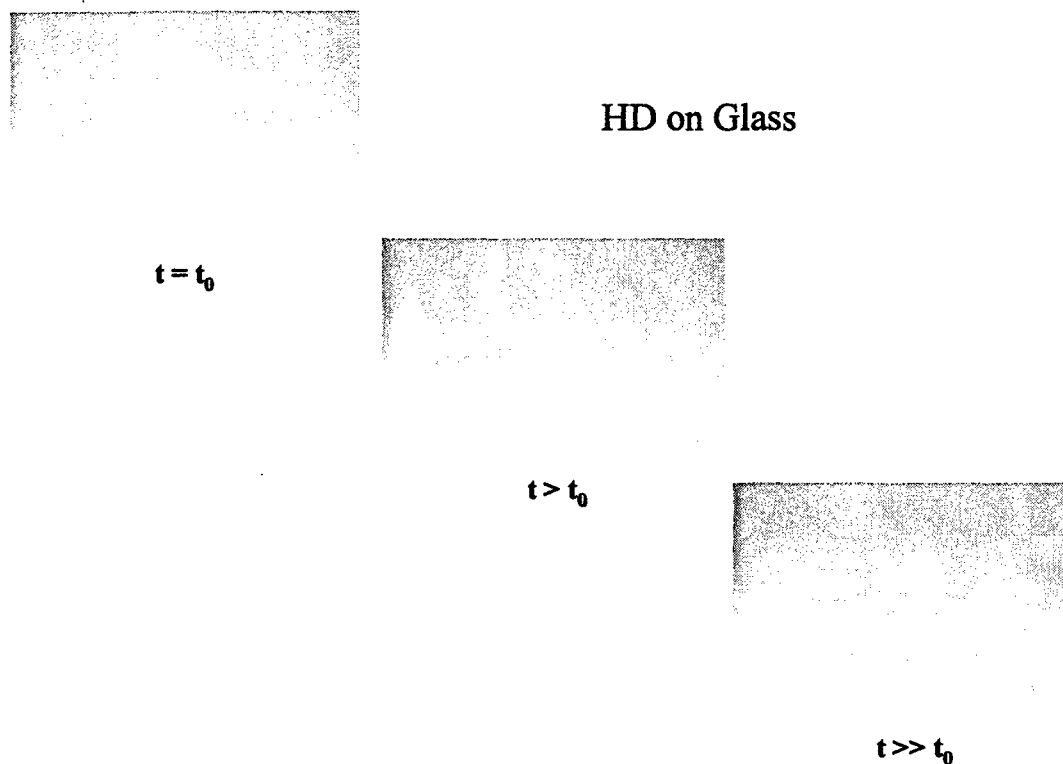


Figure 146. Evaporation of Sessile Drop on Glass<sup>30</sup>

Figure 147 depicts the results of agent deposited on samples of concrete and asphalt.<sup>30</sup> These samples have been cut in half allowing the penetration of the agent to be observed. The center photo shows a cut-away of concrete depicting the larger lateral and deep penetration of the agent and its path along the aggregates. Asphalt, shown on the right, exhibits a wider spreading, but

shallower depth of penetration. The agent also solvates in the bitumen creating a "tar-like" sludge that complicates desorption.

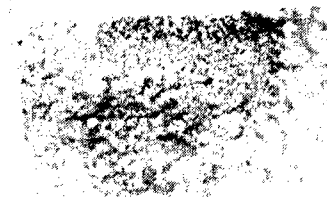
A substantial part of the Agent Fate program has been on the development of analytical methods to measure the amount of agent or its reaction products remaining in the substrate after a wind tunnel test. In addition to wind tunnel tests agents in combination with the different types of substrates, other tests are planned to evaluate the agents with variations of the same type of substrates including different sands, concretes and asphalts. While beyond the scope of this report, it points out importance of achieving an accurate agent mass balance with the wind tunnel to assist in determining residual agent in the substrate.

### Concrete



- Agent absorbs rapidly
- Spreads deep into substrate
- Follows aggregate
- Varies with concrete type

### Asphalt



- Agent absorbs rapidly
- Spreads wide over substrate
- Creates tar-like solvate
- Varies with asphalt type

Figure 147. Agent Absorption in Concrete and Asphalt



The Version 3, 5-cm wind tunnel has been used to test HD on sand, representing an absorbent, non-reactive substrate/agent combination.<sup>31</sup> Sand represents quite a different chemical/substrate interaction situation than glass. As noted previously, HD forms a sessile drop on glass. However, when deposited on sand, HD is immediately sorbed into the sand. The resulting evaporation of the HD from sand is also noticeably different as shown in Figure 148. In the case of HD on glass, the agent vapor/air concentration remains relatively constant during the earlier phase of the evaporation process and then abruptly drops to zero when the drop disappears. Whereas, for HD on sand, except for a slight initial increase as the agent spreads over the surface of the sand, the vapor/air concentration steadily decreases as the agent gradually volatilizes from the sand. This difference is further described in Figure 149 and 150, which depict the mass remaining as a function of time for HD on glass and sand, respectively. Note, that the time scales are different for these latter two figures with the sand time scale being an order of magnitude larger than for glass. The HD on glass evaporates in about 4 hr whereas 50 hr are required for the HD on sand. For the first 2 hr, the evaporation rate for HD on sand is similar to that of HD on glass. During this period of time, there is some agent on the surface of the sand. While not forming a sessile drop, the agent has a similar evaporation rate. After this top segment of the agent evaporates, the absorbed agent begins to desorb at an ever decreasing rate. This example illustrates the different nature of the agent evaporation from different types of substrates and demonstrates the ability of the 5-cm wind tunnel to measure these long term effects.

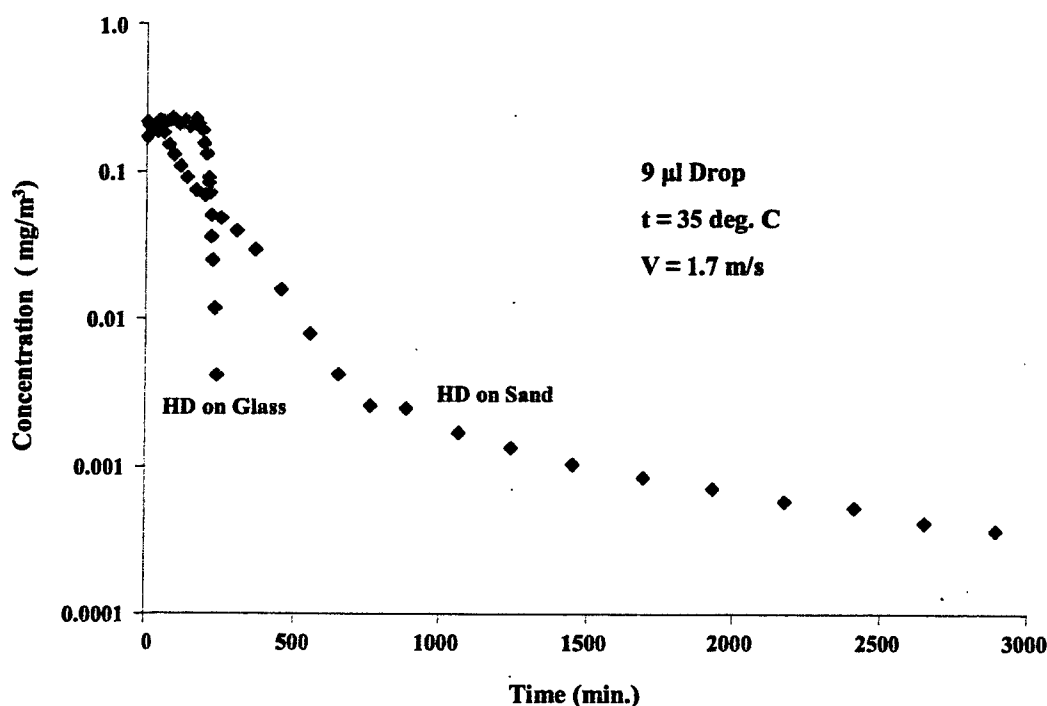
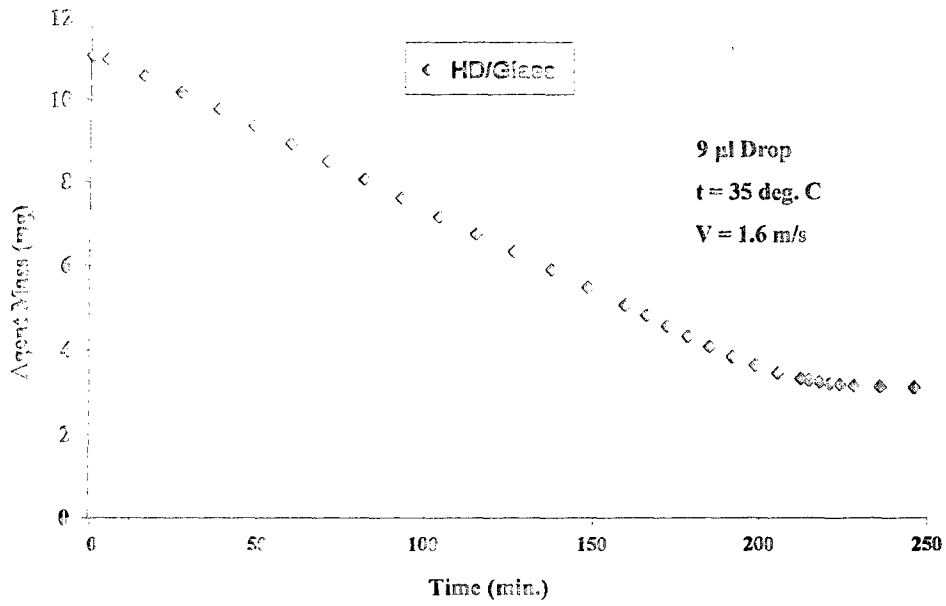
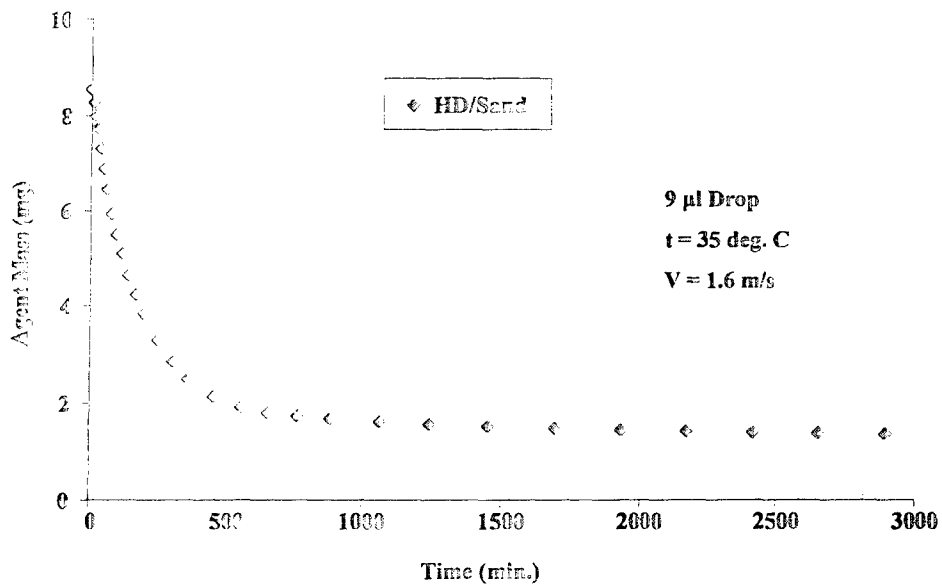


Figure 148. Comparison of Concentration vs. Time for HD on Glass and Sand



**Figure 149. Agent Mass Remaining vs. Time for HD on Glass**



**Figure 150. Agent Mass Remaining vs. Time for HD on Sand**

Figure 151 compares the evaporation rate data for a 6  $\mu\text{l}$  drop size of HD at 35  $^{\circ}\text{C}$  on glass and sand as measured in the ECBC 5-cm wind tunnel. The lower evaporation rate for the HD on sand with increasing velocity (compared with the glass case) may be due to the sand granules blocking the airflow from the agent on the surface of the sand compared with the smooth glass so that the higher velocities have less effect on the evaporation. The evaporation rate is practically the same for glass and sand at the extremely low velocities. These data not only reveal fundamental characteristics of the different substrates, but just as important, show correlation between the HD on sand data and the earlier HD on glass data, providing additional validation to the wind tunnel experimental arrangement.

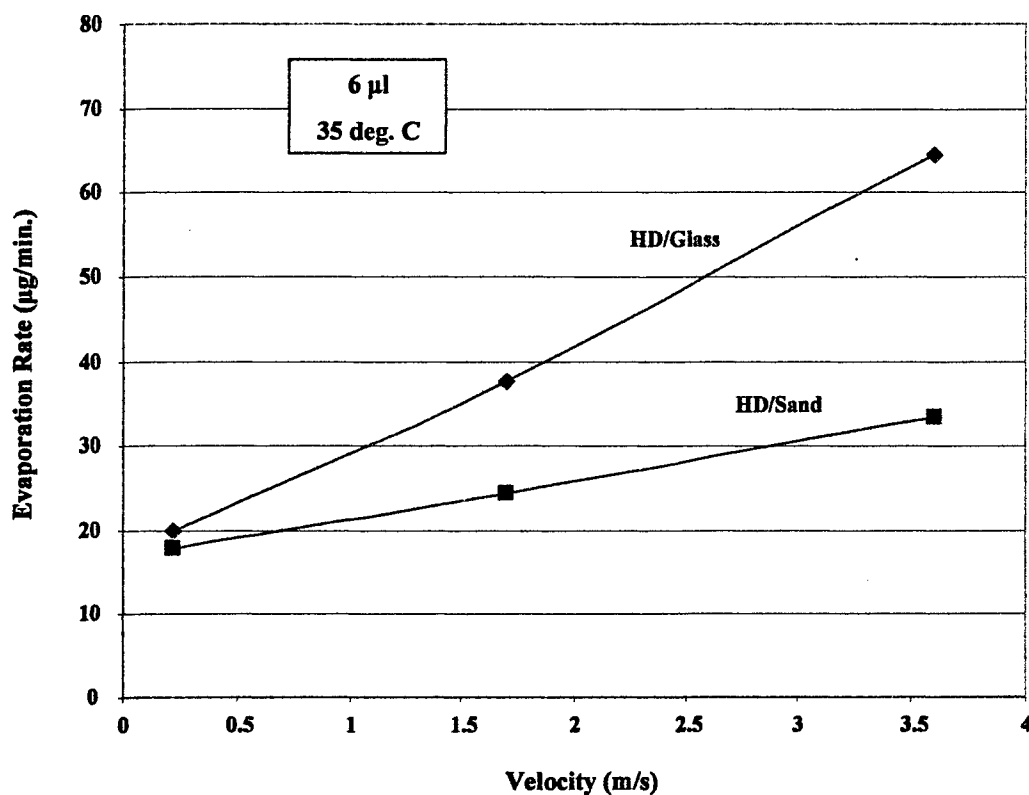


Figure 151. Comparison of Evaporation Rate of HD on Sand and Glass

16. CONCLUSIONS

1. A special 5-cm wind tunnel was designed specifically to measure the release and retention of Chemical Warfare Agents (CWA) from various materials under constant simulated environmental conditions.
2. The wind tunnel fits within the dimensions of a standard chemical fume hood that meets safety requirements for CWA operations.
3. The tunnel can create vertical velocity profiles that match the lower portion of a wind induced atmospheric boundary layer.
4. The specified velocity profiles are uniform across the substrate area in the wind tunnel test section.
5. The specified velocity profiles can be characterized by a single reference velocity at a specified height in the test section.
6. The tunnel has the capability to test single and multiple drops of CWA agent.
7. Data acquisition instrumentation has been included to measure the time history of the vapor released during the volatilization of the CWA from the material substrate whether the chemical is a sessile drop on the surface or a sorbed liquid within the substrate.
8. Dedicated 5-cm wind tunnels have been operated for medium/hot and cold environmental test conditions.
9. Remaining agent and/or its decomposition products in the substrate are determined using post-test analyses.
10. Free stream turbulence in the 5-cm wind tunnel has similar values to those of a typical atmospheric boundary layer.
11. Analysis of the operational and measured velocity profiles show that the agent, as a sessile drop and sorbed into the substrate, lies within the laminar substrate region of the boundary layer and the evaporation rate is not influenced by the level of free turbulence in the wind tunnel.
12. The 5-cm wind tunnel completed a series of validation tests that demonstrated the ability to accurately and repeatably measure the evaporation rate of HD agent on a glass substrate under specified test conditions.
13. Data trends measured in the 5-cm wind tunnel agrees with theoretical predictions, specifically that the evaporation rate for HD on glass is a non-linear function of velocity, drop size and temperature.

14. Comparison of the evaporation rate data for HD on glass measured in the 5-cm wind tunnel matched similar data obtained in a 10-cm wind tunnel demonstrating that testing can be performed interchangeably between the two sizes of Agent Fate wind tunnels.

15. Evaporation rate data for HD on glass obtained from different 5-cm wind tunnels match each other as well as similar data obtained in a TGA.

16. Video camera record of agent drop evaporation times obtained in the tunnel correlated with direct vapor measurements.

17. Simultaneous operation of two 5-cm wind tunnels in the same hood was accomplished demonstrating that multiple tunnels can be used in the same location to increase productivity.

18. An automated, computer controlled data acquisition and reduction system was incorporated into the tunnel.

19. Experiments to date have included HD on glass and HD on sand demonstrating the ability of the 5-cm wind tunnel to measure the considerably different evaporation characteristics of these two substrates.

20. Multiple 5-cm wind tunnels have been fabricated that produce the same vertical velocity profiles in their test sections demonstrating that multiple 5-cm wind tunnels can be distributed and used for Agent Fate studies at distributed research locations.

Blank

## LITERATURE CITED

1. Agent Fate Master Plan, Joint Science and Technology Panel for Chemical and Biological Defense, October 30, 2002.
2. Weber, Daniel; Molnar, John and Shuely, Wendel; "Environmental Fate of Toxic Chemicals On Surface Materials In Laboratory Wind Tunnels: Measured and Computed Wind Speeds And Flow Fields", Proceedings of the Joint Services Scientific Conference on CB Defense Research, November 2002.
3. Weber, Daniel; Molnar, John; Scudder, Mary Kate and Shuely, Wendel; "Characterization of the Flow Field and Wind Speed Profiles in Microbalance Wind Tunnels for Measurement of Agent Fate", Proceedings of the Scientific Conference on Chemical Defense Research, November 2003.
4. Shuely, Wendel; Nickol, Robert; Pence, John; Weber, Daniel; Molnar, John; Hong, Seok and Sumpter, Kenneth; "Methodology Development For Measurement Of Agent Fate In an Environmental Wind Tunnel", Proceedings of the Scientific Conference on Chemical Defense Research, November 2003.
5. Kilpatrick, William; Ling, Esther; Hin, A.R.T.; Brevett, Carol; Fagen, Mark and Murdock, Paul, Jr.; "Testing Requirements for Predictive Model Development Using Hooded Evaporation Devices (HEDs)", United States Air Force Research Laboratory, AFRL-RE-WP-TR-2004, March 2004.
6. Nickol, Robert; Shuely, Wendel; Pence, John; Flowers, Aaron; Durst, Dupont; Hong, Seok and Sumpter, Kenneth; "Vapor Sampling Methodology Development for Laboratory Measurement of the Environmental Fate of HD on Surfaces, 2004 Decontamination Conference. Palm Harbor, FL. May 2004.
7. Weber Daniel; Molnar, John; Scudder, Mary Kate; Shuely, Wendel and Nickol, Robert; "Laboratory Evaporation and Desorption Instrumentation Systems (Wind Tunnels) for Measuring the Environmental Fate of Toxic Chemicals: Design, Transducers, and Calibration", 2004 Decontamination Conference. Palm Harbor, FL. May 2004.
8. Hin, A.R.T., Droplet Reaction and Evaporation of Agents Model (DREAM), TNO Report, May 2004.
9. Weber Daniel; Molnar John; Scudder Mary Kate; Shuely, Wendel and Nickol, Robert; "Reproducing a Section of The Earth's Atmospheric Surface Layer in Small Wind Tunnels for Studies on the Environmental Fate of Chemical Warfare Agents", Proceedings of the Army Science Conference. November 2004.

10. Weber, Daniel; Scudder, Mary Kate; Shuely, Wendel; Nickol, Robert and Molnar, John; "Laboratory Evaporation and Desorption Instrumentation Systems (Wind Tunnels) for Measuring the Environmental Fate of Toxic Chemicals: Comparison of Velocity Profiles with the Earth Surface Layer Profiles", Proceedings of the Scientific Conference on Chemical Defense Research, November 2004.

11. King, Bruce; Nickol, Robert; Pence, John; Giannaras, Christopher; D'Onofrio, Terrance; Durst, Dupont; and Sumpter, Ken; "Methods for Measuring Evaporation of Chemical Agent from Solid Surfaces"; Proceedings of the Scientific Conference on Chemical and Biological Defense Research, November, 2006.

12. McFarland, A. R., Anand, N. K., Ortiz, C. A., Gupta, R., Chandra, S., McManigle, A. P.; "A Generic System for Effective Thyroid Blocking in the First Few Hours Post Exposure", Health Physics, Vol. 76(1), Pp 17 - 26, January 1999.

13. King, Bruce; Nickol, Robert; Sumpter, Ken; Pence, John; Giannaras, Christopher; D'Onofrio, Terrance; Durst, Dupont; "Methods for Measuring Evaporation of Chemical Agent from Solid Surfaces", Proceedings of the Joint Service Chemical and Biological Decontamination Conference, December 2005..

14. Shuely, Wendel; Miller, Miles; Nickol, Robert; King, Bruce; Park, Kyong; Weber, Daniel; Scudder, Mary Kate; Molnar, John; Moury, Clayton; Sumpter, Kenneth; Hong, Seok; D'Onofrio, Terrance and Durst, Dupont; "Overview of Agent Fate Laboratory Research Studies", Proceedings of the Joint Service Chemical and Biological Decontamination Conference, December 2005.

15. Weber, Daniel; Scudder, Mary Kate; Moury, Clayton; Park, Kyong; Sumpter, Kenneth; Hong, Seok; D'Onofrio, Terrance; Shuely, Wendel; Miller, Miles; Nickol, Robert; King, Bruce; Pence, John and Durst, Dupont "Agent Fate 5-cm Wind Tunnel, Version 3: Design through Testing", Proceedings of the Joint Service Chemical and Biological Decontamination Conference, December 2005.

16. Shuely, Wendel; Miller, Miles; Nickol, Robert; King, Bruce; Park, Kyong; Weber, Daniel; Scudder, Mary Kate; Molnar, John; Moury, Clayton; Sumpter, Kenneth; Hong, Seok; D'Onofrio, Terrance and Durst, Dupont; "Agent Fate Laboratory Research Studies", Proceedings of the Conference on Chemical Defense Research, November 2005.

17. Weber, Daniel; Scudder, Mary Kate; Moury, Clayton; Park, Kyong; Sumpter, Kenneth; Hong, Seok; D'Onofrio, Terrance; Shuely, Wendel; Miller, Miles; Nickol, Robert; King, Bruce; Pence, John and Durst, Dupont; "Agent Fate 5-cm Wind Tunnel: Enhancements, Characterization and Performance", Proceedings of the Conference on Chemical Defense Research, November 2005.

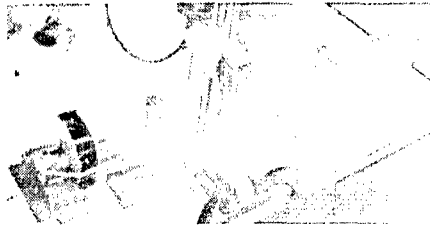


18. Shuely, Wendel; Miller, Miles; Nickol, Robert; King, Bruce; Park, Kyong; Weber, Daniel; Scudder, Mary Kate; Sumpter, Kenneth; Hong, Seok and D'Onofrio, Terrance; "Comparative Evaluation of Environmental Fate Kinetic Parameters Measured with Different Wind Tunnels, Surface Materials, and Chemical Warfare Agents", Proceedings of the Conference on Chemical Defense Research, November 2005.
19. Coutant, R. W. and Penski, E. C.; "Experimental Evaluation of Mass Transfer from Sessile Drops", Chemical Systems Laboratory, ARCSL-SP-83023, June 1983
20. Dooley, Brad; Chen, Kevin; Gharib, Mory and Navaz, Homayun; "Boundary Layer Experiments and the Agent Fate Program", Agent Fate Analytical Working Group Meeting, Kettering University, September 28-29, 2005.
21. Frehlich, R.; Meillier, Y.; Jensen, L.; Balsley, B.; and Sharman, R., "Measurements of Boundary Layer Properties in an Urban Environment", American Meteorological Society, June 2006, Pp 821-837. (National Center for Atmospheric Research (NCAR) Briefing, 2005.
22. Danberg, J.; "Evaporation Rate Data Regression Analysis", Memorandum Report, February 27, 2006/Revised December 04, 2006.
23. Donnelly, T.; "Statistical Comparison of agent Fate Wind Tunnel Evaporation Rate Data", Agent Fate Analytical Working Group Meeting, ECBC, April 24, 2006.
24. Weber, Daniel; Shuely, Wendel; Park, Kyong and Miller, Miles, "Agent Fate Wind Tunnel Data Presentation Format", Agent Fate Analytical Working Group Meeting, ECBC, April 24, 2006.
25. Davies, N. J.; Riches, J.; Walker, S.; "Evaporation of Mustard from Glass – UK Dstl (Porton Down) Evaporation Test Facility"; Dstl/CR12591 V1.0; September, 2004.
26. Riches, J.; "Chemical Agent Fate in Buildings"; Proceedings of the Scientific Conference on Chemical Biological Defense Research, Hunt Valley, MD, November, 2006.
27. Skoumal, Miroslav; "The New Czech Hooded Evaporation Device (HED): Design and First Live Agent Experimental Results"; Proceedings of the Joint Service Chemical Biological Decontamination Conference; May 2004.
28. Shuely, W. J.; McHugh, V. M.; Ince, B. S; "Development of Computer-Controlled Thermogravimetric Instrumentation for Measurement of Environmental and High Temperature Volatilization and Desorption of Contaminants from Polymeric Materials"; CRDEC-TR-88054; April, 1988.
29. Shuely, Wendel; Hong, Seok; Sumpter, Ken; Nickol, Robert; "Measurement of Chemical Agent Evaporation and Desorption In Microbalance Wind Tunnels"; Proceedings of the Scientific Conference on Chemical Defense Research, November 2003.

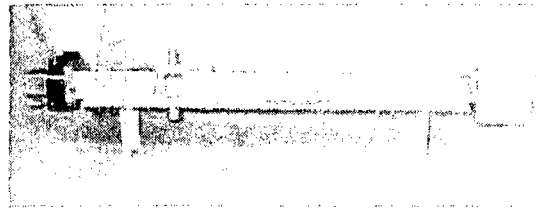
30. D'Onofrio, Terrence; "Photographic Analysis of Agent-Substrate Matrices in Controlled Wind Tunnel Environments"; Proceedings of the Joint Service Chemical Biological Decontamination Conference. December 2005.

31. Shuely, Wendel; Nickol, Robert; King, Bruce; Pence, John; Giannaras, Christopher; D'Onofrio, Terrance; Donnelly, Thomas; Durst, Dupont; "Fundamental Laboratory Measurements of the Environmental Fate of Chemical Agents on Surfaces"; Section C3 in Agent Fate Final Report. ECBC-TR. 2007.

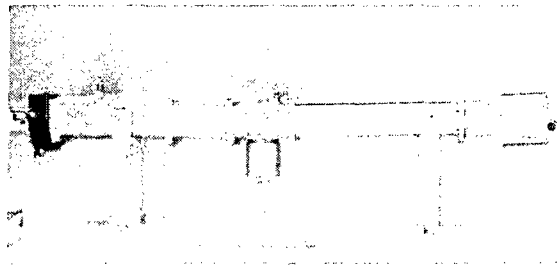
**APPENDIX A**  
**5-CM WIND TUNNEL DESIGN EVOLUTION**



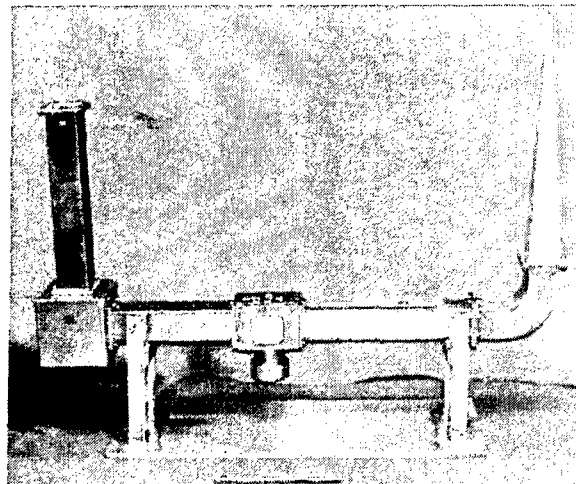
Test Fixture



Type 1 (Test Bed)



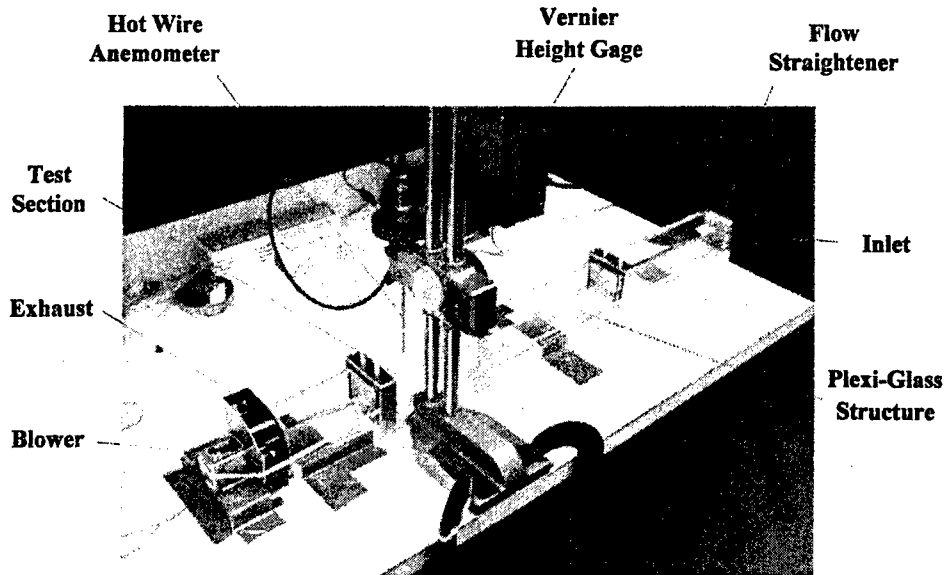
Type 2 (Prototype)



Type 3 (Production)

Evolution of 5-cm Wind Tunnel

## Tunnel Designation: Plexi-Glass Test Fixture



**Initial tests:** June 2002

**Purpose:** Investigate methods of creating and measuring boundary layer flow in small wind tunnels.

**Layout:** Straight, Open circuit

Blower downstream of test section (negative test section static pressure)

**Material/Construction:** Plexi-Glass

**Instrumentation:**

Hotwire anemometer for vertical velocity profile measurements

**Results:** Determined optimum fetch length

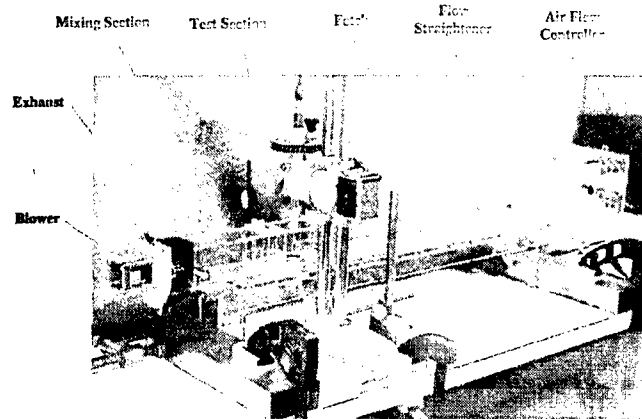
Determined need for flow straighteners in inlet

Evolved cubic flow turbulence generators for velocity profile shapers

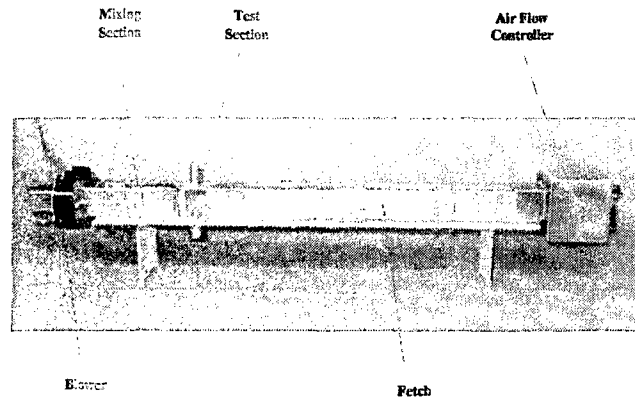
Established "no turbulence" baseline for boundary layer measurements

Demonstrated ability to produce "power law" boundary layer velocity profiles

## Tunnel Designation: Version 1 (Test Bed Tunnel)



Lexan® Tunnel



Stainless Steel Tunnel

Initial Tests: June 2003

Purpose: Evaluate methods for creating specific velocity profiles and for measuring agent vapor concentrations

Layout: Straight, Open circuit

Blower located downstream of test section (negative static test section pressure)

Sampler located upstream of blower

Material/Construction:

Lexan® tunnel used to evaluate velocity profiles

Stainless steel tunnel used to evaluate agent vapor measuring instrumentation

Squirrel cage electric blower as airflow source located downstream of test section

Components connected with slip fit attachments

Instrumentation:

Hotwire anemometer for vertical velocity profile measurements

Hapsite GC-MS for vapor concentration measurements

Results:

Determined that slip fit attachments did not provide sufficient sealing

Evaluated several different blower designs

Showed that blower voltage could not be used to accurately adjust tunnel centerline velocity

Demonstrated that exhaust tube on blower improved flow through tunnel

Investigated blower location and orientation to prevent flow asymmetries

Evaluated multi-hole/slot and Iris flow controllers

Evaluated Miller-Nelson as Environmental Control Unit

Evolved piston component for inserting/holding agent/substrate in test section

Evaluated turbulence strake designs

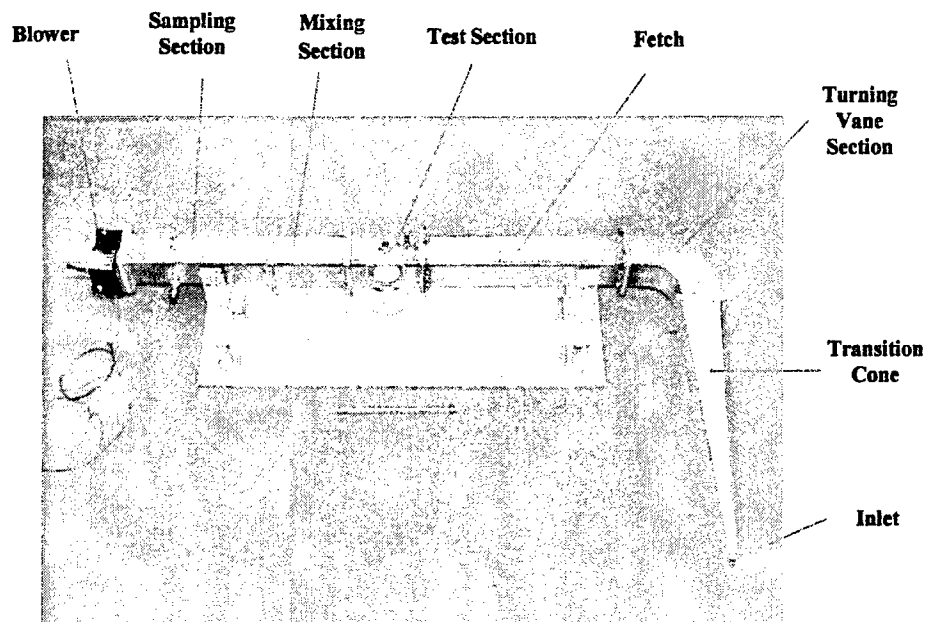
Demonstrated ability to produce "power law" boundary layer velocity profiles

Demonstrated need to directly measure reference velocity

Showed that airflow near agent/substrate could be correlated with tunnel centerline velocity

Determined need to add agent resistant coating to interior surface of tunnel

## Tunnel Designation: Version 2



**Initial tests:** July 2004

**Purpose:** Incorporated improvements determined from tests with Version 1 tunnel

**Layout:** "L" shape, Open circuit

Blower located downstream of test section (negative test section static pressure)

Temperature/RH controlled air provided by Miller-Nelson ECU

Agent concentration sampler located upstream of blower

**Material/Construction:**

Silco-Steel® coated stainless steel tubing

Reduced number of components

Components had welded flanges, connected with screws and including silicon gaskets

Welded test section

Front test section window not flush with floor due to curvature of stainless steel tubing

Screw-in agent/substrate piston

Transition cone and turning vane section to adapt tunnel to Miller-Nelson

**Instrumentation:**

Hotwire anemometer used for vertical velocity measurements

3 instrumentation ports in test section for velocity calibration and temperature

Hapsite GC-MS used as agent vapor measuring device

**Results:**

Evaluated various mixing devices (Induced air jet and Vortab)

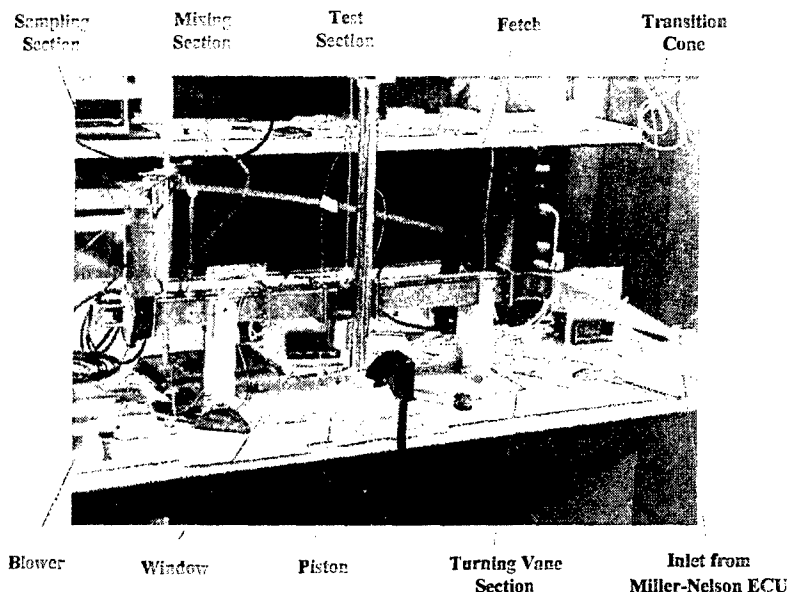
Demonstrated ability to match defined velocity profiles (defined in May 2004)

Demonstrated adequacy of single reference velocity measurement in test section

Evolved waterjet method for cutting TNO glass into disks for 5-cm wind tunnel

Demonstrated zero leakage throughout tunnel

## Tunnel Designation: Version 2, Mod 1



Initial tests: August 2004

Purpose: Incorporated improvements determined from tests with Version 1 tunnel

Layout: Twisted "L" shape, Open circuit

Blower located downstream of test section and used only for mixing

Sampler located downstream of blower

Miller-Nelson sole source of airflow

Airflow source located upstream of test section (positive test section static pressure)

Material/Construction:

Silco-Steel® coated stainless steel tubing

Reduced number of components

All components had welded flanges and were screw connected with silicon gaskets

Welded test section

Front test section window not flush with floor due to curvature of stainless steel tubing

Screw-in agent/substrate piston

Airflow provided solely by Miller-Nelson Environmental Control Unit

Vapor sampling port located downstream of blower

Transition cone and turning vane section to adapt tunnel to Miller-Nelson

Vertical exhaust component for enhanced mixing at sampling port (twisted "L" shape layout)

Instrumentation:

Hotwire anemometer used for vertical velocity measurements

3 instrumentation ports in test section for velocity calibration and temperature

Hapsite GC-MS used as agent vapor measuring device

Results:

First successful tests of HD/Glass on August 2004

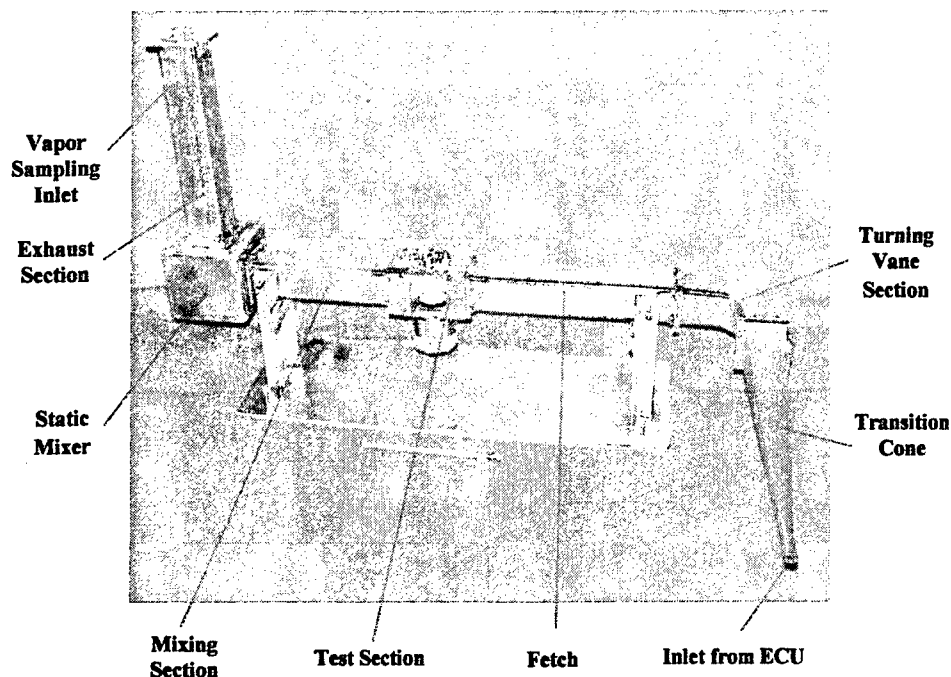
Demonstrated zero leakage throughout tunnel

Demonstrated need for insulated and temperature controlled blankets

Demonstrated need for automated flow control/meter at tunnel entrance



## Tunnel Designation: Version 3



Initial tests: April 2005

Purpose: Incorporated improvements determined from tests with Version 2 tunnel

Layout: Twisted "L" shape, Open circuit

Airflow source located upstream of test section (positive test section static pressure)

Blower eliminated

Sampler located downstream of static mixer

Material/Construction:

Silco-Steel® coated stainless steel components

All components had welded flanges and were screw connected with Kalrez gaskets

Front test section window located flush with floor for better drop viewing

Snap-fit piston evolved for rapid agent/substrate insertion

McFarland type, static mixer

Fixed, centerline position in exhaust section for vapor sampling port

Insulated and temperature controlled blankets over entire tunnel structure

Instrumentation:

6 instrumentation ports in test section for velocity, temperature, pressure and video camera

Instrumentation ports in fetch and exhaust for temperature

Hyfed used as real time vapor analysis tool

Variable Tube Sampler (VTS) evolved

Automated computer controlled airflow and temperature

Automated computer controlled data acquisition (Hapsite and VTS)

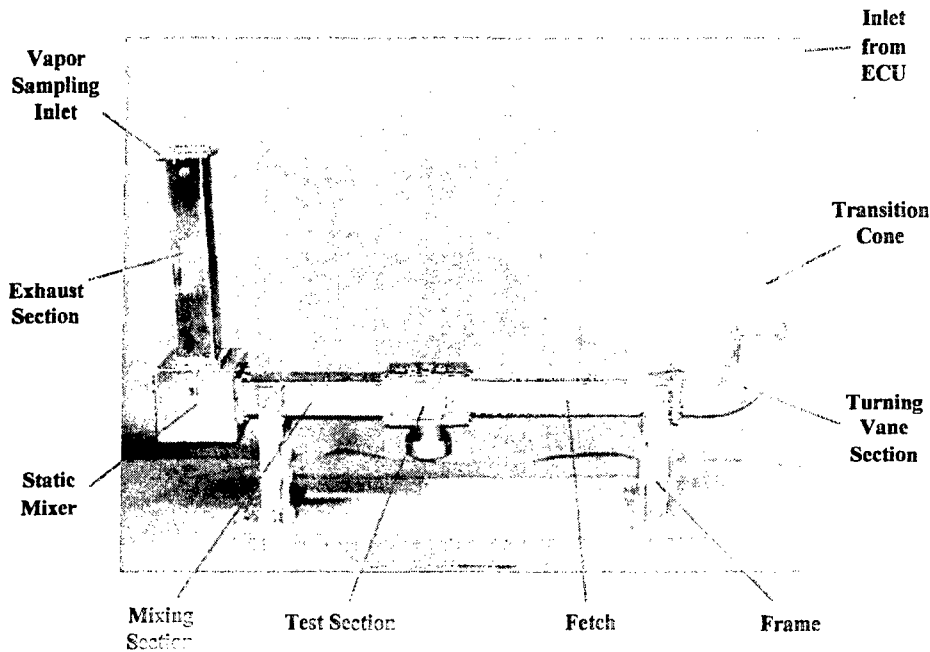
Results:

Evaporation rate data for HD/Glass matches 10-cm wind tunnel data

Evaporation rate data for HD/Glass matches between different 5-cm wind tunnels

Evaporation rate data for HD/Glass matches TGA data  
 Measured velocity profiles match all operational values stipulated by model developers  
 Video correlation of agent drop evaporation correlated with vapor measurements  
 Demonstrated simultaneous operation of two 5-cm wind tunnels in same hood  
 Operation of dedicated medium/hot and cold tunnels  
 12 duplicate tunnels fabricated  
 Tunnel provided to CUBRC

### Tunnel Designation: Version 3 Mod 1



Initial tests: May 2006

Purpose: Alter configuration to be compatible with larger fume hoods of Building E3400.

Incorporated improvements determined from tests with Version 3 tunnel

Layout: "U" shape, Open circuit

Airflow source located upstream of test section (positive test section static pressure)

Sampler located downstream of static mixer

Material/Construction:

Installation of multiple tunnels in Building E3400 hoods required vertical orientation of transition cone and turning vane section (producing "U" shape tunnel layout)

Polished, Sulfinert® coated stainless steel components (required for VX)

Instrumentation:

Use VTS solely for vapor measurement

Shorter and fully insulated transfer line between sampler port and VTS system

Results:

Screen required at entrance to fetch to smooth flow from vertically oriented turning vanes

**APPENDIX B**  
**ENGINEERING DRAWINGS OF 5-CM WIND TUNNEL - VERSION 3 MOD 1**

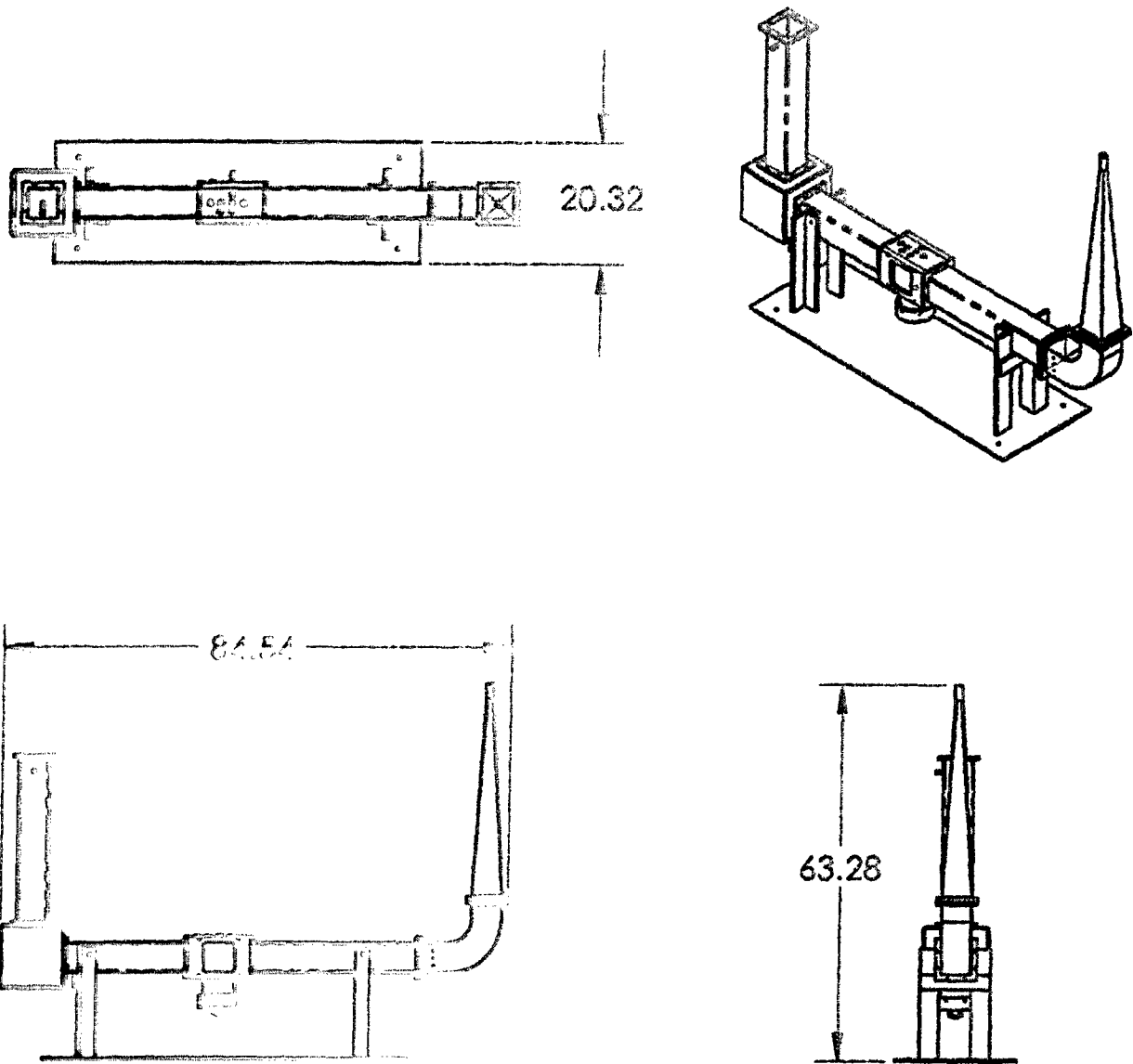


Figure B.1 - Three-Views of 5-cm Wind Tunnel (Version 3 Mod 1)  
 (Dimensions in Centimeters)

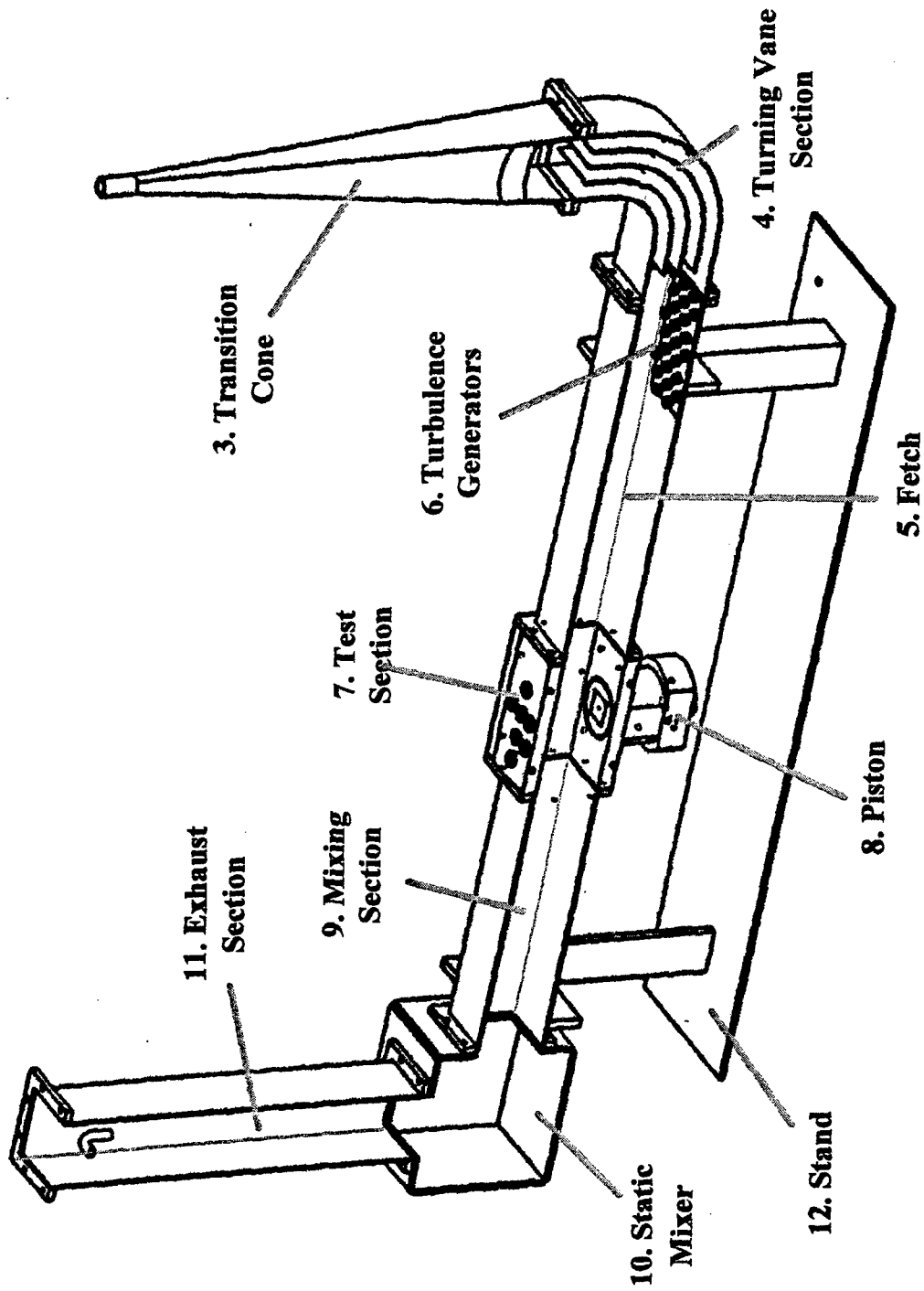


Figure B.2 - Isometric View of 5-cm Wind Tunnel (Version 3 Mod 1)  
 Highlighting Major Components

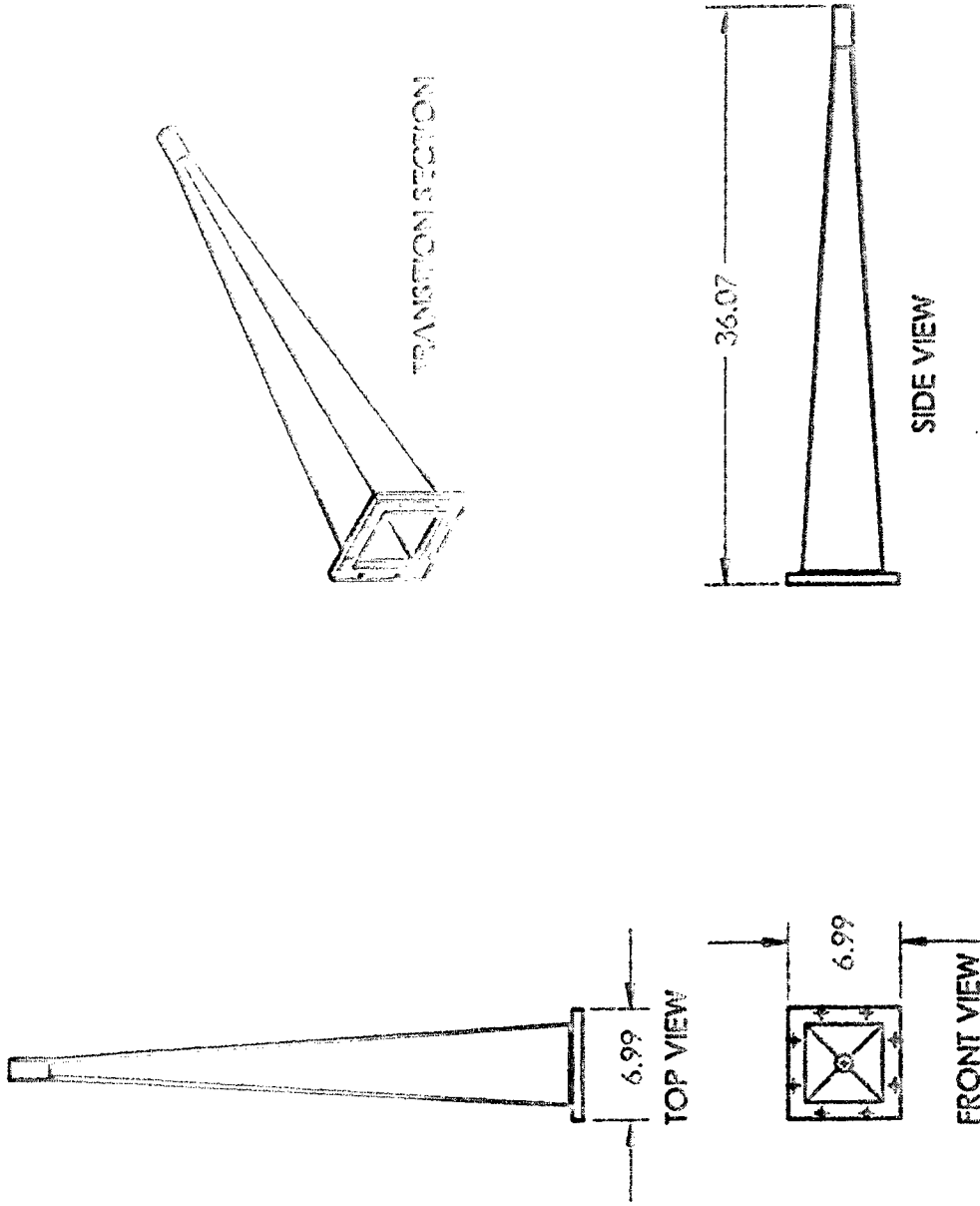


Figure B.3.1 - Three-View of Transition Cone  
(Dimensions in Centimeters)

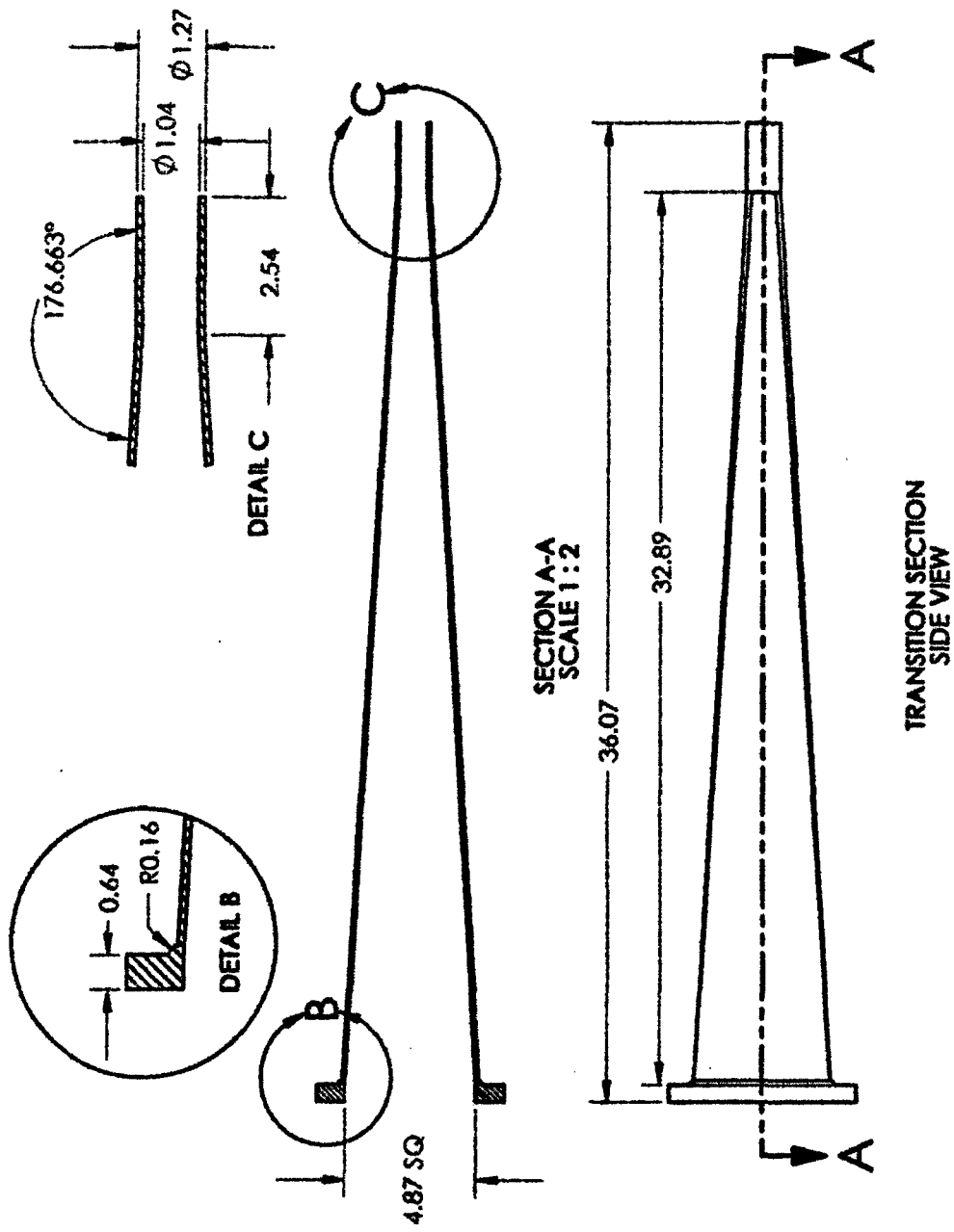
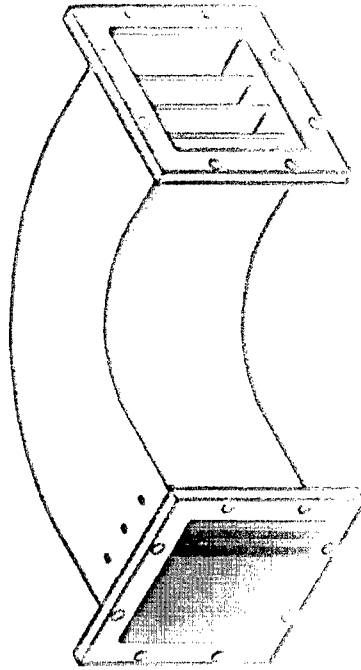
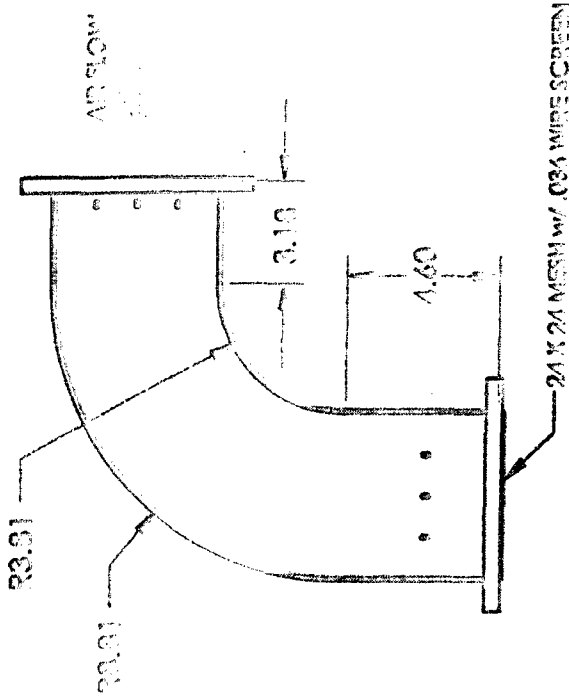


Figure B.3.2 - Details of Transition Cone  
 (Dimensions Centimeters)



TURNING VANE SECTION

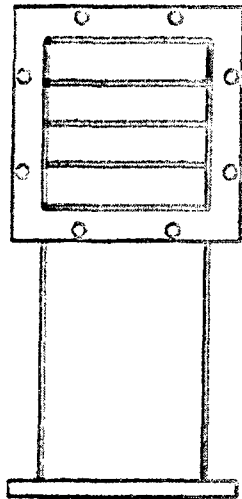
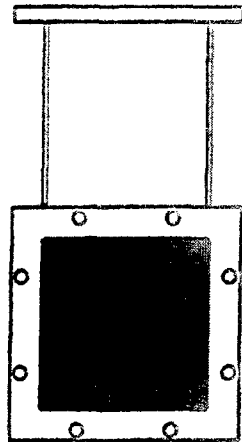


Figure B.4.1 - Three-View of Turning Vane Section  
(Dimensions in Centimeters)



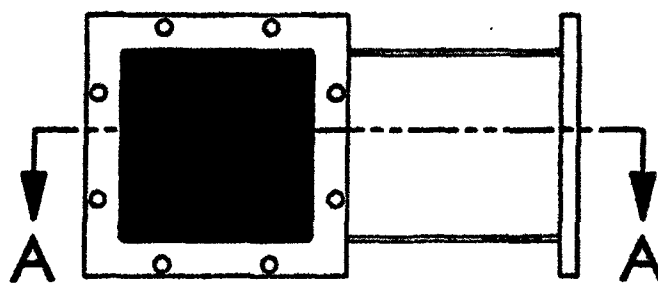
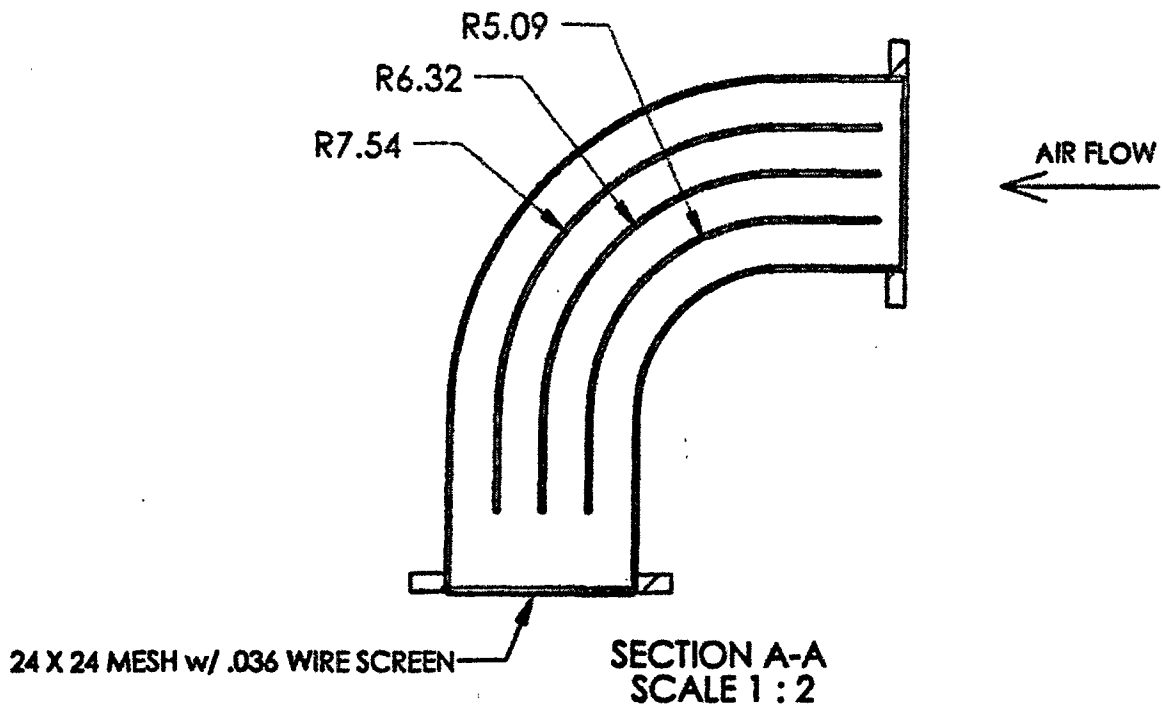


Figure B.4.2 - Details of Turning Vane Section  
(Dimensions in Centimeters)

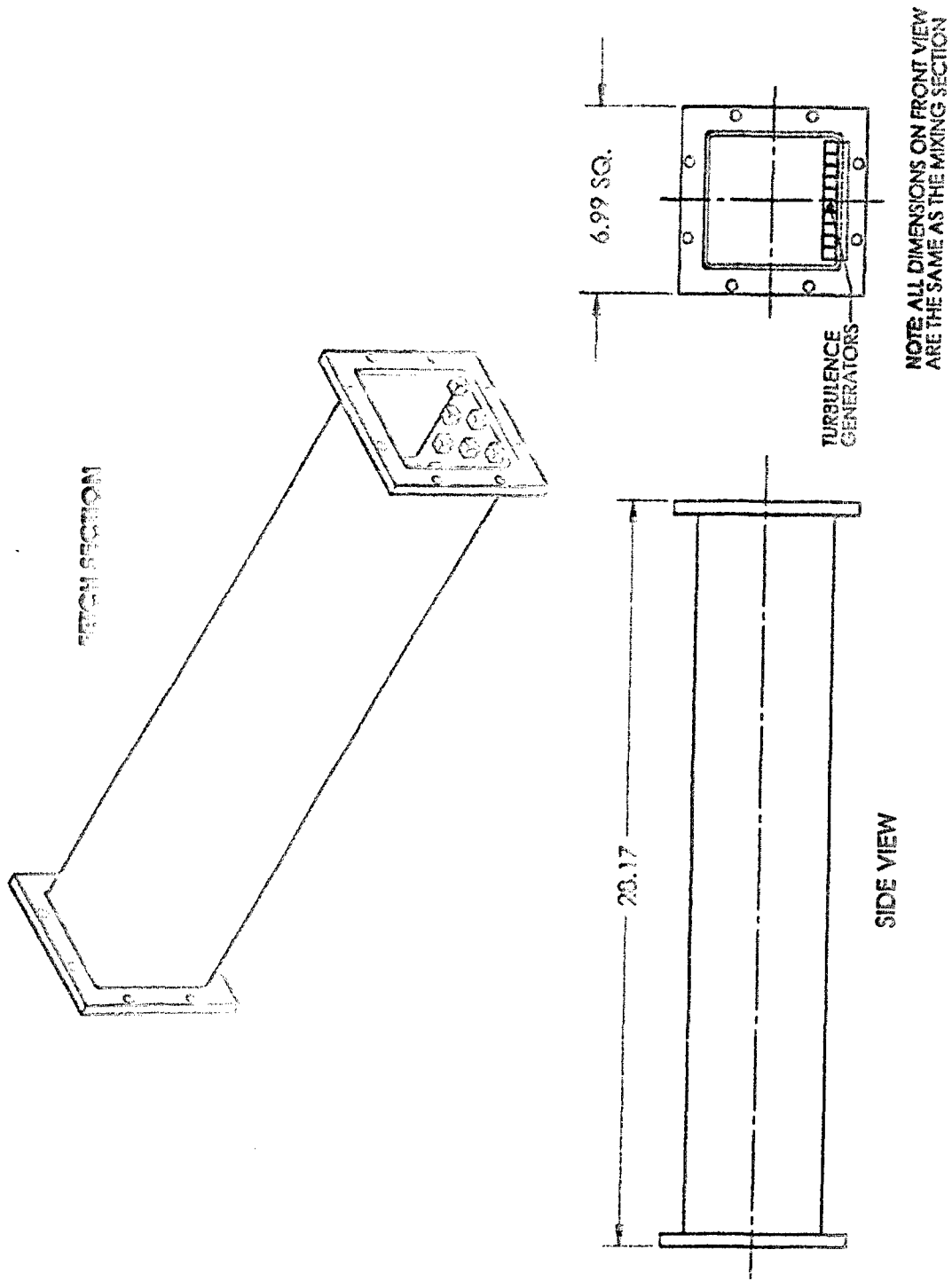


Figure B.5.1. Details of Fetch  
(Dimensions in Centimeters)

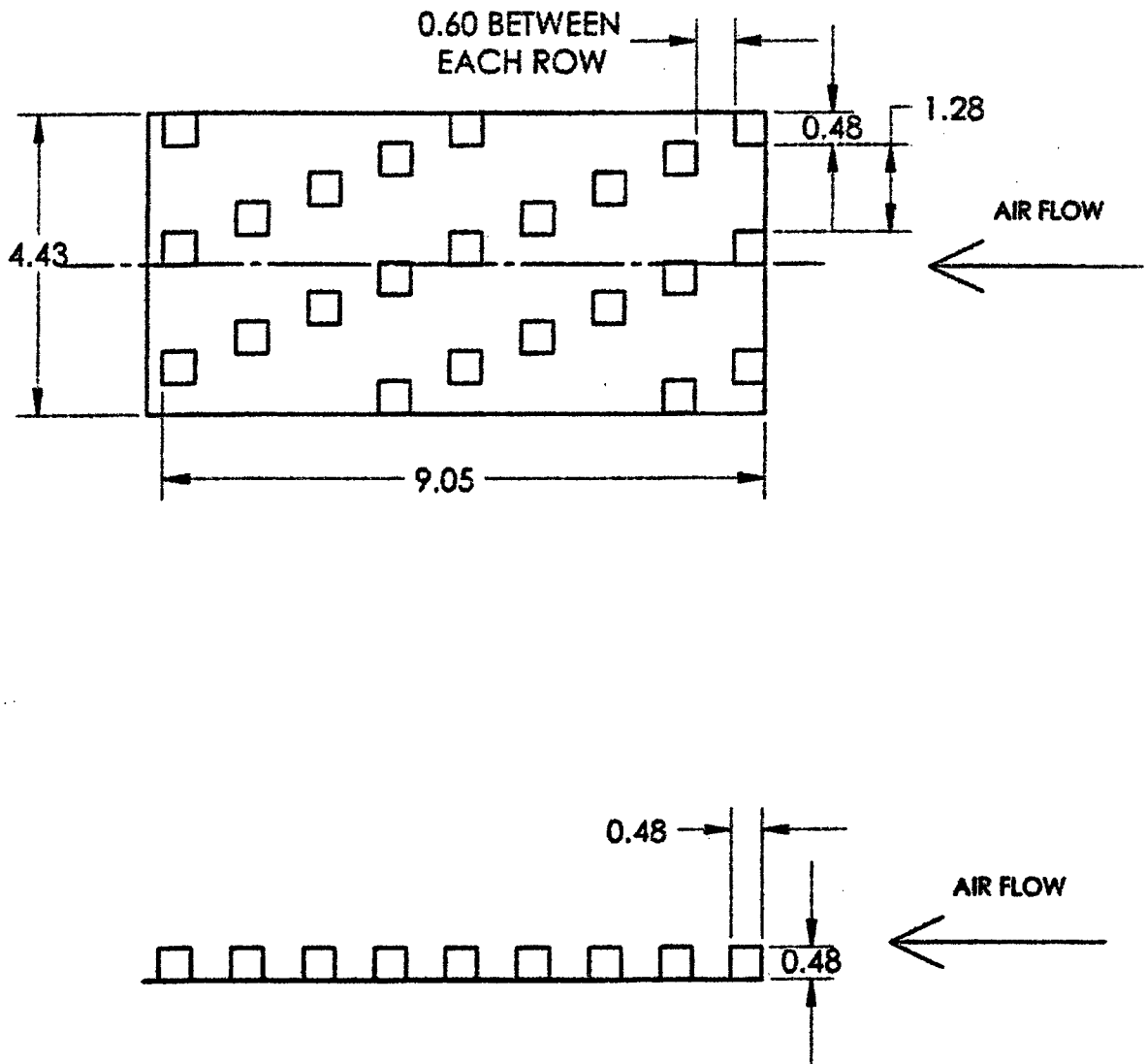


Figure B.6.1. Details of Turbulence Generators  
(Dimensions in Centimeters)

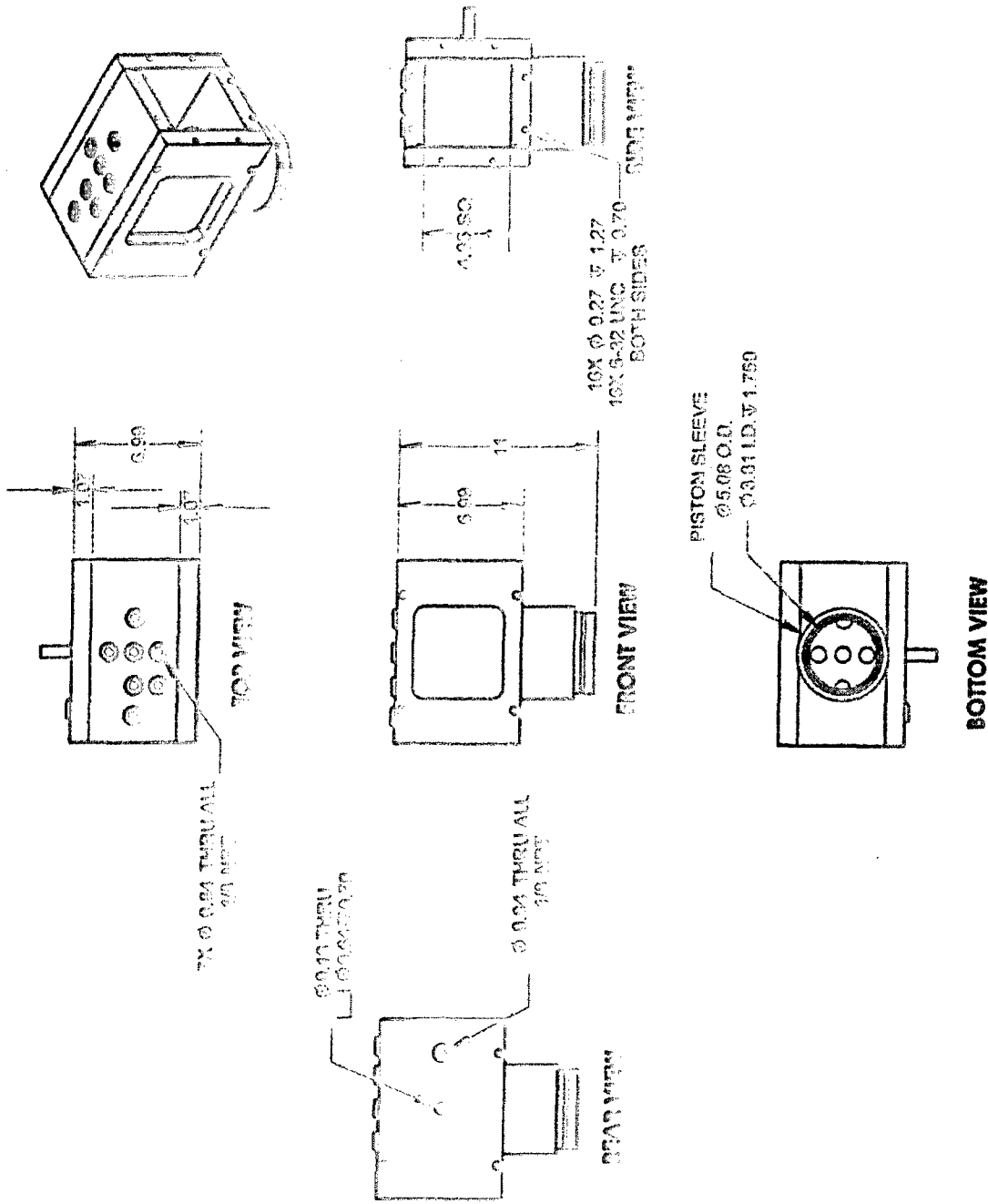


Figure B.7.1 - Five-View of Test Section  
(Dimensions in Centimeters)

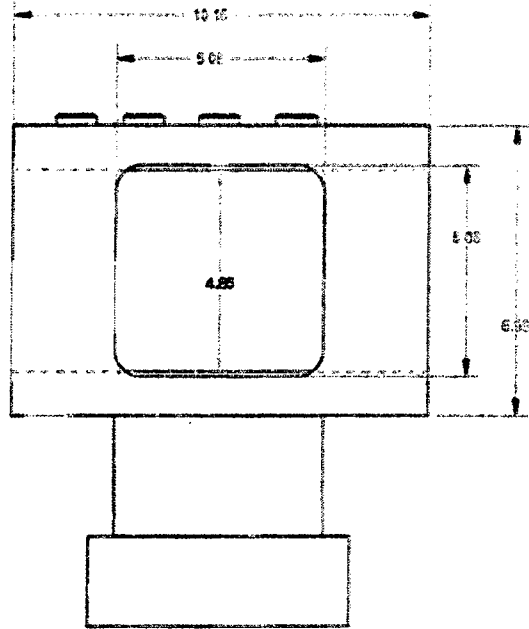


Figure B.7.2 - Details of Test Section (Front View)  
(Dimensions in Centimeters)

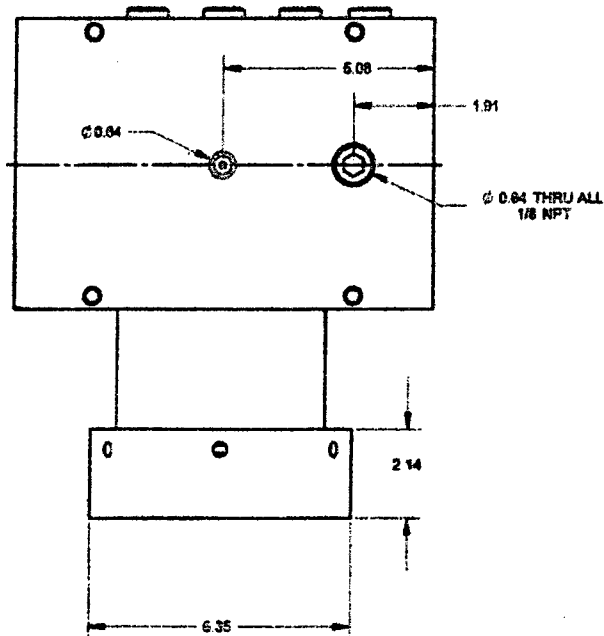


Figure B.7.3 - Details of Test Section (Back View)  
(Dimensions in Centimeters)

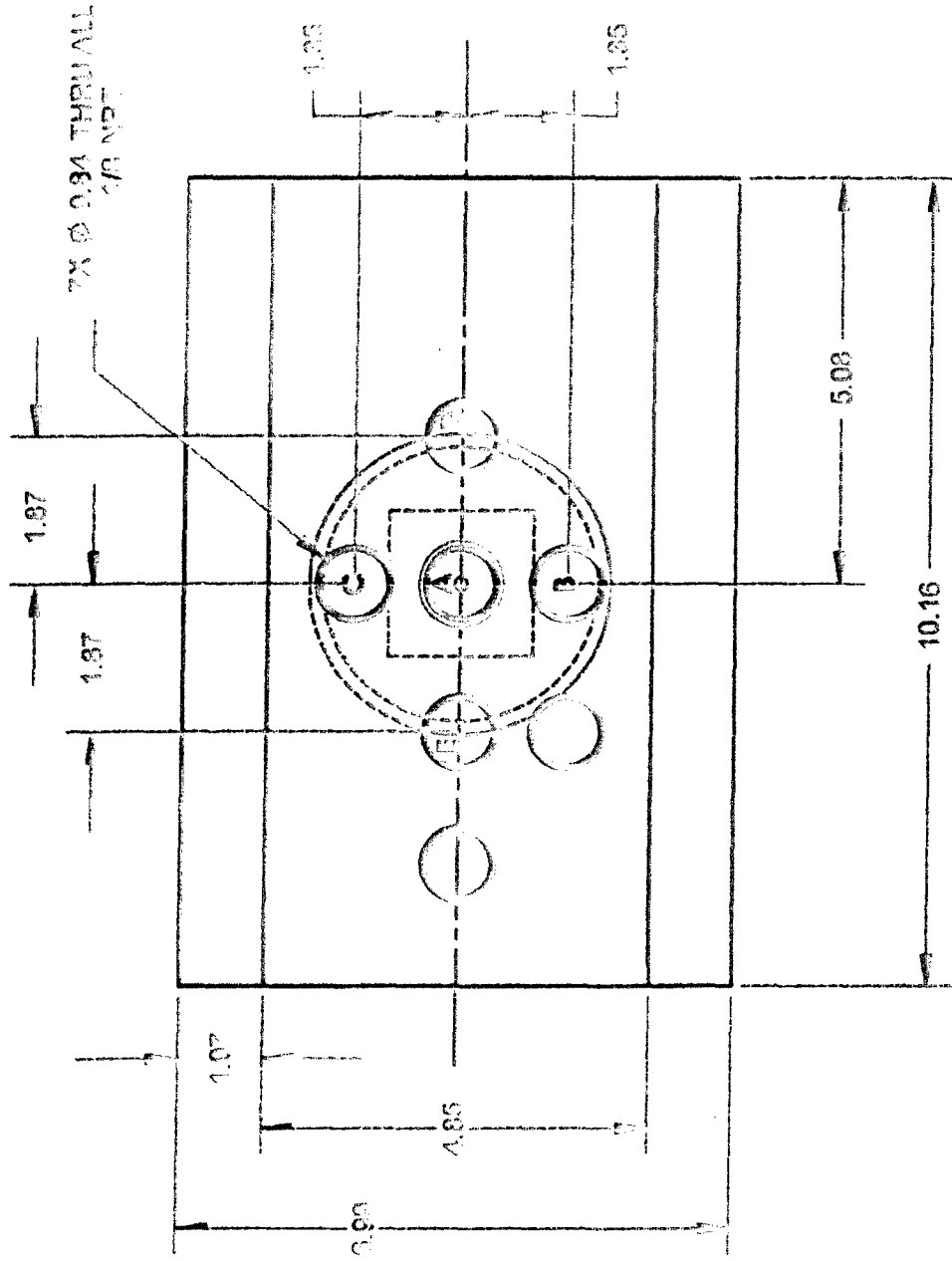


Figure B.7.4 - Details of Test Section (Top View)  
(Dimensions in Centimeters)

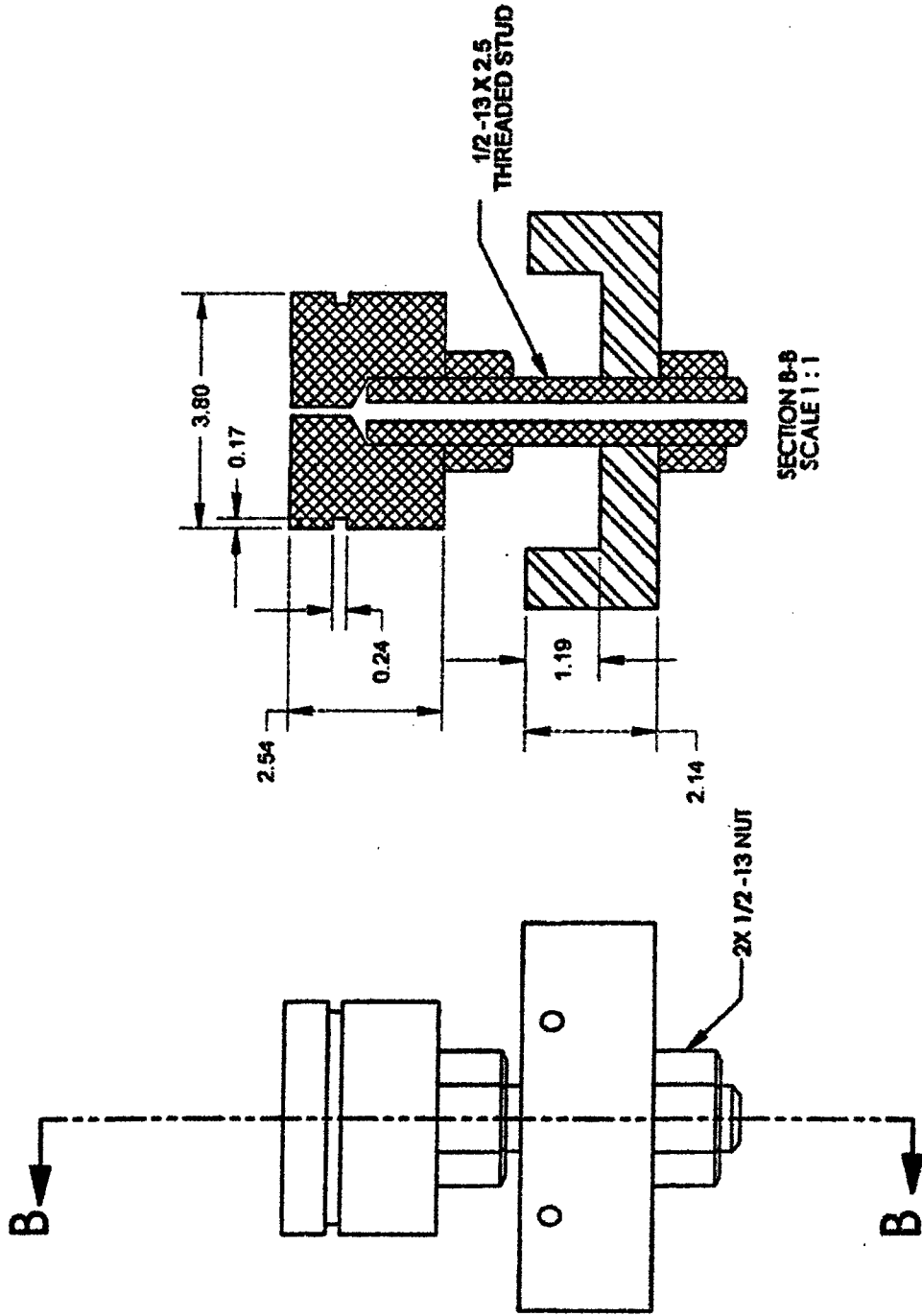


Figure B.8.1. Details of Piston  
(Dimensions in Centimeters)

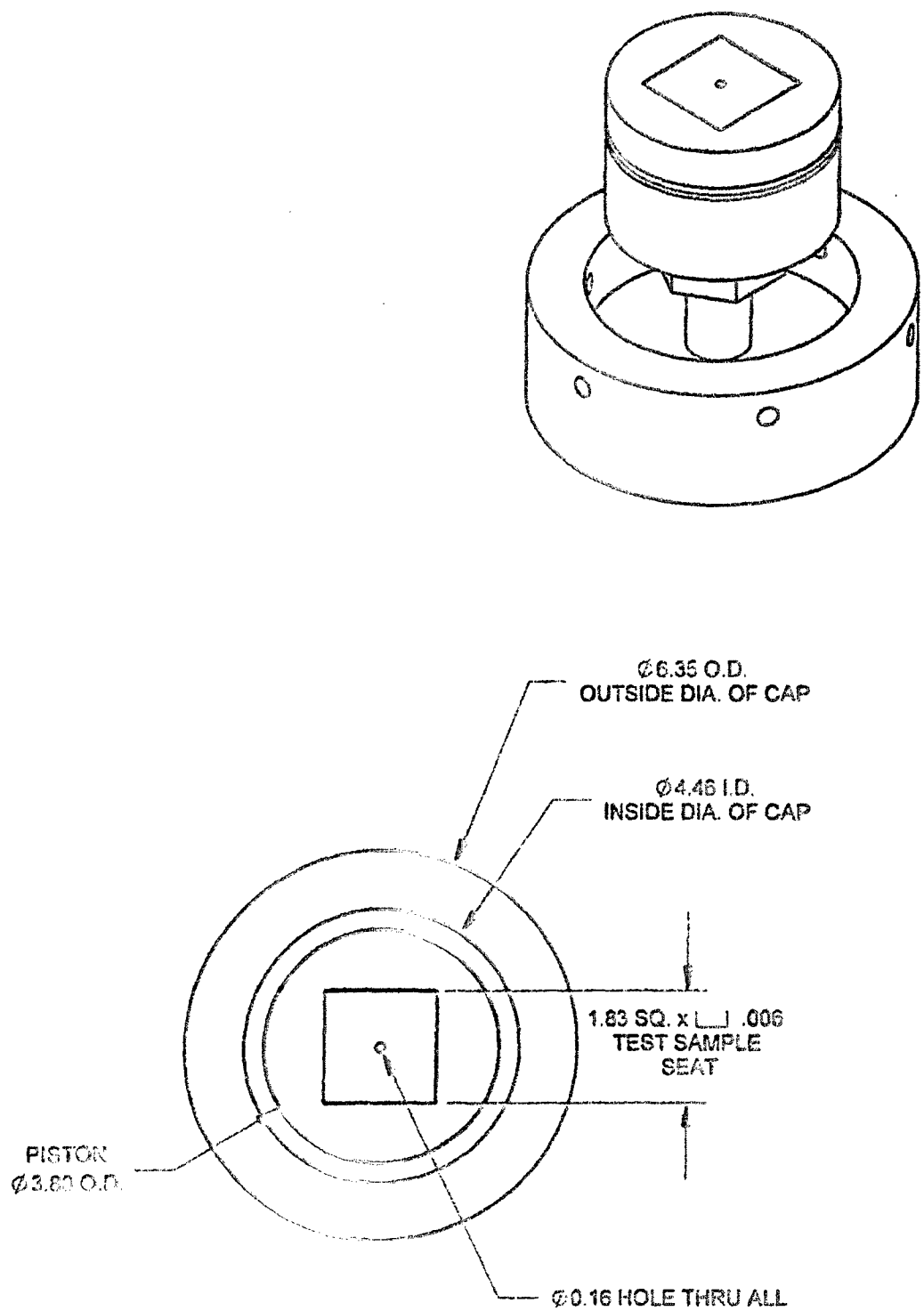


Figure B.8.2. Details of Piston  
 (Dimensions in Centimeters)



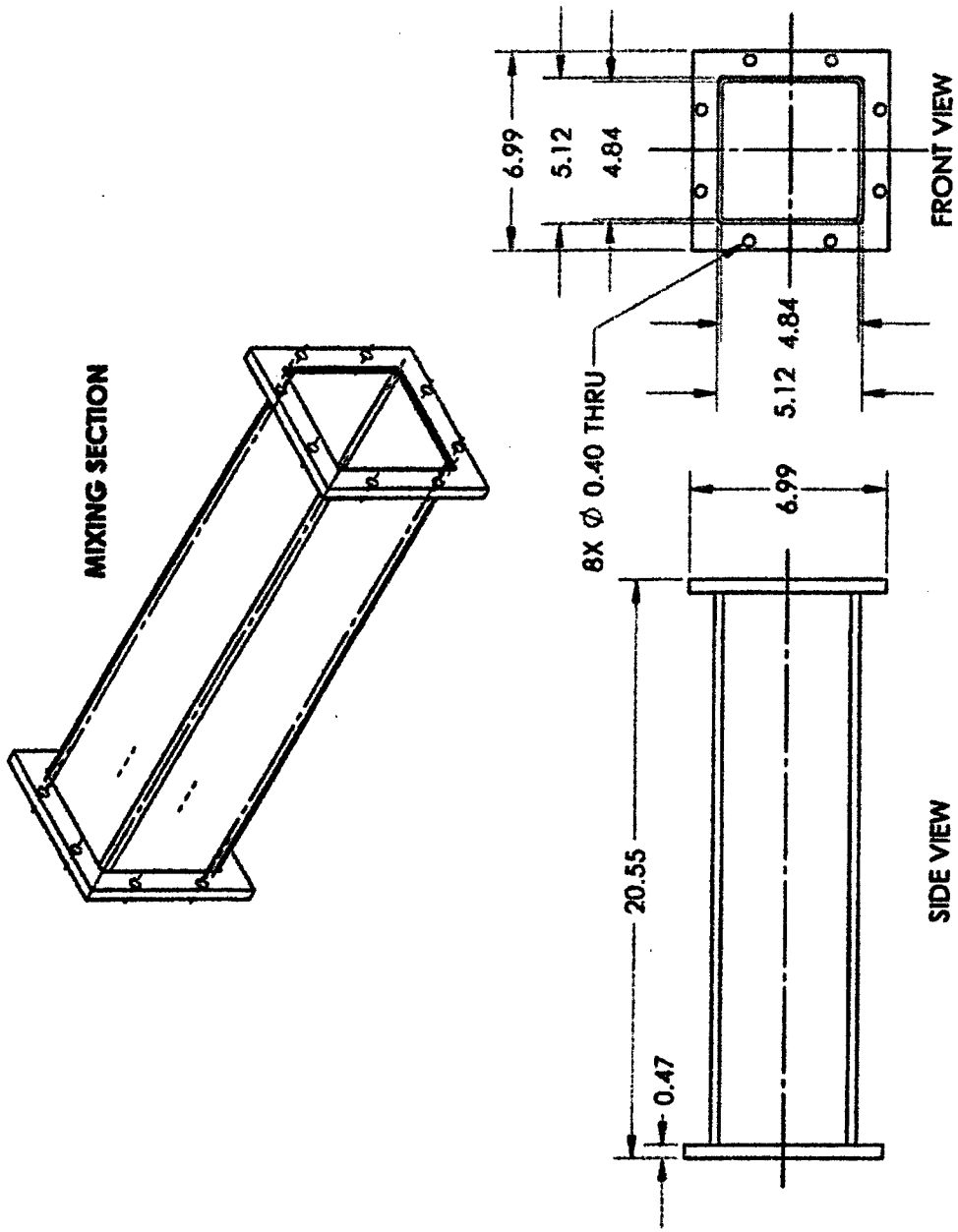


Figure B.9.1. Details of Mixing Section  
(Dimensions in Centimeters)

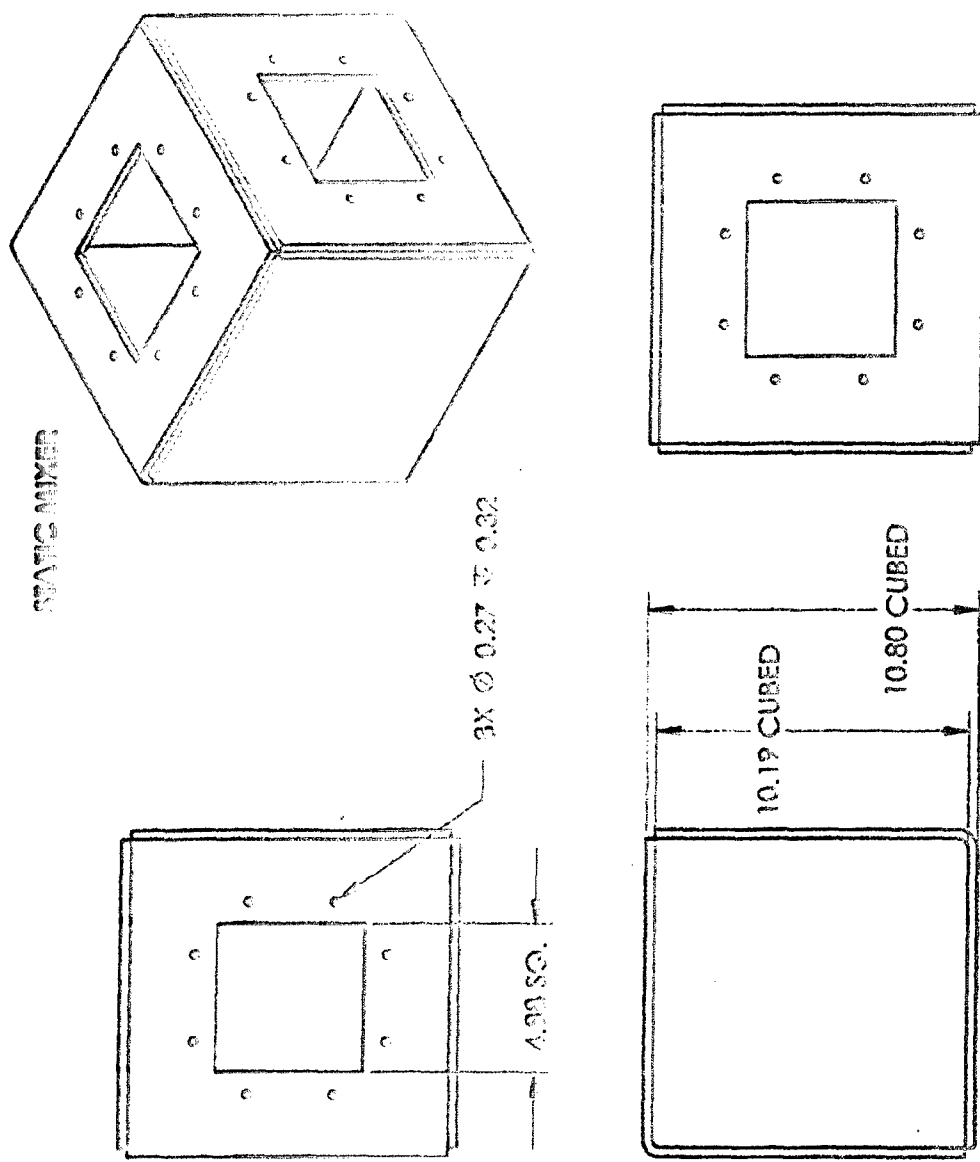


Figure B.10.1 - Three-View of Static Mixer  
(Dimensions in Centimeters)

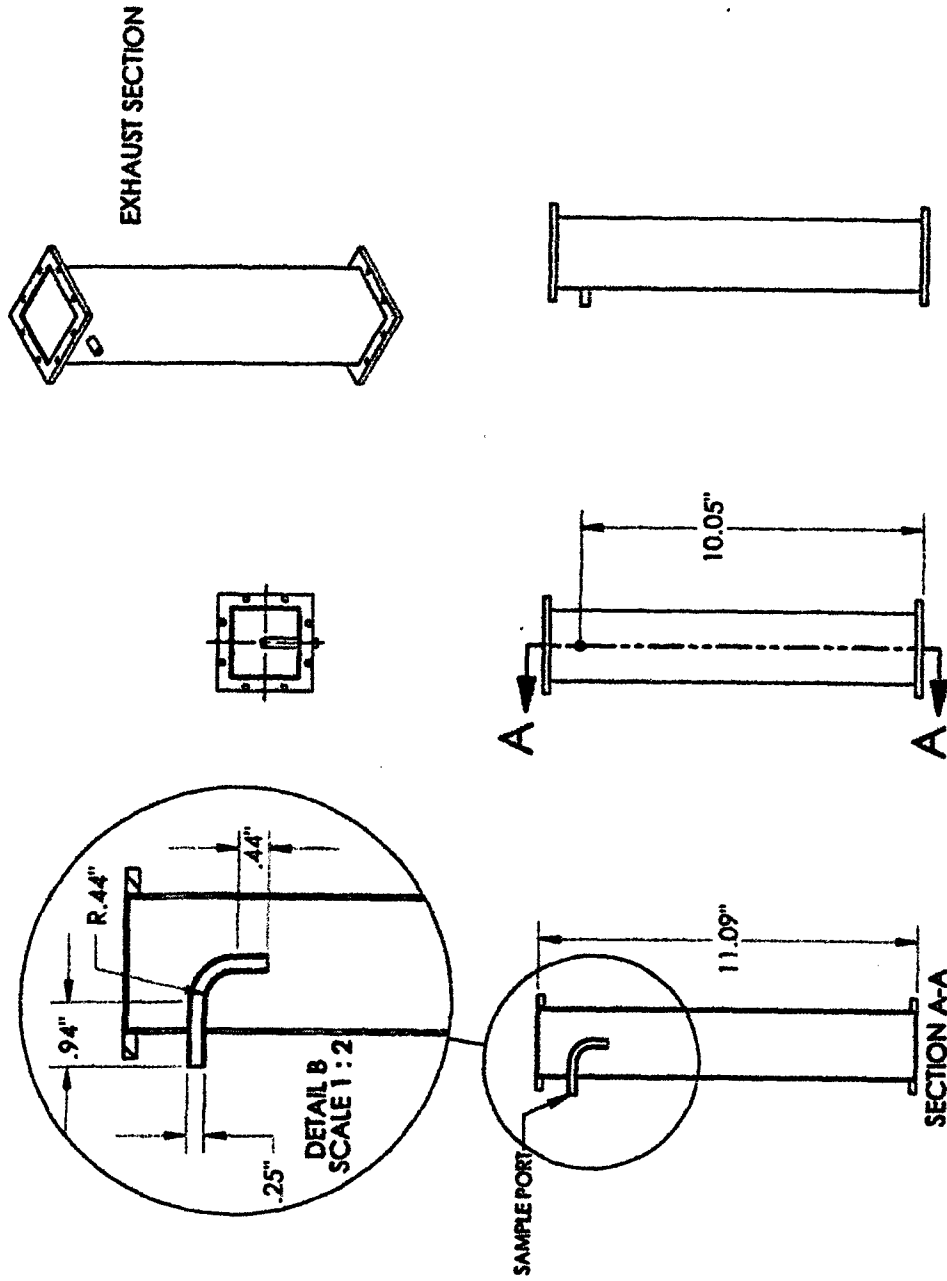


Figure B.11.1 - Three-View of Exhaust Section  
(Dimensions in Centimeters)

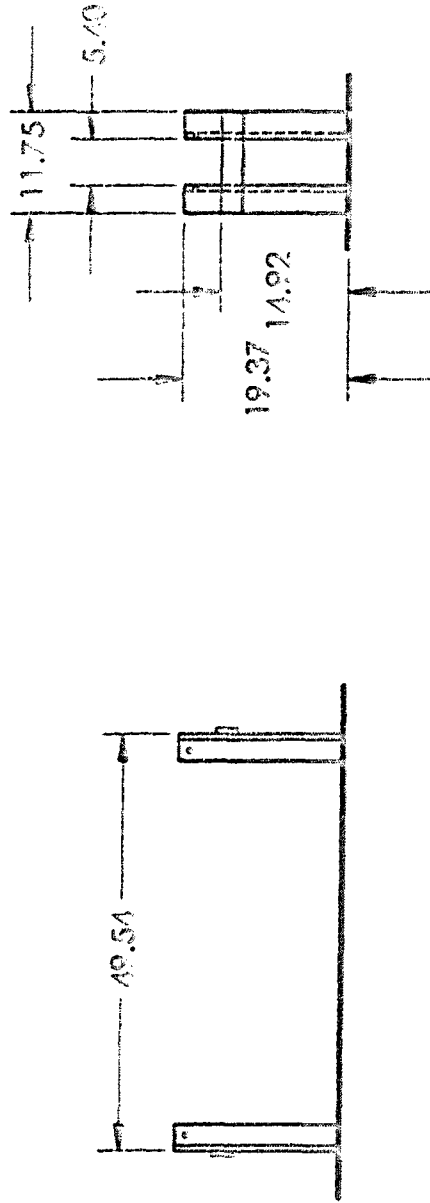
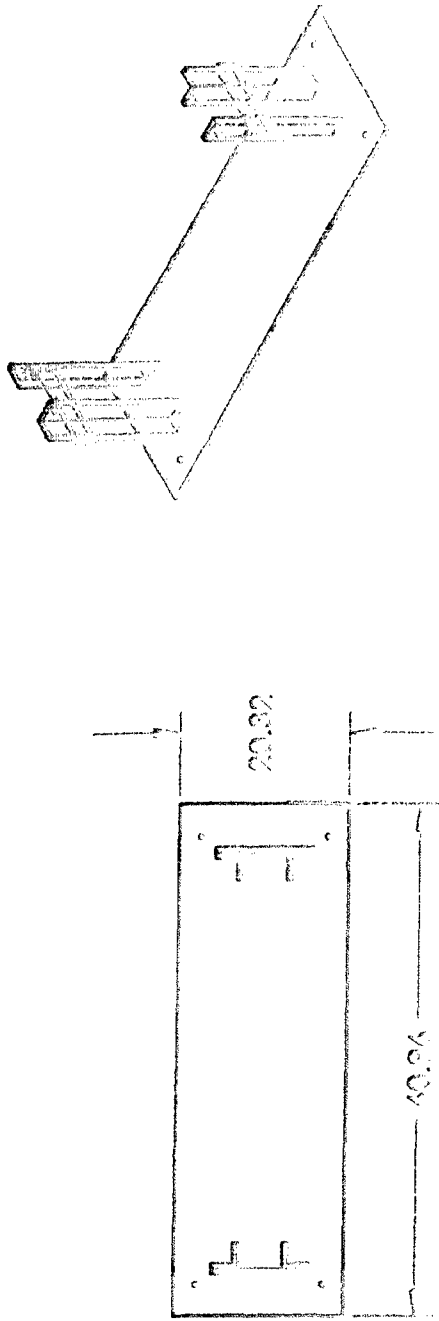


Figure B.12.1 - Three-View of Stand  
(Dimensions in Centimeters)

## APPENDIX C

### SUMMARY OF 10-CM WIND TUNNEL VALIDATION TEST DATA

Code	Temperature °C	Drop Size μl	Velocity @ 1cm m/s	Velocity @2 m m/s	Mean Evaporation Rate μg/min.
- - -	15	1	0.25	0.5	
- 0 -	15	6	0.25	0.5	
- + -	15	9	0.25	0.5	
-- 0	15	1	1.77	3	3
- 0 0	15	6	1.77	3	6.1
- + 0	15	9	1.77	3	
-- +	15	1	3.66	6	4.9
- 0 +	15	6	3.66	6	
- + +	15	9	3.00	5	12.8
0 --	35	1	0.25	0.5	7
0 0 -	35	6	0.25	0.5	11.9
0 + -	35	9	0.25	0.5	
0 - 0	35	1	1.77	3	13.9
0 0 0	35	6	1.77	3	41.3
0 + 0	35	9	1.77	3	54.3
0 - +	35	1	3.66	6	
0 0 +	35	6	3.00	5	37
0 + +	35	9	3.66	6	
+ --	50	1	0.25	0.5	
+ 0 -	50	6	0.25	0.5	
+ + -	50	9	0.25	0.5	
+ - 0	50	1	1.77	3	
+ 0 0	50	6	1.77	3	117
+ + 0	50	9	1.77	3	
+ - +	50	1	3.66	6	71.8
+ 0 +	50	6	3.66	6	
+ + +	50	9	3	5	161.7

Summary of 10-cm Wind Tunnel Validation Test Data